The novel role of semaphorin3F in neutrophilic inflammation

Suttida Eamsamarng

Submitted for the degree of Doctor of Philosophy

Department of Biomedical Science

University of Sheffield

August 2014

Abstract

Neutrophils are typically the first leukocytes to be recruited to inflamed sites to eliminate invading pathogens, and also play a prominent role in inflammatory processes. Although neutrophils are necessary for host defenses, paradoxically, they have also been involved in the pathology of chronic inflammatory conditions. Recent studies have found that at inflammatory sites characterised by low oxygen concentration, neutrophils are functionally regulated by the oxygen-sensitive hypoxia inducible factor (HIF) transcription factor, which in turn is modulated by a group of oxygen-sensing hydroxylase enzymes, principally the prolyl hydroxylases (PHDs). More recently our group found that semaphorin3F, which was originally identified as an axon guidance molecule, is significantly induced in PHD3-deficient neutrophils following hypoxic stimulation. I therefore proposed that semaphorin3F may play a role in neutrophil behaviour during inflammation. To investigate this, *in vivo* experiments were performed in the genetically tractable zebrafish, in parallel with *in vitro* experiments in human peripheral blood neutrophils.

Hypoxia and inflammatory stimuli can modulate semaphorin3F expression. Semaphorin3F is significantly upregulated in response to inflammation at both mRNA and protein levels suggesting that semaphorin3F might be important in regulating neutrophil responses during inflammation. *In vivo* zebrafish experiments show that semaphorin3F plays a role in regulating neutrophil migration in inflammation. Semaphorin3F overexpression decreases neutrophil recruitment to the site of injury, and subsequently delays neutrophil reverse migration. In contrast, semaphorin3F knockdown accelerates the movement of neutrophils away from the site of inflammation, resulting in faster resolution of inflammation. Similar results were found with TALENs-generated semaphorin3F mutant fish. Notably, the phenotypes occur in neutrophils not macrophages, suggesting a specific role for semaphorin3F in neutrophil migration.

Neuropilin-2 and plexin A3 have been identified as expressed in neutrophils and potentially as receptors for semaphorin3F in these cells. Semaphorin3F inhibits neutrophil chemotaxis to chemoattractants, but did not appear to affect cell polarity as judged by the intracellular distribution of an Akt-GFP fusion protein that reports PI-3K activity. However, semaphorin3F does appear to be implicated in neutrophil shape change during migration.

These results describe for the first time a role for semaphorin3F in regulating neutrophil migration, with consequences for inflammation initiation and particularly for resolution. This reveals a novel mechanism by which neutrophils are recruited to and maintained at sites of tissue injury. I propose therefore that semaphorin3F may be a potential therapeutic target in chronic inflammatory diseases caused by persistent neutrophilic inflammation.

Acknowledgement

I would first like to thank my supervisors, Dr Sarah Walmsley, Professor Moira Whyte and Dr Andrew Furley for all their support, patience, advice and encouragement throughout my study. I would also like to thank my advisors, Professor Stephen Renshaw and Dr Freek van Eeden for their advice and help, especially to Professor Stephen Renshaw for providing the opportunity to work in his laboratory.

My thanks go to all the staff and friends in Walmsley's and Renshaw's lab for their help and making my time in the lab so enjoyable. Special thanks go to Roger Thompson, Selina Parmar, Gary Shaw, Pranvera Sadiku, Amy Lewis, Cat Loynes, Aleksandra Bojarczuk, Katy Henry, Nikolay Ogrzyko, Anne Robertson, Lore Lambein and Phil Elks. Many thanks to the aquarium staff for their advice and help with fish stuff and maintainance.

My thanks extend to Amy Lewis for performing the experiments in murine bronchoalveolar lavage neutrophils (Figures 3.6, 6.6); Emma Connolly for performing the experiments in immunostaining (Figures 3.5, 6.4, 6.5); and Tracie Plant for permorming the experiments in neutrophil chemotaxis (Figure 6.7).

Extra special thanks go to my family and my boyfriend Suriya Chukiatsiri for their love and their moral support throughout. Finally, I thank the department of Biochemistry, Kasetsart University for giving me the opportunity to study abroad, and the Royal Thai government for the funding throughout my study in Germany and the UK.

List of Abbreviations

ANOVA	Analysis of Variance
ARNT	Aryl hydrocarbon receptor nuclear translocator
ATP	Adenosine triphosphate
BAL	Bronchoalveolar lavage
Bcl-2	B-cell Lymphoma 2
bHLH	Basic helix-loop-helix
BSA	Bovine serum albumin
$CaCl_2$	Calcium chloride
CAD (HIF)	C-terminal activation domain
CD	Cluster of differentiation
CO	Carbon monoxide
CO_2	Carbon dioxide
COPD	Chronic Obstructive Pulmonary Disease
CTL	Cytotoxic T lymphocyte
DFO	Desferrioxamine
DMEM	Dulbecco's modified Eagle's medium
DMOG	Dimethyloxaloylglycine
DMSO	Dimethyl sulphoxide
DNA	Deoxy-ribonucleic acid
dpf	Days Post Fertilisation
DTT	Dithiothreitol

ECM	Extracellular matrix
EDTA	Ethylenediamine tetraacetic acid
EGFP	Enhanced GFP
ELISA	Enzyme linked immunosorbent assay
ERK	Extracellular signal related kinase
FACS	Fluorescence activated cell sorting
FcR	IgFc-receptor
FCS	Fetal calf serum
FITC	Fluorescein isothiocyanate
fMLP	N-formyl-methionyl-leucyl-phenylalanine
FRET	Fluorescent resonant energy transfer
G-CSF	Granulocyte-colony-stimulating factor
GFP	Green Fluorecent Protein
GM-CSF	Granulocyte macrophage-colony stimulating factor
HBSS	Hanks' balanced salt solution
HCl	Hydrochloric acid
HIF-1	Hypoxia-induced factor-1
H_2O_2	Hydrogen peroxide
hpf	Hours Post Fertilisation
hpi	Hours Post Injury
HRE	Hypoxia response element
IFN	Interferon
Ig	Immunoglobulin

IgG	Immunoglobulin G
IL	Interleukin
JAM	Junctional Adhesion Molecule
KCl	potassium chloride
kDa	Kilo-Daltons
kPa	Kilo-Pascals
LFA-1	Lymphocyte Function-Associated Antigen-1
LPS	Bacterial lipopolysaccharide
MAb	Monoclonal antibody
MAPK	Mitogen-activated protein kinase
Mcl-1	Myeloid Cell Leukemia Sequence-1
MEK	MAP ERK kinase
Mg^{2+}	Magnesium ions
MIP-1	Macrophage inflammatory protein-1
MMP	Matrix metalloproteinase
MPO	Myeloperoxidase
MPX	Myeloid Specific Peroxidase
mRNA	Messenger RNA
NAD	N-terminal activation domain
NADPH	Reduced nicotinamide adenine dinucleotide phosphate
NF-κB	Nuclear factor-Kappa light chain enhancer of activated B cells
NGF	Nerve growth factor

NK	Natural killer cell
NO	Nitric oxide
O_2	Oxygen
O_2^-	Superoxide anion
PAF	Platelet-activating factor
PAGE	Polyacrylamide gel electrophoresis
PBMC	Peripheral blood mononuclear cells
PBS	Phosphate-buffered saline
PBST	Phosphate-buffered saline Tween
pCO_2	Partial pressure of O_2
PCR	Polymerase chain reaction
PDGF	Platelet derived growth factor
PFK	Phosphofructokinase
PH	Pleckstrin Homology
PI3-K	Phosphatidylinositol 3-kinase
PIP_3	Phosphatidylinositol (3,4,5)-Triphophate
pO_2	Partial pressure of O_2
PPP	Platelet-poor plasma
PMN	Polymorphonuclear Neutrophil
PTEN	Phosphatase and Tensin Homologue
RA	Rheumatoid Arthritis
RNA	Ribonucleic acid
ROI	Region Of Interest

ROS	Reactive oxygen species
RPMI	Roswell Park Memorial Institute Medium
RT	Reverse transcriptase
RT-PCR	Real time-PCR
SD	Standard deviation of the mean
SDS	Sodium dodecyl sulphate
SEM	Standard error of the mean
SIVA	CD27 binding protein
SSC	3 M sodium chloride, 0.3 M sodium citrate
STAT	Signal Transducer and Activator of Transcription
Taq	DNA polymerase with 5' exo-nuclease activity
TCA	Trichloroacetic acid
TE	Tris EDTA
TEMED	NNN'N'-Tetramethylethylene-diamine
TGF	Transforming growth factor
TLR	Toll like receptor
TNF	Tumour necrosis factor
TSA	Tyramide Signal Amplification
TUNEL	Terminal Deoxynucleotidyl Transferase dUTP Nick End Labelling
Tris	Tris[hydroxymethyl]-aminomethane
VEGF	Vascular endothelial growth factor
WISH	Whole Mount *in situ* Hybridisation

Table of contents

List of Figures and Tables

Chapter 1: Introduction

1.1 Semaphorins

1.1.1 Semaphorin family

Semaphorins are a family of genes encoding guidance molecules in the nervous system. The first semaphorin to be discovered was the grasshopper transmembrane protein semaphorin-1a (original name; Fasciclin IV) which was found in the developing grasshopper nervous system (Kolodkin et al., 1992). The first semaphorin to be found as a secreted semaphorin was semaphorin3A (original name; Collapsin) which was identified from biochemically purified neuronal growth cone collapsing factor associated with chicken brain membranes (Luo et al., 1993). The name 'semaphorin' is derived from the word 'semaphore' meaning to convey information by a signalling system (Goodman et al., 1999). Semaphorins are now a large family of secreted and membrane-bound molecules characterised by the presence of a sema domain. This domain contains approximately 500 amino acids with the 5' N-terminus being critical for semaphorin function. The sema domain forms in a seven-blade β-propeller fold having structural similarity to the extracellular domain of α-integrins (Koppel et al., 1997). Next to the C-terminus of the sema domain, semaphorins contain the PSI (plexin-semaphorin-integrin) domain which is rich in cysteines and referred to as a MET-related sequence (MRS) or a cysteine-rich domain (CRD) (Bork et al., 1999). Semaphorins also contain other distinct protein domains including immunoglobulin-like domain, basic C-terminal domain and thrombospondin domain (Figure 1.1). Semaphorins are categorised into 8 classes, 1-7 and V: invertebrate semaphorins are grouped in classes 1, 2 and 5; classes 3-7 are vertebrate semaphorins; and class V contains virally encoded semaphorins. In vertebrates, class 3 semaphorins are secreted and are distinguished by a C-terminal conserved basic-charged domain. Class 4-7 semaphorins, cell-membrane-anchored proteins, are characterised by unique structural elements, including thrombospondin repeats or a glycophosphatidylinositol (GPI) anchor (Capparuccia and Tamagnone, 2009).

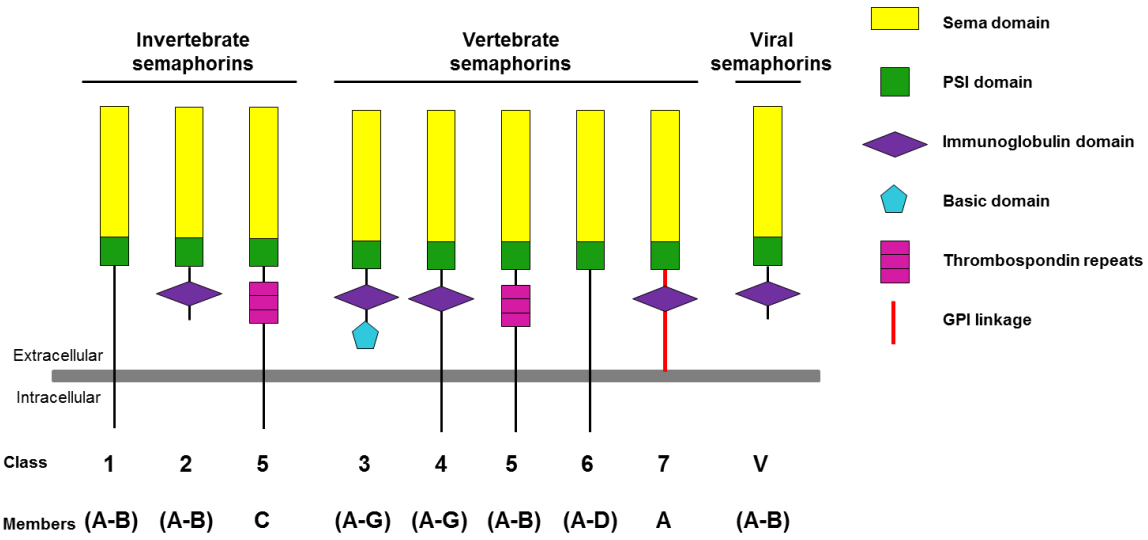

Figure 1.1: The members of the semaphorin family and their structure. There are 8 classes of semaphorins, of which class 1-2 and sema5C are invertebrate semaphorins, class 3-7 are vertebrate semaphorins (with the exception of sema5C). Semaphorins of classes 2, 3 and V are secreted, whereas the other classes are synthesized as transmembrane proteins. Class V semaphorins are found in DNA viruses. Semaphorins contain sema domains with additional domains, including PSI (Plexin, Semaphorin and Integrin) domains, Immunoglobulin (Ig)-like domains, thrombospondin repeats and GPI (Glycophosphatidylinositol) linkage. All proteins are shown with their N-termini to the top. This schematic was based on a diagram from Neufeld and Kessler (2008).

Semaphorins are expressed in both neuronal and non-neuronal tissues, and in many organ systems, including the gastrointestinal, cardiovascular, endocrine, hepatic, immune, musculoskeletal, renal, reproductive, and respiratory systems. The varied expression patterns of semaphorins suggest that they act in different roles in a variety of functions (Yazdani and Terman, 2006).

Semaphorins are best known for their roles in nervous system development, for instance, invertebrate class 1 semaphorins are required in *Drosophila* for embryonic motor and central nervous system axon guidance (Yu et al., 1998). Invertebrate semaphorin2A functions as a selective target-derived signal inhibiting the formation of specific synaptic terminal arborisations in vivo in drosophila models (Matthes et al., 1995). Class 3 semaphorins are not involved in axonal guidance through repulsive gradient and induction of growth cone collapse, but are implicated in survival and apoptosis of neurons, such as semaphorin3C effects on survival and induction of neuritogenesis of rat cerebellar neurons in culture (Moreno-Flores et al., 2003). Furthermore, semaphorin4D demonstrated neurotrophic effects by potentiating neurite outgrowth in the presence of nerve growth factor (Fujioka et al., 2003). Unlike other semaphorins, acting as repulsive guidance cues, semaphorin7A promotes central and peripheral axon growth and is necessary for axon tract formation during embryonic development (Pasterkamp et al., 2003).

Accumulated evidence has shown that, besides their roles in the nervous system, semaphorins also function in a variety of other cell processes. Class 3 semaphorins are the best example. Many studies of semaphorin3A have revealed that semaphorin3A is implicated in cell survival and proliferation, cell adhesion, cell migration, bone, heart and lung formation and cytoskeleton organisation (Yazdani and Terman, 2006). Semaphorin3A moreover can inhibit VEGF-induced cyclin D1 upregulation, with the abrogation of semaphorin3A expression responsible for VEGF-driven growth of tumour cells (Catalano et al., 2004). In the immune system, semaphorin3A expressed by tumour cells inhibited activation of cytotoxic activity in mixed lymphocyte culture with tumour cells, suggesting that semaphorin3A inhibited

primary T-cell activation and contributed to the T-cell dysfunction in the tumour microenvironment (Catalano et al., 2006). Interestingly, semaphorin3A has been reported to be involved in regulating the functional activity of macrophages (Casazza et al., 2013).

Other studies have suggested that semaphorin3B acts as a tumour suppressor by inducing apoptosis in lung and breast cancer cells and by blocking the $VEGF_{165}$ autocrine activity as a survival factor produced by tumour cells (Castro-Rivera et al., 2004). Semaphorin3B has been found to be expressed at high levels in invasive and metastatic human cancers. Silencing the expression of semaphorin3B in tumour cells results in defective IL-8 transcription, leading to reduction of tumour-associated macrophage recruitment and metastatic dissemination to the lung (Rolny et al., 2008).

Some research has indicated that semaphorin3C can enhance glomerular endothelial cell proliferation, adhesion, directional migration, and tube formation *in vitro* by activating integrin phosphorylation and $VEGF_{120}$ secretion. These effects are opposite to semaphorin3A which controls vascular morphogenesis via integrin inhibition (Banu et al., 2006). Semaphorin3C is further required for normal cardiovascular patterning, and can promote crest cell migration into the proximal cardiac outflow tract using mouse models. Semaphorin3C mutant mice showed an early mortality from congenital cardiovascular defects caused by improper septation of the cardiac outflow tract (Feiner et al., 2001).

In zebrafish models, knockdown of semaphorin3D mediated by morpholino injections inhibited the proliferation of hindbrain neuroepithelial cells, and decreased migratory neural crest cells (Berndt and Hoalloran, 2006). Furthermore, semaphorin3D is important for the normal patterning of pulmonary veins, with a defect of semaphorin3D signalling leading to total anomalous pulmonary venous connection disorder in mutant mice (Degenhardt et al., 2013). Sabag et al. reported that semaphorin3D and semaphorin3E inhibit the development of tumours from U87MG glioblastoma cells, and semaphorin3D plays a role as an inhibitor of angiogenesis (Sabag et al., 2012).

In contrast, a recent study has found that semaphorin3E enhances tumour cell survival by suppressing an apoptotic pathway. Blocking of semaphorin3E inhibited tumour growth and decreased metastasis in mouse models of breast cancer (Luchino et al., 2013). However, semaphorin3E has also been identified as a potent inhibitor of tumour-induced angiogenesis (Sakurai et al., 2010), and can regulate angiogenesis via a VEGF-induced feedback mechanism (Kim et al., 2011).

Semaphorin3G has been identified as an attractive and repulsive regulator of angiogenesis. It functions further as a molecule of angiogenic endothelial cells controlling endothelial and smooth muscle cell functions in autocrine and paracrine effects (Kutschera et al., 2011).

Interestingly, accumulated evidence has revealed that semaphorins play a crucial role in immune processes including immune cell differentiation into effector and helper cells, cell migration, clonal expansion and phagocytosis (Potiron et al., 2007). For instance, semaphorin4D expressed in leucocytes can increase macrophage recruitment to glomeruli during glomerular injury in experimental crescentic glomerulonephritis (Li et al., 2009). Semaphorin4A activates T-cell-mediated immunity by increasing proliferation and stimulation of interleukin and interferon production (Kumanogoh et al., 2002). Recent studies have demonstrated that endothelial semaphorin7A enhances neutrophil transmigration across endothelial cells during hypoxia (Morote-Garcia et al., 2012). Moreover, viral semaphorinA39R expressed on neutrophils and dendritic cells inhibited phagocytosis of bacterial particles *in vitro* by inhibiting integrin-mediated adhesion. SemaphorinA89R disrupted the ability of $CD8\alpha^+$ DC to cross –prime $CD8^+$ T-cells *ex vivo* (Walzer et al., 2005).

1.1.2 Semaphorin3F

Semaphorin 3F is a member of class 3 secreted semaphorins. The class 3 semaphorin proteins are distinguished by a conserved, basic-charged domain at the C-terminus. Semaphorin3F, previously known as H SemaIV, was originally isolated from a 3p21.3 homozygous deletion in small cell lung cancer cell lines (Xiang et al., 1996). In lung, semaphorin3F is observed at the cytoplasmic membrane and in the cytoplasm (Brambilla et al., 2000), but there is currently no literature exploring localisation of semaphorin3F in neutrophil compartments. Although semaphorin3F was initially characterised as a mediator of growth cone repulsion (Luo et al., 1993), semaphorin3F has been shown to be involved in a variety of cellular processes including cell attachment, cell migration, cell proliferation, cytoskeleton organization, lung formation, synaptic transmission, neural connectivity, cell survival, apoptosis, tumour angiogenesis, tumour metastasis, tumour suppression and immune responses (Yazdani and Terman, 2006).

In a breast cancer cell line, MCF7, semaphorin3F inhibited cell attachment and spreading by loss of lamellipodia extensions, cell-cell contacts (Nasarre et al., 2003). Semaphorin3F had a dual effect, chemoattractive and mitogenic, on embryoic oligodendrocyte precursor cells, the myelin-forming cells of the central nervous system, migrating from the site of emergence toward the final destination. Moreover, in the presence of semaphorin3F, the number of migrating oligodendrocyte precursor cells increased significantly (Spassky et al., 2002). In human U87MG glioma cells and human umbilical vein endothelial cells, semaphorin3F caused rapid cytoskeletal collapse by inactivation of a small GTPase and RhoA which is essential for cytoskeleton integrity (Shimizu et al., 2008). Semaphorin3F stimulated branching morphogenesis in the developing lung that was accompanied by an increase in the incorporation of bromodeoxyuridine into DNA in the epithelial cells (Kagoshima and Ito, 2001). Sahay et al. (2005) reported that recombinant semaphorin3F modulated fast excitatory synaptic transmission by increasing frequency and amplitude of miniature EPSC in granule cells of the dentate gyrus and pyramidal neurons in the adult hippocampus. Semaphorin3F was

identified as a ligand shown to be necessary for controlling the development of amygdaloid circuitry in the CNS (Sahay et al., 2003).

Although semaphorin3F is widely expressed in most tissues, the expression of semaphorin3F is frequently downregulated in cancer cells, indicating that alterations of semaphorin3F are involved in tumourigenesis (Kusy et al., 2005). Overexpression of semaphorin3F in tumourigenic human HEK293 cells inhibited tumour-forming ability and cell development, and had a significantly lower concentration of tumour-associated blood vessels induced by $VEGF_{165}$ (Kessler et al., 2004). Many recent studies have suggested that semaphorin3F might be a tumour-suppressor gene (Xiang et al., 1996). Experimental evidence indicated that semaphorin3F can inhibit cell migration of breast cancer cells (Nasarra et al., 2005), and induce apoptosis in ovarian cancer in vivo (Xiang et al., 2002). Some studies have suggested that Semaphorin3A and Semaphorin3F inhibit migration of endothelial cells by inhibiting activation of integrins and thereby disrupting tumour angiogenesis (Guttmann-Raviv et al., 2007). Semaphorin3F is expressed in many human tumour cell lines but is downregulated in highly metastatic tumour cells and in metastases *in* vivo (Bielenberg et al., 2004). Furthermore, overexpression of semaphorin3F inhibited cell growth of a lung cancer cell line *in vitro* and participated in p53 regulated tumour angiogenesis suppression. Semaphorin3F is also a direct transcriptional target of p53 (Futamura et al., 2007).

There is currently no literature exploring the role of semaphorin3F in regulating immune cell responses. The members of class 3 semaphorins which have been identified to be involved in the immune system are semaphorin3A and semaphorin3E. Semaphorin3A has been discovered to affect macrophage function involved in tumour growth and metastasis (Casazza et al., 2013). It was also found to inhibit human monocyte and T cell migration by inhibiting their responsiveness to chemokine gradients (Delaire et al., 2001). Furthermore, human recombinant semaphorin3A or semaphorin3A-transfected COS-7 cells can inhibit primary human T-cell proliferation and cytokine production, and inhibit the activation of the cytotoxic activity in mixed lymphocyte culture (Catalano et al., 2006).

Semaphorin3E and its receptor have been reported to be necessary in the development of thymocytes by regulating migration of maturing thymocytes into the medulla through chemokine gradients (Choi et al., 2008).

1.1.3 Receptors

Plexins and neuropilins are two groups of proteins which have been characterised as the primary semaphorin receptors. Several membrane-bound semaphorins bind directly to plexins, whereas secreted class 3 semaphorins further require neuropilins as obligate coreceptors (Takahashi et al., 1999). Therefore class 3 semaphorins signal through a specific holoreceptor complex consisting of a ligand-binding (neuropilins) and a signal-transducing subunit (plexins).

Plexins are large, phylogentically conserved transmembrane proteins (~ 200 kDa) containing a divergent extracellular semaphorin domain and a conserved cytoplasmic domain unique to plexins. Invertebrate plexins are grouped in two categories, plexin A and plexin B. In contrast, vertebrate plexins are divided into four categories, A to D. Similar to semaphorins, the extracellular domain of plexins contains a sema domain, followed by three plexin-semaphorin-integrin (PSI) domains and three immunoglobulin-like, plexin and transcription factors (IPT) domains (Bork et al., 1999). The PSI domain is rich in cysteines and referred to as a MET-related sequence (MRS) or a cysteine-rich domain (CRD), and is required for protein-protein interaction, whereas the IPT domain is essential for ligand binding. The intracellular domain of plexins is highly conserved between different classes, and contains a GTPase-binding domain and a segmented GTPase-activating protein (GAP) (Figure 1.2). The cytoplasmic tail of plexins is necessary for signal transduction upon ligand binding (Kruger et al., 2005).

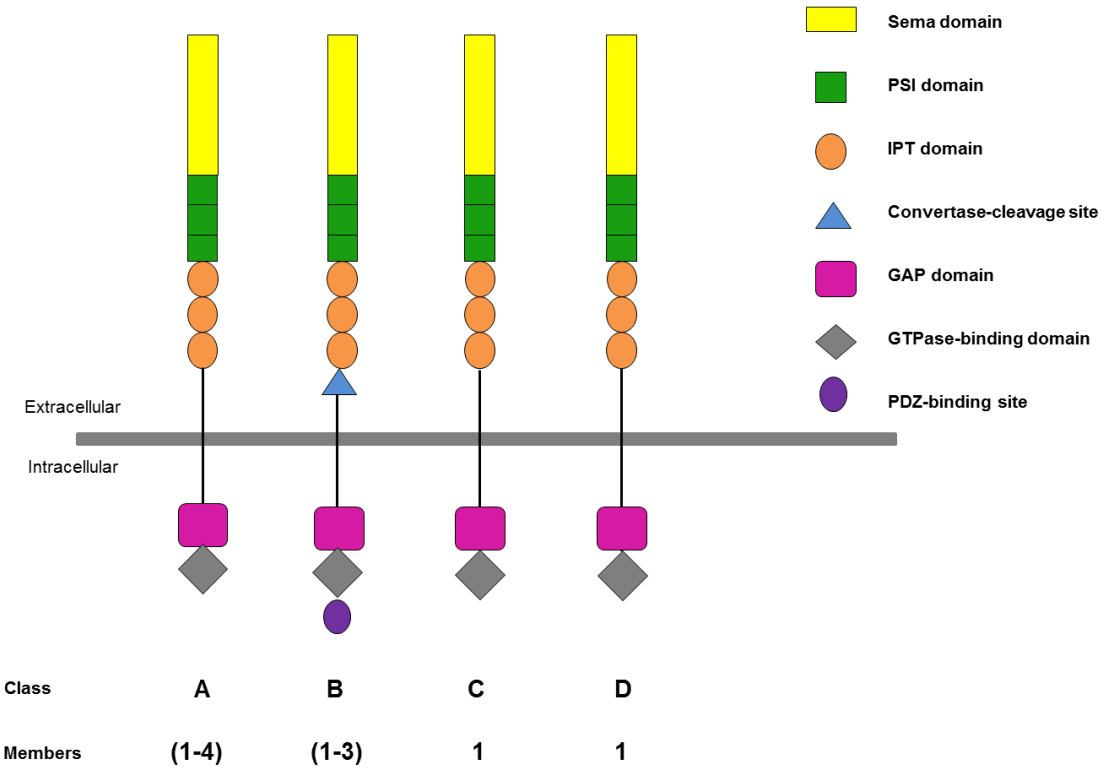

Figure 1.2: The members of the plexin family and their structure. There are four classes of plexins in vertebrates. Plexins are chracterised by a sema domain and additional domains including three plexin-semaphorin-integrin (PSI) domains, three immunoglobulin-like, plexin and transcription factors (IPT) domains, a GTPase-binding domain, and a segmented GTPase-activating protein (GAP). Class B plexins contain additional a convertase-cleavage site, and a PDZ-binding site. All proteins are shown with their N-termini to the top. This schematic was based on a diagram from Neufeld and Kessler (2008).

Neuropilins, which are found only in vertebrates, are single-spanning transmembrane glycoproteins with molecular weights of 120-130 kDa. They were first identified as an antigen of a monoclonal antibody A5 generated against the optic nerve of *Xenopus* (Takagi et al., 1991). A5 was then renamed to neuropilin based on its expression in neuropils in a specific region of the nervous system. Neuropilins are expressed on neurons, endothelial cells, epithelial cells, osteoblasts and tumour cells. Two neuropilins are classified, neuropilin-1 and neuropilin-2, that share 40% homology. The basic structure of neuropilins contains three sections; a large extracellular domain, a very short transmembrane domain, and a short cytoplasmic domain. The extracellular domain is divided into three parts; an A domain containing two repeats of CUB (complement factor C1r and C1s, Uegf (Tolloid protein) and bmp1 (Bone Morphogenetic Protein 1)) domain (a1/a2), a B domain consisting of two repeats of coagulation factors FV/VIII domain (b1/b2), and a C domain containing a MAM (Meprin, A5, μ-phosphatase) domain. The A and B extracellular domains are binding sites for neuropilin ligands. The cytoplasmic tail does not have a kinase motif, but a PDZ (PSD-95/Dlg/ZO-l) binding motif. This PDZ domain is a common protein-protein recognition module in the nervous system (Nakamura and Goshima, 2002) (Figure 1.3). Most of the class 3 semaphorins bind to one or to both of the neuropilin family. Although neuropilin was firstly identified as a direct binding receptor for class 3 semaphorins (Kolodkin et al., 1997), they alone have no ability to transduce the signals of class 3 semaphorins because of their non-kinase motif at the cytoplasmic tail. Neuropilins need therefore to form complexes with plexins (Takahashi et al., 1999). In addition, neuropilins were characterised as co-receptor for member of the vascular endothelial growth factor (VEGF) family (Soker et al., 1998), and can form complexes with other cell-surface receptors such as β1-integrin (Fukasawa et al., 2007) and transforming growth factor- β1 (TGF- β1) (Glinka et al., 2008).

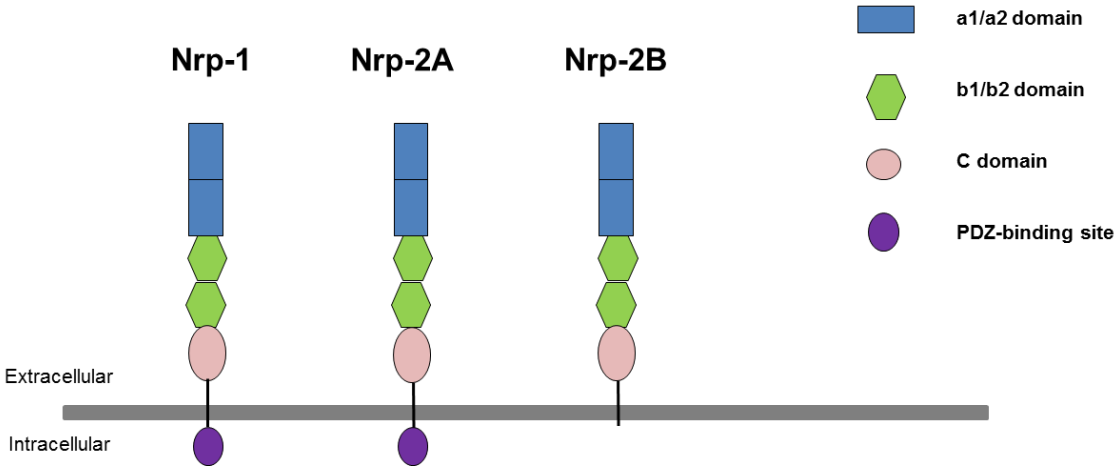

Figure 1.3: The neuropilin structure. Neuropilins consist of three extracellular domains (a1/a2, b1/b1, and c), a very short transmembrane domain, and a short cytoplasmic domain. Neuropil-1 and neuropilin-2A contain additional a PDZ-binding site at the cytoplasmic tail. All proteins are shown with their N-termini to the top. This schematic was based on a diagram from Neufeld and Kessler (2008).

Accumulated evidence has indicated that neuropilin-2 and class A plexins form a complex for semaphorin3F signalling. Chen et al. has reported that neuropilin-1 binds semaphorin3A with higher affinity than semaphorin3F, but neuropilin-2 binds semaphorin3F only, and the affinity of semaphorin3F for neuropilin-2 is ten times greater than for neuropilin-1 (Chen et al., 1997). Furthermore, semaphorin3F is the ligand for neuropilin-2-mediated axon guidance *in vivo* that plays a critical role in limbic and peripheral nervous system circuitry (Sahay et al., 2003). Experiments in metastatic human melanoma demonstrated that semaphorin3F expressed by tumour cells generated chemorepulsion of vascular and lymphatic endothelial cells expressing neuropilin-2 in a manner similar to semaphorin-induced axon repulsion. This repulsion was inhibited by neuropilin-2 RNA interference (Bielenberg et al., 2004). Studies of tumour angiogenesis showed that semaphorin3F signals through neuropilin-2 to inhibit $VEGF_{165}$-induced proliferation of human umbilical vein endothelial cells, as well as VEGF-induced phosphorylation of extracellular signal which led to inhibition of tumour angiogenesis (Kessler et al., 2004). Moreover, loss of neuropilin-2 expression in tumour cells inhibited semaphorin3F-dependent activities including inactivation of RhoA, depolymerisation of F-actin and inhibition of tumour and endothelial cells (Coma et al., 2011). Furthermore, it has been shown that, besides neuropilin-2, different members of class A plexins function as co-receptors for semaphorin3F. Takahashi et al. used a COS-7 cell contraction assay demonstrating that semaphorin3F was unable to induce the contraction of neuropilin-1/plexin A1- or neuropilin-1/plexin A2-expressing COS-7 cells, but could generate the contraction of neuropilin-2/plexin A1- or neuropilin-2/plexin A2-expressing COS-7 cells ((Takahashi and Strittmatter, 2001) Other observations revealed that semaphorin3F signals repulsion primarily through the action of plexin A3 (Yaron et al., 2005). Nervous cell migration such as oligodendrocyte precursor cell migration mediated by semaphorin3F decreased significantly in the absence of neuropilin-2 and plexin A3 (Xiang et al., 2012). In ovarian cancer cell lines, the expression of semaphorin3F and plexin A3 was markedly decreased, whereas plexin A1 expression was not altered when compared to normal human ovarian epithelial cells (Joseph et al., 2010).

1.1.4 Signalling

Whilst plexins are the most prominent semaphorin receptors, semaphorin signalling requires co-receptors forming as holoreceptor complexes with plexins. These co-receptors can act as ligand-binding subunits such as neuropilins, or modulatory subunits such as Immunoglobulin superfamily cell adhesion molecules (IgCAMs) (Tran et al., 2007), and receptor tyrosine kinases (RTKs) e.g. VEGFR2 (Toyofuku et al., 2004).

Recent studies have shown that class 3 semaphorins serve as a key regulator of cellular processes including cell motility and migration of endothelial and tumour cells, tumour growth and angiogenesis, cell survival, proliferation and apoptosis. Class 3 semaphorins mediate their activities through plexin A1-A4 and neuropilins, with the exception of semaphorin3E, which binds directly to plexin D1 without the requirement for neuropilins (Gaur et al., 2009). In addition, some class 3 semaphorin signalling needs other molecules as co-receptors, for instance, semaphorin3A binds to neuropilin-1 which assembles plexin A1 as a neuropilin-1/plexin A1 receptor complex. This complex further requires a neuron cell adhesion molecule L1 (L1CAM) for specific repulsion or attraction of the axon guidance actions (Castellani et al., 2000). One of the best known intracellular signalling events downstream of class 3 semaphorins is inhibition of integrin activity by semaphorin3A. Semaphorin3A mediates the axonal repulsion via direct binding of plexin A1 and FERM domain-containing guanine nucleotide exchange factor (GEF) FARP2. Once semaphorin3A binds to neuropilin-1, FARP2 dissociates from plexin A1 resulting in activation of Rac1 activity and recruitment of Rnd1 to plexin A1 (Toyofuku et al., 2005). Active Rac1 leads to regulation of actin dynamics, enhancing axon repulsion. Rnd1/plexin A1 interaction stimulates plexin A1/RasGAP (GTPase-activating protein) activity resulting in inactivation of R-Ras and PI3K signalling. Thus, integrin ligand-binding activity is inhibited (Zhou et al., 2008) (Figure 1.4).

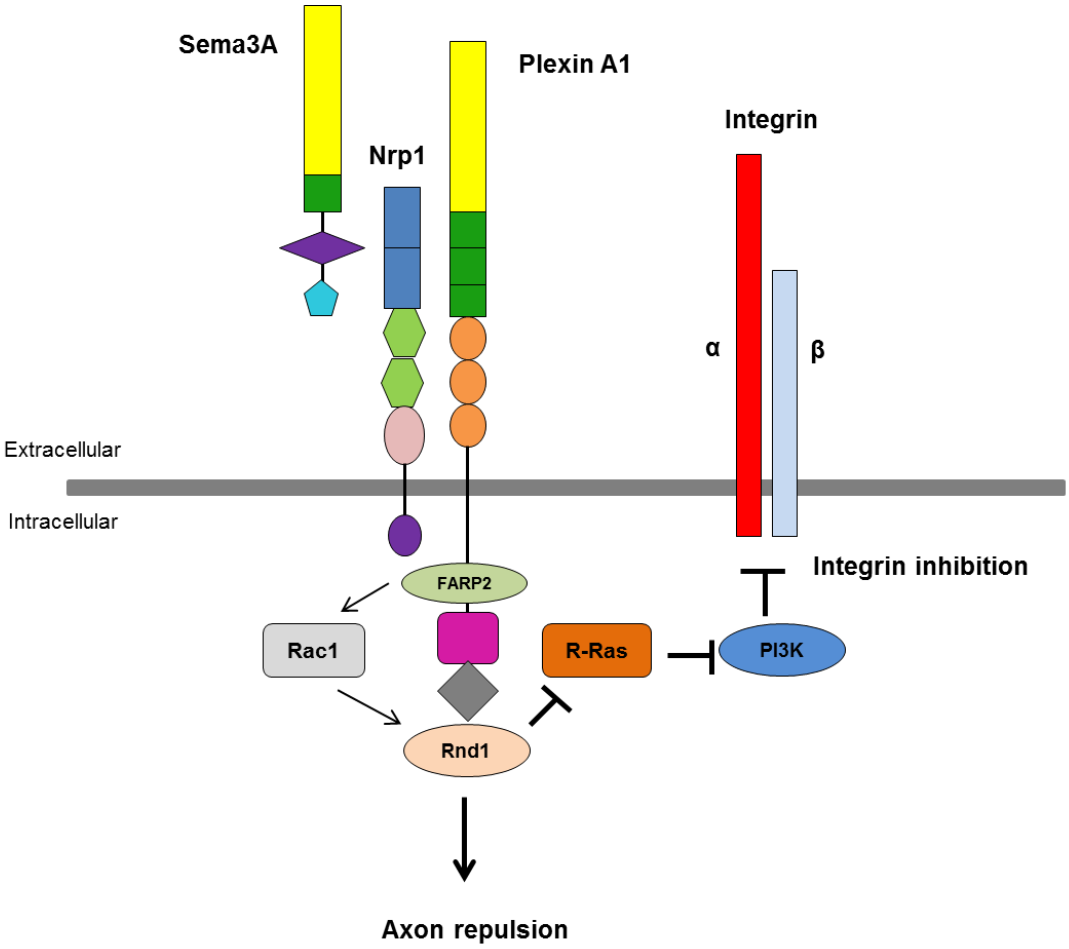

Figure 1.4: Integrin inhibition by semaphorin3A signaling. Semaphorin3A binds neuropilin-1 to assemble a neuropilin-1-plexin A1receptor complex. This binding stimulates FERM domain-containing guanine nucleotide exchange factor (GEF) (FARP2) dissociation from the plexin A1. Dissociated FARP2 activates Rac1 and recruitment of Rnd1 to plexin A1. Active Rac1 leads to regulation of actin dynamics enhancing axon repulsion. Rnd1/plexin A1 interaction stimulates plexin A1/RasGAP (GTPase-activating protein) activity resulting in inactivation of R-Ras and PI3K signalling. Thus, integrin ligand-binding activity is inhibited. This schematic was based on a diagram from Toyofuku et al. (2005) and Zhou et al. (2008).

As previously mentioned, class A plexins form a complex with neuropilin-2 to generate a functional semaphorin3F receptor in which neuropilin-2 acts as semaphorin3F binding element, and plexin A as signal transducer. It has been proposed that semaphorin3F functions as a tumour suppressor because of its downregulation of expression in tumours (Bielenberg et al., 2004). Semaphorin3F can cause loss of activated α5β3-integrin Brambilla et al., 2000), downregulation of integrin-linked kinase activity (ILK), and reduction of cell adhesion to extracellular matrix (ECM) ((Kusy et al., 2005, Potiron et al., 2007). Potiron et al. reported that semaphorin3F inhibited ILK activity in H157 lung cancer cells leading to decreased extracellular signal-regulated protein kinase 1 and 2 (ERK1/2) signalling. In parallel, semaphorin3F decreased protein kinase B or AKT and signal transducer and activator of transcription 3 (STAT3) phosphorylation in H157 cells independent from ILK-ERK1/2 signalling. As a consequence, semaphorin3F inhibited tumour growth and formation (Potiron et al., 2007). Consistently, studies of growth cone collapse in sympathetic neurons showed that semaphorin3F suppressed neurotrophin nerve growth factor (NGF)-induced activity resulting in inhibition of PI3K-AKT and mitogen-activated protein kinase kinase (MEK)-ERK pathway (Atwal et al., 2003) (Figure 1.5A).

Accumulated evidence has indicated that semaphorin3F can inhibit tumour cell migration. One mechanism by which semaphorin3F inhibits cell migration is through inactivation of RhoA. Semaphorin3F forms a complex with neuropilin-2 and plexin A1 leading to recruitment of ABL2 tyrosine kinase (v-Abl Abelson murine leukemia viral oncogene homolog 2) and p190RhoGAP to the cytoplasmic tail of plexin A1. ABL2 phosphorylates then the p190RhoGAP which inactivates RhoA, followed by inactivation of Rho kinase. As a result, cofilin, an actin depolymerisation factor, remains active, and promotes F-actin cytoskeleton depolymerisation. The migration and contractility of this cell are consequently inhibited. Moreover, semaphorin3F inactivates the small GTPase Rac1, a regulator of lamellipodia formation at the leading edge during migration, suggesting that semaphorin3F contributes to the regulation of cell migration (Shimizu et al., 2008) (Figure 1.5B).

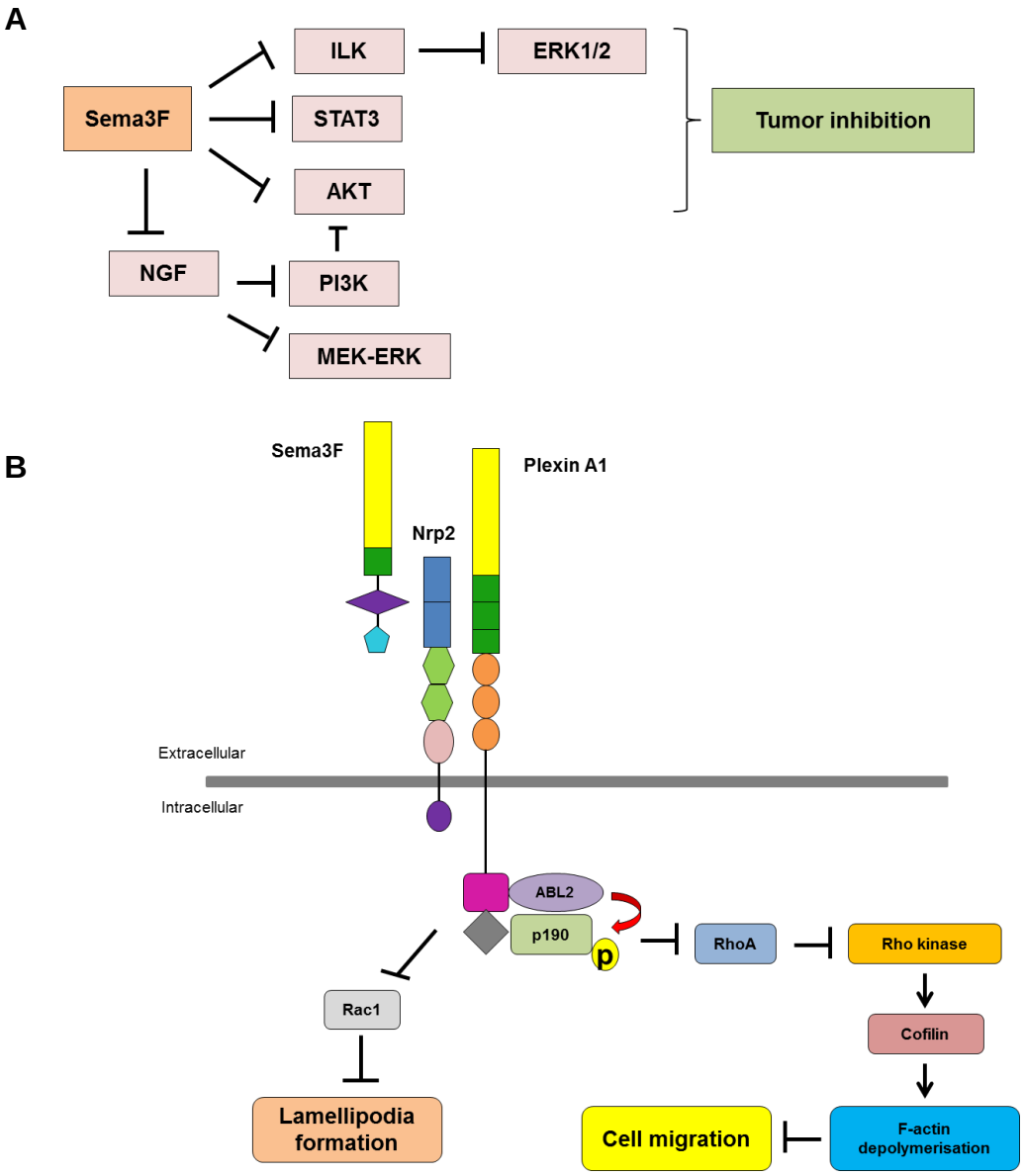

Figure 1.5: Semaphorin3F signaling. (A) Signaling pathways involved in semaphorin3F signaling. Semaphorin3F can inhibit (Integrin-linked kinase) ILK activity leading to decreased extracellular signal-regulated protein kinase 1 and 2 (ERK1/2) signalling. In parallel, semaphorin3F decreases protein kinase B or AKT and signal transducer and activator of transcription3 (STAT3) phosphorylation. As a consequence, semaphorin3F inhibits tumour progression. Consistently, studies of growth cone collapse in sympathetic neurons showed that semaphorin3F suppresses neurotrophin nerve growth factor (NGF)-induced activity resulting in inhibition of PI3K-AKT and mitogen-activated protein kinase kinase (MEK)-ERK pathway. This schematic was based on a diagram from Atwal et al. (2003) and Potiron et al. (2007). (B) Cell migration inhibition by semaphorin3F signalling. Semaphorin3F forms a complex with neuropilin-2 and plexin A1 leading to recruitment of ABL2 tyrosine kinase (v-Abl Abelson murine leukemia viral oncogene homolog 2) and p190RhoGAP to the cytoplasmic tail of plexin A1. ABL2 phosphorylates then the p190RhoGAP which inactivates RhoA, followed by inactivation of Rho kinase. As a result, cofilin, an actin depolymerisation factor, remains active, and promotes F-actin cytoskeleton depolymerisation. The migration of this cell is consequently inhibited. Moreover, semaphorin3F inactivates small GTPase Rac1, a regulator of lamellipodia formation at the leading edge during migration. This schematic was based on a diagram from Shimizu et al. (2008).

A further mechanism through which semaphorin3F inhibits tumour angiogenesis is by antagonising VEGF-mediated signalling. Both semaphorin3F and VEGF have same ligands. However, many studies have indicated that in contrast to semaphorin3A, which competes with $VEGF_{165}$ for binding to neuropilin-1, semaphorin3F does not compete with $VEGF_{165}$ for binding to neuropilin-2 (Kessler et al., 2004). Neuropilin-2 is the co-receptor for both semaphorin3F and the VEGF family of angiogenesis factors including VEGF-A (145 and 165 isoforms) VEFG-C (Gluzman-Poltorak et al., 2000, Xu et al., 2010). In principle, VEGF family members mediate their downstream effects by binding to neuropilins and forming complexes with VEGF receptors (VEGFR) analogous to the class 3 semaphorin-neuropilin-plexin complex (Soker et al., 1998). Semaphorin3F has a higher binding affinity to neuropilin-2, which functions as a splice variant specific VEGF receptor that binds VEGF165, and therefore can signal though the neuropilin-2 to inhibit $VEGF_{165}$ in angiogenesis (Serini et al., 2009). Kessler et al. reported that semaphorin3F inhibited VEGF165 and basic fibroblast growth factor (bFGF)-induced phosphorylation of ERK1/2 signaling, indicating that semaphorin3F acts as an inhibitor of angiogenesis (Kessler et al., 2004).

Nowadays, semaphorin3F has emerging roles in tumour progression and cell migration. It is interesting to consider whether semaphorin3F has other functions in cells in the immune system. In this study, the role of semaphorin3F in neutrophil function in inflammation was investigated.

1.2 Neutrophils

1.2.1 Overview of neutrophils

Polymorphonuclear neutrophils (PMNs) are a subdivision of myeloid derived granulocytes, representing the most abundant (50 to 70 percent of the total) circulating leukocytes and 95 percent of granulocytes in mammals. Neutrophils form an important part of the innate immune system, and are terminally differentiated cells rich in cytoplasmic granules which contain various enzyme components, including myeloperoxidase, serine proteases, neutrophil elastase, cathepsin and gelatinase, and antimicrobial proteins, including bactericidal/permeability increasing protein (BPI), defensins, lactoferrin and cathelicidin. Neutrophils release their granule contents during phagocytosis creating a highly toxic microenvironment (Schmidt et al., 1989).

In the circulation, neutrophils normally have a very short half-life between of 8 to 20 hours. This increases several fold once neutrophils arrive at inflamed or infected tissues where oxygen is typically rare (Edwards, 1994). Neutrophils are the first defensive cell type to be recruited to sites of inflammation, where they remove pathogens through phagocytosis. They migrate through the blood vessels, then through interstitial tissue, following chemical signals in a process called chemotaxis. Neutrophils and cells in the inflamed area express and release cytokines, which in turn have effects on neutrophil recruitment and function in inflammatory reactions. For instance, IL-1β is involved in the local recruitment of neutrophils to inflamed sites. TNF-α further promotes neutrophil migration and plays an important role in microbial defence and neutrophil apoptosis (Butterfield et al., 2006).

Although neutrophils play a crucial role in host defence against infectious agents such as bacteria, fungi, protozoa, viruses, virally infected cells and tumour cells (Ratcliffe et al., 1988), paradoxically, they also contribute to the pathogenesis of a number of human diseases (John, 1944). In these conditions, host tissue damage occurs through neutrophil-released tissue-damaging molecules such as protease during the killing of microbes.

1.2.2 Neutrophil priming

Neutrophil priming was described by McPhail as the ability of a primary agonist, typically at a substimulatory concentration, to enhance superoxide production triggered by a second stimulus (McPhail et al., 1984). Resting neutrophils can become primed by cytokines, chemokines, growth factors and bacterial products, resulting in 'primed' or 'activated' neutrophils, which recruit towards the site of infection or inflammation (Hallett and Lloyds, 1995). Priming occurs via two separate mechanisms. Priming agents can cause priming as a consequence of rapid mobilisation of secretory vesicles and secretion of cytokines, or by the activation of transcription factors that trigger the expression of cytokines or plasma membrane receptors, which then in turn regulate neutrophil function and lifespan (Wright et al., 2010).

1.2.3 Neutrophil recruitment

The recruitment of activated neutrophils from the circulation to the site of inflammation, via diapedesis, is regulated by selectins, integrin and adhesion molecules, cytokines, chemokines and products of invading microorganisms. Neutrophil rolling in blood vessels is mediated by selectins. In this, L-selectin expressed on the surface of neutrophils binds to ligands expressed on the surface of endothelial cells; E- and P-selectin, to facilitate a loose interaction, known as tethering, between neutrophils and endothelial cells leading to neutrophil rolling along the endothelium, followed by rolling arrest. This step is mediated by binding of neutrophil receptors to chemoattractants such as IL-8 or *N*-formylated peptides from bacteria (Kobayashi et al., 2005), and by adhesion molecules such as β1 (VLA-4; very late antigen-4) - and β2-integrins (LFA-1; Lymphocyte function antigen, or Mac-1; macrophage antigen-1) (Ley, 2002). Once high-affinity adhesion to the endothelium occurs, neutrophils migrate into the tissue through the junctions between neighbouring endothelial cells, a process known as paracellular migration, using surface ligands including platelet endothelial cell adhesion molecule-1(PECAM-1), intracellular adhesion molecule-1 (ICAM-1) and proteins of the

junctional adhesion molecule (JAM) family (Woodfin et al., 2009). They migrate then towards inflamed tissue along a chemotactic gradient. Neutrophils are directed by number of different chemoattractants, including N-formylmethionyl-leucyl-phenylalanine (fMLP), IL-8, and complement component 5a (C5a). These chemoattractants induce cellular polarisation and formation of actin-rich pseudopodia at the leading edge of the cells allowing neutrophils to migrate to their destination (Servant et al., 2000).

1.2.4 Neutrophil phagocytosis and respiratory burst

At the site of infection or inflammation, neutrophils bind and eliminate invading microorganisms by the process known as phagocytosis. Neutrophils can recognise pathogen-derived molecules including lipopolysaccharide (LPS), peptidoglycan or lipoporteins through their cell surface receptors such as Toll-like receptors (TLRs) and CD14 (Akira and Takeda, 2004). Phagocytosis is facilitated by specific opsonin (immunoglobulin G (IgG)) and non-specific opsonin (complement components). These opsonins bind then to receptors on neutrophils through Fc fragment of IgG, and complement C3b fragment receptors (Gomez et al., 1994). This binding triggers the formation of phagosomes, and release of lysis products depending on cytoplasmic granule types. Primary or azurophilic granules contain myeloperoxidase, bacterial permeability-increasing protein (BPI), α-defensins, elastase and cathepsin G. Scondary or specific granules contain alkaline phosphatase, lysozyme, NADH oxidase, lactoferrin and cathelicidin, whereas tertiary granules have cathepsin and gelatinase (Borregaard and Cowland, 1997). As a result, pathogens are killed at the site of infection or inflammation.

During phagocytosis, neutrophils undergo an increase in glucose and oxygen consumption known as the respiratory burst. Neutrophils begin to produce large quantities of superoxide (O_2^-), which is then catalysed by NADPH oxidase. NADPH oxidase transfers electrons from cytosolic NADPH across the plasma membrane to oxygen leading to formation of hydrogen peroxide

(H_2O_2) and reactive oxygen species (ROS), including hypochlorous acid (HOCl), singlet oxygen ($^1O_2$) and hydroxyl radical (OH^-). Superoxide and its secondary products accumulate within the phagosome, or in the extracellular environment when NADPH oxidase has been recruited to the neutrophil plasma membrane, followed by destructing of pathogens (Clark, 1999). However, the products of this process can also cause host tissue damage.

1.2.5 Neutrophil apoptosis

Once the pathogens are destroyed, neutrophils are thought to undergo apoptosis. Apoptosis, or programmed cell death, is essential to maintain the balance of cellular homeostasis under physiological conditions (Cartwright et al., 1964). Normally, aged neutrophils in the circulation without activation die by constitutive or spontaneous apoptosis after 8-20 hours (Cartwright et al., 1964), whereas neutrophils at the site of inflammation can be influenced by survival or death signals from the inflammatory environment. Here, neutrophils' life span is prolonged by pro-inflammatory mediators, including granulocyte macrophage colony-stimulating factor (GM-CSF), IL-1β, IL-6 and IL-8, or bacterial-derived products such as LPS. Conversely, pro-apoptotic stimuli, including Tumour Necrosis Factor-α (TNF-α), TNF-related apoptosis-inducing ligand (TRAIL) and Fas ligand, shorten their life span (Lee et al., 1993) (Renshaw et al., 2003). Apoptosis renders neutrophils unresponsive to extracellular stimuli and leads to external "eat-me" signals, so that neutrophils can be recognised and removed by macrophages through phagocytosis (Savill et al., 1989). However, macrophages can promote neutrophil apoptosis at the inflamed site by releasing Fas ligand and triggering Fas-mediated neutrophil apoptosis (Brown et al., 1999). Furthermore, macrophages induce apoptosis of neighbouring neutrophils through cell-cell contact-dependent mechanism involving integrin-ligand binding (Meszaros et al., 2000). Many studies suggest that enhanced neutrophil survival occurs during the early stage of inflammation promoting the clearance of invading organisms, followed by downregulation of pro-inflammatory capacity towards resolution of inflammation (Kobayashi et al.,

2003). Since neutrophils are the most abundant type of leukocyte with potent cytotoxic components, appropriate neutrophil apoptosis provides a balance between neutrophil defense functions and their clearance. Loynes et al. demonstrated that pharmacological compounds, such as pyocyanin and roscovitine, which accelerate neutrophil apoptosis, reduced neutrophil numbers at the site of injury in zebrafish models. This led to acceleration of inflammation resolution (Loynes et al., 2010). Thus, the regulation of neutrophil apoptosis is important for prevention of tissue damage and trauma associated with inflammatory disease, and plays a crucial role in the resolution of inflammation.

1.2.6 Neutrophil reverse migration

Recent evidence has indicated that, in addition to neutrophil apoptosis, movement of neutrophils away from the site of inflammation, defined as reverse migration, is an alternative mechanism in inflammation resolution. *In vivo* a zebrafish model was the first demonstration that neutrophil reverse migration was largely responsible for clearance of neutrophils from inflamed sites. Mathias et al. had previously shown that neutrophils undergo retrograde chemotaxis back toward the vasculature after rapid chemotaxis to the wound site during inflammation (Mathias et al., 2006). More recently, work from Elks et al. has revealed that hypoxia-inducible factor-1α (HIF-1α) delays inflammation resolution by reducing neutrophil reverse migration in zebrafish (Elks et al., 2011). Molecules with pro-resolution activity such as Tanshinone IIA can also promote reverse migration of neutrophils resulting in facilitation of inflammation resolution (Robertson et al., 2014). Notably, a similar observation was recently made in a mammalian system. Woodfin et al. showed that mice with junctional adhesion molecule C (JAM-C)-deficient endothelial cells displayed an increase in reverse transendothelial migration of neutrophils compared to WT in intrascrotal inflammation induced by ischemia-reperfusion injury. However, this neutrophil population was also found in the lungs, suggesting that these transendothelial migrating neutrophils might enhance inflammation at sites distant from the actual injury

(Woodfin et al., 2011). Moreover, studies of rheumatoid arthritis showed that in patients with rheumatoid arthritis, 1-2% of their peripheral blood neutrophils were reverse-transmigrating neutrophils which were more resistant to apoptosis (Buckley et al., 2006).

Thus neutrophil reverse migration may function as an alternative mechanism removing activated neutrophils from the site of inflammation. This can promote inflammation resolution, and may prevent the tissue damage from cytotoxic molecules secreted by activated neutrophils at the site of inflammation. However, it is possible that reverse migration of neutrophils back to the circulation might disseminate inflammation into other organs, retrieve antigen from extravascular tissue, and influence the adaptive immune response.

1.2.7 Neutrophil-mediated inflammatory diseases

Although neutrophil recruitment to the site of infection or inflammation is essential for host defense, neutrophil recruitment and inflammatory responses may be detrimental. As mentioned previously, primed or activated neutrophils release cytotoxic molecules such as proteinases, and reactive oxygen species (ROS), to kill invading organisms. Uncontrolled or impaired neutrophil activation can thus lead to persisting tissue damage from these cytotoxic molecules. In addition, activated neutrophils synthesise and secrete immune cell-stimulating agents including cytokines and chemokines such as TNF-α, IL-1β, IL-8, MIP-1α and IP-10, which can activate other neutrophils and other cells of the immune system, and prolong inflammation (Helen et al., 2010). Thus, the termination of inflammation is crucial and must be strictly regulated to prevent excessive inflammatory responses towards chronicity. Unresolved neutrophilic inflammation caused by neutrophil persistence has been associated with a wide variety of inflammatory diseases, including chronic obstructive pulmonary disease (COPD) (Quint and Wedzicha, 2007), inflammatory bowel disease (IBD) (Taylor and Colgan, 2007), rheumatoid arthritis (Hallett et al., 2008) and cystic fibrosis (Elizur *et*

al., 2008) (Figure 1.6). As observed in rheumatoid arthritis, neutrophils are present in high numbers in the synovial tissues and tend to persist in synovial fluid (Cascao et al., 2009). Chakravati et al. also reported that under inflammatory conditions, neutrophils have the potential of persistence for more than 72 hours, in contrast to the short circulating half-life of neutrophils (Chakravati et al., 2008).

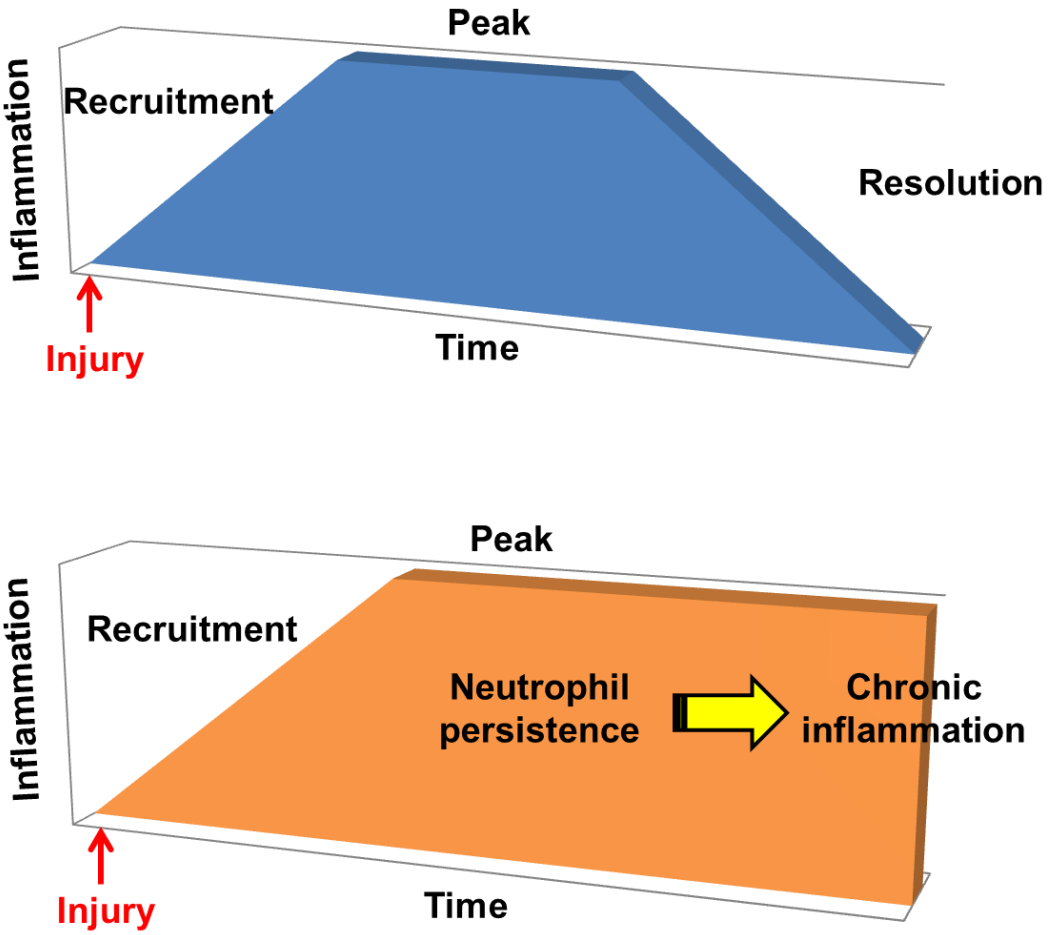

Figure 1.6: Neutrophilic inflammation. A diagram showing the phases of neutrophilic inflammation. After an injurious stimulus, neutrophils are recruited to the site of injury and perform their destructive capacity to kill invading pathogens. Moreover, activated neutrophils release cytokines and chemokines modulating inflammation and other immune cells. In the top picture, the acute inflammatory response is resolved by neutrophil clearance mostly by phagocytosis of apoptotic neutrophils by macrophages, followed by the restoration of normal tissue homeostasis. In the bottom picture, dysregulation of inflammation resolution caused by persistence of neutrophils at the site of injury leads to chronic inflammation. This schematic was based on a diagram from Serhan et al. (2007).

1.3 Hypoxia

1.3.1 Hypoxia and its regulation

The microenvironment of inflamed tissue and tumours is characterised by low levels of oxygen, described as hypoxia (Frede et al., 2007). Oxygen delivery is absolutely critical for the survival of mammalian cells. Insufficient oxygen availability in tissue mediated by pathogenic conditions can lead to an imbalance of oxygen homeostasis, followed by cellular dysfunction. Therefore, mammals have developed sophisticated mechanisms to sense oxygen levels and execute an appropriate response such as adaptive changes in gene expression that either enhance oxygen delivery or promote survival in a hypoxic environment. A pathway mediated by oxygen-dependent posttranslational hydroxylation of HIF plays a crucial role in this process (Schofield and Ratcliffe, 2004).

HIF (Hypoxia Inducible Factor) is a heterodimeric transcription factor, a heterodimer of bHLH-PAS proteins, and consists of two basic helix-loop-helix proteins, namely the HIFα-subunit and HIFβ-subunit. This HIFα/β dimer binds DNA at a core DNA motif (G/ACGTG) located in hypoxia response elements (HREs) (Figure 1.7). There are three closely related forms of HIFα proteins (HIF-1α, HIF-2α, HIF-3α) in higher organisms, but only HIF-1α and HIF-2α show a similar regulatory manner and have been most extensively researched (Hogenesch et al., 1997). HIF plays a central role in the transcriptional response to changes in oxygen availability. Due to HIF-directed transcriptional activation, a series of target genes involved in systemic responses to hypoxic environment and in cellular responses is transcribed. HIFα is an unstable subunit highly induced by hypoxia; by contrast, HIFβ is a stable, constitutively expressed nuclear protein (Kaelin and Ratcliffe, 2008).

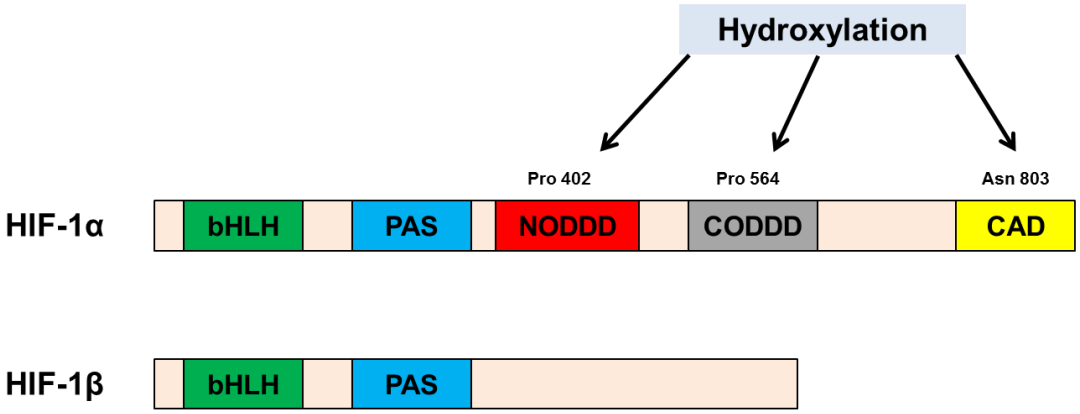

Figure 1.7: The domain structure of HIF-1α and HIF-1β. A schematic showing of the structures of HIF-1α and HIF-1β subunits. HIF-1α subunit is composed of a bHLH (basic helix-loop-helix) domain, PAS (period-ARNT-sim) domain, NODDD (the amino-terminal oxygen-dependent degradation domain), carboxy-terminal oxygen-dependent degradation domain (CODDD), and CAD (the carboxy-terminal activation domain). The prolyl hydroxylase (PHD) enzymes can hydroxylate prolyl (Pro) residues, whereas factor inhibiting-HIF (FIH) hydroxylates asparaginyl (Asn) on HIF-1α. HIF-1β subunit contains a bHLH (basic helix-loop-helix) domain and a PAS (period-ARNT-sim) domain. This schematic was based on a diagram from Schofield and Ratcliffe (2004).

Members of the prolyl hydroxylase domain (PHD) family play a pivotal role in regulation of HIFα stability. Under normoxic conditions, HIFα are hydroxylated at two highly conserved prolyl residues (Pro-402 and Pro-564) in the amino-terminal oxygen-dependent degradation domain (NODDD) and the carboxy-terminal oxygen-dependent degradation domain (CODDD) by PHD. As a result, the specific prolyl hydroxylation creates a binding site for the von Hippel-Lindau tumour suppressor protein (pVHL) which is the recognition component of an ubiquitin ligase complex. Due to this post-translational modification, HIFα becomes polyubiquitylated and terminated by proteasomal degradation. In hypoxia, in contrast, the prolyl hydroxylation is inhibited. Thus, the HIFα subunit is not degraded by pVHL-mediated destruction which enables HIFα to accumulate and dimerize with a HIFβ subunit. This heterodimer can therefore transcriptionally activate several hundred target genes involved in adaptation to low oxygen conditions (Kaelin and Ratcliffe, 2008).

Four PHD proteins, known as prolyl hydroxylase domain, (PHD1, PHD2, PHD3 and P4H-TM) have been identified to date. PHDs belong to the Fe(II) and 2-oxoglutarate-dependent oxygenase superfamily with the ability to catalyse HIF prolyl hydroxylation which is strongly dependent on oxygen because of an absolute requirement for molecular oxygen as a co-substrate (Koivunen et al., 2007). Whilst all PHDs have closely related domains, only PHD2 has been suggested to be the primary HIF prolyl hydroxylase for normoxic HIF-1α levels. Experimental evidence has shown that specific silencing of PHD2 is sufficient to stabilize HIF-1α steady-state levels in normoxia in all the human cells, fully protect HIF-1α degradation upon re-oxygenation of hypoxia-stressed cells, and trigger HIF-1α nuclear accumulation and HIF-dependent transcriptional activation in normoxia (Berra et al., 2003). Interestingly, many studies have shown that the PHD enzymes, especially PHD2 and PHD3, but not PHD1, are induced to a high level in response to inflammatory stimuli and hypoxia *in vivo* and *in vitro*, providing an HIF-dependent auto-regulatory mechanism driven by the oxygen tension (Bruick and McKnight, 2001).

In addition to the prolyl hydroxylation, the HIFα subunit is also hydroxylated at a specific conserved asparaginyl residue. This asparagine is hydroxylated by factor inhibiting HIF (FIH); an Fe(II)- and 2-oxoglutarate-dependent dioxygenase (like the PHD family members). Asparaginyl hydroxylation blocks the protein-protein interaction between HIFα and the transcriptional coactivator p300 leading to inactivation of HIF transcriptional activity. Therefore, asparaginyl hydroxylation provides a second oxygen-regulated mechanism by inhibition of the activity of HIFα proteins that escape the prolyl hydroxylation/degradation pathway (Schofield and Ratcliffe, 2004).

The association of angiogenesis with chronic inflammation is becoming clearer. An inflammatory state can promote angiogenesis, and angiogenesis can facilitate chronic inflammation. At sites of inflammation where oxygen is typically scarce, VEGF is a part of the hypoxic response. VEGF is an endothelial cell-specific growth factor; a multifunctional cytokine; that plays a key role in vasculogenesis and angiogenesis. Due to its effect on stimulating vessel hyperpermeability and endothelial cell proliferation is VEGF involved in both physiological and pathological angiogenesis. VEGF contains the conserved consensus sequence for the hypoxic response element (HRE) within its promoter. This highly conserved HRE is recognized by hypoxia inducible factor (HIF), which has been identified as a key regulator of VEGF expression. Thus, HIF accumulation causes an increase in VEGF that is postulated to drive angiogenesis resulting in raised oxygen delivery to the inflamed sites. Moreover, new blood vessels can maintain the chronic inflammatory state by transporting inflammatory cells to the site of inflammation (Forsythe et al., 1996).

The VEGF family possesses several members, consisting VEGF-A, -B, -C, -D, and placental growth factor (PIGF-1, -2), with VEGF-A often simply referred to as VEGF. VEGF-A has four relatively abundant isoforms (206, 189, 165 and 121 amino acids in human) resulting from alternative splicing. $VEGF_{165}$ is the predominant isoform and is soluble. VEGF can bind multiple receptors. There are three major receptors, namely VEGFR1, -R2 and –R3, which are characterized by protein-tyrosine kinase activity. As previously described, VEGF also binds to the same receptors for the class 3

semaphorin, neuropilins (NRP) 1 and 2. NRP1 interacts only with $VEGF_{165}$, whereas NRP2 binds $VEGF_{165}$ and $VEGF_{145}$. To induce intracellular signalling, VEGF and its receptor necessarily complex with VEGF receptor and/or plexins that contain a kinase domain (Ferrara and Davis-Smyth, 1997).

Inflammatory cells, such as neutrophils, also contribute to angiogenesis. Neutrophils recently have been shown to express VEGF, and are a potential cell source of VEGF (Scapini et al, 1999). Interestingly, using a model of corneal angiogenesis demonstrated that neutrophil depletion significantly suppressed corneal angiogenesis resulting in reduction of microvessel density and neovascularisation. Neutrophils can also causally promote inflammatory angiogenesis via release of preformed VEGF *in vivo (*Gong and Koh, 2010).

1.3.2 Hypoxia and neutrophilic inflammation

The crucially important cellular events of the innate immune response during inflammation are leukocyte extravasation to sites of infection by means of chemoattractants, cell adhesion molecules, and especially, oxygen gradient. An oxygen gradient is a low oxygen signal for neutrophils to increase their extravasation through endothelial cells to sites of inflammation characterized by hypoxia. The hypoxic microenvironments also signal neutrophils to adhere to endothelial cells, and increase the adhesive properties of endothelial cells for neutrophils so that neutrophils effectively infiltrate into the injured tissues (Figure 1.8) (Ginis et al., 1993) (Borroni et al., 2009).

At inflammatory sites characterised by low levels of oxygen and glucose, neutrophils have adapted to provide their antimicrobicidal function. Hypoxia, in turn, prolongs neutrophil life span through delaying apoptosis (Walmsley et al., 2005). This evidence is consistent with some observations that hypoxia can cause a dramatic decrease in neutrophil apoptosis *in vitro* (Hannah et al., 1995). Additionally, hypoxia can regulate neutrophil apoptosis *in vivo* in rheumatoid synovial fluid (Cross et al., 2006). As a result, neutrophils have

an ability to survive in hypoxia and become rescued from the constitutive apoptotic pathway.

In particular, HIF-1α has been identified as a critical regulator of neutrophil survial under hypoxic condition at sites of inflammation. Walmsley et al. reported that in human and murine neutrophils, hypoxia caused an inhibition of neutrophil apoptosis mediated by HIF-1α –dependent NF-ϰB activity (Walmsley et al., 2005). Similarly, in a zebrafish inflammation model, activation of HIF-1α decreased neutrophil apoptosis (Elks et al., 2011). Besides HIF-1α, Thompson et al. revealed that HIF-2α overexpression also reduced neutrophil apoptosis both in humans, and in a zebrafish model (Thompson et al., 2013).

Furthermore, accumulated evidence has shown that hypoxia plays a role in key neutrophil functions at the site of infection or inflammation. Murine HIF-1α knockout in myeloid cells can lead to impairment of neutrophil aggregation, bacterial killing, invasion and motility in the inflammatory microenvironment (Cramer et al., 2003). However, hypoxia selectively inhibits respriratory burst activity and killing of *Staphylococcus aureus* in human neutrophils, without affecting expression of the NADPH oxidase subunits (McGovern et al., 2011). Elks et al. revealed that activation of HIF-1α further decreased neutrophil reverse migration, resulting in delay of inflammation resolution using a zebrafish model (Elks et al., 2011). Similarly, overexpression of HIF-2α in zebrafish resulted in delayed resolution of inflammation, accompanied with increased collagen deposition at the site of injury (Thompson et al., 2013).

Work from our group has further shown that PHD3, a component of HIF hydroxylase pathway, also functions as a critical regulator of neutrophil apoptosis in inflammation. PHD3-deficient neutrophils result in a loss of hypoxic survival. *In vivo*, using an acute lung injury model, $PHD3^{-/-}$ mice showed increased levels of neutrophil apoptosis. PHD3 also prolongs neutrophil survival during hypoxia (Walmsley et al., 2011).

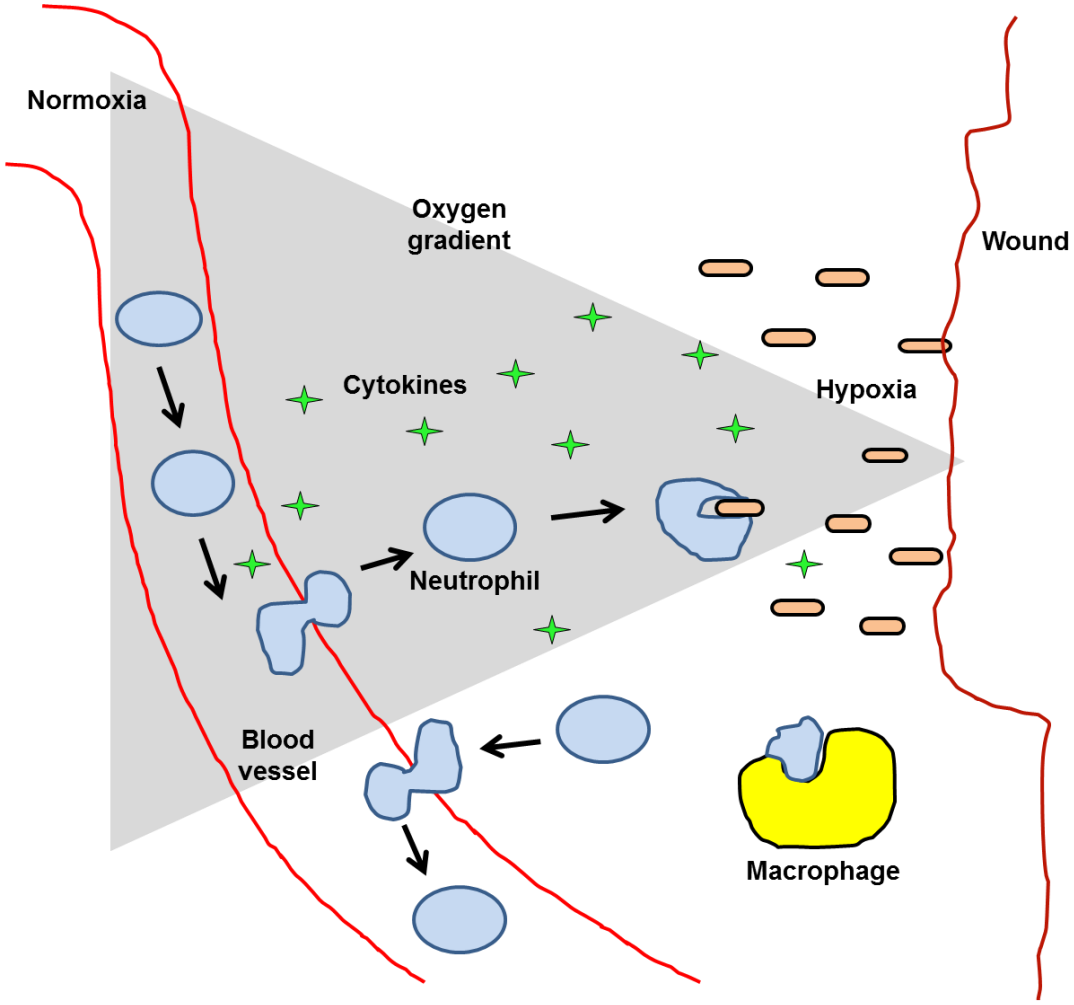

Figure 1.8: Neutrophil behavior in inflammation. Once an infection or injury occurs, neutrophils are recruited from the circulation to the site of injury by alarm signal from hypoxia and pro-inflammatory cytokines. At the wound site characterized by hypoxic microenvironment, neutrophils kill invading organisms by releasing cytotoxic molecules or phagocytosis. The inflammation is then resolved through apoptotic neutrophils which are removed by macrophages. An alternative mechanism promoting inflammation resolution is neutrophil reverse migration from the site of injury to circulation.

1.3.3 Hypoxia and semaphorins

Recent accumulated evidence has indicated that hypoxia is mostly associated with semaphorins in the context of the tumour microenvironments and hypoxia. Sun et al. reported that semaphorin4D in head and neck squamous cell carcinoma (HNSCC) cells is strongly induced by hypoxia in a HIF-1-dependent manner. Semaphorin4D knockdown decreases endothelial cell migration, growth and vascularity of HNSCC expressing a degradation resistant HIF-1α subunit *in vitro*. They also suggested that semaphorin4D may be involved in hypoxia adaptive response (Sun et al., 2009). Consistently, Zhou et al. demonstrated that semaphorin4D expression regulated by the HIF-1 transcription factor works together with VEGF to promote tumour growth and angiogenesis in oral squamous cell carcinoma (Zhou et al., 2012).

Recently, study of anti-angiogenic treatment in cancer using a small-molecule tyrosine kinase inhibitor; sunitinib, has shown that semaphorin3A expression counteracts sunitinib-induced HIF-1α activation, and also reduces sunitinib-elicited cancer hypoxia, so that this may lead to anti-angiogenic treatment of tumours (Maione et al., 2012). Moreover, semaphorin3A/neuropilin-1 signalling blockade inhibits tumour growth and angiogenesis through inhibition of macrophage recruitment to hypoxic tumour areas (Casazza et al., 2013). Conversely, another class 3 semaphorin such as semaphorin3E is upregulated in hypoxia resulting in enhanced postnatal angiogenesis. Moriya et al. suggested that inhibition of semaphorin3E may also be a strategy for therapeutic angiogenesis (Moriya et al., 2010).

Some studies have demonstrated the correlation between hypoxia and semaphorin3F expression in tumours. Semaphorin3F expression causes loss of HIF-1α and VEGF mRNA levels in the lung cancer cell line H157 by reduction of AKT and of signal transducer and activator of transcription 3 (STAT3) phosphorylation. This leads to decreased microvessel density and tumour growth (Potiron et al., 2007). Notably, hypoxia can inhibit semaphorin3F-dependent activities through direct repression of neuropilin-2

expression by HIF-1α. Loss of neuropilin-2 expression in tumour cells causes an increase in VEGF protein which then promotes tumour and endothelial cell migration (Coma et al., 2011).

With regard to neutrophilic inflammation, semaphorin7A has been identified to function in association with hypoxia. During hypoxia, HIF-1α induces semaphorin7A expression in endothelial cells. This upregulated endothelial semaphorin7A promotes transmigration process of neutrophils through endothelia during hypoxia (Morote-Garcia et al., 2012). Interestingly, our group has recently found that in addition to the function of PHD3, a component of HIF hydroxylase pathway, as a regulator of neutrophil life span in inflammation, hypoxia also influences semaphorin3F expression in neutrophils. Results of gene array experiment profiling of hypoxic PHD3$^{-/-}$ neutrophils compared with WT controls have shown that loss of PHD3 results in increased levels of semaphorin3F (Walmsley et al., 2011). However, the mechanism behind this increase is still incompletely described and remains to be elucidated.

1.4 Thesis aims

There is a general acceptance that neutrophilic inflammation is closely associated with chronic inflammatory diseases. Once the processes that initiate neutrophil recruitment are completed, mechanisms of neutrophil removal, driving inflammation resolution, need to take place. During inflammation characterised by a hypoxic microenvironment, neutrophils utilise a wide range of signalling pathways for their activities. In this regard, semaphorin3F, which has been shown to be regulated in response to hypoxia, may have a critical functional role in regulating neutrophil recruitment and persistence. I sought to provide understanding of the role of semaphorin3F in regulating neutrophilic inflammation. More specially, I proposed to

- Characterise semaphorin3F expression in human and mouse neutrophils in response to hypoxia and pro-inflammatory mediators *in vitro* using human neutrophils, and in local inflammation *in vivo* using a murine acute inflammation model,
- Investigate the role of semaphorin3F in neutrophil behaviour in inflammation *in vivo* using a zebrafish model that can reveal the effects of semaphorin3F on neutrophilic recruitment and resolution of neutrophilic inflammation,
- Identify the phenotype of neutrophil migration in semaphorin3F whole fish mutation using the Transcription Activator-Like Effector Nucleases (TALENs) technique that can better define the action of semaphorin3F on neutrophil migratory behaviour,
- Investigate the mechanism by which semaphorin3F regulates neutrophilic inflammation, its dependence on co-receptors, the role of semaphorin3F in human neutrophil chemotactic response *in vitro*, and the association between semaphorin3F and Phosphoinositide 3-Kinase (PI-3K) activity during inflammation *in vivo* using a zebrafish model.

Chapter 2: Materials and Methods

2.1 Materials

The following reagents were purchased from Abcam® (Cambridge, UK), anti-semaphorin3F; anti-neuropilin1; anti-neuropilin2; anti-plexin A1; anti-plexin A2; anti-plexin A3; anti-plexin D1.

The following reagents were purchased from Invitrogen Gibco Life Technologies (Paisley, Scotland, UK), RPMI 1640 media; culture supplements penicillin (50 U/ml), streptomycin (50 U/ml); Hanks Balanced salt solution; foetal bovine serum (FBS); phosphate buffered saline (PBS); Top10 competent cells; SOC media; mMessage mMachine® High Yield Capped RNA Transcription kit.

The following reagents were obtained from R+D Systems Europe Ltd (Oxon UK), recombinant Human TNF-alpha; recombinant Human IL-1beta.

The following reagents were obtained from New England Biolabs (NEB) (Herts, UK), restriction enzymes PmeI; NotI; NheI; BamHI; Esp3I; MwoI; BslI; XbaI; T4 ligase, BSA; appropriate buffers; 10-beta competent cells.

The following reagent was obtained from Cell signalling Technology (Danvers, USA), anti-p38 MAPK.

The following reagents were obtained from QIAGEN (Manchester, UK), mini-prep kit; midi-prep kit.

The following reagents were obtained from Dako UK Ltd. (Cambridge, UK), anti-rabbit Immunoglobulina/HRP; anti-mouse Immunoglobulina/HRP.

The following reagent was purchased from Bio-Rad Laboratories Ltd (Hertfordshire, UK), rainbow marker.

The following reagent was purchased from Martindale Pharmaceuticals (Essex, UK), Sodium citrate.

The following reagent was obtained from Axis-Shield (Huntingdon, UK), OptiPrep™ .

All other reagents were purchased from Sigma Chemical Company (Poole, Dorset, UK).

96-well 'Flexiwell' plates were obtained from BD Falcon (Oxford, UK or Costar, High Wycombe, UK). Falcon 96 well polyvinyl chloride flexiplates and lids were purchased from Fred Baker Scientific (Reading, UK). Incubator was purchased from Sanyo Electric Co Ltd. (Japan). Invivo$_2$ 400 hypoxic work station was purchased from Ruskinn (Bridgend, UK). Blood gas analyser (Model ABL5) was obtained from Radiometer (Copenhagen, Denmark). Mini PROTEAN®II electrophoresis cell system was purchased from Bio-Rad laboratories (Hemel Hempstead, UK). PVDF Immobilon-P transfer membranes were purchased from Millipore (Bedford, USA). Enhanced Chemi-Luminescent™ (ECL) system was obtained from EZ-ECL, Geneflow Ltd. (Fradley, UK). X-ray films were obtained from Amersham Hyperfilm™. Petri dishes were purchased from Scientific Laboratory Supplies Ltd. (SLS), (Coatbridge, UK). Non-filament glass capillary needles were obtained from Kwik-Fil™ Borosilicate Glass Capillaries, World Precision Instruments (WPI) (Herts, UK). Flaming Brown micropipette puller was obtained from Sutter Instrument Co. (Novato, USA). Fluorescent dissecting stereomicroscope was purchased from Leica Microsystems GmbH (Wetzlar, Germany). Volocity® sorfware was purchased from Improvision, Perkin Elmer Inc. (Massachusetts, USA). Nikon Eclipse TE2000-U Inverted Compound Fluorescence Microscope was purchased from Nikon (Tokyo, Japan). Nanodrop™ 1000 spectrophotometer was obtained from Thermo Scientific (Hemel Hempstead, UK). Gel documentation was purchased from Syngene (Cambridge, UK).

2.2 Methods

2.2.1 Human neutrophil assays

2.2.1.1 Human neutrophil preparation

Human neutrophils were isolated from the peripheral blood of healthy volunteers under the approval of the Sheffield Research Ethics Committee. Initially, 3.8% sodium citrate (Martindale Pharmaceuticals, Essex, UK) was added at one tenth of total blood volume to avoid coagulation. Falcon tubes were gently mixed and spun at 1200 rpm at 20^{o}C for 20 minutes (MSE centrifuge, Sanyo, Loughborough, UK). The upper phase was aspirated into clean tubes and centrifuged at 2000 rpm at 20^{o}C for 20 minutes to form platelet-poor plasma (PPP). The lower blood cell phase from the first spin was made up to 50 ml by adding 6 ml of 6% dextran (Sigma-Aldrich Company Ltd.,Gillingham, UK) and 0.9% sterile saline, following by gently inverting the tubes. Air bubbles were removed and the contents were allowed to sediment at 37^{o}C for 20-30 minutes to separate the red blood cells from the white blood cells. Then, the upper layer was transferred to clean tubes and centrifuged at 1000 rpm at 20^{o}C for 6 minutes. After this spin, neutrophils were isolated from other white blood cells using either Optiprep^{TM} or Percoll® method (according to the department's agreement on cost). Optiprep^{TM} was used for the experiments in expression of semaphorin3F and VEGF (Figures 3.1, 3.2, 3.3, 3.4); Percoll® was used for the experiments in expression of neuropilins and plexins (Figures 6.1, 6.2, 6.3). Both methods yield similar purity of neutrophils with identical functional properties.

Optiprep^{TM} Method

Following 100 rpm centrifigution, the white blood cell pellet was re-suspended in a solution of 8 ml Hank's balanced salt solution (HBSS) without Ca^{2+}/Mg^{2+} (Invitrogen) with 20% PPP, then 4 ml OptiPrep^{TM} (Axis-Shield, Huntingdon, UK) was added. The 1080 layer (10.435 ml HBSS with 20% PPP and 3 ml OptiPrep^{TM}) was first gently pipetted over the contents, followed by the 1095 layer (8.036 ml HBSS with 20% PPP and 3 ml

OptiPrep™). Another 10 ml of HBSS with 20% PPP was added. The contents were spun at 10000 rpm at 20°C for 30 minutes. Three separate cell layers were produced; erythrocytes at the bottom, a neutrophil band between 1095 and 1080 layer, and an upper band of peripheral blood mononuclear cells (PBMCs) above the 1080 layer. The PBMCs and neutrophils were carefully transferred into separate clean tubes and counted using a haemocytometer. Neutrophils were centrifuged at 1500 rpm at 20°C for 6 minutes, then, re-suspended to give $5x10^6$ neutrophils per ml in RPMI 1640 media (Gibco®, Invitrogen Ltd., Paisley, UK) containing 1% penicillin and streptomycin (Life Technologies,Paisley, UK) and 10% foetal bovine serum (FBS) (Invitrogen) (Figure 2.1).

Percoll® Method

90% Percoll® was prepared with 10% saline. Discontinuous plasma-Percoll gradients were prepared; a lower layer consisting of 0.98 ml 90% Percoll® and 1.02 ml PPP and an upper layer consisting of 0.84 ml 90% Percoll® and 1.16 ml PPP. The white blood cell pellet was re-suspended in 2 ml PPP and layered on top of the upper layer of the plasma-Percoll gradient, and then spun at 11000 rpm at 20°C for 11 minutes. This resulted in three separate cell layers, with erythrocytes at the bottom, a layer of neutrophils and eosinophils above this between two plasma-Percoll layers, and an upper layer of PBMCs. The PBMCs and neutrophils were carefully transferred into separate clean tubes and counted using a haemocytometer. Neutrophils were centrifuged at 1500 rpm at 20°C for 6 minutes, then, re-suspended to give 5x106 neutrophils per ml in RPMI 1640 media (Gibco®, Invitrogen Ltd., Paisley, UK) containing 1% penicillin and streptomycin (Life Technologies,Paisley, UK) and 10% foetal bovine serum (FBS) (Invitrogen) (Figure 2.1).

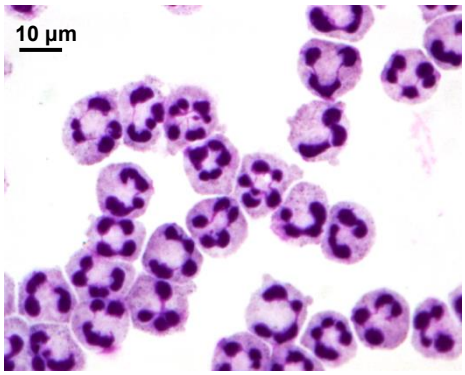

Figure 2.1: Human neutrophil isolation. Neutrophils were isolated from human peripheral blood as previously described (2.2.1.1). Freshly isolated human neutrophils on a cytocentrifugation slide were imaged. Magnification x1000.

2.2.1.2 Human neutrophil culture

Human neutrophils were cultured in RPMI 1640 media (Gibco®, Invitrogen Ltd., Paisley, UK) containing 1% penicillin and streptomycin (Life Technologies,Paisley, UK) and 10% foetal bovine serum (FBS) (Invitrogen) at a concentration of $5x10^6$/ml in 96-well 'Flexiwell' plates (BD Falcon, Oxford, UK or Costar, High Wycombe, UK). Neutrophils were incubated in normoxic conditions (19 kPa O_2) at 37°C in a humidified incubator with 5% supplemental CO_2 (Sanyo Electric Co Ltd., Japan). For hypoxic culture, cells were re-suspended in media pre-equilibrated in 1% O_2, 5% CO_2 at 37°C (Walmsley et al., 2011), using an Invivo$_2$ 400 hypoxic work station (Ruskinn, Bridgend, UK). The O_2 and CO_2 tension, pH and pCO_2 of the hypoxic culture media were analysed using a blood gas analyser (Model ABL5, Radiometer, Copenhagen, Denmark) and mean values from experiments remained constant throughout (Table 2.1).

Conditions	pH	PO_2 (kPa)	PCO_2 (kPa)
Normoxia (n=6)	7.35 +/- 0.02	19.01 +/- 0.14	4.67+/- 0.14
Hypoxia (n=6)	7.34 +/- 0.01	3.55 +/- 0.15	4.53 +/- 0.09

Table 2.1: The standardised O_2 tension, pCO_2 and pH for culture conditions. Following 4 hours culture in normoxic and hypoxic incubators, neutrophil culture media were analysed by an automated blood gas machine (Radiometer). Mean gas tension and corresponding pH values are shown for n=6 separate experiments +/- SEM.

2.2.1.3 Western blotting of human neutrophil lysates

Preparation of human neutrophil lysates

$10x10^6$ neutrophils per condition were gently harvested from 96-well culture plates and centrifuged at 2000 rpm at 4^oC for 2 minutes. Cells were washed in ice cold phosphate buffered saline (PBS) (Gibco®, Invitrogen Ltd., Paisley, UK), followed by centrifugation at 2000 rpm at 4^oC for 2 minutes. Cell pellets were suspended in 1 ml of hypotonic sonication lysis buffer (Appendix 2). Supernatant was discarded and cell pellets were re-suspended in 100 µl sonication lysis buffer and incubated on ice for 10 minutes. Cells were sonicated in a Bioruptor^{TM} (Diagenode Europe SA, Liege, Belgium) using 30 second on-off high power cycles for 10 minutes. Whole cell fractions were collected and spun at 12000 g at 4^oC for 10 minutes. Supernatant was transferred into clean 1.5 ml tubes and 100 µl of 2x SDS lysis buffer (Appendix 2) was added. Lysates were boiled at 95^oC for 5 minutes, then either run immediately on SDS gels or stored at -80^oC.

Protein separation

Proteins were separated by sodium dodecyl sulphate polyacrylamide electrophoresis (SDS-PAGE) using the Bio-Rad mini PROTEAN®II electrophoresis cell system (Bio-Rad laboratories, Hemel Hempstead, UK) on appropriate percentage of SDS gels (resolving and stacking gel) (Appendix 2). Gels were immersed with running buffer (Appendix 2). Neutrophil lysates were loaded into lanes with one lane of 5 µl rainbow marker (Bio-Rad laboratories). Gels were run at 120 volts (PowerPac 300, Bio-Rad Laboratories) until samples reached the resolving gel, then at 150 volts until samples reached the bottom of the gel.

Protein transfer

The stacking gel was removed and the resolving gel was soaked in transfer buffer (Appendix 2). PVDF Immobilon-P transfer membranes (Millipore, Bedford, USA) were soaked in methanol for 2 minutes to activate, then in

transfer buffer. Gels were then transferred to PVDF membranes with a constant voltage of 100 volts for 70 minutes in ice-cold transfer buffer.

Immunoblotting and detection

Membranes were blocked in blocking buffer (Appendix 2) for 1 hour on an orbital shaker. Primary antibody was prepared in 4 ml blocking buffer at the appropriate concentration required in 50 ml falcon tubes. Membranes were transferred to the tubes and incubated at 4^{o}C overnight on a rolling platform. The following day, membranes were washed in Tris-buffered saline + 0.1% tween 20 (TBS-Tween) (Appendix 2) and incubated at room temperature for 1 hour with the appropriate horseradish peroxidase (HRP)-conjugated secondary antibody diluted in 4 ml blocking buffer. Membranes were then washed in TBS Tween. Proteins were detected using the Enhanced Chemi-Luminescent^{TM} (ECL) system (EZ-ECL, Geneflow Ltd., Fradley, UK) and exposed to X-ray film (Amersham Hyperfilm^{TM}) in a dark room.

Membranes were stripped and re-probed using the following method: membranes were washed in distilled water for 7 minutes on an orbital shaker, then washed in 0.2 M Sodium hydroxide (NaOH) for 15 minutes. Membranes were washed again in distilled water, followed by blocking in blocking buffer for 1 hour and then incubation with another primary antibody at 4^{o}C overnight on a rolling platform.

2.2.2 General zebrafish techniques and assays

2.2.2.1 Zebrafish husbandry

Zebrafish were maintained according to standard protocols (Nusslein-Volhard, 2002), in a closed aquarium system at 28^{o}C with a light cycle of 14 light hours and 10 dark hours, in UK Home Office approved facilities in the MRC Centre for Developmental and Biomedical Genetics aquaria at the University of Sheffield. Zebrafish larvae at 5 days post fertilisation (dpf) were fed Tetra A-Z powdered fish feed. Zebrafish older than 13 dpf were fed live artemia twice daily.

Fertilised, healthy embryos were collected and maintained in E3 medium (Appendix 2) in Petri dishes (Scientific Laboratory Supplies Ltd. (SLS), Coatbridge, UK), and incubated at 28^{o}C. After the end of each experiment and prior to 5.2 dpf, embryos were culled by immersion in bleach according to UK Home Office legislation, which permits use of zebrafish embryos up to 5.2 dpf outside of the Animals Act (Scientific Procedures).

2.2.2.2 Microinjection of zebrafish embryos

Ribonucleic acid (RNA) or morpholino was diluted with sterile water, and 10% phenol red to allow visualisation, at the appropriate concentration required. RNA or morpholino was injected into the one-cell stage embryos using non-filament glass capillary needles (Kwik-Fil^{TM} Borosilicate Glass Capillaries, World Precision Instruments (WPI), Herts, UK) pulled by a Flaming Brown micropipette puller (Sutter Instrument Co., Novato, USA). Following injection, embryos were incubated in E3 medium at 28^{o}C.

2.2.2.3 Inflammation assay

To investigate the inflammatory responses of neutrophils, zebrafish embryos of the neutrophil or macrophage specific fluorescent lines *Tg(mpx:GFP)i114* or *Tg(fms: GAL4;UNM)* respectively (Appendix 3) were injured by tail fin transection as previously described (Renshaw et al., 2006) (Figure 2.2). Embryos were anesthetized at 2 dpf by immersion in 0.168 mg/ml Tricaine (Sigma-Aldrich, Poole, UK) and transection of the tail was performed with a micro-scalpel (WPI) to initiate an inflammatory response. At 6 hours after injury (hpi) and 24 hpi, neutrophils were counted at the site of injury by eye using a fluorescent dissecting stereomicroscope (Leica Microsystems GmbH, Wetzlar, Germany). Counting was performed blind to experimental conditions.

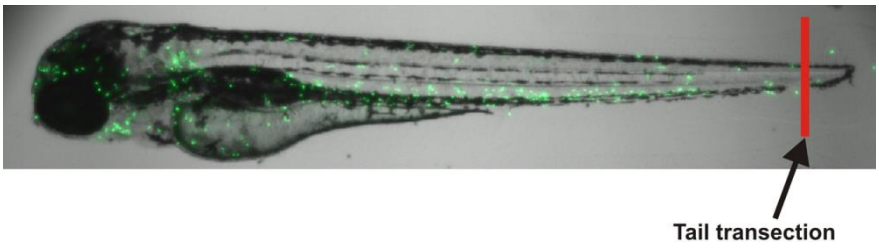

Figure 2.2: Tail fin transection. Image shows a 2 dpf *Tg(mpx:GFP)i114* zebrafish embryo. Injury was performed within the region with pigment disruption (as illustrated by the red line) using a micro-scalpel.

2.2.2.4 Neutrophil tracking during recruitment to the site of injury

To examine the speed and meandering index of neutrophil migration towards the site of tail injury by *in vivo* tracking, 2 dpf *mpx*:GFP embryos were anaesthetised in tricaine then injured. Embryos were mounted in a 1% solution of low melting point (LMP) agarose dissolved in sterile water containing 0.017% tricaine. Neutrophils were tracked over 1 hour during the initial recruitment phase using a 1394 ORCA-ERA camera on an Eclipse TE2000-U inverted compound fluorescence microscope. Tracking analysis

was performed using Volocity® software (Improvision, Perkin Elmer Inc.), which detected the intensity of fluorescence to examine individual GFP-labelled neutrophils with various parameters for each track (Figure 2.3).

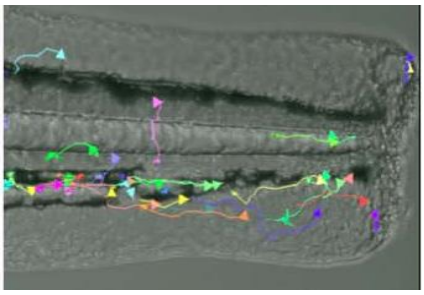

Figure 2.3: Tracking experiment. A typical tracking experiment with arrows indicating the path of individual neutrophils' movements over 1 hour during the initial recruitment phase of inflammation. Speed and meandering index (direction) were calculated by Volocity® software.

2.2.2.5 Reverse migration assay

To investigate the migration of neutrophils away from the site of injury, a reverse migration assay was performed. *Tg(mpx:Gal4:Kaede)i222* or *mpx*:Kaede (Appendix 2) transgenic fish have embryos expressing Kaede, a photoconvertible protein that fluoresces red in neutrophils, and can be converted from green to red fluorescence in individual cells. 2 dpf *mpx*:Kaede were anaesthetised and tailfin transection was performed. At 6 hpi, embryos were mounted in a chamber slide in a 1% solution of low melting point (LMP) agarose dissolved in sterile water containing 0.017% tricaine. Kaede-labelled neutrophils present at the site of injury were photoconverted at 10x magnification using a PerkinElmer UltraVIEW PhotoKinesis^{TM} device (PerkinElmer Life and Analytical Sciences) on an UltraVIEWVoX spinning disk confocal microscope using 120 pulses of the 405 nm laser at 40% laser energy (Dixon et al., 2012). Embryos were then transferred to Nikon Eclipse TE2000-U Inverted Compound Fluorescence Microscope (Nikon, Tokyo, Japan) and a time-lapse series was captured. Neutrophils fluorescing in the red channel were tracked over 3.5 hour.

Reverse migration analysis was performed using Volocity® sorfware (Improvision, Perkin Elmer Inc.).

2.2.2.6 Apoptosis assay

To examine the amount of neutrophil apoptosis at the site of injury, 2 dpf embryos were anaesthetised and injured at tailfin. At 12 hpi, embryos were then fixed in 4% paraformaldehyde (PFA) (Fisher Scientific, Loughborough, UK) overnight at 4^{o}C. The next day, embryos were washed in phosphate buffered saline (PBS). Tyramide Signal Amplification (TSA) staining was performed using the TSA^{TM}-Plus Fluorescein System Kit (PerkinElmer Life and Analytical Sciences). Before staining, embryos were washed in amp diluent, then incubated in 1:50 FITC TSA;amp diluent in the dark for 10 minutes at 28^{o}C. Background staining was removed by washing in PBS. Embryos were then fixed in 4%PFA at 4^{o}C overnight. This TSA staining labels myeloperoxidase in neutrophils with green fluorescence.

The following day, embryos were washed in PBS + 0.1% tween 20 (PBT), digested with proteinaseK at 10 µg/ml at room temperature for 90 minutes, then washed in PBT. Embryos were fixed in 4% PFA at room temperature for 20 minutes, washed in PBT, followed by immersion in 1:2 acetone:ethanol at -20^{o}C for 7 minutes, then washed in PBT. The ApopTag® Red *In situ* Apoptosis Detection Kit (Millipore Corporation, Herts, UK) was used for terminal deoxynucleotidyl transferase (TdT) dUTP nick end labelling (TUNEL). Embryos were incubated in 50 µl equilibration buffer from the kit at room temperature for 45 minutes. Liquid was removed, 30 µl reaction buffer and 16 µl TdT enzyme were then added to the embryos, and incubated at 37^{o}C for 90 minutes. Liquid was removed and embryos were incubated with 200 µl stop buffer at 37^{o}C for 3 hours, and washed in PBT. Embryos were then incubated with 62 µl anti-dig-rhodamine and 68 µl blocking solution with gentle shaking at 4^{o}C overnight. The following day, embryos were washed in PBT, fixed in 4% PFA at room temperature for 30 minutes, and mounted in 80% glycerol at 4^{o}C until imaging.

Neutrophils at the site of injury were imaged using the Ultra*VIEW*VoX spinning disk confocal imaging system (PerkinElmer Life and Analytical Sciences). The neutrophil apoptosis was assessed by counting the number of apoptotic neutrophils at the site of injury (cells labelled with both TSA (green) and TUNEL (red)) divided by the total neutrophil number at the site of injury (cells labelled with TSA (green)).

2.2.3 General molecular biology techniques

2.2.3.1 Extraction of DNA from filter paper

The filter paper containing plasmid was cut out and placed in a 1.5 ml eppendorf tube. 50 µl of 10 mM TE-buffer (Endotoxin-free) (QIAGEN, Manchester, UK) was added to the tube, followed by vortex for 1 minute. The contents were incubated at room temperature for at least 5 minutes before transformation.

2.2.3.2 Transformation

1-2 µl DNA of plasmid indicated was added to 25 µl of Top10 competent cells (Invitrogen, Paisley, UK) without mixing and incubated on ice for 30 minutes. The mixture was then heat-shocked at 42^{o}C for 45 seconds before returning to ice for 2 minutes. 250 µl of SOC media (Invitrogen) was added to the mixture, and the cells were then incubated at 37^{o}C with vigorous shaking at 200-250 rpm for 1 hour. The cells were spread onto dry selection plates (autoclaved LB agar containing 50 µl/ml appropriate antibiotic) and incubated at 37^{o}C overnight.

The following day, individual colonies were picked and grown overnight in 100 ml of autoclaved LB broth containing 50 µl/ml of appropriate antibiotic at 37^{o}C with vigorous shaking at 200-250 rpm.

2.2.3.3 DNA purification

Following transformation, DNA was purified using a HiSpeed Plasmid Midi kit (QIAGEN, Manchester, UK), as directed by the manufacturer. The DNA concentration was quantified using a Nanodrop^{TM} 1000 spectrophotometer (Thermo Scientific, Hemel Hempstead, UK).

DNA was identified by diagnostic digest using the following method: 2 µl DNA, 1 µl restriction enzyme, 1 µl appropriate 10x buffer (and 0.1 µl Bovine Serum Albumin) were added to an eppendorf tube. The contents were made up to 10 µl by adding sterile water and incubated at 37^{o}C for 2 hours. The samples were then run on 0.8% agarose gel (Bioline) containing 0.03% Ethidium bromide (Severn Biotech Ltd., Kidderminster, UK) at 100 volts for 45 minutes, and visualised by gel documentation (Syngene, Cambridge, UK).

2.2.3.4 RNA synthesis

Following DNA purification, RNA synthesis was performed using the mMessage mMachine® High Yield Capped RNA Transcription kit (Invitrogen), as per the manufacturer's instructions. 6 µl of DNA was incubated with 2 µl SP6 enzyme mix, 10 µl 2x NTP/CAP and 10 µl 10x reaction buffer at 37^{o}C for 2 hours. After this incubation, 1 µl of TURBO DNAse was mixed to the sample, followed by incubation at 37^{o}C for 30 minutes. This reaction was stopped by adding 115 µl nuclease free water and 15 µl ammonium acetate stop solution. RNA was extracted by addition of 150 µl phenol:chloroform and spin at 14000 rpm at 4^{o}C for 15 minutes. The upper phase was then transferred to a new tube prior to adding an equal volume of isopropanol. The sample was centrifuged at 14000 rpm at 4^{o}C for 15 minutes. The pellet was then re-suspended in 20 µl sterile RNAse free water and stored at -80^{o}C. The RNA concentration was quantified using a Nanodrop^{TM} 1000 spectrophotometer (Thermo Scientific, Hemel Hempstead, UK).

2.2.3.5 Whole mount in situ Hybridisation probe synthesis

Following transformation and DNA purification of plasmid vectors containing the zebrafish semaphorin3Fa or semaphorin3Fb coding sequence (Yu and Moens, 2005), the vectors were linearised by restriction digest with PmeI or NotI, respectively (New England Biolabs (NEB), Herts, UK) using the following method: 20 µg of vector DNA, 1 µl of Not1 and 20 µl of Not1 buffer were added to an eppendorf tube, made up to 200 µl by adding sterile water and incubated at 37^{o}C for 2 hours. To extract the linearised DNA, 200 µl of phenol:chloroform was added. The mixtures were vortexed then spun at 14000 rpm at 4^{o}C for 7 minutes. The upper phase was transferred to a new tube, followed by adding an equal volume of chloroform. The samples were vortexed, then centrifuged at 14000 rpm at 4^{o}C for 5 minutes. The upper phase was again transferred to a new tube, followed by adding one tenth of this volume of 3 M sodium acetate and an equal volume of isopropanol. The samples were stored at -20^{o}C for 20 minutes and spun at 14000 rpm at 4^{o}C for 20 minutes. The pellet was washed in 70% ethanol, then spun 14000 rpm at 4^{o}C for 5 minutes. The ethanol was removed and the pellet air-dried before re-suspension in 20 µl of sterile water. The DNA concentration was quantified using a Nanodrop^{TM} 1000 spectrophotometer (Thermo Scientific, Hemel Hempstead, UK).

Transcription of RNA probe was performed using an SP6 RNA digoxigenin-labelling kit (Roche). 1 µg of linearised DNA was incubated with 2 µl NTP-DIG-RNA labelling mix, 2 µl SP6 polymerase, 1 µl RNAse inhibitor and 2 µl transcription buffer in a final volume of 20 µl with RNAse free water at 37^{o}C for 2 hours, followed by adding 4 µl DNAse and incubating at 37^{o}C for 30 minutes. For precipitation, 1 µl of 0.5 M EDTA pH8, 2.5 µl of 4 M LiCl and 75 µl of 100% ethanol were added to the sample, then stored at -80^{o}C for 1 hour. The sample was centrifuged at 14000 at 4^{o}C for 10 minutes. The pellet was air-dried before re-suspension in 20 µl of sterile water. After addition of 80 µl of formamide, the RNA probe was stored at -80^{o}C.

2.2.3.6 Whole mount in situ Hybridisation

To determine the expression of semaphorin3Fa and semaphorin3Fb in zebrafish embryos, 20-somite and 3 dpf zebrafish embryos were fixed in 4% paraformaldehyde (PFA) (Fisher Scientific, Loughborough, UK) at 4^{o}C overnight. Embryos were immersed in a methanol series (25%, 50% and 75%) and stored in 100% methanol at -20^{o}C. Embryos were then re-hydrated though a reverse methanol series and washed in phosphate buffered saline+ 0.1% tween 20 (PBT), followed by digestion with proteinaseK at 10 µg/ml for 30 minutes (for 20-somite) or 70 minutes (for 3dpf embryos). After re-washing in PBT, embryos were then fixed in 4% PFA at room temperature for 20 minutes and re-washed in PBT. Pre-hybridisation was performed by incubating embryos with PreHyb buffer (Appendix 2) horizontally at 70^{o}C for 3 hours. The PreHyb was removed and ProbeHyb (Appendix 2) was added to embryos. Embryos were then incubated horizontally at 70^{o}C overnight. The next day, the ProbHyb was replaced with a series of HybWash/2x SSC (75%, 50% and 25%), then another wash in 2x SSC at 70^{o}C. Embryos were washed in a series of 0.2x SSC/PBT (75%, 50% and 25%) and then PBT at room temperature. To minimise non-specific binding, embryos were incubated with blocking solution (Appendix 2) at room temperature for 1 hour with gentle rocking. Embryos were then incubated with an anti-DIG-AP antibody (Roche, Herts, UK) at a 1:5000 dilution in blocking solution at 4^{o}C overnight with gentle rocking. The following day, embryos were washed in PBT, then in staining wash (Appendix 2). Staining solution (Appendix 2) was added to embryos. This was incubated at room temperature with gentle rocking until staining developed. The reaction was stopped by adding 1 mM EDTA. Embryos were washed in PBT, fixed in 4% PFA at room temperature for 20 minutes then stored in methanol at -20^{o}C until imaging.

Before imaging, embryos were re-hydrated in a reverse methanol series (75%, 50% and 25%) then in 80% glycerol. Imaging was performed by fluorescent dissecting microscope with a Leica DFC310 camera and Leica Application Suite software.

2.2.3.7 Semaphorin3F whole fish overexpression

Semaphorin3Fa or semaphorin3Fb whole fish overexpression and knockdown were carried out using RNA and morpholino oligonucleotide (Appendix 1) microinjections into one-cell stage embryos of *Tg(mpx:GFP)i114*, respectively. Injections were performed into the yolk. Following injection, embryos were incubated in E3 media at 28^{o}C. 3 dpf embryos were then tested using whole mount *in situ* hybridisation for semphorin3F whole fish overexpression or by RT-PRC for semaphorin3F whole fish knockdown.

Semaphorin3Fa or semaphorin3Fb whole fish overexpression

3 dpf embryos injected with semaphorin3Fa or semaphorin3fb RNA (50ng/µl) were collected and fixed in 4% PFA overnight at 4^{o}C, then followed by whole mount *in situ* hybridisation method as described above. The embryos were imaged using a fluorescent dissecting microscope (Figure 2.4). Non-injected embryos were used as controls.

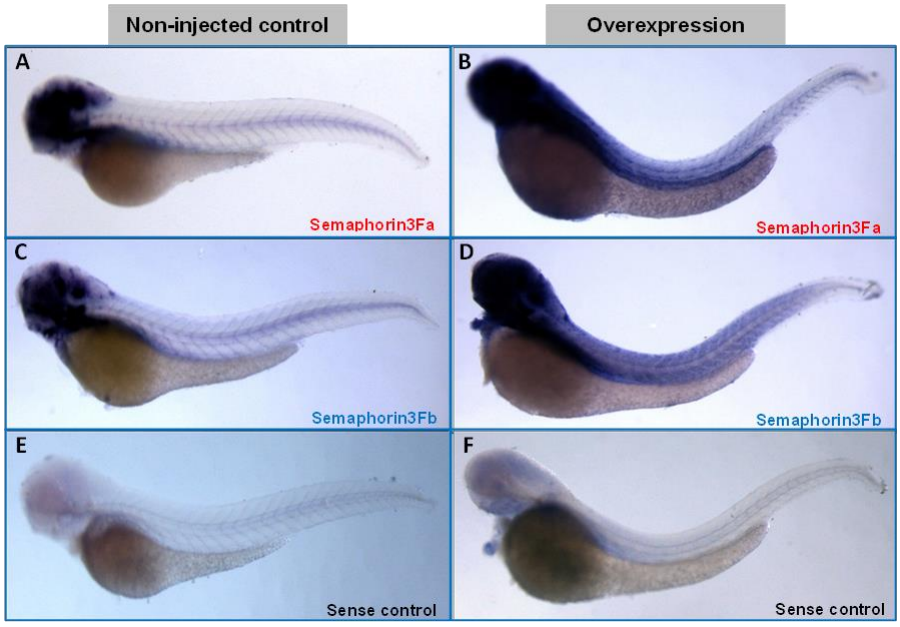

Figure 2.4: Semaphorin3Fa or semphorin3Fb whole fish overexpression by RNA injection. The whole fish overexpression of zebrafish semaphorin3Fa and b was identified by whole mount *in situ* hybridization. 3dpf embryos were stained with sema3Fa (A-B), sema3Fb (C-D) and sense probes, respectively. RNA-injected embryos showed stronger blue stain than in non-injected embryos providing the overexpression of semaphorin3Fa or b in the RNA-injected embryos.

2.2.3.8 Semaphorin3F whole fish knockdown

Additionally, the efficacy of semaphorin3F morpholinos to generate the whole fish knockdown in zebrafish embryos was confirmed by Reverse Transcription polymerase chain reaction (RT-PCR). Two antisense morpholino oligonucleotides were designed to target the translation start sites of semaphorin3Fa (Yu and Moens, 2005) and semaphorin3Fb (Tanaka et al., 2007). To enable proofing by molecular methods, another antisense morpholino oligonucleotide of semaphorin3Fb which targets an exon-intron boundary between exon 3 and exon 5 and interrupts pre-mRNA splicing, was designed by Dr.Stephen Renshaw (University of Sheffield).

Embryos were injected with semaphorin3Fb splice blocking morpholino. A single 3 dpf injected embryo was transferred to a 96-well plate. For the genomic DNA extraction, the single embryos were incubated with 100 µl of 50 mM NaOH at 95^{o}C for 20 minutes, followed by adding of 10 µl of 1 M Tris-HCl pH 8.0 and mixing. After centrifugation at 14000 rpm at 4^{o}C for 30 minutes, 2 µl of supernatant was applied to separate 96-well plate with 10 µl ReddyMix PCR master mix (Thermo Scientific), 1 µl of 10 µM of each forward and reverse primer (Appendix 1) and 6 µl of dH_2O, mixed gently and run using this cycle:

98^{o}C	30 seconds	
98^{o}C	10 seconds	34x
65^{o}C	30 seconds	
72^{o}C	30 seconds	
72^{o}C	10 minutes	
10^{o}C	forever	

Samples were run in parallel with primer for zebrafish ef1α (Appendix 1) as control. The PCR products were then run on 2.5% agarose gel (Bioline) (Figure 2.5).

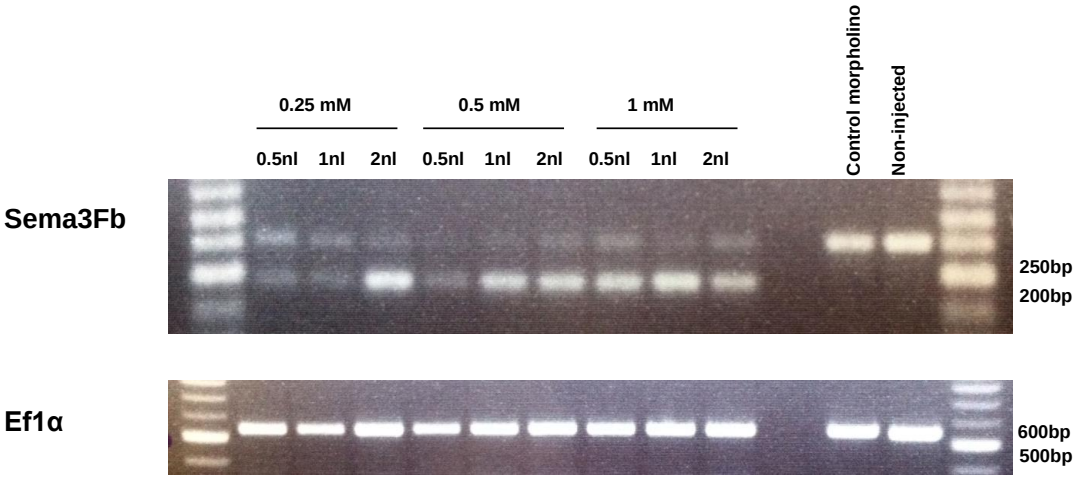

Figure 2.5: Semaphorin3Fa or semphorin3Fb whole fish knockdown by semaphorin3Fb splice blocker morpholino injection. Semaphorin3Fb morpholino inhibited splicing. The gel represents genomic DNA from morpholino-injected fish subject to PCR analysis targeting the translation start site of semaphorin3Fa or b. Semaphorin3Fb splice blocking morpholino (0.25 mM – 1 mM) was injected into 1-cell stage zebrafish mpx:GFP embryos. In addition, 1 mM mismatch morpholino which has no effect on zebrafish development, was used as a control. The upper band provided the WT band, in contrast, the lower band showed misspliced bands with exon4 deletion. A loading control was quantified by EF1α.

The semaphorin3Fb splice blocking morpholino showed mis-splicing with exon 4 deletion resulting in a shorter band compared to WT in a dose-dependent manner. This confirmed whole fish knockdown of semaphorin3Fb. The effect of all three morpholinos was then compared by inflammation assay as described previously. Neutrophil numbers at the injury site at 6hpi and 24 hpi were counted. Semaphorin3Fa translation blocking, semaphorin3Fb translation blocking and semaphorin3Fb splice blocking morpholino showed no significant difference in neutrophil numbers at the site of injury both at recruitment and resolution phase (Figure 2.6). Therefore, all three morpholinos had the equivalent effects on inflammatory responses of neutrophils by generating whole fish semaphorin3F knockdown. I also selected semaphorin3Fa translation blocking morpholino and semaphorin3Fb translation blocking morpholino for all experiments in chapter 4.

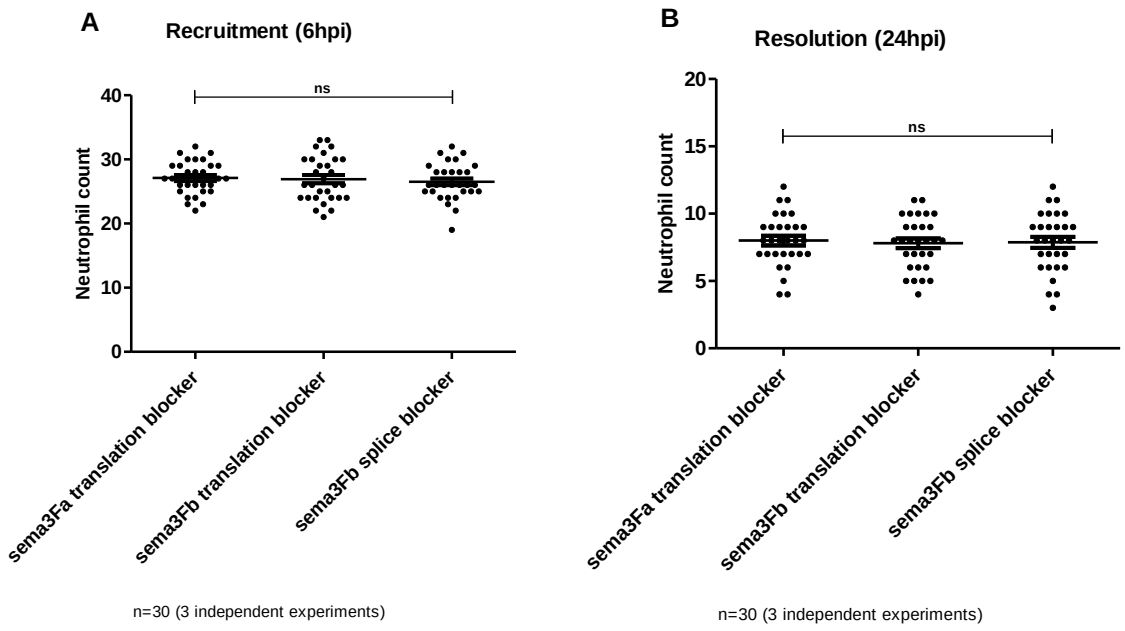

Figure 2.6: All three antisense morpholino oligonucleotides showed no significant difference in neutrophil numbers at the site of injury both at recruitment and resolution phase. Each morpholino (1 nl of 0.5mM) was injected into 1-cell stage zebrafish mpx:GFP embryos. Tailfin transection was performed at 2dpf, and neutrophils counted at 6 and 24 hpi. (A) 6 hpi timepoint neutrophil counts (recruitment). (B) 24 hpi timepoint neutrophil counts (resolution). Data shown are mean ± SEM. n= 30 performed as 3 independent experiments, P values were calculated using one-way ANOVA ****P<0.001.*

2.2.3.9 Transcription activator-like effector nuclease (TALEN)

To generate site-specific DNA double-strand breaks resulting in mutations of semaphorin3Fa and semaphorin3Fb gene, transcription activator-like effector nuclease (TALEN) was performed according to previously described protocols (Cermark et al., 2011) (Zu et al., 2013). A heterodimer with a left and a right subunit containing a C-terminal Fok1 nucleases domain and an N-terminal site specific DNA binding domain, at a target site was first designed by website http://tale-nt.cac.cornell.edu/node/add/talen-old. The target genomic sequence should have a wide spanning restriction enzyme that cuts well in reddymix to allow saving on time and cost for screening process. The DNA binding domain should be comprised of between 15-21 repeat variable domain (RVD) units and have a space between two subunits about 15 bp. All plasmids were provided by Golden Gate TALEN kit

(Addgene, Cambridge, UK) and obtained as a kind gift from Dr. Stone Elworthy (University of Sheffield).

Preparing TALEN constructs

In assembly stage 1, part A and part B of each subunit were assembled. The part A was assembled into pFusA plasmid with the first ten RVD plasmids. The part B was assembled into pFusB plasmid with the rest of RVD plasmids. Each of four reactions was transferred to 0.2 ml PCR tubes on ice. Following this, 2 µl of T4 ligase (NEB), 2 µl of T4 ligase buffer (NEB) and 1 µl of BsaI (NEB) were added to each tube. The contents were made up to a total volume of 20 µl by adding dH_2O and mixed gently. All reactions were run using the program 'TALEN' with not hot-lid option.

10x (37°C/5 min + 16°C/10 min) + 50°C/5 min + 80°C/5 min

After this cycle, the reactions were incubated with 0.3 µl of 25 mM ATP and 1 µl of plasmid safe nuclease at 37°C for 1 hour to eliminate all unligated linear dsDNA fragments including incomplete ligation products. Each reaction was transformed into 12.5 µl of 10-Beta competent cells (NEB), as directed by the NEB manufacturer, and then spread on spectinomycin (50 µg/ml) Xgal (1:1000) LB agar plate using flat toothpicks, followed by incubation at 37°C overnight. The next day, three white colonies of each reaction were picked then incubated separately in 6 ml of autoclaved LB broth containing 50 µl/ml spectinomycin at 37°C with vigorous shaking at 200-250 rpm overnight.

In assembly stage 2, the heterodimer (a left and a right subunit) were combined together. For this, DNA of the previous overnight cultures above were purified using a Mini kit (QIAGEN, Manchester, UK), as per the manufacturer's instructions. The DNA was then eluted into 50 µl dH_2O and checked by restriction digest with NheI + XbaI (NEB) using the following method: 4 µl of mini prep DNA, 0.5 µl of NheI, 0.5 µl of XbaI, 0.1 µl of 10mg/ml BSA and 1 µl of 10x NEB2 buffer were added to an eppendorf tube, made up to 10 µl by adding sterile water and incubated at 37°C for 1 hour. The samples were then run on 1.1% agarose gel (Bioline). The expected

band sizes were 266 bp, 2132 bp and 500-1100 bp (depending on RVD number).

The correct clones of each part A and part B were transferred to 0.2 ml PCR tubes on ice. Following this, 4 µl of part A mini prep DNA, 4 µl of part B mini prep DNA, 1 µl of 150 ng/µl the appropriate final RVD plasmid, 1 µl of 75 ng/µl pCAGT7TALEN plasmid, 2 µl of T4 ligase (NEB), 2 µl of T4 ligase buffer (NEB), 1 µl of Esp3I (NEB) and 5 µl of dH_2O were added to each tube. The contents were made up to a total volume of 20 µl by adding dH_2O and mixed gently. All reactions were run using program 'TALEN' with not hot-lid option.

10x (37°C/5 min + 16°C/10 min) + 50°C/5 min + 80°C/5 min

Each reaction was transformed into 12.5 µl of 10-Beta competent cells (NEB), as directed by the NEB manufacturer, and then spread on carbenecillin (50 µg/ml) Xgal (1:1000) LB agar plate using flat toothpicks, followed by incubation at 37°C overnight. The next day, one white colony of each reaction was picked, then incubated separately in 100 ml of autoclaved LB broth containing 50 µl/ml carbenecillin at 37°C with vigorous shaking at 200-250 rpm overnight. The following day, DNA of the previous overnight cultures above were purified using a nucleobond Midi kit (QIAGEN, Manchester, UK), as per the manufacturer's instructions. The DNA was then eluted into 120 µl dH_2O and the DNA concentration was quantified by a spectrophotometer using a wavelength A260. The clone DNA was checked by sequencing using TAL_R2 and SeqTALEN_5-1 primers and by restriction digest with BamHI + XbaI (NEB) using the following method: 1.5 µl of 100 ng/µl DNA, 0.5 µl of BamHI, 0.5 µl of XbaI, 0.1 µl of 10mg/ml BSA and 1 µl of 10x NEB3 buffer were added to an eppendorf tube, made up to 10 µl by adding sterile water and incubated at 37°C for 1 hour. The samples were then run on 1.1% agarose gel (Bioline). The expected band sizes were 4346 bp and 3669 bp (depending on RVD number).

To linearization the constructs, the DNA of correct clones was digested with NotI using this method: 6 µg of left construct DNA, 6 µg of right construct DNA, 30 µl of 10x NEB3 buffer, 3 µl of 10mg/ml BSA and 10 µl of NotI (NEB)

were added to an eppendorf tube, made up to 300 µl by adding sterile water, mixed gently and incubated at 37^{o}C for 1 hour. The linearized DNA was then purified by PCR clean up columns (QIAGEN, Manchester, UK), as directed by the manufacturer, and eluted into 30 µl dH_2O.

Preparing mRNA for injecting

RNA from the NotI linearized DNA was performed using Epicenter messageMax^{TM} T7 ARCA-Capped Message Transcription kit (Cambio Ltd., Cambridge, UK). For this, 5.5 µl of 400 ng/µl DNA, 2 µl of 10x buffer, 8 µl of NTP CAP mix, 2 µl of 100 mM DTT, 0.5 µl of scriptguard and 2 µl of enzyme mix were added to a 0.2 ml PCR tube, mixed gently and incubated in PCR machine at 37^{o}C for 30 minutes. Following this, 1 µl of DNAase was added, mixed gently and incubated 37^{o}C for 15 minutes. For RNA purification, the RNA was applied to RNA minelute column (QIAGEN, Manchester, UK) following instruction and eluted into 14 µl RNAase free water. The RNA was stored immediately at -80^{o}C.

Microinjection

3.5 µl of RNA was added with 0.5 µl phenol red to allow visualisation, and injected into the one-cell stage *mpx*:GFP embryos using non-filament glass capillary needles (Kwik-Fil^{TM} Borosilicate Glass Capillaries, World Precision Instruments (WPI), Herts, UK). Following injection, embryos were incubated in E3 medium at 28^{o}C.

Mutation analysis

A single 3 dpf injected embryo was transferred to a 96-well plate. For the genomic DNA extraction, the single embryos were incubated with 100 µl of 50 mM NaOH at 95^{o}C for 20 minutes, followed by adding of 10 µl of 1 M Tris-HCl pH 8.0 and mixing. After centrifugation at 14000 rpm at 4^{o}C for 30 minutes, 2 µl of supernatant was applied to another 96-well plate with 10 µl ReddyMix PCR master mix (Thermo Scientific), 1 µl of 10 µM forward primer (Sema3Fa MwoI (F) or Sema3Fb BslI (F)), 1 µl of 10 µM reverse primer (Sema3Fa MwoI (R) or Sema3Fb BslI (R)) and 6 µl of dH_2O, mixed gently and run using this cycle:

94°C	2 minutes	
94°C	20 seconds	34x
55°C	20 seconds	
72°C	45 seconds	
72°C	3 minutes	
10°C	forever	

The PCR products were analysed by restriction digest with 0.5 µl MwoI (for semaphorin3Fa) or BslI (for semaphorin3Fb) at appropriate temperature for 1 hour prior to run on 2.5% agarose gel (Bioline). The rest of the mutated embryos were allowed to grow in the aquarium system.

Screening potential founder fish

Once the mutated fish were about 2-3 months old, these fish were crossed with *mpx*:GFP, and put into individual tanks. Their progeny embryos were tested using the previous described mutation analysis method above. From each potential founder, three 3 dpf embryos were transferred to each of eight wells in a 96-well plate. The positive digestion results were then accurately analysed by sequencing using the same primers for PCR. The embryos of potential founder with frameshift mutation were allowed to grow in the aquarium system.

Screening F1 carriers

Once the offspring of the potential founder were 2-3 months old, the screening of these F1 fish was performed by fin clipping and mutation analysis. Fish were anaesthetised by immersion in 4.2% tricaine until gill movement was slowed. A small amount of fin from the end of the tail was clipped with the scissors and transferred to a 96-well plate. The genomic DNA was extracted and tested using the previous described mutation analysis method. The positive digestion results were then analysed by sequencing using the same primers for PCR. Fish with the same mutation as the founder were maintained in aquarium system for further experiments.

2.2.3.10 Analysis of PI-3K activity

To examine PI-3K activation during neutrophil recruitment *in vivo*, the zebrafish transgenic line *Tg(lyz:PHAkt-EGFP)*, subsequently referred to as *lyz/*PHAkt, were injured at the tail fin as described above at 3 dpf. Embryos were then mounted in a 1% solution of low melting point (LMP) agarose dissolved in sterile water containing 0.017% tricaine, and imaged on an Ultra*VIEWVoX* spinning disk confocal imaging system (PerkinElmer Life and Analytical Sciences) with an inverted Olympus IX81 microscope at 60x magnification with oil immersion objective (Hamburg, Germany). Neutrophils in the region between the site of injury and the posterior blood island were individually imaged using the 488 nm laser line with 20 Z slices. Single slices in which a leading edge and trailing edge of each cell could be defined were exported as *.tif* files and analysed using ImageJ. In this, using the straight-line tool, a transecting line was drawn through each cell from the trailing edge towards the leading edge. A plot profile was generated to measure the fluorescence intensity per pixel along the length of the line. The values were then inserted into a Microsoft® Excel worksheet. Using Microsoft Excel, the mean intensity values for each parameter, as illustrated in Figure 2.7, were entered into the equation to calculate the polarity index:

$$\text{Polarity index} = (\log_{10} a / b) \times [(a + b) / c]$$

where a = trailing edge of cell; b = leading edge of cell; c = whole cell

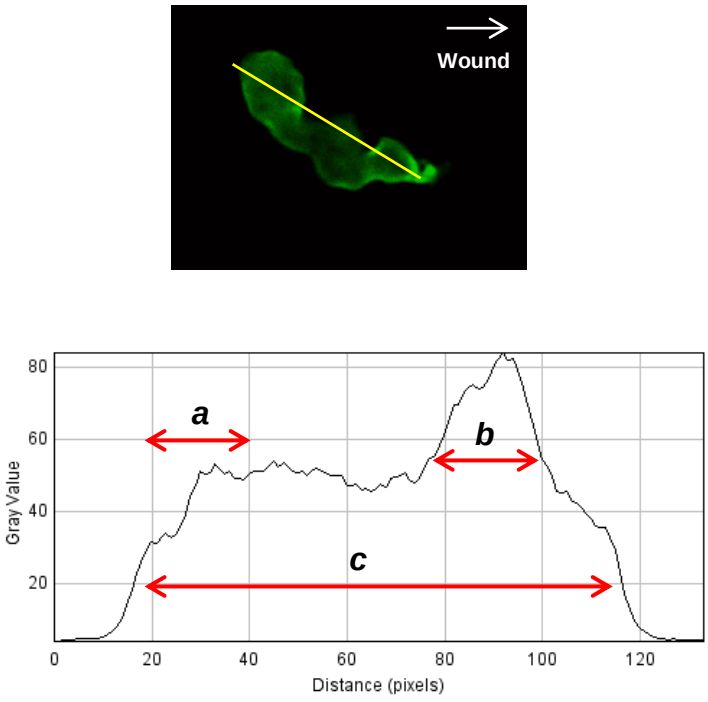

Figure 2.7: A neutrophil with straight-line tool and fluorescence intensity plot profile of a migrating neutrophil. A representative recruited neutrophil with straight-line tool as illustrated in yellow line is matched to a representative plot profile generated in imageJ by drawing a straight line through a migrating neutrophil from the trailing edge towards the leading edge. The fluorescence intensities per pixel were imported into Excel, a threshold was applied and the appropriate pixels were selected to define the trailing edge (a), the leading edge (b) and the whole cell (c).

Subsequently, neutrophil roundness was measured using the 'analyse' function of imageJ (Yoo et al., 2012). In this, using the freehand selections tool, a freehand line was drawn around each cell, and the roundness of each neutrophil was quantified by 'measure' of the analyse function (Figure 2.8). To measure roundness,

$$Roundness = 4 \times [Area] / \pi \times [Major\ axis]^2$$

The value is between 0 and 1, which 0 is a line segment, and 1 is actually a circle.

was calculated.

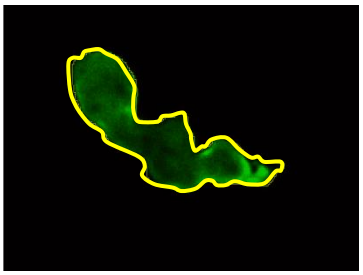

Figure 2.8: A neutrophil with freehand selections tool. A representative recruited neutrophil with freehand line as illustrated in yellow line was analysed using measure of the analyse function of imageJ to calculate the neutrophil roundness.

2.2.4 Murine experiments

2.2.4.1 Murine neutrophil RNA extraction

Murine peripheral blood or bone marrow neutrophil RNA was extracted using the mirVana™ total RNA isolation protocol (Ambion, Austin, USA). Cells ($1x10^6$ per condition) were lysed in 300 µl of mirVana lysis/binding buffer and stored at -80 ˚C if not being extracted immediately. To extract the RNA, miRNA homogenate ($1/10^{th}$ of the lysate volume) was added to the lysate to stabilise the RNA and inactivate RNases. Samples were vortexed (Vortex Genie®2, Scientific Industries, Bohemia, USA) to mix and incubated on ice for 10 minutes. A volume of Acid-Phenol:Chloroform equivalent to that of the initial lysate was added, mixed well using a vortex mixer and spun at 13400 rpm (Eppendorf Mini Spin Hamburg, Germany) for 5 minutes at room temperature. The upper aqueous layer was carefully removed and transferred to a clean RNase-free 1.5 ml eppendorf tube. The volume removed was noted to enable 1.25 volumes of ethanol to be added. Samples were vortexed and a maximum of 700 µl of this aqueous layer/ethanol mixture was transferred onto a filter cartridge within a labelled mirVana kit collection tube. These tubes were spun for 15 seconds at room temperature at 10000 rpm. The flow through was discarded and any remaining aqueous/ethanol mixture was added to the filter cartridge. Once all the aqueous/ethanol mixture had been spun over the cartridge, 700 µl miRNA wash-solution 1 was added to the filter cartridge. Tubes were again spun for

15 seconds at 10000 rpm, the flow through was discarded and washing of the filter cartridge was repeated a further two times using 500 µl miRNA wash-solution 2/3, discarding the flow through after each wash. After the final wash, the tubes were spun for a further 60 seconds to dry the filter cartridge. Cartridges were then placed into a clean labelled collection tube and 30 µl of RNase free water pre-heated to 95 °C was added to the filter cartridge. Tubes were spun again for 20-30 seconds at 13400 rpm. The flow through containing the RNA was then analysed using a NanoDrop™ 1000 spectrophotometer (Fisher Scientific UK Ltd.). cDNA synthesis was performed but due to the low numbers of murine neutrophils and low yield of RNA, 500 ng of RNA were used to make each cDNA sample.

2.2.4.2 Acute lung injury models

Intratracheal instillation of lipopolysaccharide (LPS)

Mice were anaesthetised with ketamine (100 mg/kg i.p; Willows Francis Veterinary, Crawley, U.K.) and acepromazine (5 mg/kg i.p.; C-Vet Veterinary Products, Lancashire, UK) before fur was shaved from their necks. A small (<1 cm) midline incision was made and the trachea exposed through gentle blunt dissection until it could be cannulated under direct vision with a 24G cannula (Jelco® radiopaque cannula, Smiths Medical International Ltd. Rossendale, UK). LPS from *Salmonella minnesota* R595 (TLR*grade*™, Enzo Life Sciences, Exeter, UK) was directly instilled (0.3 µg in 20 µl) via the cannula and the animals recovered for 6 hours in a warmed cage in room air (Rowe *et al.*, 2002).

2.2.5 Statistical analyses

GraphPad Prism® software was used for all Statistical analyses. To compare between two groups, an unpaired two-tailed- t-test was used, and the variances were analysed by an F test. For simultaneous comparisons between multiple groups, a one-way or two-way ANOVA was used with Bonferroni's multiple comparison post-test, and the equal variances were analysed by Bartlett's test. For reverse migration assays, results were analysed by using either linear regression to compare the difference between slopes or non-linear regression to compare the difference between curves, depending on data. On all figures, where * $p<0.05$, where ** $p<0.01$ and where *** $p<0.001$.

Chapter 3: Characterisation of Semaphorin3F expression in human and mouse neutrophils

3.1 Introduction

Neutrophils as key host defence cells are required to migrate to and function at sites of infection or inflammation. In the circulation, resting neutrophils can become activated by bacterial products, cytokines or chemokines such as TNF-α, IL-1β, IL-8, GM-CSF and IFN-γ (Hallett and Lloyds, 1995). Once activated neutrophils leave the circulation and transmigrate through the endothelium towards the inflamed tissue where oxygen is typically scarce (hypoxia), along a chemotactic gradient (Servant et al., 2000).

Recently, the oxygen- sensitive hypoxia inducible factor (HIF) has been identified as a critical regulator of neutrophil survival (Walmsley et al. 2005), and also of important neutrophil functions such as chemotaxis and bacterial killing (Cramer et al. 2003, Peyssonnaux et al. 2005, Peyssonnaux et al. 2007). The oxygen-sensitive hypoxia inducible factor (HIF) transcription factor is modulated by a group of oxygen-sensing hydroxylase enzymes, principally the prolyl hydroxylases (PHDs) (Kaelin and Ratcliffe 2008). Interestingly, our group examined transcript abundance between WT mouse neutrophils and PHD3 (one of the prolyl hydroxylase enzymes)-deficient mouse neutrophils using a whole mouse genome Affymetrix array. While confirming PHD3 was essential for hypoxic regulation of neutrophilic inflammation, we also found that semaphorin3F, which was originally identified as an axon guidance molecule (Dickson, 2002), was the most significantly induced gene in PHD3-deficient neutrophils following hypoxic stimulation (Walmsley et al., 2011). On the basis of these findings, we hypothesised that semaphorin3F may have a role in neutrophil function in response to hypoxia or to inflammation.

Semaphorin3F has also been crucially implicated in the cross talk between tumour cells and the surrounding micro-environment and in the negative feedback on Vascular Endothelial Growth Factor (VEGF)-mediated signals, which are themselves in part HIF-regulated (Capparuccia and Tamagnone 2009). Accumulating evidence has indicated that semaphorin3F antagonises VEGF effects in the context of hypoxic conditions. For example, semaphorin3F negatively affects integrin-linked kinase (ILK)-phosphor-extracellular signal-regulated kinase 1/2 (ERK 1/2) and AKT-signal transducer and activator of transcription 3 (STAT3) signalling, which extend downstream to hypoxia-inducible factor-1α (HIF-1α) protein and VEGF mRNA levels. As a consequence, both HIF-1α and VEGF were reduced in semaphorin3F-transfected lung cancer cell lines (Potiron et al., 2007). In breast cancer cell lines, semaphorin3F and VEGF had opposing effects on cell attachment and spreading (Nasarreet al., 2003). Guo et al. has reported that VEGF and semaphorin3F have opposing roles in regulating neuropilin-2 vascular function in angiogenesis. Thereby, VEGF functions as a potent pro-angiogenic cytokine, whereas semaphorin3F is a potent endogenous angiogenesis inhibitor (Guo et al., 2013). Semaphorin3F is also able to inhibit human endothelial cell survival and migration induced by VEGF (Favier et al., 2006). Antagonism between semaphorin3F and VEFG is also seen to control cell migration and gangliogenesis in the nervous system (Shwarz et al., 2008).

In this chapter, I therefore sought to characterise the expression of semaphorin3F and VEGF in parallel in human neutrophils in response to hypoxia and pro-inflammatory mediators (TNF-α and IL-1β), using human neutrophils isolated from healthy volunteers. Furthermore, semaphorin3F expression in neutrophils recruited to the lung in acute models of neutrophilic inflammation in mouse lung section and semaphorin3F mRNA in murine bronchoalveolar lavage (BAL) neutrophils were investigated.

Aims and hypotheses

Our initial aim is to characterise neutrophil expression of semaphorin 3F in response to culture under physiologically relevant hypoxia and in the presence of pro-inflammatory mediators *in vitro* using human neutrophils. In addition, semaphorin3F expression in inflammatory neutrophils was determined *in vivo* using mouse models as acute models of neutrophilic inflammation.

3.2 Results

3.2.1 Human neutrophils constitutively express semaphorin3F and this is downregulated in response to hypoxia.

First, to investigate whether human neutrophils express semaphorin3F, and how hypoxia regulates semaphorin3F expression, freshly isolated peripheral blood neutrophils from healthy volunteers were cultured in normoxic (21% O_2, 5% CO_2 at 37^oC) and hypoxic (1% O_2, 5% CO_2 at 37^oC) conditions for 4 hours. Cells were lysed using hypotonic sonication lysis buffer, the lysates were then separated by SDA-PAGE with 8% resolving gels. In parallel, breast cancer cell line lysates (MCF7) were run as positive control, and p38-MAPK was used as a loading control.

Figure 3.1A shows a full length blot of semaphorin3F in human neutrophils. Semaphorin3F has an approximate molecular weight of 88 kDa which was apparent in the MCF7 positive control. Although neutrophil-derived semaphorin3F represents slightly different molecular weight from the positive control, it thought to be the correct band regarding the different cell types. Other bands lower in the gel could be non-specific bands from a serum contamination. Figure 3.1 showed that human neutrophils constitutively expressed semaphorin3F protein. This expression was greatest in freshly isolated neutrophils without culture (T0), and was significantly downregulated in neutrophils aged in hypoxia compared to normoxia (densitometry performed relative to p38, *$P<0.05$, n=5 performed as 5 independent experiments) (Figure 3.1).

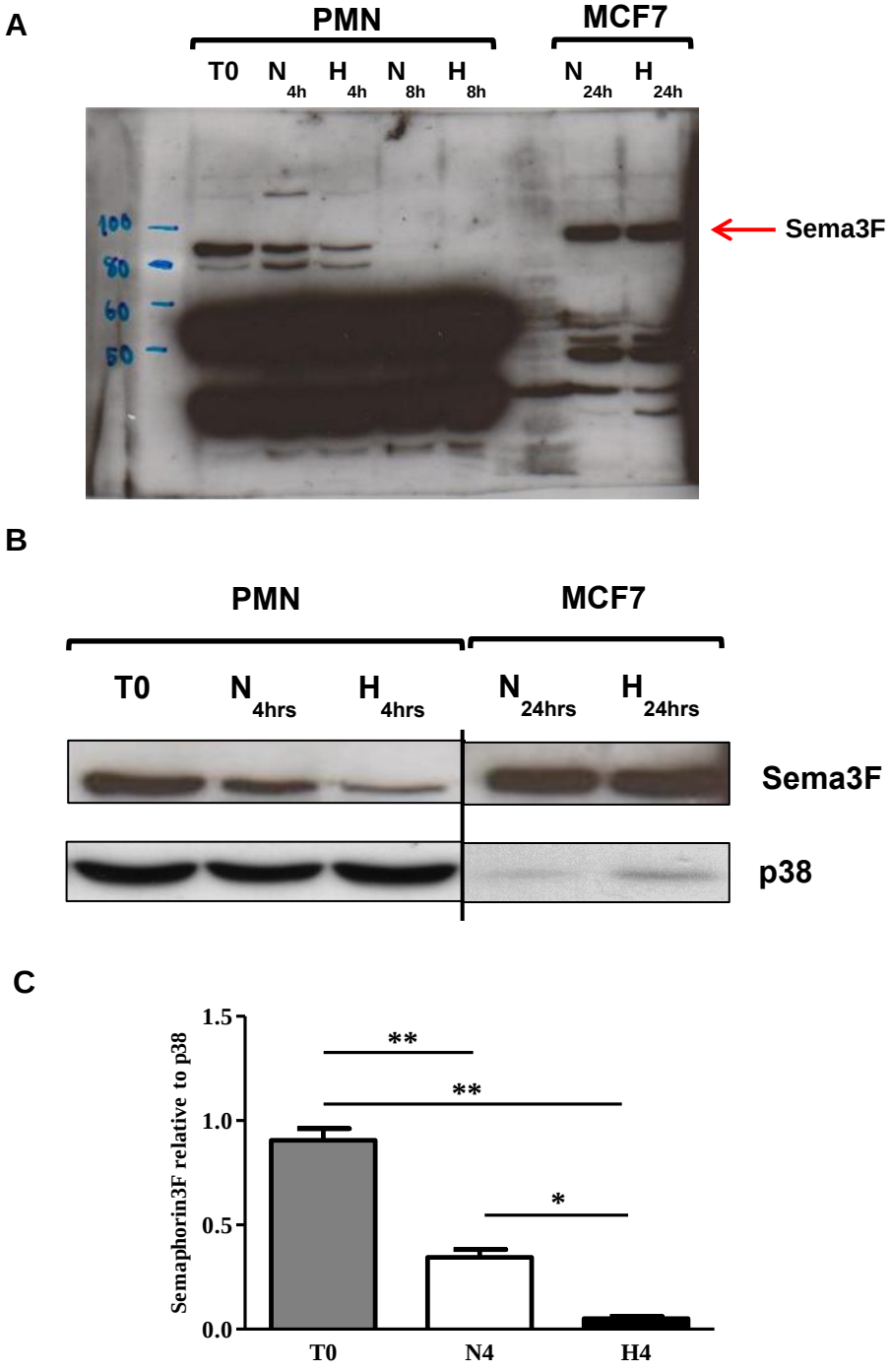

Figure 3.1: Human neutrophils expressed semaphorin3F constitutively and this was downregulated in response to hypoxia. (A) A full length blot of semaphorin3F in human neutrophils (PMNs). Neutrophils were lysed at time 0 or following 4 and 8 hours, and cultured in normoxia (N) or hypoxia (H) (B) Representative blot of semaphorin3F protein in human neutrophils. Human peripheral blood neutrophils (PMNs) and breast cancer cell line (MCF7) cells were sonication lysed in hypotonic lysis buffer at time 0 or following 4 hours for PMNs, and 24 hours for MCF7, cultured in normoxia (N) or hypoxia (H), with p38-MAPK used as a loading control. (B) Densitometry performed relative to p38 in normoxia and hypoxia (n=5), P values were calculated using one-way ANOVA, **P<0.05, **P<0.01.*

3.2.2 The expression of VEGF in human neutrophils is increased in aged hypoxic neutrophils.

Since semaphorin3F and VEGF are known to be antagonistic in other circumstances, I considered that VEGF expression might be regulated differently to semaphorin3F in response to hypoxia. Although VEGF is the downstream target of the hypoxia-inducible factor-1α (HIF-1α), the expression of VEGF in human neutrophils under hypoxic conditions has not been previously investigated. To further understand the previous finding of semaphorin3F expression, I therefore sought to determine VEGF expression in human neutrophils in response to hypoxia. Neutrophils were harvested and lysed using hypotonic sonication lysis buffer, the lysates were then separated by SDA-PAGE with 8% resolving gels. MCF7 cells were used as positive controls, and antibody to p38-MAPK was applied as a loading control. Initially, isolated neutrophils were incubated in normoxia and hypoxia for 4 hours, but I was unable to detect a difference in the intensity of the 46 kDa VEGF band between normoxic and hypoxic conditions. I considered the possibility that VEGF regulation might be delayed compared to semaphorin3F. I therefore incubated neutrophils in both conditions longer for 8 and 20 hours, allowing sufficient time for HIF itself to be induced and to enhance the transcription of its downstream target genes including VEGF.

As a result, hypoxic neutrophils exhibited considerable expression of VEGF and this was significantly upregulated after 20 hours compared to normoxia (densitometry performed relative to p38, $*P<0.05$, n=3 performed as 3 independent experiments) (Figure 3.2). Moreover, VEGF expression declined in aged normoxic neutrophils.

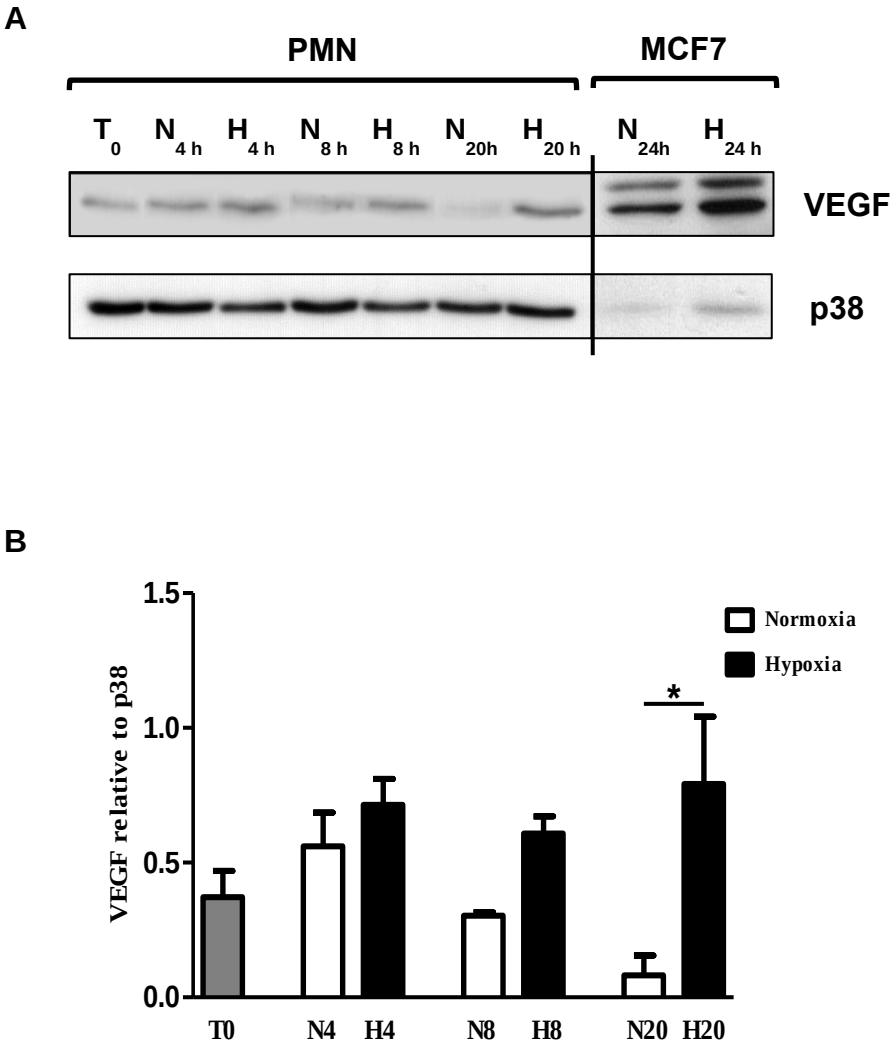

Figure 3.2: Human neutrophils expressed VEGF and this was significantly upregulated in response to hypoxia after 20 hours compared to normoxia. (A) Western blot analysis of sema3F protein in human neutrophils. Human peripheral blood neutrophils (PMNs) and breast cancer cell line (MCF7) cells were sonication lysed in hypotonic lysis buffer at time 0 or following 4, 8 and 20 hours for PMNs, and 24 hours for MCF7, cultured in normoxia (N) or hypoxia (H), with p38-MAPK used as a loading control. (B) Densitometry performed relative to p38 in normoxia and hypoxia (n=3), P values were calculated using one-way ANOVA **P<0.05*.

3.2.3 Pro-inflammatory cytokines (TNF-α, IL-1β) overcome hypoxic suppression of semaphorin3F expression.

In this section, I focused on semaphorin3F expression in response to inflammatory conditions including hypoxia and the presence of pro-inflammatory mediators. Since neutrophil function in inflammation is a highly regulated process requiring pro-inflammatory cytokines, this led me to question how pro-inflammatory cytokines such as TNF-α and IL-1β, which are required for local recruitment of neutrophils to the site of inflammation (Blond et al., 2002) (Vieira et al., 20009), modulate the expression of semaphorin3F in hypoxia. I decided to choose TNF-α and IL-1β for this experiment as neutrophil migration during inflammation was particularly investigated. To address this question, normoxic or hypoxic aged human neutrophils were incubated in the presence or absence of TNF-α and IL-1β for 4 hours. Western blot was carried out to analyse the expression of semaphorin3F protein.

Hypoxic suppression of semaphorin3F expression was partially rescued by co-incubation of neutrophils with TNF-α and IL-1β (densitometry performed relative to p38, $^{**}P<0.01$, $^{*}P<0.05$, n=4 performed as 4 independent experiments) (Figure 3.3).

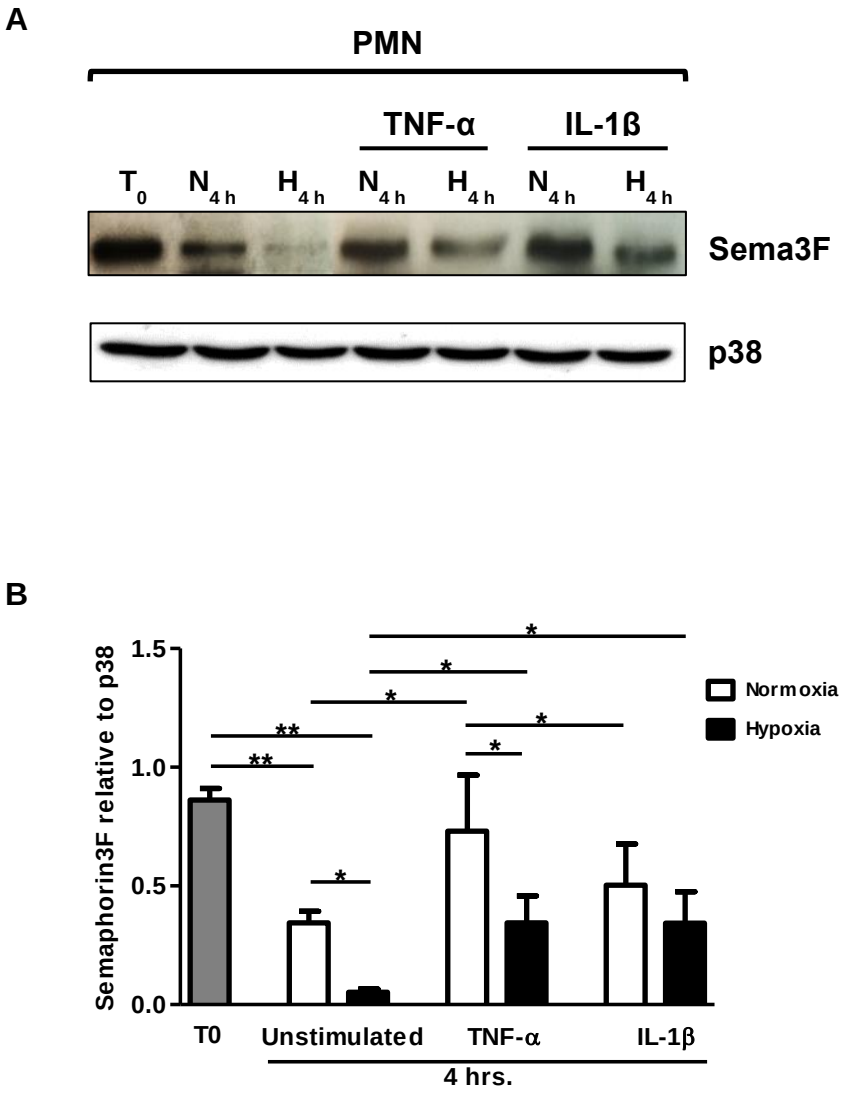

Figure 3.3: Pro-inflammatory cytokines (TNF-α, IL-1β) overcome hypoxic suppression of semaphorin3F expression. (A) Western blot analysis of sema3F protein in human neutrophils. Human peripheral blood neutrophils (PMNs) were lysed at time 0 or following 4 hours +/- TNF-α or IL-1β PMNs culture in normoxia (N) or hypoxia (H), with p38-MAPK used as a loading control. (B) Densitometry performed relative to p38 of sema3F at time 0 or following 4 hours in normoxia and hypoxia (n=4), P values were calculated using one-way ANOVA **P<0.05, **P<0.01*.

3.2.4 Proinflammatory cytokines (TNF-α, IL-1β) enhance VEGF expression in hypoxia.

To determine the expression of VEGF, which might be affected by pro-inflammatory cytokines, freshly isolated human neutrophils were cultured in the presence and absence of TNF-α and IL-1β for 4 hours in normoxic or hypoxic conditions. Western blot was performed to assess the expression of VEGF protein.

TNF-α and IL-1β similarly enhanced VEGF expression in hypoxia. VEGF expression in the presence of TNF-α and IL-1β was significantly induced in hypoxia compared to normoxia with the same stimulation or compared to unstimulated neutrophils (densitometry performed relative to p38*, *P<0.05*, n=3 performed as 3 independent experiments) (Figure 3.4).

These findings indicated that pro-inflammatory cytokines TNF-α and IL-1β could modulate the expression of semphorin3F as well as VEGF under hypoxic conditions.

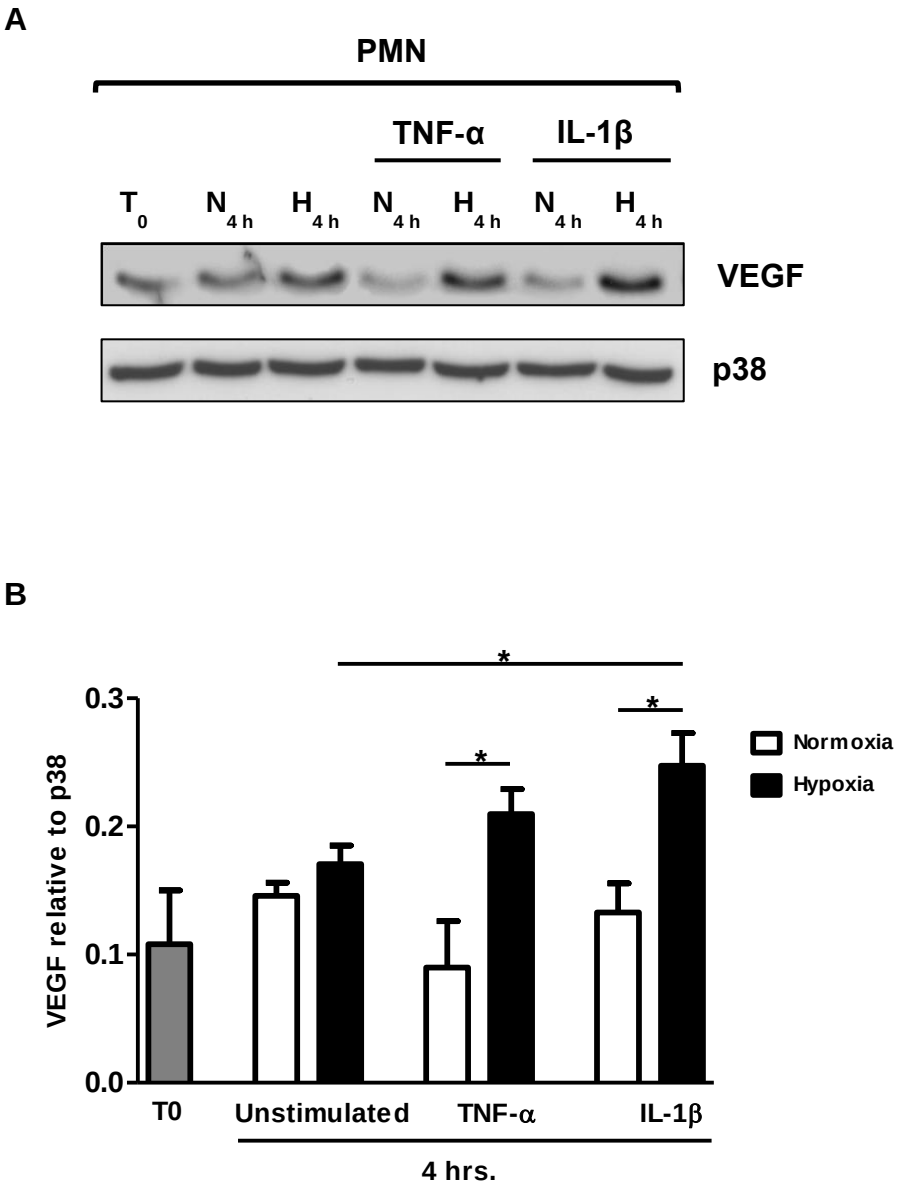

Figure 3.4: Pro-inflammatory cytokines (TNF-α, IL-1β) enhance VEGF expression in hypoxia. (A) Western blot analysis of VEGF protein in human neutrophils. Human peripheral blood neutrophils (PMNs) were sonication lysed in hypotonic lysis buffer at time 0 or following 4 hours +/- TNF-α (10 ng/ml) or IL-1β (10 ng/ml) PMNs culture in normoxia (N) or hypoxia (H), with p38-MAPK used as a loading control. (B) Densitometry performed relative to p38 of VEGF at time 0 or following 4 hours in normoxia and hypoxia (n=3), P values were calculated using one-way ANOVA *$P<0.05$.

3.2.5 Semaphorin3F expression in acute models of neutrophilic inflammation

To explore the expression of semaphorin3F in neutrophilic inflammation in *vivo,* an acute model of lung injury in mice was performed. LPS was directly instilled via the intratracheal route, inducing acute lung injury. Six hours after LPS instillation, mice were recovered in environmental normoxia or hypoxia. Mice were sacrificed at 24 hours, lung sections were stained for expression of the neutrophil marker myeloperoxidase (MPO) and semaphorin3F (data with permission from Dr.Sarah Walmsley).

Semaphorin3F was co-localised to MPO positive cells (i.e. neutrophils) both in normoxia and hypoxia. Semaphorin3F expression was markedly induced in neutrophils in hypoxic conditions compared to normoxia (Figure 3.5). This finding indicated that semaphorin3F was upregulated in neutrophils recruited to the lung in acute models of neutrophilic inflammation (data with permission from Dr.Sarah Walmsley).

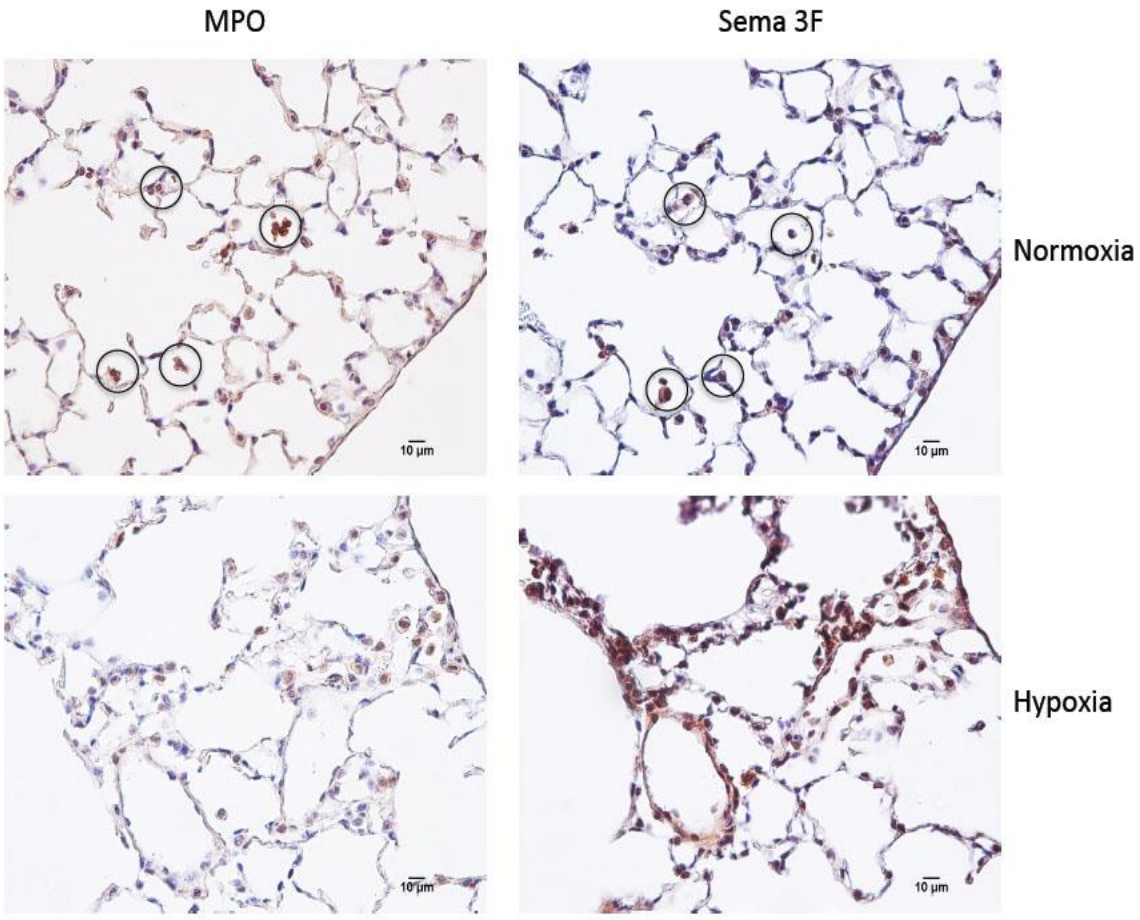

Figure 3.5: Semaphorin3F expression was marked induced in neutrophils recruited to the lung in acute models of neutrophilic inflammation. An acute lung injury was induced by intratracheal LPS installation. Six hours after LPS, mice were recovered in environmental normoxia or hypoxia. Mice were sacrificed at 24 hours. Lung sections were stained for expression of the neutrophil marker MPO and semaphorin3F (deep purple/black staining) (data with permission from Dr.Sarah Walmsley).

3.2.6 Semaphorin3F mRNA expression was upregulated in murine bronchoalveolar lavage (BAL) neutrophils.

To further characterise the semaphorin3F expression in response to inflammation *in vivo*, semaphorin3F mRNA in murine bronchoalveolar lavage (BAL) neutrophils was quantified. Acute lung injury in mice was induced by intratracheal LPS installtion. Then, 6, 24 and 48 hours after LPS, mice were recovered in environmental hypoxia. Mice were sacrificed, BAL cell pellets were collected, and cDNA was then extracted. The cDNA samples of each condition were applied to TaqMan® gene expression assays. Beta-actin (ACTB) was selected as the endogenous control as it is highly expressed and expression is not altered by hypoxia (data with permission from Dr.Sarah Walmsley).

The expression of semaphorin3F mRNA was significantly upregulated in BAL neutrophils at all time points (6, 24 and 48 hours) compared to peripheral blood neutrophils (PBT0) (data normalized to beta-actin expression, ****P<0.001*, n=4) (Figure 3.6). These results demonstrated that semaphorin3F was markedly induced in neutrophilic inflammation at mRNA level using a murine acute lung injury model (data with permission from Dr.Sarah Walmsley).

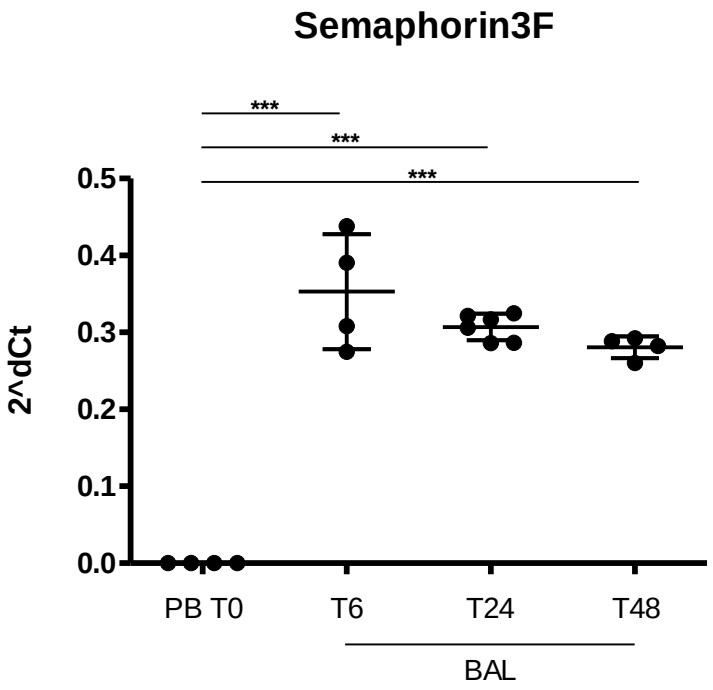

Figure 3.6: Semaphorin3F mRNA expression was upregulated in murine bronchoalveolar lavage (BAL) neutrophils. Fold change in expression of semaphorin3F following acute lung injury with LPS. Mice were recovered for 6, 24 and 48 hours in hypoxia. BAL cells were then collected, and cDNA was extracted. TaqMan analysis of cDNA was performed with data normalized to beta-actin (*ACTB)* expression. Data show mean and SEM of fold change compared to peripheral blood neutrophils (PBT0), n=4-6 (1 independent experiment), analysed by ANOVA, ****P<0.001* (data with permission from Dr.Sarah Walmsley).

3.3 Discussion

Semaphorin3F is widely expressed in most tissues both in neuronal and non-neuronal tissues (Luo et al., 1993), but no evidence for the expression of semaphorin3F in neutrophils has been identified. In this chapter, I have characterised semaphorin3F expression in human and mouse neutrophils in response to hypoxic and to inflammatory conditions. In parallel, the expression of a well-known downstream target of HIF-1α, VEGF, in human neutrophils was determined.

3.3.1 The expression of VEGF

VEGF is a part of the hypoxic response that is upregulated by the HIF hydroxylase pathway (Shweiki et al., 1992). Recently, VEGF expression and secretion have been characterised in a variety of human cell types such as human vascular smooth muscle cells (HSMC) (Breier et al., 1992), mononuclear cells (Iijima et al., 1993), and neutrophils (Gaudry et al., 1997). Human neutrophils express mRNA for the two common VEGF splice variants, namely $VEGF_{121}$ and $VEGF_{165}$ ((Webb et al., 1998). The release of VEGF by human neutrophils under hypoxic conditions was investigated by other groups demonstrating that the incubation of human neutrophils in hypoxia for time period between 0.5 to 24 hours did not cause a significant increase in soluble VEGF in supernatants compared to normoxic conditions. Moreover, detection of mRNA expression of VEGF in neutrophils revealed no significant differences in VEGF mRNA after 8, 12 or 24 hours exposure to normoxia or hypoxia (Koehne et al., 2000). Here, I provide evidence that protein levels of VEGF in human neutrophils are unchanged between normoxia and hypoxia after 4 or 8 hours incubation, whereas VEGF expression is significantly induced in response to hypoxia after 20 hours. One possibility for the delayed upregulation of VEGF protein is that cells exposed to hypoxia require an increase of VEGF transcription rate mediated by binding of HIF-1 to a hypoxia responsive element located in the 5'-flanking region of the VEGF gene. Once the VEGF gene is transcribed, VEGF mRNA

is bound by RNA-binding proteins that inhibit its degradation under hypoxic conditions. Following an increase in the stability of VEGF mRNA, VEGF protein is then efficiently translated (Levy et al., 1998). Another possibility is the relationship between VEGF and semaphorin3F. Potiron et al. reported that in lung cancer cells, semaphorin3F expression reduces AKT and signal transducer and activator of transcription 3 (STAT3) phosphorylation, which changes downstream VEGF mRNA levels (Potiron et al., 2007). Here, after incubation of neutrophils under hypoxic conditions for 8 hours, semaphorin3F expression totally disappears suggesting that the inhibition of VEGF expression by semaphorin3F is abrogated after 8 hours.

By contrast, VEGF expression in neutrophils cultured with TNF-α or IL-1β is significantly increased after 4 hours under hypoxic conditions compared to normoxic control suggesting that neutrophil-derived VEGF is modulated during inflammation. Likewise, other groups have shown association between activated neutrophils and VEGF expression in the acute inflammatory response. Isolated neutrophils incubated in the presence of TNF-α for 4 hours significantly produce VEGF compared with control (Webb et al., 1998). Taichman et al. demonstrated that neutrophils infiltrating inflamed tissues are a potential source of VEGF. VEGF release is significantly induced by neutrophils exposed to an inflammatory stimulus after 30 minutes, over 70% compared to unstimulated control (Taichman et al., 1997). Furthermore, neutrophil-derived VEGF is upregulated in numerous human inflammatory lesions such as mucosa in mucus extravasation phenomenon or mucocele (Taichman et al., 1997), synovial fluids and rheumatoid synovial tissue (Fava et al., 1994), healing wounds (Brown et al., 1992), and in delayed hypersensitivity reactions (Brown et al., 1995).

3.3.2 The expression of semaphorin3F

Whilst semaphorin3F has been reported to be expressed in a variety of cell types, there is currently little literature regarding semaphorin3F expression in neutrophils. Here, I reveal a series of semaphorin3F expression patterns in response to hypoxia, to pro-inflammatory mediators, and in an acute model of neutrophilic inflammation. I initially found that isolated peripheral blood neutrophils express semaphorin3F, which is significantly downregulated in response to hypoxia. However, this suppression of semaphorin3F is rescued by pro-inflammatory cytokines; TNF-α and IL-1β. These findings indicate that hypoxia can regulate neutrophil-derived semaphorin3F expression. Consistently, other cell types demonstrate a similar correlation between hypoxia and semaphorin3F expression. Human U87MG glioblastoma and A375SM melanoma cells cultured in hypoxic conditions show an inhibition of semaphorin3F-induced biological activity. In addition, when those cells are treated with an inhibitor of prolyl hydroxylation of HIF-1; DFO, semaphorin3F activity is also suppressed, suggesting that besides physical hypoxia, semaphorin3F is regulated by HIF-1 (Silvia et al., 2011). In turn, semaphorin3F shows an ability to modulate HIF-1 expression. Recent evidence has revealed that semaphorin3F expression caused loss of HIF-1α mRNA levels in lung cancer cell line H157 cells (Potiron et al., 2007). Furthermore, based on our previous observation in PHD3-deficient neutrophils following hypoxic stimulation, semaphorin3F transcript was the most upregulated in the context of inhibition of prolyl hydroxylation of HIF-1α. These findings also support the findings here that hypoxia and HIF regulate the expression of semaphorin3F in neutrophils.

On the other hand, in the presence of TNF-α and IL-1β, the hypoxic suppression of semaphorin3F protein in human neutrophils was significantly inhibited. Semaphorin3F expression of mouse lung sections with acute neutrophilic inflammation was markedly induced in hypoxia compared to normoxia. This is consistent with the finding that semaphorin3F mRNA was significantly upregulated in bronchoalveolar lavage (BAL) mouse neutrophils compared to peripheral blood neutrophils. These findings indicate that

semaphorin3F expression is upregulated in response to inflammation both at mRNA and protein level. It has been seen that semaphorin3F is further regulated by the activity of additional factors released in the inflammatory microenvironment. Here, semaphorin3F might be inducible in neutrophils with the presence of pro-inflammatory cytokines or other inflammatory responses or signals rather than by hypoxia alone. For example, in multiple sclerosis, an inflammatory condition, increased semaphorin3F mRNA expression is seen in multiple sclerosis lesions. Semaphorin3F is also only detected around active inflammatory lesions suggesting that it is associated with inflammatory processes of plaque formation (Williams et al., 2007). Furthermore, kruppel-like factor 2 (KLF2), known as a regulator of endothelial pro-inflammatory activation, can potently induce semaphorin3F expression during inflammation (Dekker et al., 2006). Notably, semaphorin3F expression in response to hypoxia was markedly induced in neutrophils in incubation with TNF-α and IL-1β, which are required for local recruitment of neutrophils to the site of inflammation (Blond et al., 2002) (Vieira et al., 20009), suggesting that semaphorin3F might be upregulated once neutrophils receive recruitment signals or once they reach the site of inflammation.

This led me to question how semaphorin3F may regulate neutrophil function during inflammation, including neutrophil recruitment to the inflamed site, and the biological functions of recruited neutrophils at the site of inflammation or after during the resolution phase. Thus, in the next chapter, I determined the role of semaphorin3F in neutrophilic inflammation *in vivo* using zebrafish models.

3.3.3 Conclusions

In conclusion, I have provided evidence that human neutrophils express semaphorin3F, which is modulated by hypoxia or inflammatory stimuli. Semaphorin3F is significantly upregulated in response to inflammation both at mRNA and protein levels. Isolated human neutrophils also express VEGF. Under hypoxic conditions, VEGF expression is the inverse of semaphorin3F. I hypothesised that the markedly regulatable semaphorin3F expression in inflammation might be instrumental in regulating neutrophil responses during inflammation.

Chapter 4: Investigation of the role of semaphorin3F in neutrophil behaviour in inflammation using the genetically tractable zebrafish

4.1 Introduction

In the previous chapter, assessment of semaphorin3F expression in human peripheral blood neutrophils suggested that semaphorin3F expression is modulated in response both to inflammatory mediators and by regional hypoxia. The marked induction of semaphorin3F in neutrophils recruited to the lung in acute models of neutrophilic inflammation led me to question whether semaphorin3F, acting either in an autocrine or paracrine fashion, may itself be regulating neutrophil recruitment to or persistence at sites of inflammation.

Since the first semaphorin protein, semaphorin4D, was described to have immunoregulatory functions in B-cell/dendritic cell activation (Kumanogoh et al., 2000), emerging evidence indicates that several semaphorins are crucially involved in immune responses. For instance, semaphorin4A is produced by mature macrophages recruited at injury sites suggesting that it regulates macrophage functions during inflammation (Meda et al., 2012). Hypoxia-induced semaphorin3A acts as an attractant for tumour-associated macrophage recruitment to and retention in hypoxic environment (Casazza et al., 2013). Furthermore, semaphorin7A induction on endothelia through HIF-1α can promote neutrophil migration during hypoxia (Morote-Garcia et al., 2012). Taken together with my observation that semaphorin3F expression is modified in human neutrophils in the context of infection, I therefore questioned whether semaphorin3F may specifically have a role in neutrophil migration.

To directly investigate the effect of semaphorin3F on neutrophil recruitment to and resolution of an inflammatory response *in vivo*, I turned to the zebrafish. Zebrafish (Danio rerio) is a small tropical fresh-water fish that has recently emerged as an excellent non-mammalian vertebrate model organism to enable real-time study of the vertebrate immune system (Trede et al., 2004). It is a genetically tractable organism, possessing many similar cell types, including neutrophils, macrophages and eosinophils, and immune pathways to mammalian systems (Bennett et al., 2001). Moreover, zebrafish has advantages of large number of offspring, short generation time and transparency of embryos.

Prior to study of zebrafish models of tissue injury and repair, I addressed whether semaphorin3F is conserved across species and more specifically whether zebrafish carry orthologs to human. Importantly, I identified that zebrafish do express semaphorin3F, but unlike humans and mice where one copy of semaphorin3F is described, and in keeping with the reported duplication of many other genes, zebrafish have two copies of semaphorin3F, namely semaphorin3Fa and semaphorin3Fb. Both copies are orthologs of human semaphorin3F and have 70% DNA sequence identity to human semaphorin3F, compared to 96% identity between murine and human semaphorin3F. In addition, zebrafish semaphorin3F is the most closely related to human semaphorin3F compared to other class 3 zebrafish semaphorins. Although semaphorin3G was also reported to be similar to human semaphorin3F, it maps to a region of the genome that is syntenic with a region of the human X chromosome that no longer contains semaphorin genes, suggesting that semaphorin3G orthologs have been lost during evolution (Yu and Moens, 2005) (ENSEMBL BLAST) (Figure 4.1). Although zebrafish semaphorin3F has less similarity to the human than mouse semaphorin3F, the zebrafish system provides the opportunity to study the inflammatory response of neutrophils *in vivo* using real time imaging to follow neutrophil migration to and from the site of injury (Renshaw et al., 2006).

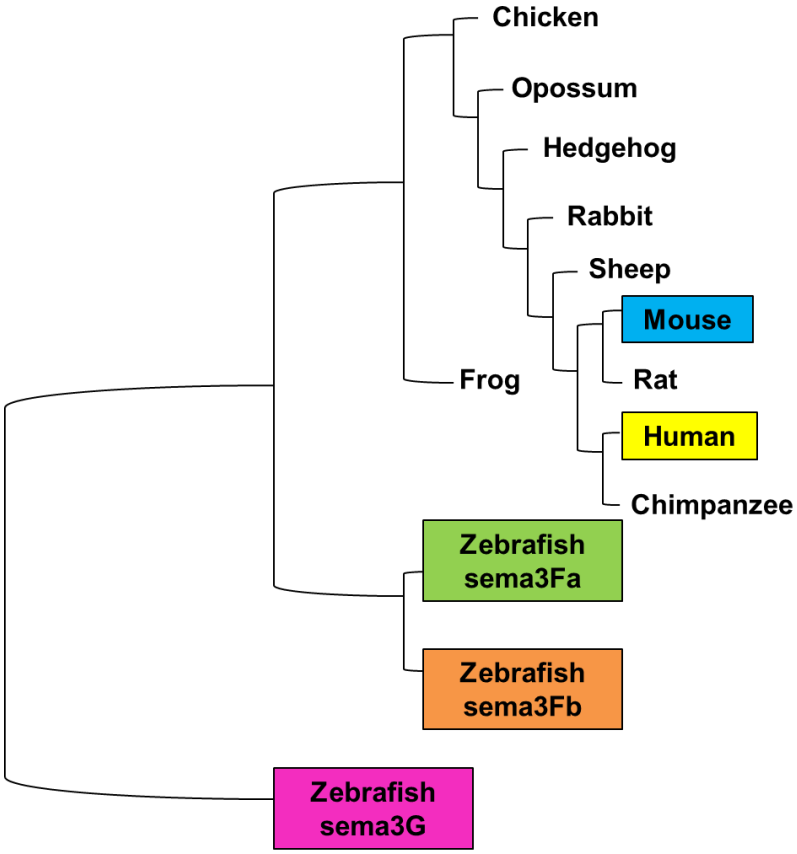

Figure 4.1: The phylogenetic tree of zebafish semaphorin3F gene and other vertebrate semaphorin3 referred to ENSEMBL (http://www.ensembl.org). Zebrafish has two copies of semaphorin3F; semaphorin3Fa and semaphorin3Fb. These both copies are duplicated orthologs to human semaphorin3F and have similarities to human semaphorin3F 70 percent. Zebrafish semaphorin3F is the most closely related to mammalian semaphorin3F compared to other class 3 zebrafish semaphorins. Mouse semaphorin3F has similarity to human semaphorin3F 96 percent. In all cases, the zebrafish semaphorin3F is more closely related to the semaphorin3F of other species than to other class 3 semaphorins of those species, and is also more closely related to those semaphorin3F than any of the other zebrafish class 3 semaphorins (zebrafish semaphorin3G, the next most closely related, is included for comparison).

To examine neutrophil behaviour during inflammation, an established transgenic zebrafish line Tg(*mpx:GFP*)*i114*, subsequently referred to as *mpx*:GFP, was used. The *mpx*:GFP zebrafish expresses green fluorescent protein (GFP) under the *mpx* promotor which allows the visualisation and quantitation of neutrophils (Renshaw et al., 2006). Due to the transparency of

zebrafish embryos, the inflammatory responses of neutrophils can be easily observed *in vivo* using such transgenically labelled neutrophil populations (Martin and Renshaw, 2009). The migratory behaviour of neutrophils during inflammation, including the number of neutrophils recruiting to the site of injury at the recruitment phase and the number of neutrophils persisting at the site of injury at the resolution phase, was assessed using the previously described injury model (Renshaw et al., 2006).

After injury to the tail fin of zebrafish embryos, *mpx*:GFP labelled neutrophils can be imaged as they migrate to the injury site. The recruitment of neutrophils to the injury site occurs with the highest number of neutrophils present at the wound at 6 hours after injury, followed by spontaneous resolution by 24 hours after injury. The data can be quantified by counting of green fluorescent neutrophils at the site of injury. The time course of the zebrafish response followed in this way is comparable with mammalian models of neutrophilic inflammation (Renshaw et al., 2006).

In addition, the *mpx*:GFP zebrafish provides a model in which individual labelled neutrophils can be identified and tracked *in vivo* to investigate their motility in real-time allowing quantification of the speed and direction of individual neutrophil migration (Elks et al., 2011).

Aims and hypotheses

My hypothesis is that semaphorin3F will affect neutrophil migration *in vivo*. My aim in this chapter is to test this *in vivo* by manipulating semaphorin3Fa and semaphorin3Fb expression (overexpression and knockdown) in zebrafish while following neutrophil migration to and from the injury site.

4.2 Results

4.2.1 Identification of zebrafish semaphorin3Fa and semaphorin3Fb expression

Unpublished microarray data from Professor Stephen Renshaw's group, which profiled GFP sorted neutrophils from *mpx*:GFP fish, showed that zebrafish neutrophils express semaphorin3Fa and semaphorin3Fb at low levels. I subsequently performed whole mount *in situ* hybridisation to further quantify semaphorin3Fa and semaphorin3Fb expression at 20-somite stage and 3 day postfertilization (dpf) of *mpx*:GFP embryos.

Embryos were collected and fixed at 20-somite stage and 3 dpf, then stained with semaphorin3Fa or semaphorin3Fb anti-sense probes. In addition, semaphorin3Fa or semaphorin3Fb sense probes were used as controls. 20-somite stage embryos expressed both copies of semaphorin3F, but in different patterns (Figure 4.2). Semaphorin3Fa was expressed in the root of zona limitans intrathalamica, anterior dorsal portion in the midbrain and hindbrain, and pharyngeal arches. Semaphorin3Fb was observed in the anterior neural ridge, rhombomeres 3 and 5, and notochord. Meanwhile, in 3 dpf embryos, both semaphorin3Fa and semaphorin3Fb were expressed in head and blood vessels, however, semaphorin3Fb is additionally observed in the spinal cord (Figure 4.3).

These observations are in general agreement with previous studies (Yu and Moens, 2005). However, these did not address expression in neutrophils. Unfortunately, due to the inability to resolve *in situ* hybridisation labelling to the level of single cell expression, we were unable to confirm whether neutrophils expressed semaphorin3Fa and semaphorin3Fb *in vivo* by *in situ* hybridisation on intact whole embryos.

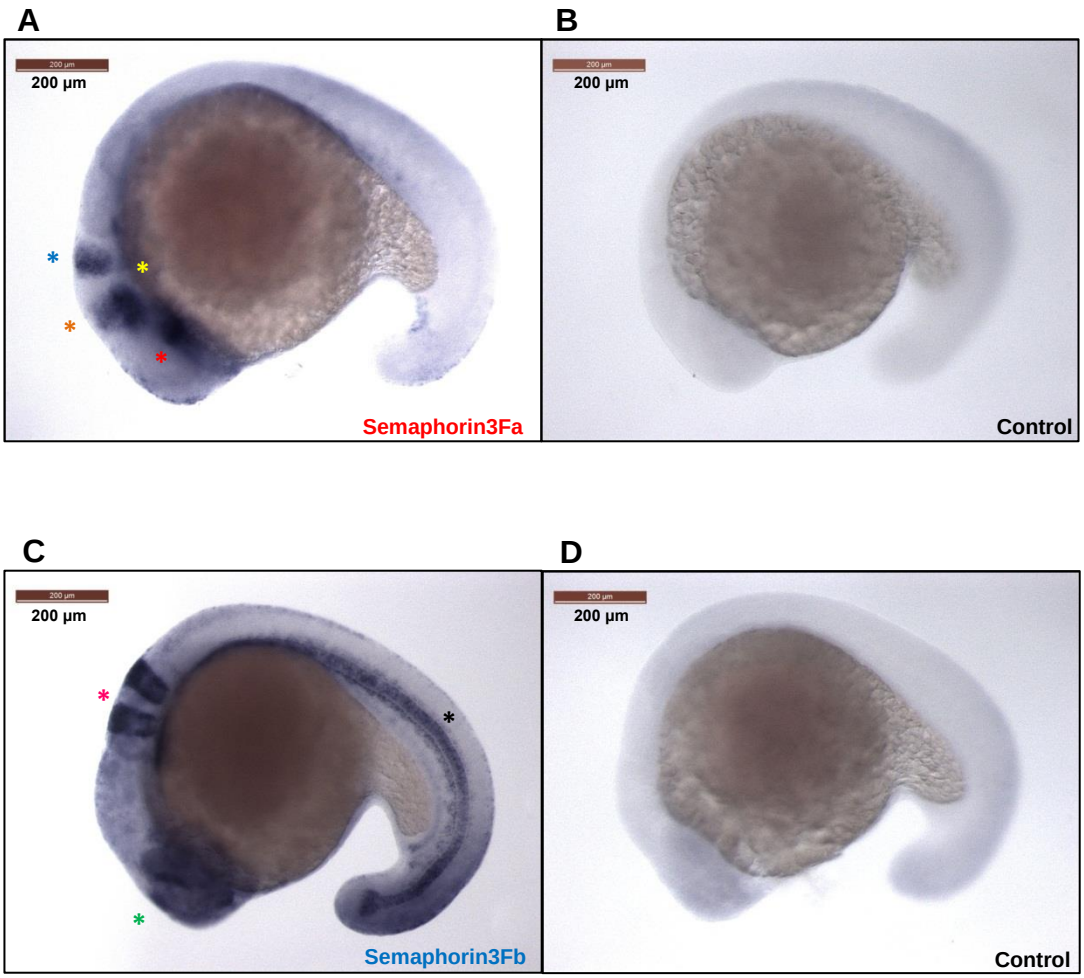

Figure 4.2: 20-somite stage embryos showed differential expression of semaphorin3Fa and semaphorin3Fb. Expression of zebrafish semaphorin3F was identified by in situ hybridisation. RNA Probes include 2 copies of zebrafish semaphorin3F (*semaphorin3Fa* and *semaphorin3Fb*). (A-B) 20somite stage embryos were stained with semaphorin3Fa. The expression of semaphorin3Fa was observed in the root of zona limitans intrathalamica (*), anterior dorsal portion (in the midbrain (*) and hindbrain (*)), and pharyngeal arches (*). (C-D) 20somite stage embryos were stained with semaphorin3Fb. Semaphorin3Fb was expressed in the anterior neural ridge (*), rhombomeres 3/5 (*) and notochord (*).

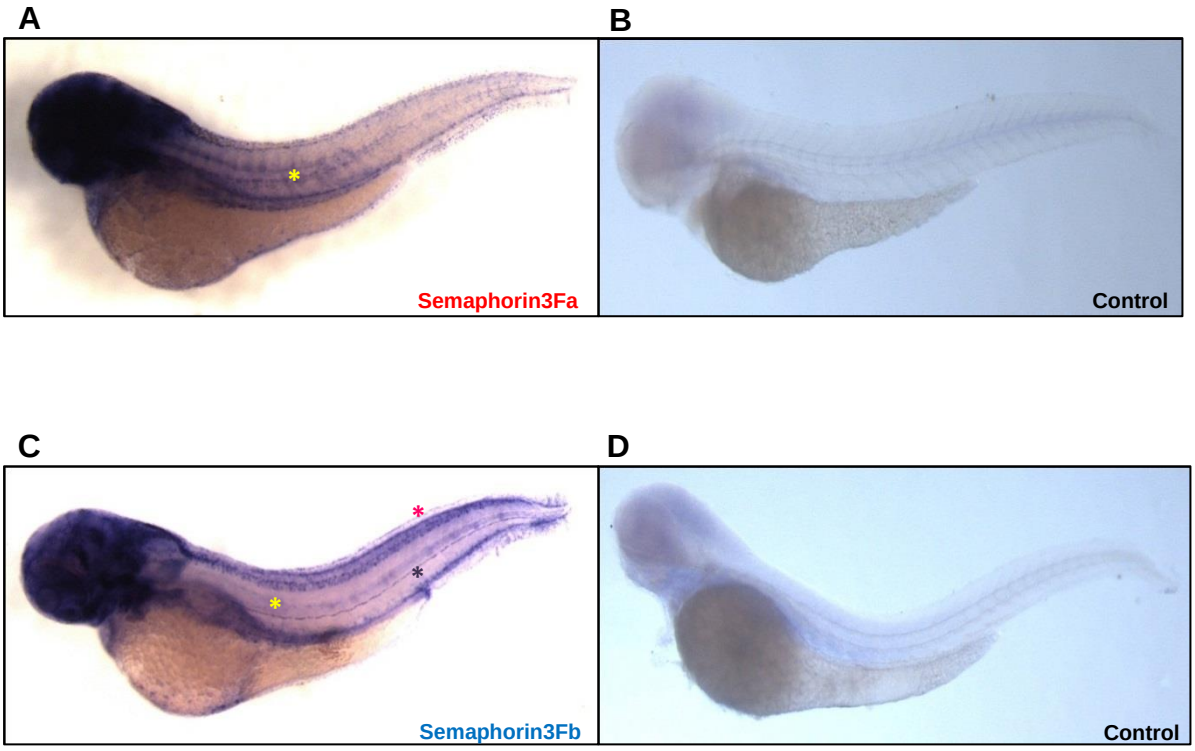

Figure 4.3: 3 days post fertilization (dpf) embryos showed differential expression of semaphorin3Fa and semaphorin3Fb. Expression of zebrafish semaphorin3F was identified by in situ hybridisation. RNA Probes include 2 copies of zebrafish semaphorin3F (*semaphorin3Fa* and *semaphorin3Fb*). (A-B) 3dpf embryos were stained with semaphorin3Fa and (C-D) semaphorin3Fb, respectively. Both semaphorin3Fa and semaphorin3Fb are expressed in head and blood vessels (*), however, semaphorin3Fb is additionally observed in the spinal cord (*). Note that by this time semaphorin3Fb expression in the notochord (*) has diminished.

Because we could not discern whether neutrophils expressed semaphorin3F in neutrophils in uninjured embryos, I hypothesised that if semaphorin3F was induced in embryos in parallel with inflammation, the expression of semaphorin3F from neutrophil cells might be visible after tissue injury. For this, *mpx*:GFP embryos were injured at 2 dpf. Then, embryos were fixed at 3, 6 and 24 hours post injury (hpi), and stained with semaphorin3Fa or semaphorin3Fb RNA probe.

Semaphorin3Fa expression in the injured embryos in general was similar to that found previously in uninjured embryos. Semaphorin3Fa was expressed in the head, blood vessels, muscles, tissues and epithelial cells through all time points. However, at 6 hpi and 24 hpi, semaphorin3Fa expression was also notably upregulated in the tissues adjacent to the site of tail transection (Figure 4.4).

In the same manner, semaphorin3Fb expression was observed in the head, blood vessels, muscles, tissues, epithelial cells and spinal cord. Interestingly, injured embryos again showed marked upregulation adjacent to the upper region of the site of injury at 6 and, to a lesser extent, at 24 hpi (Figure 4.5).

The strong expression adjacent to the site of tail transection at 6 hpi and 24 hpi is clearly affecting a veriety of cell types, including most obviously notochord, but also possibly neural cells in the spinal cord. Whether this also includes neutrophils remains difficult to determine, particularly against the background of expression in these other tissues. However, it is clear that in the injured fish semaphorin3F expression is upregulated in inflamed tissues *in vivo*. These findings are consistent with the previous result of semaphorin3F expression in mouse lung sections of acute models of neutrophilic inflammation. Given our evidence of semaphorin3F expression in human neutrophils and the marked upregulation of semaphorin3F in inflamed tissues, I next tested the effect of manipulating semaphorin3F expression *in vivo*.

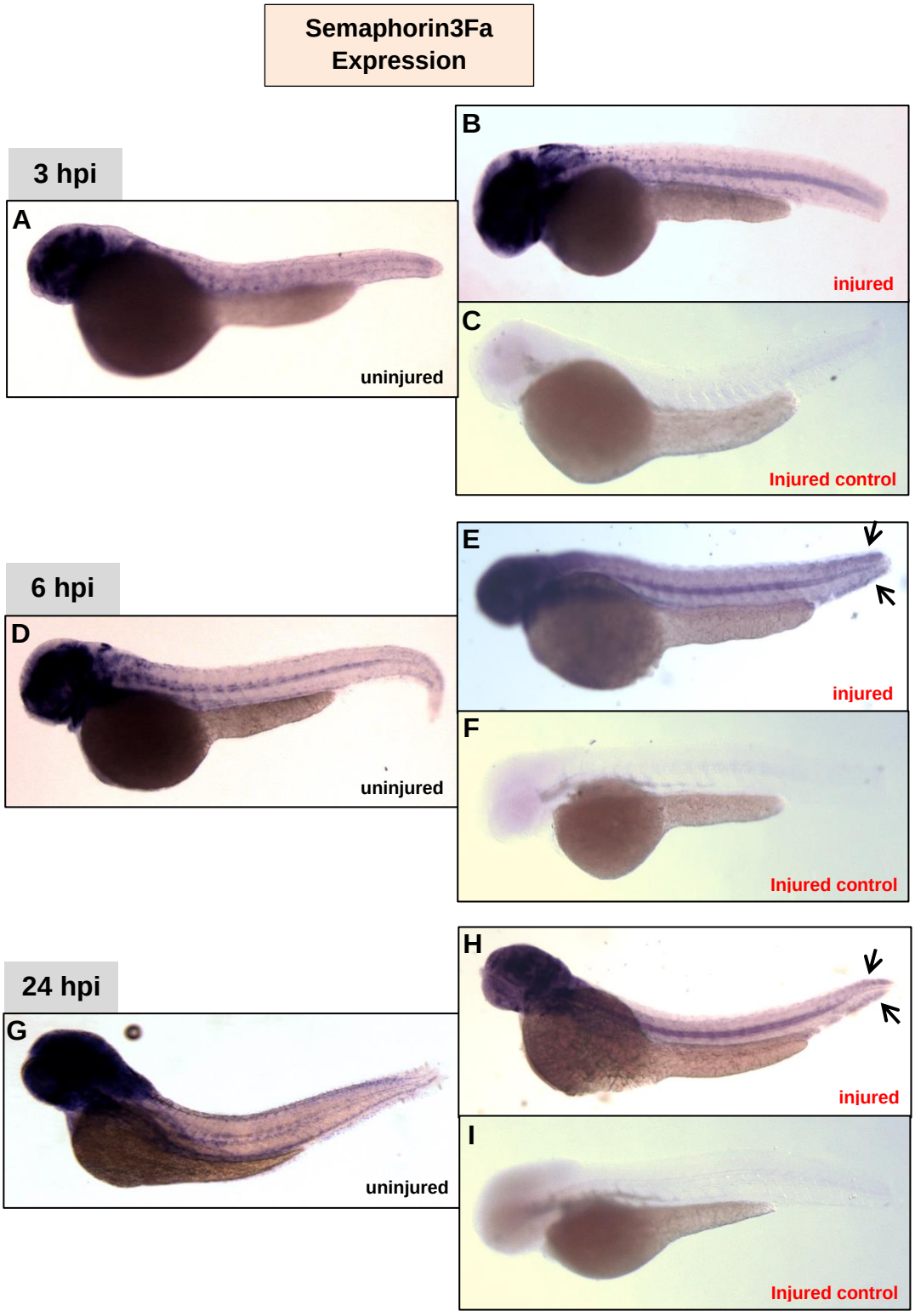

Figure 4.4: Semaphorin3Fa expression with tail fin injury. Tailfin transection was performed in 2dpf mpx:GFP embryos, then the embryos were fixed at 3 hpi (A-C), 6 hpi (D-F) and 24 hpi (G-I). The expression of zebrafish semaphorin3Fa was identified by in situ hybridization. All embryos were stained with semaphorin3Fa probe. Semaphorin3Fa was expressed in the same pattern at each time point both in uninjured and injured embryos. Interestingly, at 6 hpi and 24 hpi semaphorin3Fa expression was additionally observed at the injury sites (arrows).

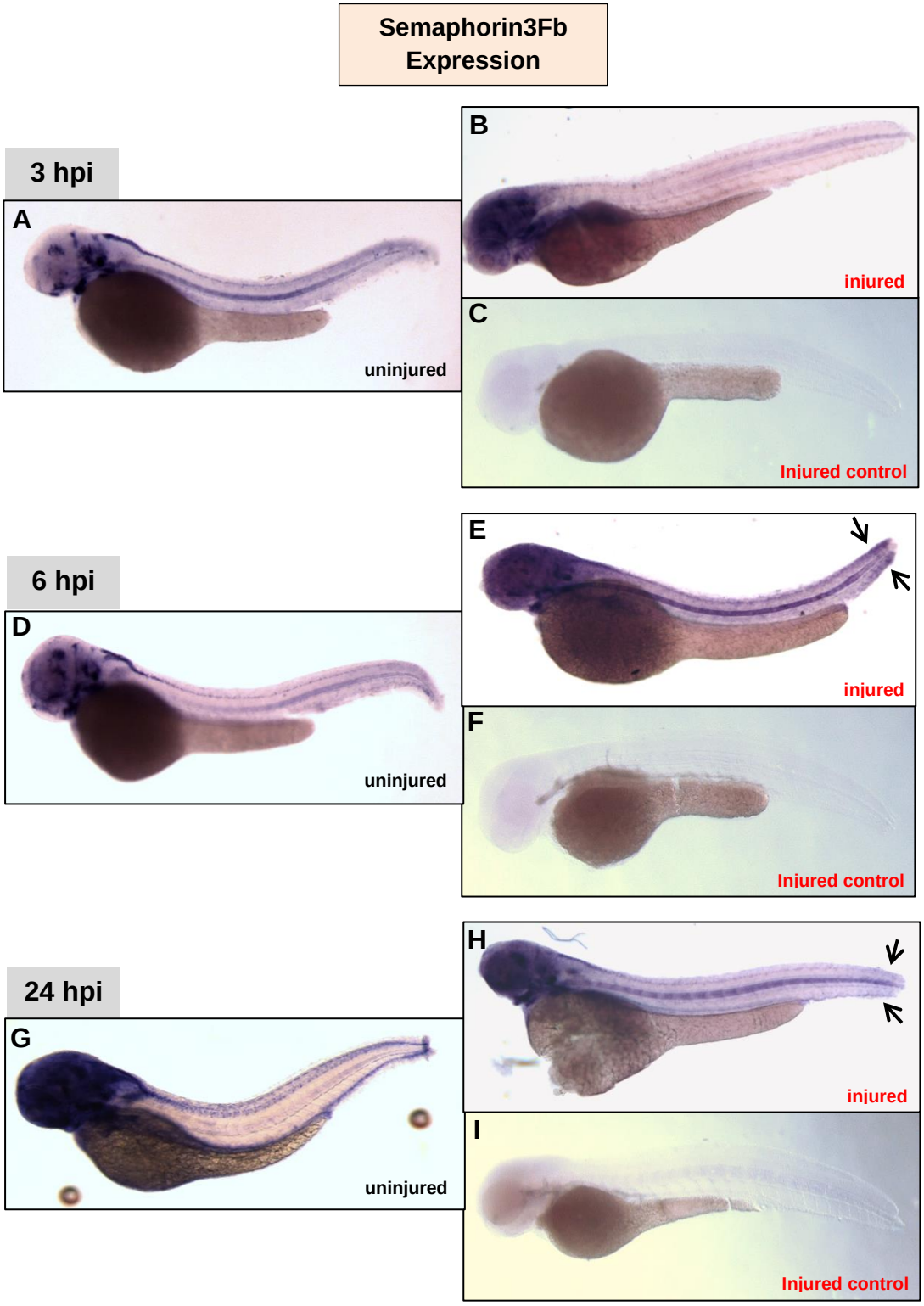

Figure 4.5: Semaphorin3Fb expression with tail fin injury. Tailfin transection was performed in 2dpf mpx:GFP embryos, then the embryos were fixed at 3 hpi (A-C), 6 hpi (D-F) and 24 hpi (G-I). The expression of zebrafish semaphorin3Fb was identified by in situ hybridization. All embryos were stained with semaphorin3Fb probe. Semaphorin3Fb was expressed in the same pattern at each time point both in uninjured and injured embryos. Interestingly, at 6 hpi and, to a lesser extent at 24 hpi, semaphorin3Fa expression was additionally observed at the injury sites (arrows).

4.2.2 Semaphorin3F whole fish overexpression decreased neutrophil recruitment and delayed neutrophil resolution.

I began by testing the effect of ubiquitous semaphorin3F overexpression on neutrophilic inflammation. Overexpression was achieved by microinjection of semaphorin3F RNA into one cell stage *mpx:*GFP embryos (methods chapter 2 section 2.2.3.7). To determine inflammatory responses of neutrophils, tail transection was performed at 2 days after fertilization (dpf). The numbers of neutrophils at the injury site were assessed by counting green fluorescent cells at injured sites at 6 and 24 hours after injury (hpi). These times were chosen because neutrophils are recruited with the highest numbers at 6 hpi, followed by spontaneous resolution over 24 hpi (Renshaw et al., 2006). Embryos injected with mCherry (red fluorescent protein) RNA were used as controls, besides non-injected embryos, to ensure that RNA microinjections did not affect inflammatory responses of neutrophils.

As shown in figures 4.6 and 4.7, during the recruitment phase (6 hpi), semaphorin3Fa as well as semaphorin3Fb whole fish overexpression caused a significant reduction in neutrophil numbers (semaphorin3Fa mean=19.4$\pm$0.60, semaphorin3Fb mean=18.7$\pm$0.66) at the injury site compared to mCherry injected (mean=26.4$\pm$0.61) and non-injected controls (mean=26.6$\pm$0.53) (*P<0.001*, n= 30 performed as 3 independent experiments). Co-injection of semaphorin3Fa and semaphorin3Fb together decreased neutrophil recruitment (mean= 19.2$\pm$0.54) only to the same extent as single injection of semaphorin3Fa or semaphorin3Fb RNA. At 24 hours after injury, semaphorin3Fa or semaphorin3Fb overexpression increased significantly the number of neutrophils (semaphorin3Fa mean=14.9$\pm$0.42, semaphorin3Fb mean=15.1$\pm$0.44) at the site of tail transection compared to controls (non-injected mean=10.7$\pm$0.34, mCherry mean=11.0$\pm$0.44) (*P<0.001*, n= 30 performed as 3 independent experiments). This had the same effects as co-injection of both semaphorin3Fa and semaphorin3Fb (mean=14.4$\pm$0.39). Thus, overexpression of semaphorin3F was sufficient to both decrease neutrophil recruitment to the site of injury, and delay neutrophil resolution away from the injury site (Figure 4.6, Figure 4.7).

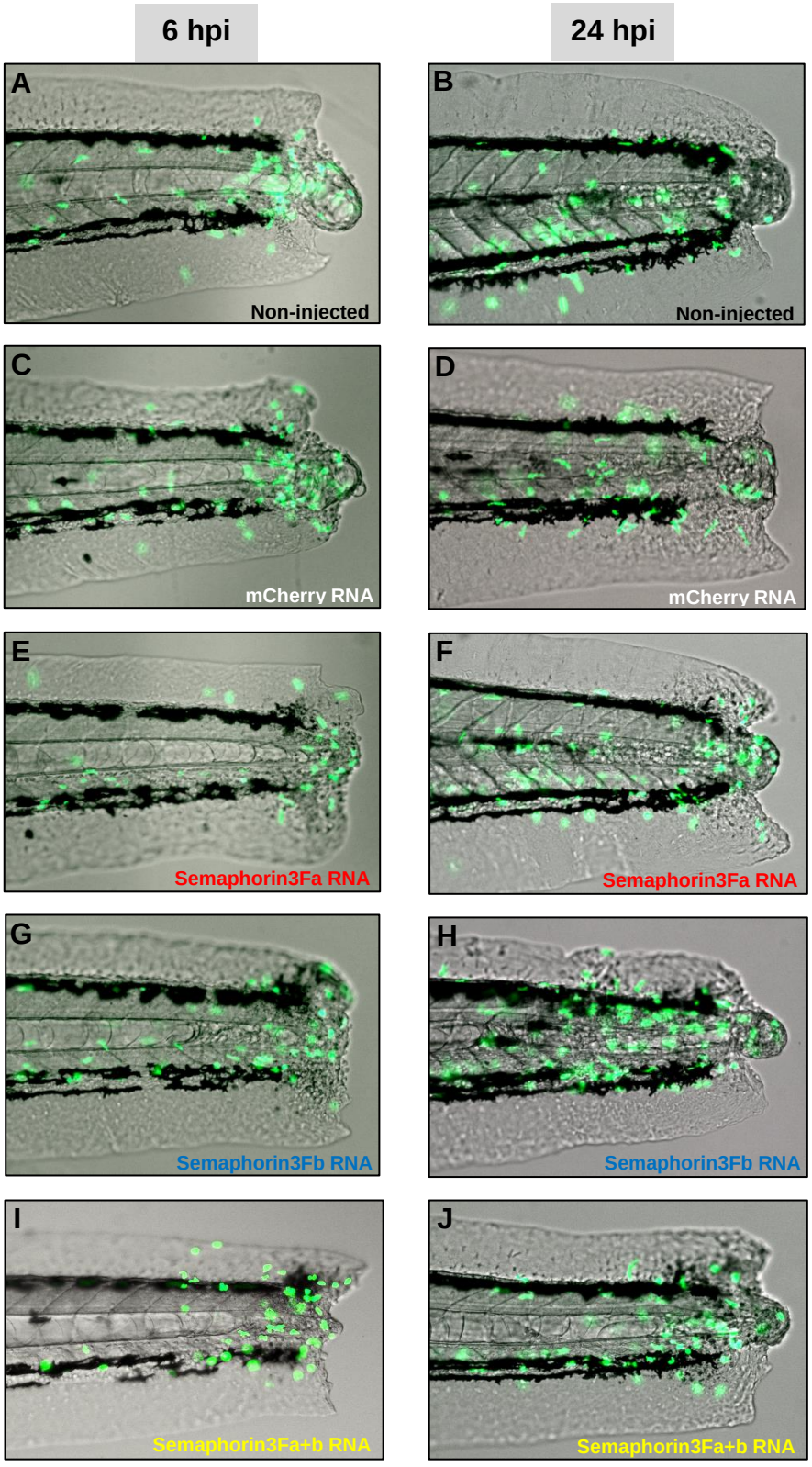

Figure 4.6: Semaphorin3F whole fish overexpression in zebrafish significantly decreased neutrophil recruitment and delayed resolution. Semaphorin3Fa or semaphorin3Fb RNA (50ng/µl) was injected into 1-cell stage zebrafish mpx:GFP embryos. In addition, 50ng/µl mCherry RNA was used as control. Tailfin transection was performed at 2dpf, and neutrophils counted at 6 and 24 hpi. (A-H) Overlaid fluorescence and brightfield photomicrographs of injured 2dpf embryos at 6hpi and 24 hpi, (A-B) non-injected, (C-D) mCherry RNA-injected, (E-F) semaphorin3Fa-injected,(G-H) semaphorin3Fb RNA-injected and (I-J) semaphorin3Fa+b RNA injected zebrafish embryos.

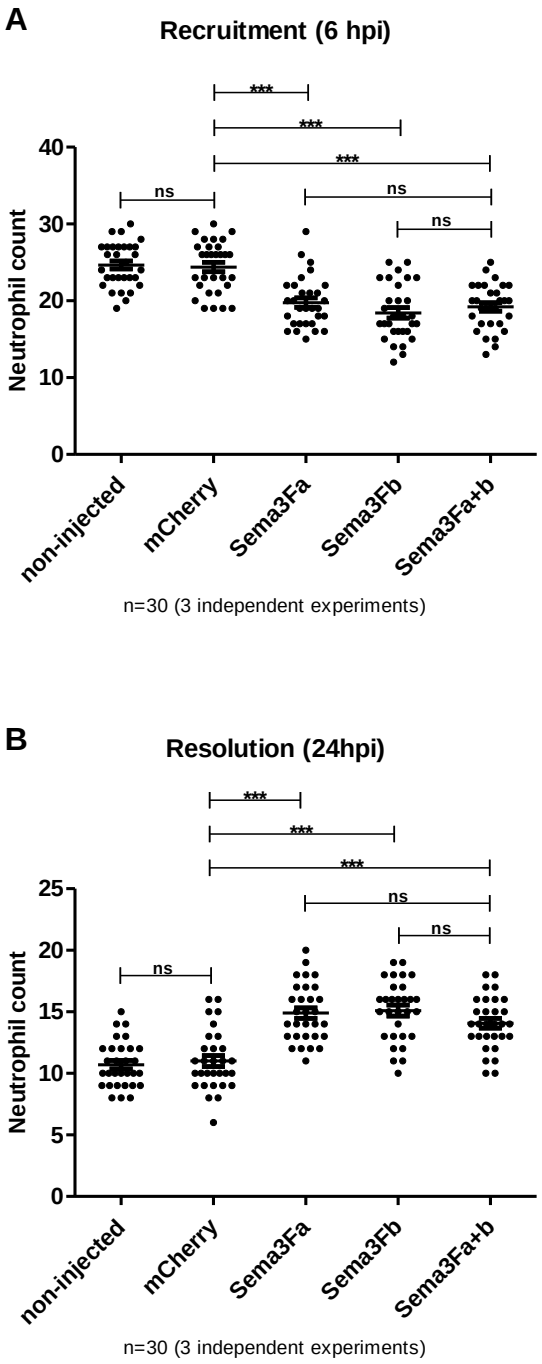

Figure 4.7: Semaphorin3F whole fish overexpression in zebrafish significantly decreased neutrophil recruitment and delayed resolution. Semaphorin3Fa or semaphorin3Fb RNA (50ng/µl) was injected into 1-cell stage zebrafish mpx:GFP embryos. In addition, 50ng/µl mCherry RNA was used as control. Tailfin transection was performed at 2dpf, and neutrophils counted at 6 and 24 hpi. (A) 6 hpi time point neutrophil counts (recruitment). Data shown are mean ± SEM. n= 30 performed as 3 independent experiments. (B) 24 hpi time point neutrophil counts (resolution). Data shown are mean ± SEM. n= 30 performed as 3 independent experiments, P values were calculated using one-way ANOVA and Bonferroni multiple comparison test, ****P<0.001.*

4.2.3 Semaphorin3F whole fish knockdown accelerated resolution of inflammation

To determine whether semaphorin3F expression is required for normal neutrophil migration, semaphorin3F whole fish knockdown was induced (methods chapter 2 section 2.2.3.8). *mpx*:GFP embryos were microinjected with morpholino-modified antisense oligonucleotide specific to semaphorin3Fa or semaphorin3Fb sequence to generate semaphorin3Fa or semaphorin3Fb whole fish knockdown. Morpholinos are synthetic molecules of about 25 bases with altered backbone linkages. A morpholino specifically binds to a target sequence to inhibit access of necessary components to that specific site. This enables it to block translation or splicing, and it also has effective targeted gene knockdown in zebrafish (Nasevicius and Ekker, 2000). As described in the Methods, semaphorin3Fa translation blocking morpholino (Yu and Moens, 2005) as well as semaphorin3Fb translation blocking morpholino (Tanaka et al., 2007) were injected into *mpx*:GFP embryos to induce whole fish knockdown of semaphorin3F (Figure 2.4&2.5). A mismatch morpholino which has no effect on zebrafish development, was used as control. Neutrophils were counted at 6 hpi for the numbers present in the recruitment phase, and at 24 hpi for the numbers of neutrophils remaining at the site of injury.

Semaphorin3Fa or semaphorin3Fb knockdown caused no significant changes in recruited neutrophil numbers (semaphorin3Fa mean=27.7$\pm$0.52, semaphorin3Fb mean=26.9$\pm$0.48) at the injury site compared to non-injected (mean=27.6$\pm$0.45) and control morpholino injected embryos (mean=27.9$\pm$0.45). Likewise, the double knockdown of semaphorin3Fa and semaphorin3Fb showed no effect on neutrophil recruitment at 6 hpi (mean=27.7$\pm$0.53). In contrast, at 24 hpi, semaphorin3Fa or semaphorin3Fb knockdown resulted in fewer neutrophil numbers (semaphorin3Fa mean=6.7$\pm$0.28, semaphorin3Fb mean=6.8$\pm$0.36) at the site of injury than the controls (non-injected mean=10.7$\pm$0.30, control morpholino mean=10.8$\pm$0.36) (*P<0.001*, n= 30 performed as 3 independent experiments). Thus, semaphorin3F knockdown by morpholino accelerated

significantly neutrophil resolution. Interestingly, the double semaphorin3F knockdown caused significantly faster neutrophil resolution from the injury site (mean=3.0±0.34) than knockdown of either semaphorin3F alone (Figure 4.8 and Figure 4.9).

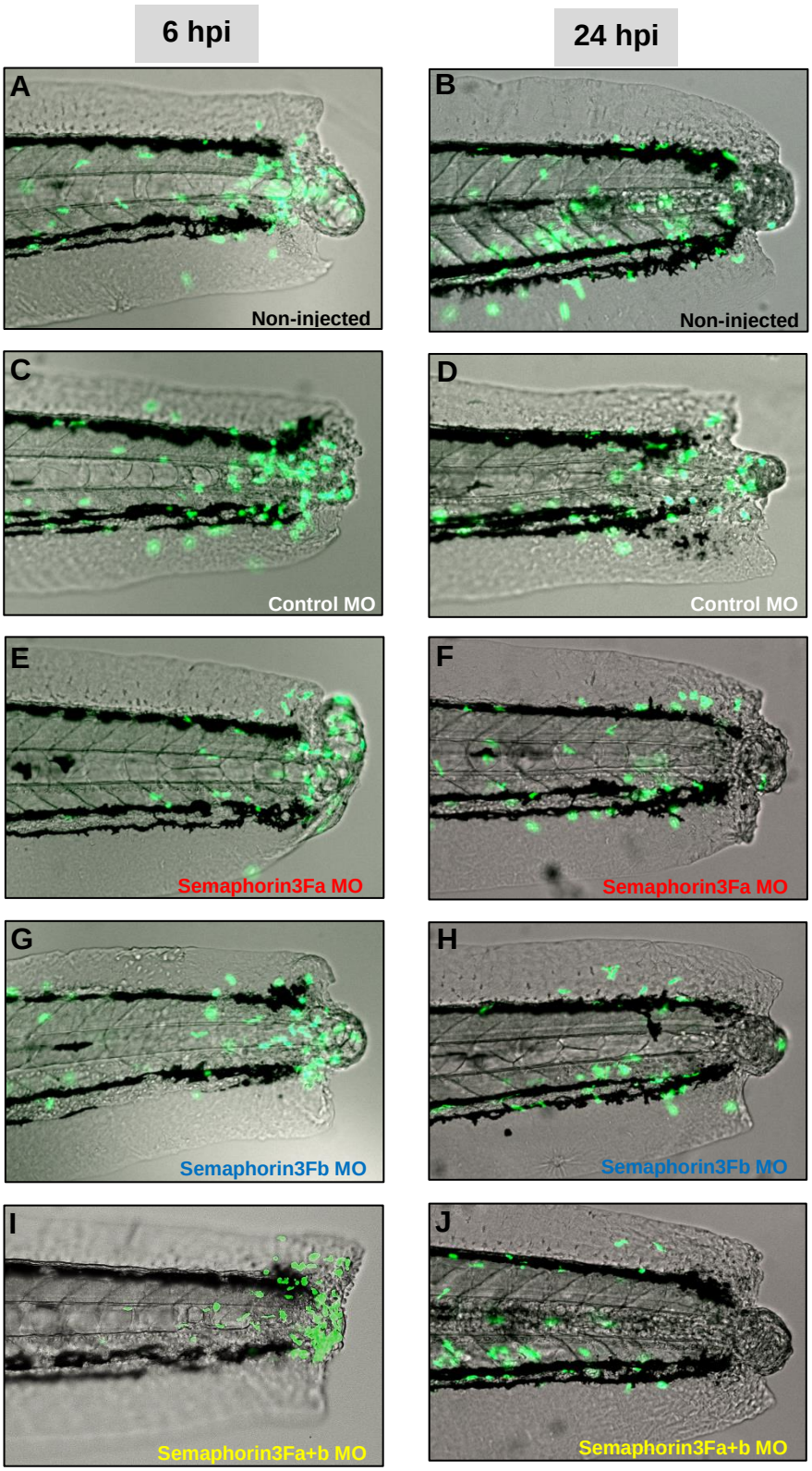

Figure 4.8: Knockdown of semaphorin3F by morpholino-injection showed a significant increased level of resolution of neutrophilic inflammation. Semaphorin3Fa or semaphorin3Fb morpholino ((1 nl of 0.5mM)) was injected into 1-cell stage zebrafish mpx:GFP embryos. In addition, 1 nl of 0.5mM of control morpholino was used as control. Tailfin transection was performed at 2dpf, and neutrophils counted at 6 and 24 hpi. (A-H) Overlaid fluorescence and brightfield photomicrographs of injured 2dpf embryos at 6hpi and 24 hpi, (A-B) non-injected, (C-D) control MO injected, (E-F) semaphorin3Fa MO injected, (G-H) semaphorin3Fb MO-injected and (I-J)semaphorin3Fa+b MO injected zebrafish embryos.

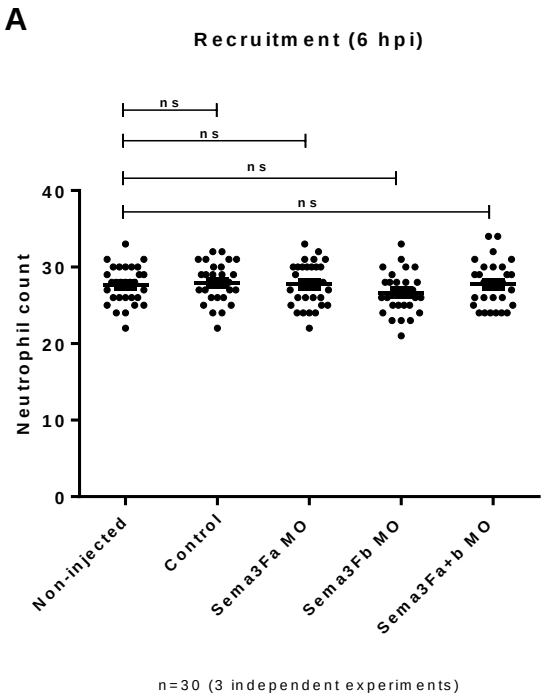

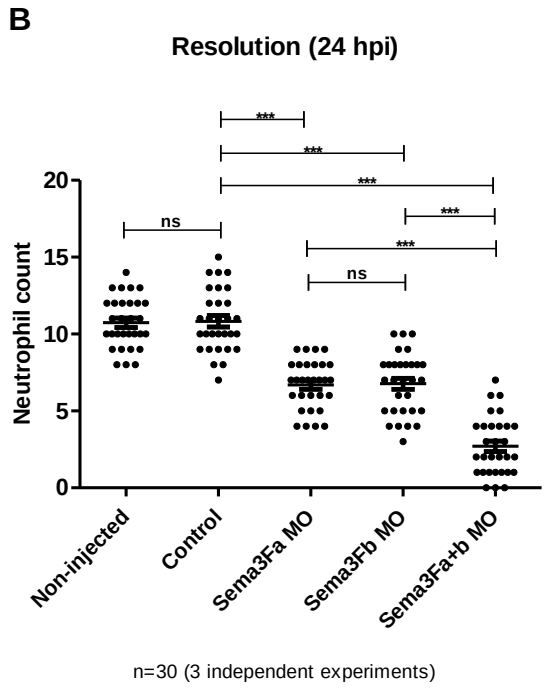

Figure 4.9: Knockdown of semaphorin3F by morpholino-injection showed a significant increased level of resolution of neutrophilic inflammation. Semaphorin3Fa or semaphorin3Fb morpholino ((1 nl of 0.5mM)) was injected into 1-cell stage zebrafish mpx:GFP embryos. In addition, 1 nl of 0.5mM of control morpholino was used as control. Tailfin transection was performed at 2dpf, and neutrophils counted at 6 and 24 hpi. (A) 6 hpi timepoint neutrophil counts (recruitment). Data shown are mean ± SEM. n= 30 performed as 3 independent experiments. (B) 24 hpi timepoint neutrophil counts (resolution). Data shown are mean ± SEM. n= 30 performed as 3 independent experiments, P values were calculated using one-way ANOVA and Bonferroni multiple comparison test, ****P<0.001.*

4.2.4 Microinjection of semaphorin3F RNA and morpholinos caused no changes in total neutrophil numbers.

To determine whether the microinjection of semaphorin3F RNA and semaphorin3F morpholinos had any effects on whole body neutrophil numbers, *mpx*:GFP embryos were injected with semaphorin3F RNA or semaphorin3F morpholino. At 3 dpf, total neutrophils were counted. Neither semaphorin3F overexpression nor knockdown caused any significant changes in the whole body neutrophil population compared to the controls (Figure 4.10).

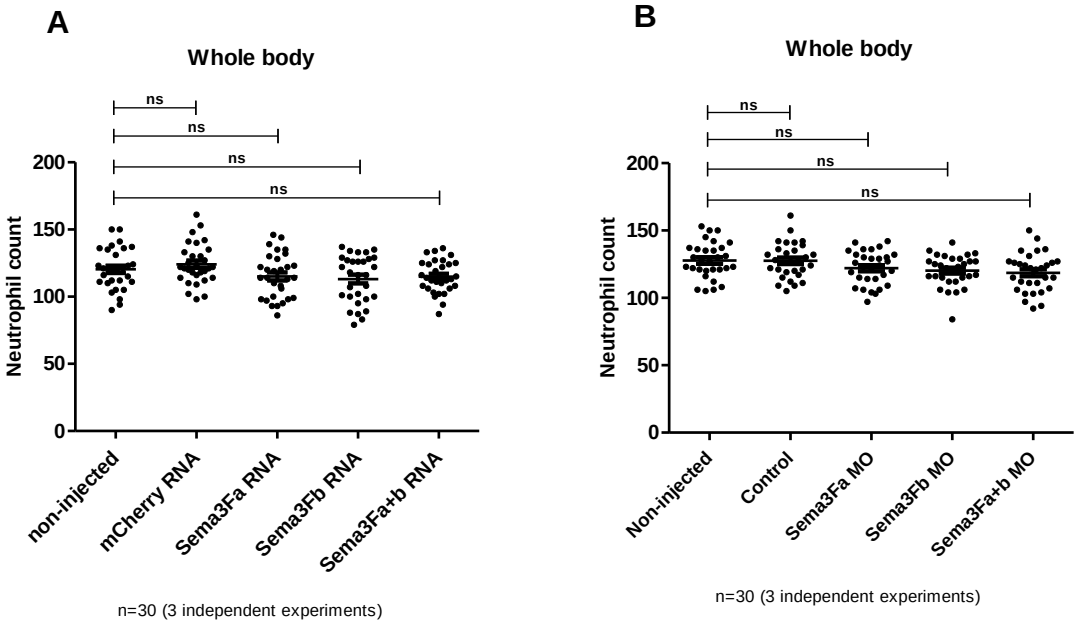

Figure 4.10: The injection of semaphorin3F RNA as well as semaphorin3F morpholinos had no effect on the whole body neutrophil numbers. (A) Semaphorin3Fa or semaphorin3Fb RNA (50ng/µl) or (B) Semaphorin3Fa or semaphorin3Fb morpholino (1 nl of 0.5mM) was injected into 1-cell stage zebrafish mpx:GFP embryos. Whole body total neutrophil numbers were counted at 3dpf. n= 30 performed as 3 independent experiments, P values were calculated using one-way ANOVA and Bonferroni multiple comparison test.

4.2.5 Semaphorin3F whole fish overexpression reduced speed of neutrophil migration towards the site of injury.

The initial findings demonstrated that semaphorin3F overexpression significantly inhibited neutrophil recruitment. Neutrophil counts were inadequate to evaluate the neutrophil migratory behaviour. To more thoroughly investigate the mechanism behind the neutrophil recruitment phenotype and to confirm the previous findings, neutrophil movements during the recruitment phase were tracked for one hour to analyse the speed and meandering index of each individual neutrophil cell.

For this, 2 dpf *mpx*:GFP embryos injected with semaphorin3Fa or semaphorin3Fb RNA were injured and mounted in agarose for timelapse imaging on a fluorescence microscope. Between 1-2 hpi, each green fluorescent neutrophil was tracked during migration towards the injury site. The speed and meandering index were analysed using Volocity® software. Meandering index is a ratio of displacement of each cell from origin to track length giving an indication of cell movement direction. A meandering index of 1 indicates that neutrophil moves in a straight line.

Semaphorin3F overexpression significantly reduced neutrophil speed towards the site of injury (Figure 4.11 A), but this had no effect on meandering index (Figure 4.11 B). It seems that semaphorin3F overexpression inhibited neutrophil movement causing most neutrophils either to move more slowly to the site of injury or to remain stationary.

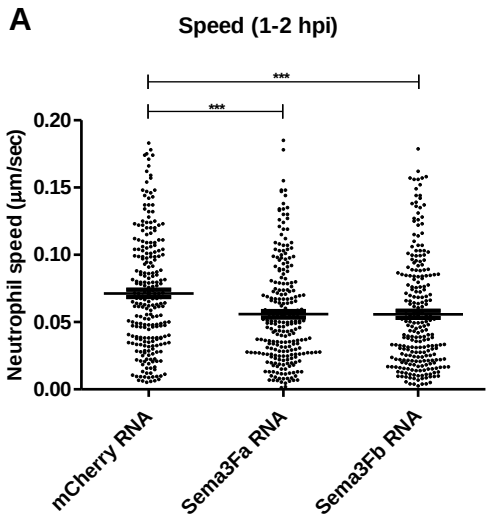

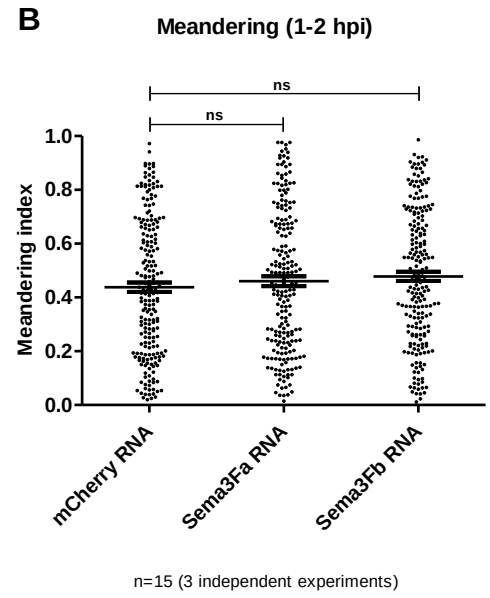

Figure 4.11: Semaphorin3F whole fish overexpression significantly decreased speed of neutrophil migration towards the site of injury, but had no effect on meandering index. Semaphorin3Fa or semaphorin3Fb RNA (50ng/µl) was injected into 1-cell stage zebrafish *mpx*:GFP embryos. In addition, 50ng/µl mCherry RNA was used as control. Tailfin transection was performed at 2dpf. Tracking of neutrophil movement over a 1 hour timelapse during the recruitment phase of inflammation (1-2hpi). Significant changes were observed in the speed of neutrophil migration (A), but there was no difference (B) in meandering index (displacement/path length). Data shown are mean ± SEM, n = 15 fish performed as 3 independent experiments (each point represents a single neutrophil), P values were calculated using one-way ANOVA and Bonferroni multiple comparison test, ****P<0.001*.

4.2.6 Semaphorin3F whole fish knockdown had no effect on speed and meandering index of neutrophil migration to the site of injury.

The initial results showed that semaphorin3F knockdown did not affect the recruited neutrophil numbers at the transection site compared to controls. To confirm this finding, the speed and meandering index of each individual neutrophil was analysed as it migrated towards the site of injury.

In the same way, semaphorin3Fa or semaphorin3Fb morpholino was injected to *mpx*:GFP 1 cell-stage embryos, tail fin transection was performed at 2 dpf embryos. Following injury, GFP-labelled neutrophils were tracked for 1 hour between 1-2 hpi, the neutrophil speed and meandering index were then calculated using Volocity® software. Embryos injected with mismatch control morpholino were used as controls.

As expected, no significant difference in the neutrophil speed was observed in semaphorin3F knockdown compared to control (Figure 4.12 A), and the meandering index was unchanged (Figure 4.12 B). This observation was consistent with the previous results confirming that semaphorin3F knockdown has no detectable effect on neutrophil migration during neutrophil recruitment to the site of injury.

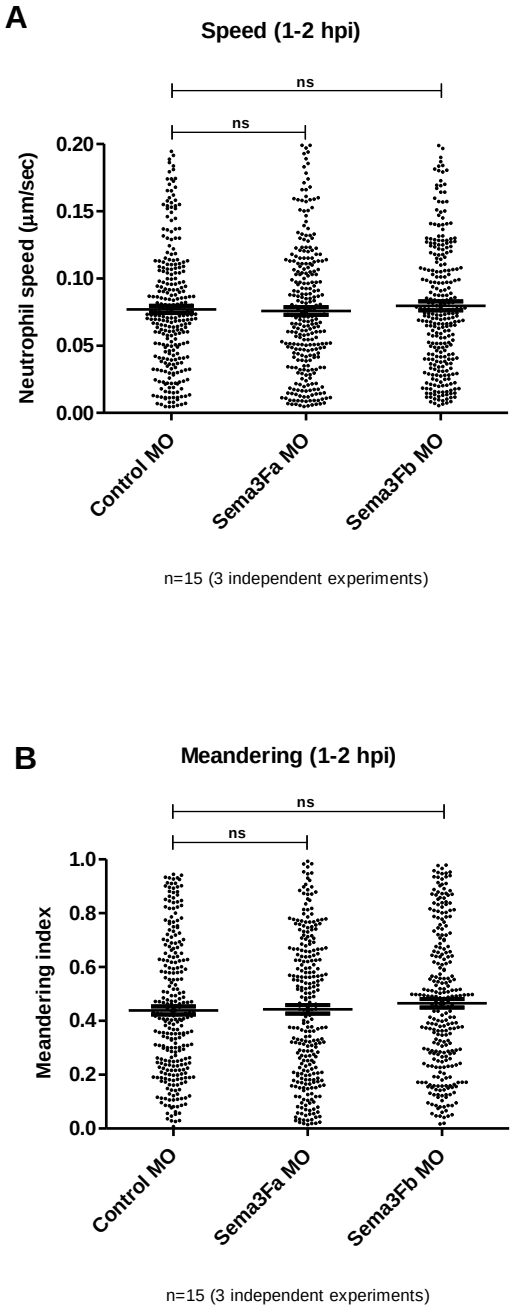

Figure 4.12: Semaphorin3F whole fish knockdown had no effect on speed and meandering index of neutrophil migration towards the site of injury. Semaphorin3Fa or semaphorin3Fb morpholino ((1 nl of 0.5mM)) was injected into 1-cell stage zebrafish mpx:GFP embryos. In addition, 1 nl of 0.5mM of control morpholino was used as control. Tailfin transection was performed at 2dpf. Tracking of neutrophil movement over a 1-hour timelapse during the recruitment phase of inflammation (1-2hpi). No change was observed in the speed of neutrophil migration (A), or (B) meandering index (displacement/path length). Data shown are mean ± SEM, n = 15 fish performed as 3 independent experiments (each point represents a single neutrophil), P values were calculated using one-way ANOVA and Bonferroni multiple comparison test.

4.2.7 Neutrophil resolution was not caused by neutrophil apoptosis at the site of injury.

The effects of semaphorin3F overexpression and knockdown on neutrophil resolution at 24hpi, together with effect of overexpression on migration to the injury site, are consistent with the idea that semaphorin3F upregulation slows neutrophil migration either to or from the site of injury. However, previous studies of neutrophil resolution have suggested that the mechanism by which neutrophil-mediated inflammation is resolved is by neutrophil apoptosis at the injury site. This mechanism is thought to support neutrophil clearance to prevent tissue damage (Haslett, 1999; Bratton and Henson, 2011). Thus, it is possible that semaphorin3F expression could alter the rates of neutrophil apoptosis at the injury site.

I therefore investigated neutrophil apoptosis at the site of injury using dual TSA/TUNEL staining. TSA or Tyramide signal amplification is an enzyme-mediated detection of endogenous neutrophil-specific myeloperoxidase activity staining neutrophils in green. TUNEL or Terminal deoxynucleotidyl transferase (TdT) dUTP Nick-End Labelling can detect double stranded DNA breaks of apoptotic cells in red colour. An apoptotic neutrophil will therefore be dual-labelled with green and red. Following injection of semaphorin3F RNA or morpholinos into 1-cell stage *mpx*:GFP embryos, tail transection was performed on 2 dpf *mpx*:GFP embryos. At 24 hpi, embryos were fixed in 4% PFA, followed by TSA staining, then TUNEL staining. The total neutrophil number at the site of injury and number of dual-labelled apoptotic neutrophils was examined in each embryo to calculate the mean percentage of neutrophil apoptosis.

Neither semaphorin3F overexpression (Figure 4.13) nor knockdown (Figure 4.14) showed any significant difference of the percentage of neutrophil apoptosis at the injury site compared to controls. This lack of difference suggests that the neutrophil resolution phenotype affected by semaphorin3F was not caused by altered neutrophil apoptosis, but by another mechanism.

A

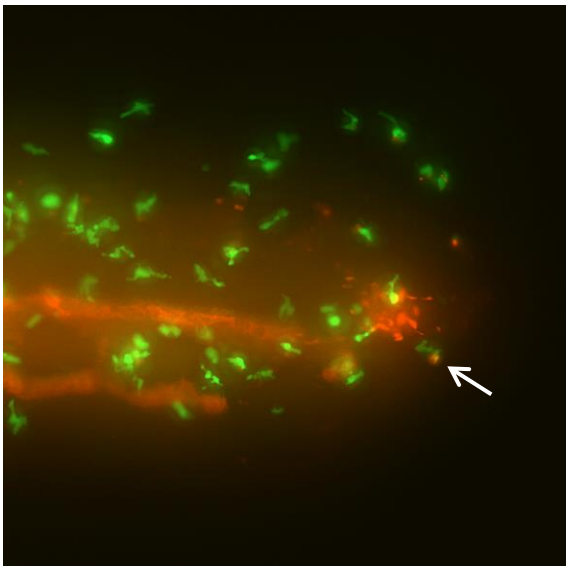

B

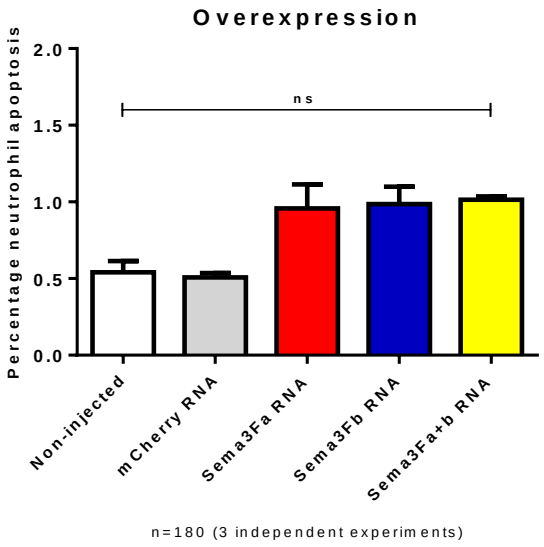

Figure 4.13: Semaphorin3F whole fish overexpression has no effect on neutrophil apoptosis at the site of injury. Semaphorin3Fa or semaphorin3Fb RNA (50ng/µl) was injected into 1-cell stage zebrafish mpx:GFP embryos. Tail transection was performed on 2 dpf. Embryos were fixed in 4% PFA at 24 hpi and stained with TSA and TUNEL. (A) Injured tail. Represented apoptotic neutrophil is indicated by the white arrows. (B) TUNEL and TSA co-localisation shows the percentage of apoptotic neutrophils at the injury site. Data shown are mean ± SEM, n = 180 performed as 3 independent experiments.

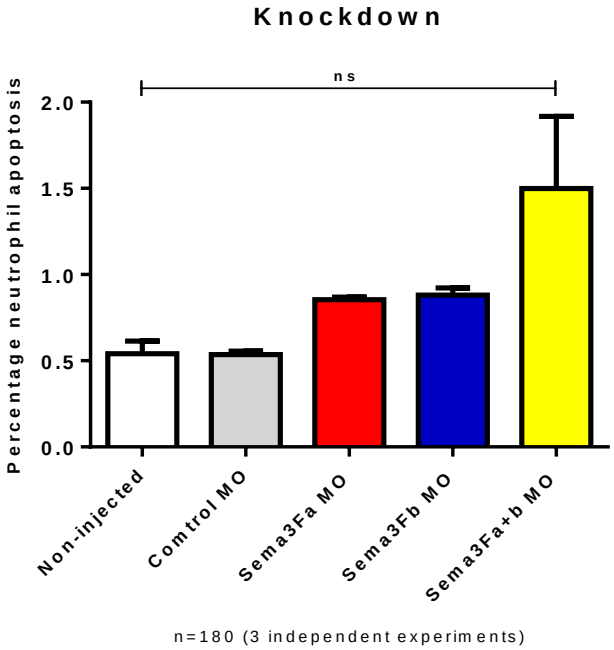

Figure 4.14: Semaphorin3F whole fish knockdown has no effect on neutrophil apoptosis at the site of injury. Semaphorin3Fa or semaphorin3Fb morpholino (1 nl of 0.5mM) was injected into 1-cell stage zebrafish mpx:GFP embryos. Tail transection was performed on 2 dpf. Embryos were fixed in 4% PFA at 24 hpi and stained with TSA and TUNEL. TUNEL and TSA co-localisation shows the percentage of apoptotic neutrophils at the injury site. Data shown are mean ± SEM, n = 180 performed as 3 independent experiments.

4.2.8 Semaphorin3F overexpression decreased neutrophil resolution by decreasing their reverse migration.

The previous results suggested that altered neutrophil apoptosis did not affect the numbers of neutrophils remaining at the site of injury at resolution phase following modulation of semaphorin3F expression. Recent studies have suggested an alternative mechanism by which neutrophils might be removed from the injury site. Robertson et al. has shown that neutrophil clearance from the wound *in vivo* resulted from neutrophil apoptosis and an additional mechanism, neutrophil reverse migration (Robertson et al., 2014). Similarly, studies from other groups have demonstrated this phenomenon and its importance for inflammation resolution (Mathias et al., 2006) (Elks et al., 2011) (Starnes and Huttenlocher, 2012).

To investigate whether semaphorin3F affects this mechanism, a reverse migration assay was performed by using double transgenic zebrafish line *Tg(mpx:Gal4; UAS:Kaede)i222* or *mpx:*Kaede*.* Kaede, a photoactivatable fluorescent protein, was originally found in stony coral. Green fluorescent neutrophils of this line can express the kaede protein, which is photoconvertible from green to red fluorescence by certain wavelengths of light. Thereby the recruited green fluorescent neutrophils at the site of injury are converted to red fluorescence using 120 pulses of the 405 nm laser at 40% laser power (Figure 4.16a&4.18a) (Elks et al., 2011). The resulting red fluorescent neutrophils were then tracked for 3.5 hours, and the numbers of red neutrophils reverse migrating from the site of injury into a defined distal region were quantified (Figure 4.16a&4.18a). In order to examine the effect of semaphorin3F overexpression on neutrophil reverse migration, *mpx:*Kaede embryos were injected with semaphorin3F RNA. Tail fin transection was performed at 2 dpf. At 6hpi, the neutrophils present at the transection site were photoconverted to red fluorescence, and the numbers of these red neutrophils were assessed.

Semaphorin3Fa or semaphorin3Fb overexpressing fish had significantly fewer red neutrophils (semaphorin3Fa mean=4.8$\pm$0.18, semaphorin3Fb mean=4.5$\pm$0.15) moving away from the injury site than mChery injected

controls (mean=9.8±0.22). As with the previous assays, overexpression of semaphorin3Fa and b together did not enhance this effect (mean=5.0±0.14) (*P<0.0001*, n= 9 performed as 3 independent experiments).

Linear regression analysis of three graphs combining displayed that single overexpression of semaphorin3Fa or semaphorin3Fb as well as the double overexpression had similar slopes (semaphorin3Fa slope=0.026±0.001, semaphorin3Fb slope=0.022±0.001, semaphorin3Fa and b slope=0.020±0.002), and showed significant difference from control (slope=0.031±0.002) (*P<0.0001*, n= 9 performed as 3 independent experiments) (Figure 4.15&4.16b). These results indicated that semaphorin3F whole fish overexpression decreased neutrophil resolution by decreasing the rate of reverse migration of neutrophils during inflammation resolution.

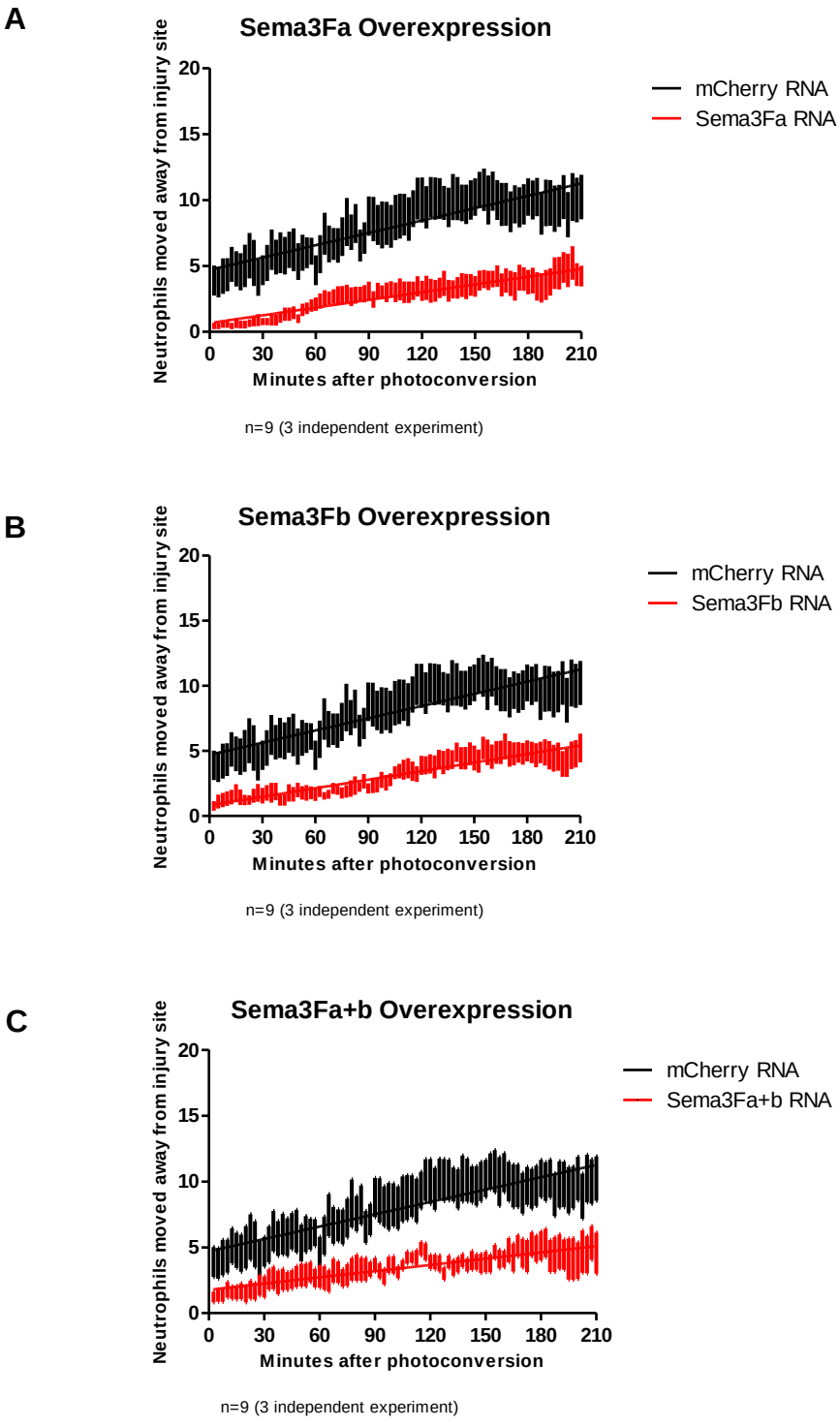

Figure 4.15: Semaphorin3F wholefish overexpression decreased reverse migration of neutrophils during inflammation resolution. (A)Semaphorin3Fa,(B)semaphorin3Fb or (C) semaphorin3Fa+b RNA (50ng/µl) was injected into 1-cell stage zebrafish *mpx*:Kaede embryos. In addition, 50ng/µl mCherry RNA was used as control. Tailfin transection was performed at 2dpf, and kaede labelled neutrophils were photoconverted at 6hpi. The numbers of photoconverted red neutrophils leaving the area of transection over a time period of 3.5 hours were analysed. Data shown are mean ± SEM, n = 9 performed as 3 independent experiments.

A

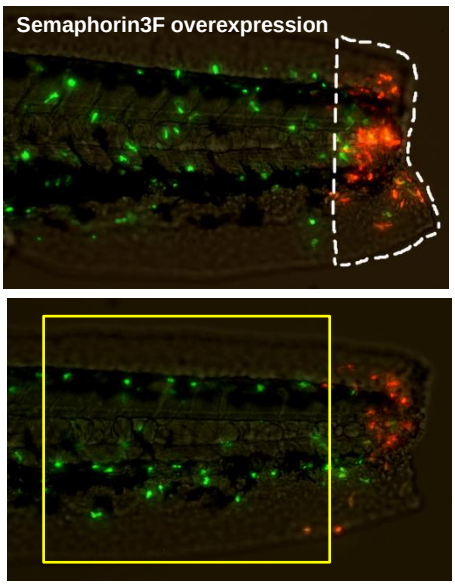

B

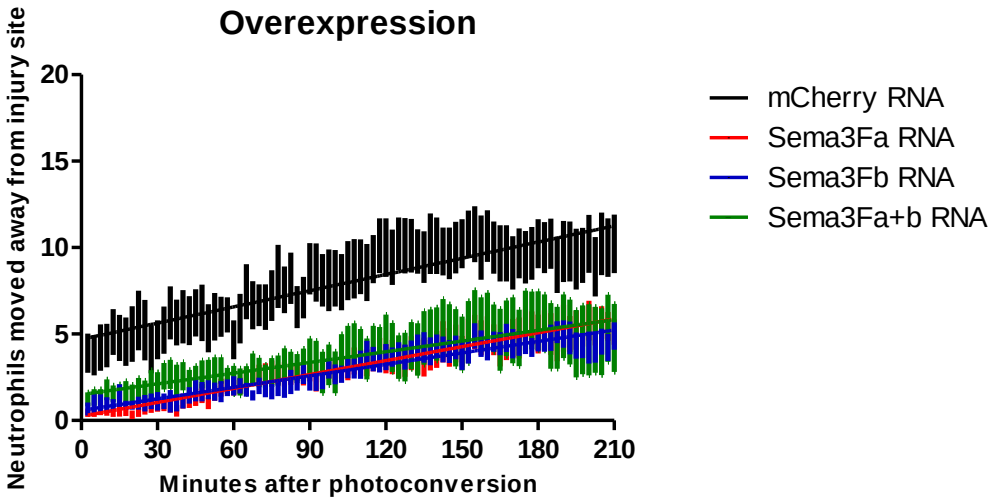

n=9 (3 independent experiment)

Figure 4.16: Semaphorin3F wholefish overexpression decreased reverse migration of neutrophils during inflammation resolution. Semaphorin3Fa, semaphorin3Fb or semaphorin3Fa+b RNA (50ng/µl) was injected into 1-cell stage zebrafish *mpx*:Kaede embryos. In addition, 50ng/µl mCherry RNA was used as control. Tailfin transection was performed at 2dpf. (A, above) Representative pictures of semaphorin3F overexpression. At 6hpi the recruited green fluorescent neutrophils at the site of injury are photoconverted to red fluorescence using120 pulses of the 405 nm laser at 40% laser power (as illustrated). (A, below) The red fluorescent neutrophils were tracked for 3.5 hours, and the numbers of red neutrophils migrating reverse from the site of injury into a defined region as illustrated were quantified. (B) Combining of three graphs of semaphorin3F overexpression. Data shown are mean ± SEM, n = 9 performed as 3 independent experiments.

4.2.9 Semaphorin3F knockdown increased reverse migration of neutrophils during inflammation resolution.

Neutrophil counts revealed that semaphorin3F whole fish knockdown significantly lowered neutrophil numbers at the transection site at 24 hpi. In order to investigate the migration behaviour of neutrophils during the resolution phase, the reverse migration assay was performed. Semaphorin3F morpholinos were injected into 1 cell-stage of *mpx*:Kaede embryos. Tailfin transection was performed at 2 dpf, and at 6 hpi the neutrophils at the site of injury were photoconverted to red fluorescence. The numbers of these red neutrophils leaving the area of transection over a time period of 3.5 hours were calculated.

As expected, there were more photoconverted red neutrophils moving away from the site of injury in semaphorin3Fa knockdown (mean=15.4$\pm$0.35) than in mismatch morpholino injected negative control embryos (mean=9.5$\pm$0.20). Semaphorin3Fa knockdown had similar numbers of neutrophils leaving the injury site as semaphorin3Fb knockdown (mean=14.8$\pm$0.29). However, it was observed that the double knockdown of semaphorin3Fa and semaphorin3Fb (mean=16.9$\pm$0.27) caused much more neutrophil reverse migration away from the site of injury than the single knockdown (*P<0.0001*, n= 9 performed as 3 independent experiments).

Linear regression analysis of three graphs combining displayed that single knockdown of semaphorin3Fa or semaphorin3Fb had similar slopes (semaphorin3Fa slope=0.050$\pm$0.002, semaphorin3Fb slope=0.043$\pm$0.002), and showed significant differences from control (slope=0.029$\pm$0.003). The double knockdown of semaphorin3Fa and semaphorin3Fb (slope=0.067$\pm$0.002) caused much faster neutrophil reverse migration (*P<0.0001*, n= 9 performed as 3 independent experiments) (Figure 4.17&4.18b).

In summary, semaphorin3F knockdown accelerated neutrophil clearance from sites of inflammation by increased reverse migration of neutrophils during the resolution phase.

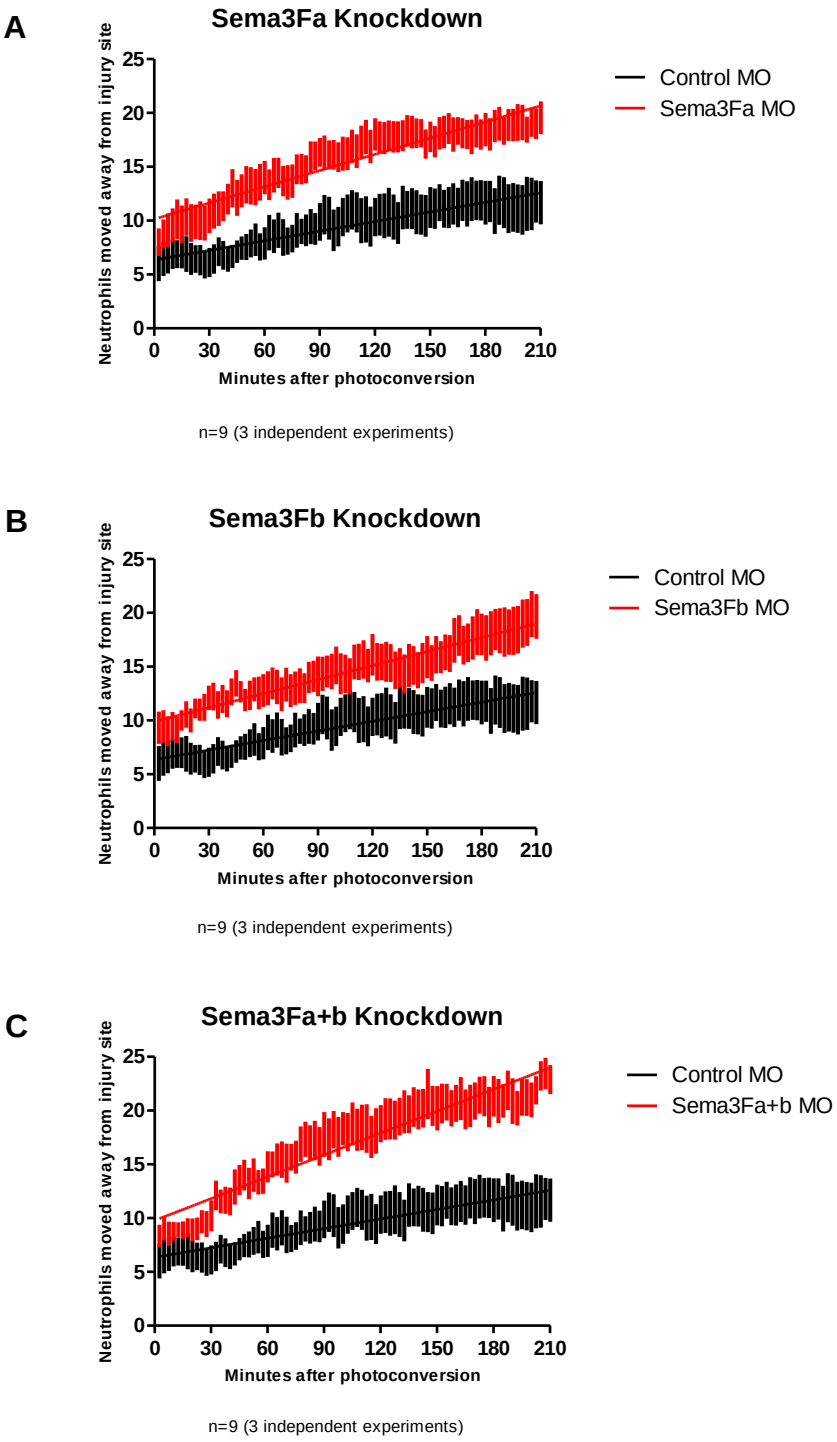

Figure 4.17: Semaphorin3F wholefish knockdown accelerates neutrophilic inflammation resolution by increase in neutrophil reverse migration. (A)semaphorin3Fa, (B)semaphorin3Fb or (C)semaphorin3Fa+b morpholino (1 nl of 0.5mM) was injected into 1-cell stage zebrafish *mpx*:Kaede embryos. In addition, 1 nl of 0.5mM control morpholino was used as control. Tailfin transection was performed at 2dpf, and kaede labeled neutrophils were photoconverted at 6hpi. The numbers of photoconverted red neutrophils leaving the area of transection over a time period of 3.5 hours were analysed. Data shown are mean ± SEM, n = 9 performed as 3 independent experiments.

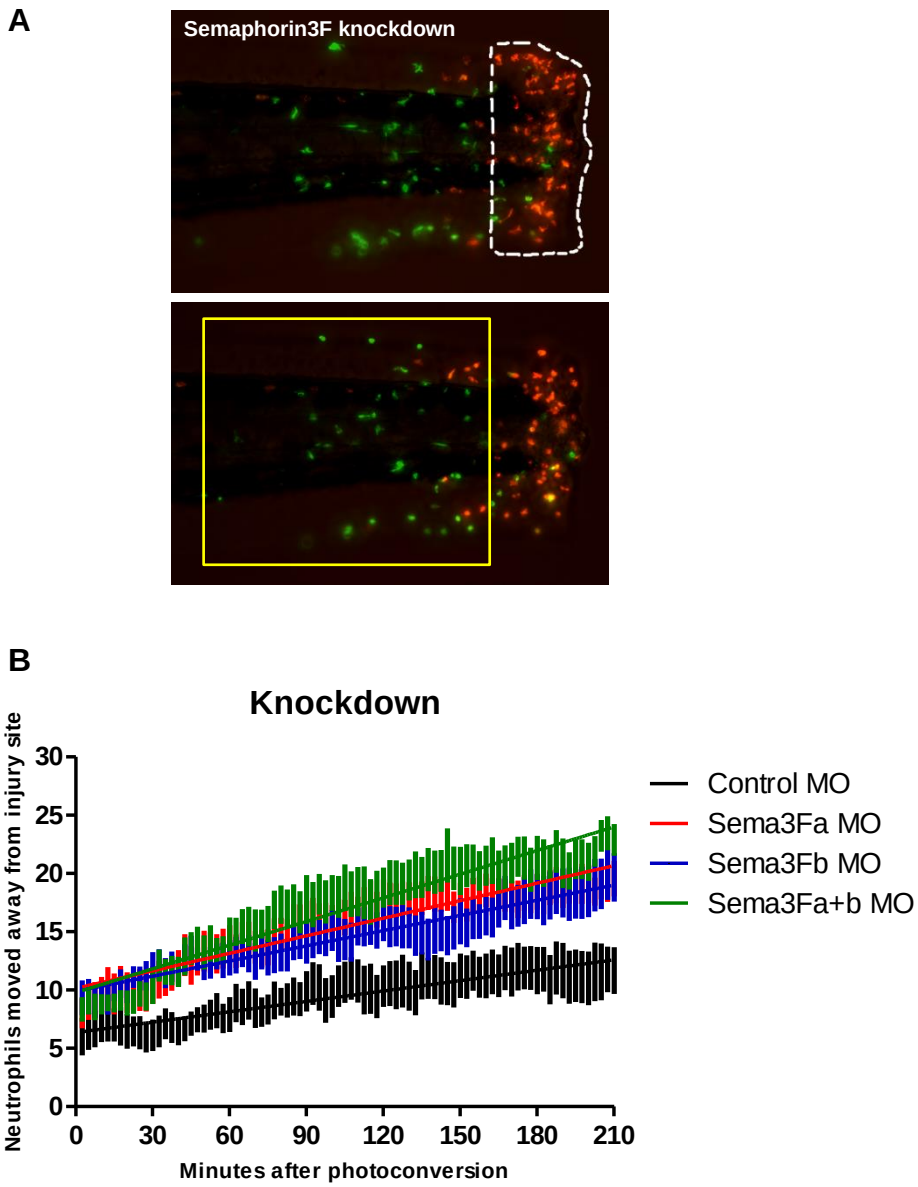

Figure 4.18: Semaphorin3F wholefish knockdown accelerates neutrophilic inflammation resolution by increase in neutrophil reverse migration. (A)semaphorin3Fa, (B)semaphorin3Fb or (C)semaphorin3Fa+b morpholino (1 nl of 0.5mM) was injected into 1-cell stage zebrafish *mpx*:Kaede embryos. In addition, 1 nl of 0.5mM control morpholino was used as control. Tailfin transection was performed at 2dpf. (A, above) Representative pictrures of semaphorin3F knockdown. At 6hpi the recruited green fluorescent neutrophils at the site of injury are photoconverted to red fluorescence using120 pulses of the 405 nm laser at 40% laser power (as illustrated). (A, below) The red fluorescent neutrophils were tracked for 3.5 hours, and the numbers of red neutrophils migrating reverse from the site of injury into a defined region as illustrated were quantified. (B) Combining of three graphs of semaphorin3F overexpression. Data shown are mean ± SEM, n = 9 performed as 3 independent experiments.

4.2.10 Semaphorin3F phenotype is specific to the neutrophils.

Since semaphorin3F affected the migration behaviour of neutrophils recruiting to the site of injury and leaving from the site of injury, it was interesting to examine the effect of semaphorin3F on other inflammatory cells. Besides neutrophils, macrophages play also an important role in the initiation, maintenance and resolution of inflammation. I therefore wished to investigate the effect of semaphorin3F on macrophage recruitment and resolution during the inflammation.

To address this, a macrophage specific fluorescent zebrafish line *Tg(fms:GAL4;UNM),* which has mCherry labelled macrophages, subsequently referred to as *fms*:UNM, was used. Semaphorin3F RNA or morpholino was injected into 1 cell-stage of *fms*:UNM embryos. At 2 dpf, tail fin injury was performed. Macrophages tend to persist at the transection site beyond the time when neutrophilic inflammation has resolved, and the number of recruited macrophages at the site of injury approaches its peak at 8 hpi (Loynes et al., 2010). However, in order to comply with the UK Home Office legislation, all procedures must end prior to 5.2 dpf and so the number of macrophages at the site of injury for the resolution phase was counted at 72 hpi even though this is prior to complete resolution.

At 8 hpi, semaphorin3Fa and semaphorin3Fb whole fish overexpression exhibited no significant change in macrophage numbers at the inflammation site compared to mCherry injected and non-injected controls. Co-injection of semaphorin3Fa and semaphorin3Fb also showed the similar effects (Figure 4.19a). Furthermore, there was no significant difference in macrophage numbers at the site of injury at 72 hpi in all conditions (Figure 4.19b).

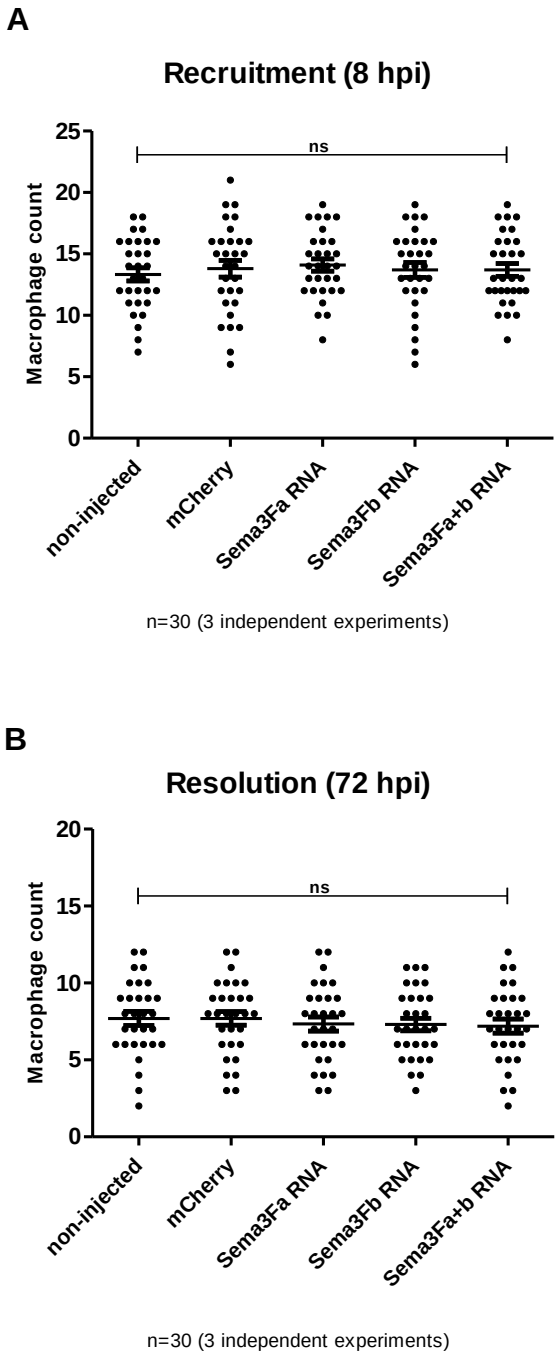

Figure 4.19: Semaphorin3F wholefish overexpression has no effect on macrophage recruitment and resolution. Semaphorin3Fa or semaphorin3Fb RNA (50 ng/µl) was injected into 1-cell stage zebrafish *fms*:UNM embryos. In addition, 50 ng/µl mCherry RNA was used as control. Tailfin transection was performed at 2dpf, and macrophages counted at 8 hpi (A) and 72hpi (B). Data shown are mean $\pm$ SEM. n= 30 performed as 3 independent experiments, P values were calculated using one-way ANOVA.

Similarly, single morpholino knockdown of semaphorin3Fa or semaphorin3Fb, as well as double knockdown caused no significant change in the number of macrophages recruiting to the injury site (Figure 4.20a) and leaving the injury site (Figure 4.20a) compared to control morpholino injected and non-injected controls.

These experiments have shown that semaphorin3F did not affect the migratory behaviour of macrophages. The numbers of macrophages at the site of injury both in recruitment phase and defined resolution phase were unchanged compared to controls. These findings indicate that semaphorin3F specifically plays a role in neutrophil migration during inflammation and does not affect macrophage recruitment or resolution.

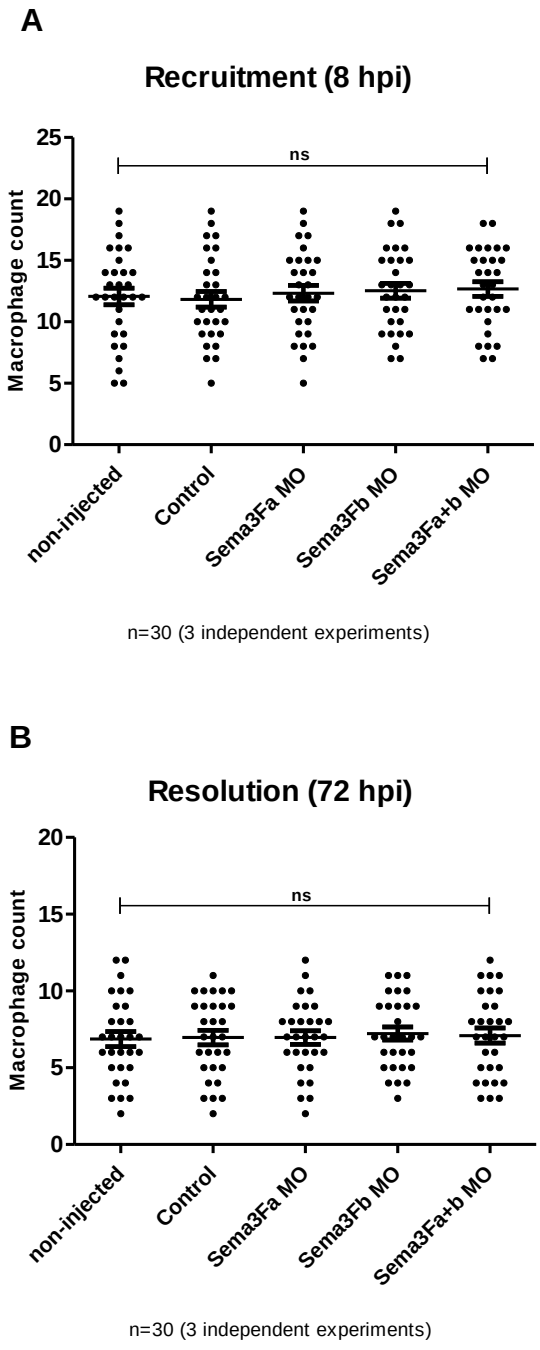

Figure 4.20: Semaphorin3F wholefish knockdown has no effect on macrophage recruitment and resolution. Semaphorin3Fa or semaphorin3Fb morpholino (1 nl of 0.5mM) was injected into 1-cell stage zebrafish fms:GAL4.UNM embryos. In addition, 1 nl of 0.5mM control morpholino was used as control. Tailfin transection was performed at 2dpf, and macrophages counted at 8 hpi (A) and 72hpi (B). Data shown are mean $\pm$ SEM. n= 30 performed as 3 independent experiments, P values were calculated using one-way ANOVA.

4.3 Discussion

In this chapter, I have characterised the expression patterns of semaphorin3Fa and semaphorin3Fb in zebrafish embryos, and have investigated the role of semaphorin3F in neutrophil behaviour during inflammation using the genetically tractable zebrafish. Semaphorin3F overexpression delays neutrophil recruitment and reverse migration resulting in a persistent inflammatory response. On the other hand, semaphorin3F knockdown enhances resolution of inflammation by accelerating neutrophil reverse migration. These manipulations do not affect the behaviour of macrophages in the same injury model. This suggests that semaphorin3F acts as a critical and specific regulator of neutrophil persistence at the inflamed site.

4.3.1 Zebrafish as *in vivo* model for neutrophilic inflammation

One of the most important examples of directed cell movement is the inflammatory response. Inflammation occurs at the injury sites leading to the migration of immune cells to the site of inflammation to protect the host from infection. Neutrophils are the most abundant leukocytes recruiting rapidly to sites of inflammation. Recently, translucent zebrafish embryos have been used as *in vivo* model for inflammation assay allowing live imaging or visualisation of fluorescent proteins in cellular processes. Zebrafish immune system shares also a wide range of features of mammalian systems. Here, we utilise the zebrafish transgenic line *Tg(mpx:GFP)i114* as an *in vivo* model for study of neutrophilic inflammation. The established Tg(*mpx:GFP*)*i114*, expresses the neutrophil-specific protein myeloid-specific peroxidase (mpx) which is homologue of the mammalian myeloperoxidase (mpo) (Lieschke et al., 2001). Following tail transection, inflammation is induced at the site of injury, and green fluorescent neutrophils are recruited to the wound site. This inflammation subsequently resolves and proceeds with kinetics similar to those in mammalian systems. Counting of neutrophil number at the tail fin wound enables us to assay the degree of inflammation. This established

inflammation model thus provides quantifiable neutrophil recruitment and resolution (Renshaw et al., 2006). Moreover, we can use the model for *in vivo* tracking of neutrophils in real-time, so that neutrophil speed and direction can be explicitly observed. Importantly, numerous studies in mammalian models have reported that neutrophil reverse migration from the site of injury is an alternative mechanism by which neutrophils can be cleared from the injury site (Hughes et al., 1997) (Mathias et al., 2006) (Buckley et al., 2006). This phenomenon can be also determined using generated transgenic zebrafish line *Tg(mpx:Gal4; UAS:Kaede)i222* with photoactivatable fluorescent protein. Study from several groups has defined the role of neutrophil reverse migration in inflammation resolution using this zebrafish transgenic line (Yoo and Huttenlocher, 2011) (Elks et al., 2011). The observation in zebrafish immunity has also many aspects with consequences for the important knowledge of mammalian immune function.

4.3.2 Semaphorin3Fa and semaphorin3Fb expression in zebrafish embryos

Due to a whole genome duplication through vertebrate evolution, semaphorin3F gene has two related members, namely semaphorin3Fa and semaphorin3Fb. As a first step toward understanding semaphorin3F role *in vivo*, I identified the expression pattern of both copies in 20-somite stage and 3 dpf zebrafish embryos. Consistent with the finding of other groups, I found semaphorin3Fa and semaphorin3Fb are expressed mostly in cells of zebrafish nervous system (Yu and Moens, 2005) (Callander et al., 2007). With regard to the microarray data from Professor Stephen Renshaw's group profiling zebrafish neutrophils, it was also difficult to determine whether zebrafish neutrophils expressed semaphorin3Fa or semaphorin3Fb. In addition, the whole mount *in situ* hybridisation technique was not sensitive enough to detect the expression of these both copies in neutrophils. However, human neutrophils demonstrate constitutive semaphorin3F expression, with the convincing evidence that semaphorin3F mRNA expression is markedly induced in BAL neutrophils in response to

inflammation. Moreover, zebrafish semaphorin3Fa and semaphorin3Fb expression is observed adjacent to the site of injury suggesting that expression of both genes is upregulated in the inflamed tissues. These results are also consistent with semaphorin3F expression in mouse lung sections of acute models of neutrophilic inflammation. Together, these findings persuade me of the role of semaphorin3F in inflammation.

4.3.3 Role of semaphorin3F in migratory behaviour of neutrophils during inflammation

Recent research has shown a role of zebrafish semaphorin3F in neural crest cell migration *in vivo*. Yu et al. reported that semaphorin3F is expressed in cranial neural crest-free zone in the head periphery of zebrafish embryos, whereas its receptors, nrp2a and nrp2b are expressed in the neural crest cells (NCCs) themselves, pluripotent migratory cells, which are important for the development of the peripheral nervous system. Repulsive semaphorin3F-neuropilin2 signalling is involved in signalling processes of neural cells leading to guidance of cranial neural crest cell migration (Yu and Moens, 2005). However, semaphorin3F has not previously been identified to be involved in regulating cell migration in the immune system.

Neutrophils contribute to the pathogenesis of a number of human diseases caused by persistence of neutrophilic inflammation. Thus, regulation of neutrophil clearance is a critical prerequisite for successful inflammation resolution. In addition to neutrophil apoptosis followed by macrophage uptake, neutrophil clearance is accomplished by the retrograde migration of neutrophils from sites of inflammation (Mathias et al., 2006). Other semaphorin members have been identified to be a regulator of neutrophil migration. *In vitro*, semaphorin3B showed an ability to increase the basal migration of neutrophils with direct correlation with IL-8 levels in those cells (Rolny et al., 2008), in contrast, semaphorin3E acted as a potent inhibitor of neutrophil migration induced by chemoattractant stimuli, CXCL8/IL-8 (Saati, 2013).

Here, we have found for the first time a role for semaphorin3F in regulating neutrophil migration during inflammation. Semaphorin3F overexpression decreases neutrophil recruitment to the site of injury by reducing speed of neutrophils. As a consequence, neutrophils stay persistently at the wound site accompanied by delayed inflammation resolution. By contrast, semaphorin3F knockdown causes faster neutrophil reverse migration from the site of injury. This also accelerates resolution of neutrophilic inflammation. Interestingly, the double knockdown of semaphorin3F copies leads to much faster neutrophil migration away from the injury site than the single knockdown, whereas the double overexpression of both copies and the single overexpression reveal no significant difference in neutrophil recruitment as well as neutrophil resolution. These findings indicate that loss of function in duplicate affects the regulation of neutrophil migration more than gain of functions. This suggests that the role of semaphorin3Fa in regulating neutrophil movement is equivalent to that of semaphorin3Fb, and that there is some redundancy between the proteins. Notably, semaphorin3F knockdown has no effect on neutrophil recruitment to the site of injury. In light of the data on semaphorin3F expression in mouse lung lesions and in bronchoalveolar lavage (BAL) mouse neutrophils in the previous chapter, which demonstrates that semaphorin3F expression is upregulated by the additional factors released in the inflammatory microenvironment, this suggests that semaphorin3F expression may not be induced until neutrophils reach the inflamed site. This would explain why the knockdown of semaphorin3F at the beginning of inflammation shows no considerable influence on neutrophil migration.

Having determined that semaphorin3F does not have significant effect on neutrophil apoptosis rate at the inflamed site compared to controls. This also suggests that semaphorin3F is unlikely to be involved in any of the pathways of programmed neutrophil death, including extrinsic, intrinsic, or endoplasmic reticulum stress pathways (El Kebir and Filep, 2010). Consistent with this, the number of macrophages at the site of injury is unaffected by either semaphorin3F overexpression or knockdown, suggesting that the rate of phagocytosis of apoptotic neutrophils by macrophages is not different to

controls. Thus, bearing in mind the effect of semaphorin3F on neutrophil reverse migration, it seems plausible that the levels of semaphorin3F expression may cause either neutrophil persistence at the site of inflammation or acceleration of inflammation resolution depending on the amount of expression that occurs during inflammation.

Exactly how semaphorin3F affects neutrophil migration during inflammation is not clear. Recent studies have implicated semaphorin3F activity in migration of endothelial cells and tumour cells. Work by other groups has identified that semaphorin3F can inhibit migration of endothelial cells by inhibiting activation of integrins and thereby disrupting tumour angiogenesis (Guttmann-Raviv et al., 2007). Interestingly, numerous studies of tumourigenesis have demonstrated the ability of semaphorin3F to inhibit tumour cell migration. Semaphorin3F inactivates RhoA, a member of the Rho family of GTPases that stabilises the F-actin cytoskeleton (Shimizu et al., 2008). Semaphorin3F also inactivates small GTPase Rac1, a regulator of lamellipodia formation at the leading edge during migration by inactivation of RhoA (Burridge and Wennerberg, 2004). As a result, the migration and contractility of the tumour cells are inhibited. Another approach to identification of the mechanism regulating neutrophil migration during inflammation is to study dynamic processes involving in neutrophil motility such as chemotaxis and neutrophil polarity via PI-3 kinase signalling. My investigations into this area are presented in Chapter 6.

Another thing that remains unclear is whether semaphorin3F regulates neutrophil migration through autocrine or paracrine signalling. RNA- and morpholino-injections can generate only in the whole fish overexpression and knockdown, respectively. To specifically address in which cells semaphorin3F is required *in vivo*, will require the creation of zebrafish transgenic lines in which semaphorin3F expression is specifically modified in neutrophils.

4.3.4 Conclusions

All findings in this chapter imply that semaphorin3F not only plays a role in endothelial cell or tumour cell migration (Bielenberg et al., 2004) (Guttmann-Raviv et al., 2007) (Guttmann-Raviv et al., 2007) (Shimizu et al., 2008), but also triggers neutrophil migration in response to inflammation *in vivo*. I found that semaphorin3F overexpression decreases neutrophil recruitment to the site of injury, and delays subsequent neutrophil reverse migration. In contrast, semaphorin3F knockdown accelerates the retrograde movement of neutrophils away from the site of injury, without affecting recruitment, resulting in faster resolution of neutrophilic inflammation. Notably, these phenotypes occur specifically in neutrophils, not in macrophages, suggesting the specific role of semaphorin3F in neutrophil migration.

Chapter 5: Phenotype of neutrophil migration in semaphorin3F mutant in zebrafish using TALENs

5.1 Introduction

On the basis of our observation that semaphorin3F whole fish knockdown by morpholino injection accelerates neutrophil reverse migration during inflammation, I sought to confirm the phenotype of neutrophil migration by generating a semaphorin3F mutation zebrafish transgenic line. For this, I generated zebrafish semaphorin3F mutant using Transcription Activator-Like Effector Nucleases (TALENs) technique.

Although morpholinos are easily delivered to cells and have high efficacy to specifically knockdown genes throughout zebrafish embryonic and larval development, they become progressively less effective as development proceeds due to spatiotemporal gene expression, dilution and degradation (Bedell et al., 2011). Morpholinos are normally injected into the yolk sacs of 1-cell-stage zebrafish embryos. Most morpholino phenotypes are identified within the first 3 days of development, with effects rarely persisting after the first 5 days following injection (Bill et al., 2008). This is believed to be a consequence of the rapid increase in numbers of nuclei over this period of time, resulting in a significant decrease in intranuclear concentration. The use of higher dosages of morpholinos is precluded by their effects on embryonic development. Morpholinos may also act ‘off target’ in that they can have effects on the production of other gene products, thereby resulting in the observed phenotype being unrelated to the gene of interest (Eisen and Smith, 2008). Another reason for limited effectiveness of morpholinos is that they are ineffective when the cognate maternal protein is present (Kardash, 2012), or when the maternal transmission of the gene under study suppresses the phenotype of interest (Nasevicius and Ekker, 2000).

Consequently, I sought to study the phenotype of neutrophil migration by generating a stable semaphorin3F mutant transgenic line.

TALENs are a newly developed technology that can efficiently modify any sequence of interest in living cells or organisms. TALENs are artificial proteins containing a DNA binding domain and a non-specific FokI endonuclease domain. A novel DNA binding domain, Transcription Activator-Like Effector (TALE) protein, is produced by a plant pathogen in the genus Xanthomonas (*Xanthomonas* bacteria) (Boch and Bonas, 2010). This domain is a customizable sequence-specific domain composed of multiple sets of highly conserved repeat domains of 34 identical or near identical tandem amino acids in tandems (Schornack et al., 2006). The individual TALE repeat recognises a specific single base of the target DNA sequence determined by the identity of a hyper variable pair of amino acids (the repeat variable diresidue (RVD)) typically found at position 12 and 13 of the repeat (Boch et al., 2009). Recently, four domains with the RVD NI, NG, HD and NN have been used for the recognition of A, T, C and G, respectively (Figure 5.1). TALE binds specifically to the target sequence, which is cleaved by FokI endonuclease resulting in double-stand breaks into that specific DNA site. The double-stand breaks are then repaired by normal DNA repair mechanisms including non-homologous end-joining (NHEJ) or homologous recombination (HR) to enable target genome alternations at the cleavage site resulting in the creation of insertion or deletion mutations (Urnov et al., 2010) (Figure 5.1).

Recently, TALENs have enabled alteration of target genes in a number of model organisms including zebrafish (Sander et al., 2011, Huang et al., 2011, Bedell et al., 2012). The TALENs system can efficiently cause double-stand breaks in target endogenous genes of interest in zebrafish following error-prone repair. As a result, the introduction of small insertions or deletions at cleavage sites frequently induces frameshift knockout mutations at the somatic cell level that pass through the germline to create mutant fish (Sander et al., 2011). Moreover, TALENs offer an easy and rapid method to edit and create potentially targeted mutations in a greater range of DNA sequences.

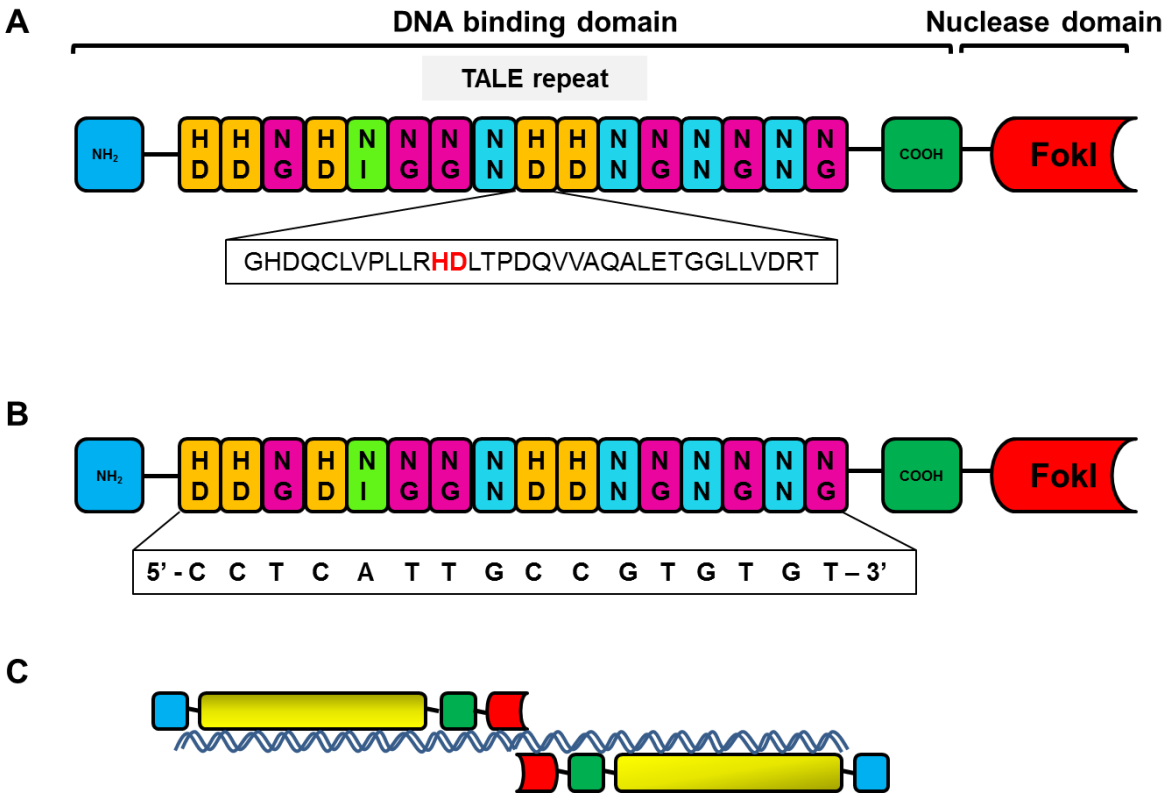

Figure 5.1: Overview of TALENs and TALE repeat. (A) Schematic diagram of a TALEN. DNA binding domain is composed of 34 amino acids TALE repeat modules with an N-terminal domain and a C-terminal domain. TALE repeats are shown as coloured squares. Letters inside each repeat represent the two repeat variable diresidue (RVD) typically found at position 12 and 13 of the repeat. The amino acid sequence of a single TALE repeat is expanded below with the RVD highlighted in red and bold text. The non-specific nuclease domain from the FokI endonuclease is shown as a red figure. (B) TALE-derived DNA binding domain aligned with its target DNA sequence. The targeted nucleotides of each RVD are expanded below. NI, NG, HD and NN are used for the recognition of A, T, C and G, respectively. (C) TALENs bind to a half-site with dimeric FokI nuclease domains cleaving the targeted DNA site within the intervening spacer region. The nuclease-induced double-strand breaks are repaired by error-prone non-homologous end-joining (NHEJ) or homologous recombination (HR) resulting in the creation of insertion or deletion mutation.

In this chapter, I sought to determine whether semaphorin3F mutation using TALENs affected the migratory behaviour of neutrophils during inflammation, including the number of neutrophils recruiting to the site of injury during the recruitment phase and the number of neutrophils persisting at the site of injury at the resolution phase. I also determined whether this semaphorin3F mutant zebrafish line demonstrated the same phenotypes as seen in semaphorin3F whole fish knockdown using morpholino-injections. For this, I created semaphorin3Fa mutant and semaphorin3Fb mutant lines. To examine neutrophil migration during inflammation, the previously described injury model was performed (Renshaw et al., 2006).

Aims and hypotheses

The aim of this chapter is to investigate the role of semaphorin3F in the migratory behaviour of neutrophils during inflammation *in vivo* using TALENs technology to create semaphorin3Fa and semaphorin3Fb mutant zebrafish lines. The findings of this chapter will let us further understand the role of semaphorin3F in neutrophilic inflammation.

5.2 Results

5.2.1 Design of DNA binding domain

A heterodimer with a left and a right subunit containing a C-terminal Fok1 nuclease domain and an N-terminal site specific DNA binding domain, at a target site was first designed by using the website http://tale-nt.cac.cornell.edu/node/add/talen-old. The target genomic sequence should have a wide spanning restriction enzyme that cuts well in Reddymix to allow saving on time and cost for screening process. The DNA binding domain should be comprised of between 15-21 repeat variable domain (RVD) units and have a space between two subunits about 15-18 bp. All plasmids were provided by Golden Gate TALEN kit (Addgene, Cambridge, UK) and obtained as a kind gift from Dr.Stone Elworthy (University of Sheffield).

DNA binding domain of semaphorin3Fa

I targeted semaphorin3Fa gene at exon 8 because of its position in the middle of the gene and its specific cleavage site recognised by MwoI restriction endonuclease. A left and a right subunit of semaphorin3Fa TALE repeat (Figure 5.2) were designed by using http://tale-nt.cac.cornell.edu/node/add/talen-old recognising the targeted sequence in exon 8. The space between two subunits is the cleavage site of MwoI. Primers were then designed for genotype test by digest array. The PCR product size is 228 bp in length, which is digested by MwoI to give approximately 130 bp and 80 bp products (Figure 5.2).

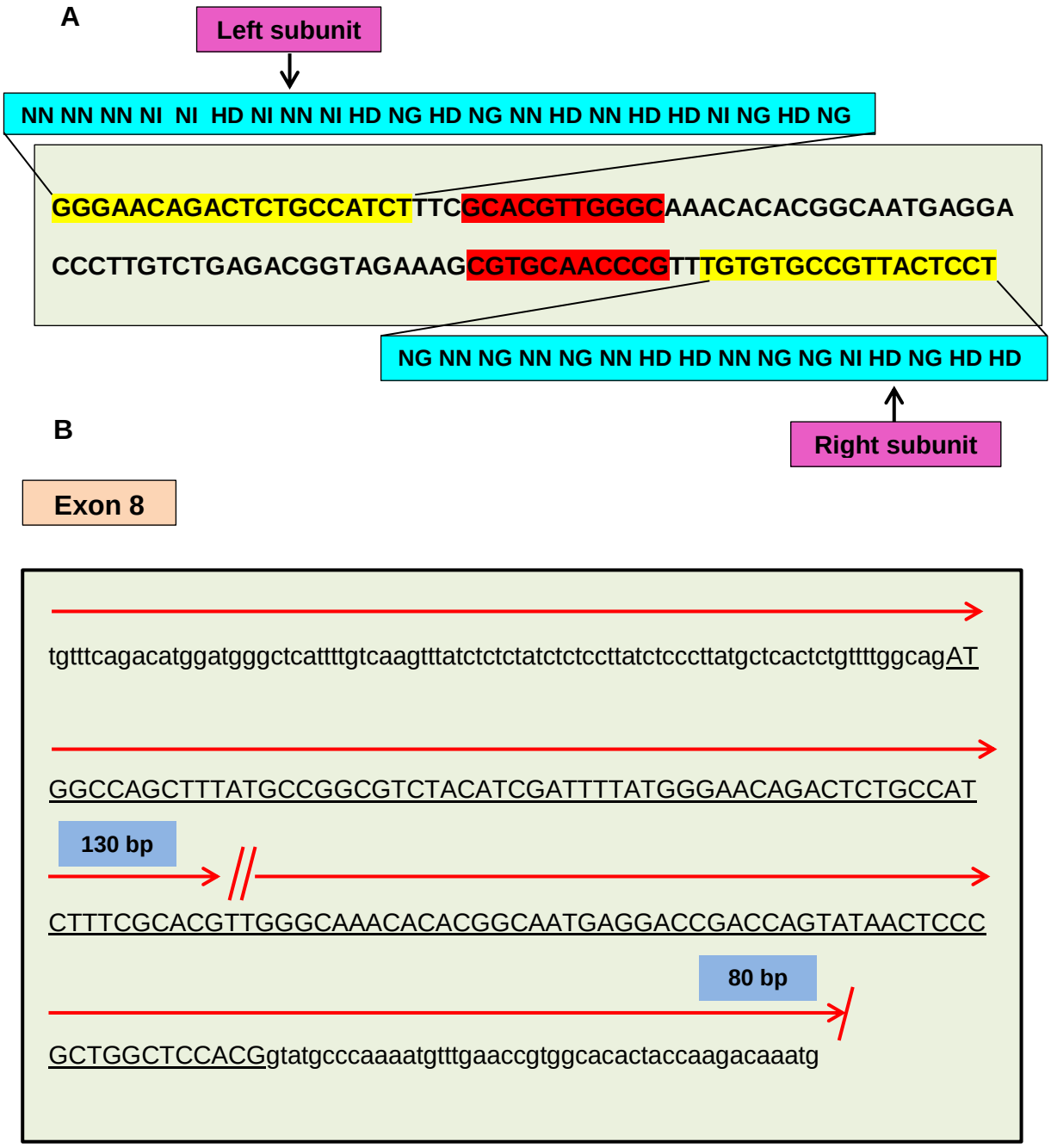

Figure 5.2: TALEN design for inducing double-strand breaks at the endogenous zebrafish semaphorin3Fa gene at exon 8. (A) A left and a right subunit of semaphorin3Fa TALE repeat aligned with its target DNA sequence in exon 8. The targeted nucleotides (as highlighted in yellow) of each RVD (as highlighted in blue) are expanded above or below. NI, NG, HD and NN are used for the recognition of A, T, C and G, respectively. The specific cleavage site of MwoI restriction endonuclease is highlighted in red. (B) The targeted DNA sequence of exon 8 with designed primers. A left and a right TALE repeat of DNA binding domain are highlighted in yellow. The specific cleavage site of MwoI restriction endonuclease is highlighted in red. A left and a right primer are highlighted in green. PCR product sizes (as illustrated in red arrow) after MwoI digestion are 130 bp and 80 bp. Uppercase = exon; lowercase = intron.

DNA binding domain of semaphorin3Fb

Likewise, I targeted semaphorin3Fb gene at exon 8 because of its position in the middle of the gene and its specific cleavage site recognised by BslI restriction endonuclease. A left and a right subunit of semaphorin3Fa TALE repeat (Figure 5.3) were designed by using http://tale-nt.cac.cornell.edu/node/add/talen-old recognising the targeted sequence in exon 8. The space between two subunits is the cleavage site of BslI.

Primers were then designed for genotype test by digest array. The PCR product size is 252 bp length, which digested by BslI gives approximately 125 bp and 110 bp products (Figure 5.3).

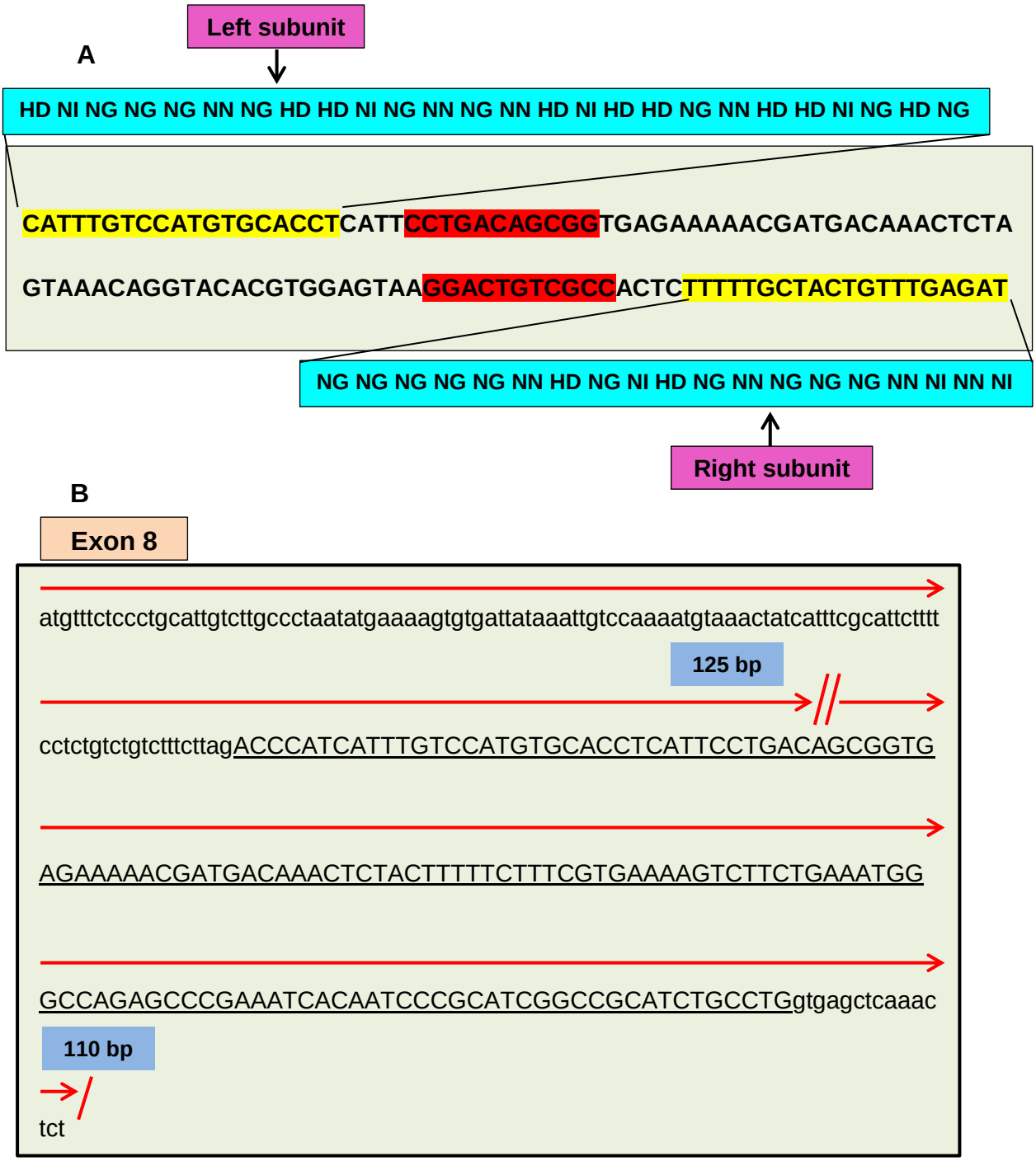

Figure 5.3: TALEN design for inducing double-strand breaks at the endogenous zebrafish semaphorin3Fb gene at exon 8. (A) A left and a right subunit of semaphorin3Fb TALE repeat aligned with its target DNA sequence in exon 8. The targeted nucleotides (as highlighted in yellow) of each RVD (as highlighted in blue) are expanded above or below. NI, NG, HD and NN are used for the recognition of A, T, C and G, respectively. The specific cleavage site of BslI restriction endonuclease is highlighted in red. (B) The targeted DNA sequence of exon 8 with designed primers. A left and a right TALE repeat of DNA binding domain are highlighted in yellow. The specific cleavage site of MwoI restriction endonuclease is highlighted in red. A left and a right primer are highlighted in green. PCR product sizes (as illustrated in red arrow) after BslI digestion are 125 bp and 110 bp. Uppercase = exon; lowercase = intron.

5.2.2 Identification of mutations induced by TALENs in embryonic zebrafish cells

The TALENs constructs of semaphorin3Fa and semaphorin3Fb were prepared and made as previously described (methods chapter 2 section 2.2.3.9). RNA of the TALENs was then injected into the one-cell stage of *mpx*:GFP embryos. Once the injected fish were about 2-3 months old, these fish were crossed with *mpx*:GFP. Their progeny embryos were tested using the previously described mutation analysis method (methods chapter 2 section 2.2.3.9) for screening of potential founder fish. The positive digestion results were then accurately analysed by sequencing using the same primers for PCR (semaphorin3Fa in Figure 5.4, semaphorin3Fb in Figure 5.5). The embryos of the potential founder with frameshift mutations were allowed to grow in the aquarium system. Once the offspring of the potential founder were 2-3 months old, the screening of these F1 fish was performed by fin clipping and mutation analysis. The genomic DNA was extracted and tested using the previously described mutation analysis method (methods chapter 2 section 2.2.3.9). The positive digest arrays were then analysed by sequencing.

The F1 generation of mutated fish of both semaphorin3Fa and semaphorin3Fb showed frameshift mutation at the somatic cell level. TALENs induced 1 bp deletion in semaphorin3Fa gene in exon 8, likewise, semaphorin3Fb gene had 1 bp deletion in exon 8 (Figure 5.6).

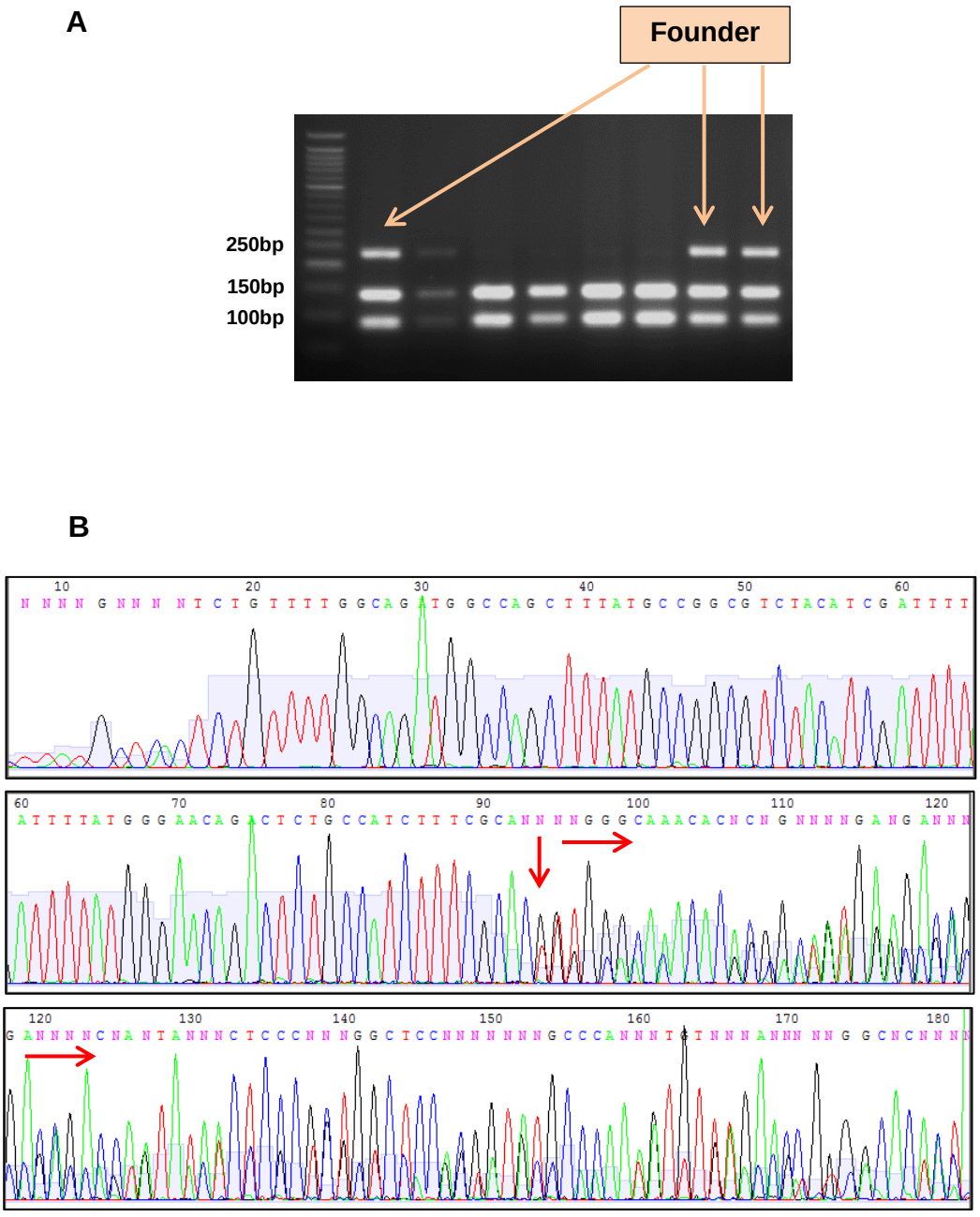

Figure 5.4: Screening of mutated semaphorin3Fa founder. (A) Gel showing MwoI digestion of PCR products amplified from genomic DNA of progeny embryos of semaphorin3Fa mutated fish. The uncleaved PCR products were shown as pointed by orange arrows. (B) The positive digestion results (with uncleaved product) were then accurately analysed by sequencing. Screenshot from FinchTV showing the sequence of this product. The overlapped peaks demonstrated nucleotide changes between WT and mutated sequence (as pointed by red arrows) starting from the cleavage site.

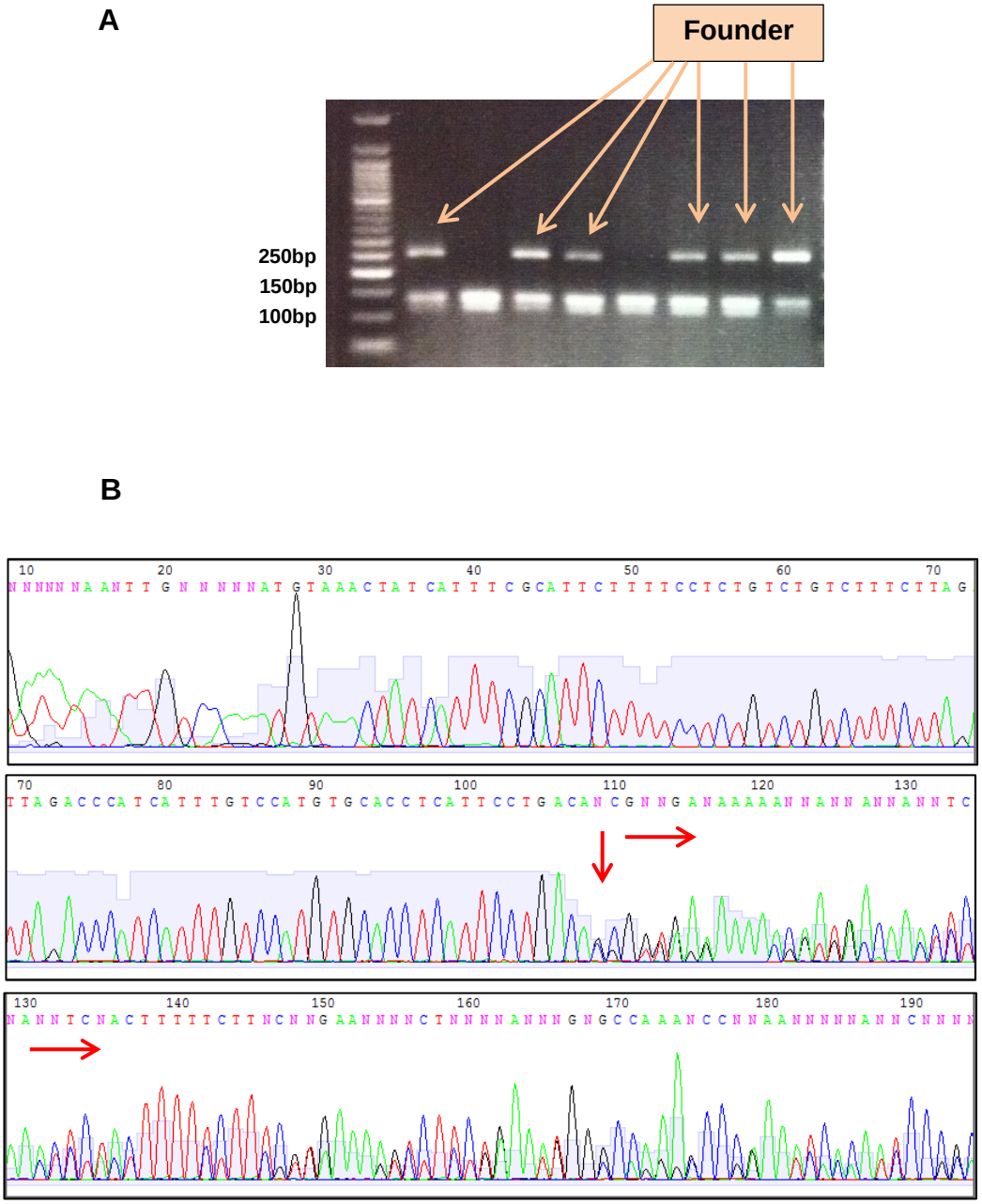

Figure 5.5: Screening of mutated semaphorin3Fb founder. (A) Gel showing BslI digestion of PCR products amplified from genomic DNA of progeny embryos of semaphorin3Fb mutated fish. The uncleaved PCR products were shown as pointed by orange arrows. (B) The positive digestion results (with uncleaved product) were then accurately analysed by sequencing. Screenshot from FinchTV showing the sequence of this product. The overlapped peaks demonstrated nucleotide changes between WT and mutated sequence (as pointed by red arrows) starting from the cleavage site.

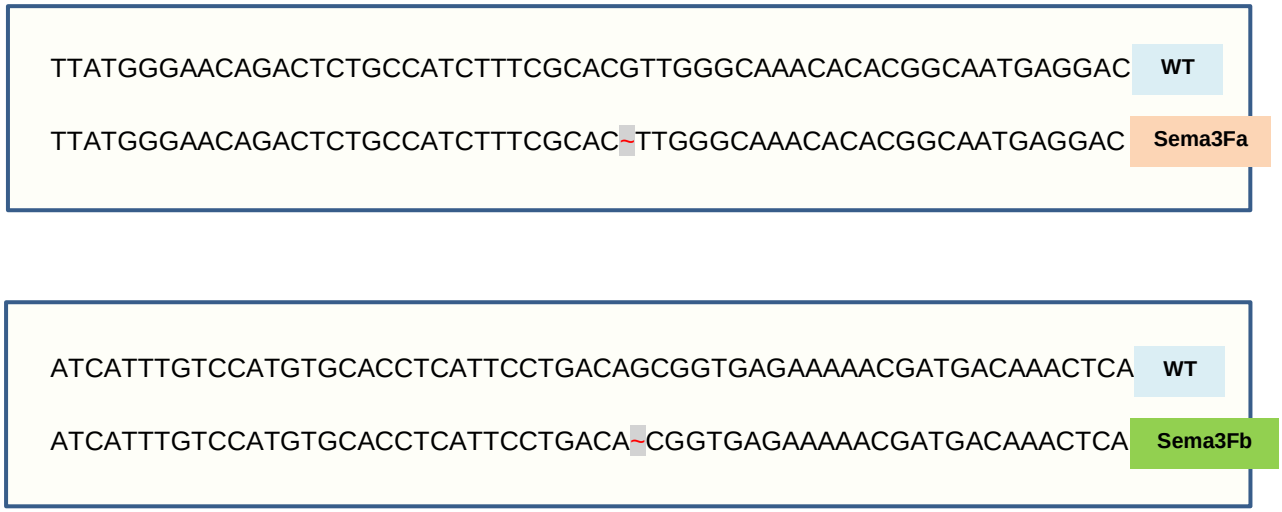

Figure 5.6: Target sequence and sequence of somatic mutation induced by TALENs in embryonic zebrafish cells at their intended target loci. For each pair of TALENs (semaphorin3Fa and semaphorin3Fb), the wild-type (WT) target sequence is shown at the top with the intended target sites of the TALE nucleases marked in yellow. Deletion is indicated by grey highlighted red dash.

The protein sequence of each mutated gene was aligned with its WT sequence using NCBI/Blast. Both mutated genes induced by TALENs of semaphorin3Fa and semaphorin3Fb demonstrated a large number of stop codons compared to WT (Figure 5.7 and Figure 5.8). This showed that introduction of a 1 bp deletion at the cleavage sites of each mutated gene could potentially induce frameshift knockout mutations at the somatic cell level passing through the germline to create mutant fish.

Semaphorin3Fa WT protein sequence

MDKVIMQGAGTLVLGTLLVSVFSAVSVHSSPLSSLPPASVPRVFLSFKELKSTGTAHHFAFL
LNSTDYRILRMDEDHDRMYVGSKDYILSLDLNDINKEPLIIHWPVAPQKRTECVLSGKDINGE
CGNFIRLIEPWNRTHLYVCGTGAYNPICTYVDRGQRAQGFLQDQMPRAGGRTSRAADPSA
SPEPYAPKEYIFRLEPGKVDSGKGKCPYDPKLNSVSALINGQLYAGVYIDFMGTDSAIFRTL
GKHTAMRTDQYNSRWLHDPTFVHAQLIPDSAEKNDDKLYFFFREKASEMGQTPMAQSRIG
RICLNDDGGHCCLVNKWSTFLKARLICSVTGSDGIETHFDELRDVYIQKTQDTKNPVIYGVF
SVSGSVFKGSAVCVYSMADVRMVFNGPFAHKEGPNYQWVAYQGKIPYPRPGTCPGGTFT
PNMKSTKDYPDEVINFMRTHPTMFNAVYPVHKRPLVVRTNVDYEFTTITVDQVAAADGNYE
VLFLGTDRGTVQKVIVLPRDDLQTEELVLEEVEVFRVPTSITTMKISPKRQQLYVSSAVGVTH
LALHRCDVYGEACADCCLARDPYCAWDGKSCSRYSANQKRRSRRQDVKYGNPIRQCRG
YNSNANKNTLETVQYGVEGSTAFLECQARSPHVSIKWHFQKENSDRRREIRSDGRVVRTE
QGLLLRSLQLSDSGVYQCTSTEKNFKHTLVKLQLVVLSAHTVNSIQTESGAPAAPPLQSSA
WTPSAEQYKDLLTILSQPEMGLINQYCQDYWQIGDDPMAHKKKDLKELQKDLRKPRNRRH
HQEQSSMAET*

Semaphorin3Fa mutant protein sequence

MDKVIMQGAGTLVLGTLLVSVFSAVSVHSSPLSSLPPASVPRVFLSFKELKSTGTAHHFAFL
LNSTDYRILRMDEDHDRMYVGSKDYILSLDLNDINKEPLIIHWPVAPQKRTECVLSGKDINGE
CGNFIRLIEPWNRTHLYVCGTGAYNPICTYVDRGQRAQGFLQDQMPRAGGRTSRAADPSA
SPEPYAPKEYIFRLEPGKVDSGKGKCPYDPKLNSVSALINGQLYAGVYIDFMGTDSAIFRTW
ANTRQ*GPTSITPAGSTIQHLSMLSSSLIVQKRMTTSCISSSVRRPLRWVRLPWLNLGLAEF
A*MMMEDTAVW*TSGAPS*RLGSSALSPALMASRRISMSSGTCTSRRLKTQRILSSTASFPC
PGLCLKAQQYVFIQWLMCAWSSMGLSLIKKAQTTNGLHTRAKSHTLAQEHVQEGRLPPT*S
LLKITQMR*STSCAHIPPCSMQFIQSTSAPWWYEPTWIMSSPPSLWTKWLQLMATMKFCS*
EQTGEQFRK*LSCPEMIYRLKSWFWRRWRSSEFQLQSLL*RFLQNDNSCMSVRRWASHIW
LCTDVMFTERPVPTAAWPETHTVPGTESPALATQQTKKGGVEGKT*SMETL*GNAEATTRM
PIRTHWRQCSME*REAQPFWSVRPDLLMCPSSGISRRRTATGEERSVLTGVWFARNRASS
CAPSSCLTAVFTSAPQLRRTSNTPLSNSSSWFSPPTQSTASRLKAAPRPPHPFSPAPGRPA
QNNTKTS*PSSANLRWASSTSTAKTTGR*GTTPWPTRRRTSRSSRRTCGSLEIGDTTRSRA
AWLRH

Figure 5.7: Representative protein sequence alignment between semaphorin3Fa WT and semaphorin3Fa mutant. Semaphorin3Fa mutant revealed a large number of stop codons (shown as red highlighted star) compared to WT.

Semaphorin3Fb WT protein sequence

MLLDSLWPVQVLLVLSVLTLVLGNEPQNAPRVFLSFKDLRSTGTAHYFSFLLNTSDYRILRM
DEDHDRMYVGSKDYILSLDLHDINREPLIIHWPVSPQRKTECVLSGKDTNGECGNFIRLIEP
WNRTHLYICGTGAYNPVCTYVNRGRKPMTAMHLQMPQTRGRASRAAEPETVFDETGLQE
YVFHLEPGKEDSGKGKCPYDPKLNSVSALINGELYAGVYIDFMGTDSAIFRTLGKNAVMRT
DQYNSRWLNDPSFVHVHLIPDSGEKNDDKLYFFFREKSSEMGQSPKSQSRIGRICLNDDG
GHCCLVNKWSTFLKARLICSVPGADGIETHFDELRDVYIQPTQDTKNPVIYGVFSVSGSVFK
GSAVCVYSMADIRMVFNGPFAHKEGPNYQWVAYTGKIPYPRPGTCPGGTFTPNMKSTKD
YPDEVINFMRNHPTMYNSVYPVHKRPLVVRTNVDYEFTTITVDQVTAADGNYEVLFLGTDR
GTVQKVIVLPSDDLQTEELVLEEVEVFKVPTSITTMKISSKRQQLYVASAVGVTHMALHRCD
VYGEACADCCLARDPYCAWDGKSCSRYSASQKRRSRRQDVKYGNPIRQCRGYNSNINKN
TLETVQYGVEGSSTFLECQARSPHAAIKWHLHRDNSDRRREVRSDGRVLKTDQGLLLRSL
QSSDSGIYICTATEKNFKHTLVKLQLLVLTNQAVNNILVDTGRPVVSPLQSSAWTPSAGQYK
DLLTILSQPEMGLINQYCQDYWQYGDPLTGVIKAKDLKELKEQKKPRNRRHHGDEEET*

Semaphorin3Fb mutant protein sequence

MLLDSLWPVQVLLVLSVLTLVLGNEPQNAPRVFLSFKDLRSTGTAHYFSFLLNTSDYRILRM
DEDHDRMYVGSKDYILSLDLHDINREPLIIHWPVSPQRKTECVLSGKDTNGECGNFIRLIEP
WNRTHLYICGTGAYNPVCTYVNRGRKPMTAMHLQMPQTRGRASRAAEPETVFDETGLQE
YVFHLEPGKEDSGKGKCPYDPKLNSVSALINGELYAGVYIDFMGTDSAIFRTLGKNAVMRT
DQYNSRWLNDPSFVHVHLIPDTVRKTMTNSTFSFVKSLLKWARARNHNPASAASA*TMTVV
TAAWSTSGAPS*KPVSSAQSQELTGLKRTSMSSEMCTYSPRRTLKTQSSTGSSLCPALYS
RARRSASTPWRTFGWCSMDLLPTKKVPITSGWPTLGKSPTPVREHVLVGLSPRT*SPLRTT
QTRSSTSCGIIPPCITPCIQCTSAPWWSGLTWTMSSQPSLWIRSQRPTETMRCSSWEQTE
EQCRR*SSYPVMTCRQRSLCWRKWRSLRSLLLSQQ*RFLQNGNNCMWPLRWE*RIWLCT
AVMSTARPVLTAVWPGTPIVHGTANPALDTQPRRRDAAVDKT*NTGTPYASAEDTIPTLIRT
HWRQCSMGWRAAAPFWSARPDHHTLPSSGTFTETTATGGEKSAVMAVC*RRIKVCFCAL
SSPQTPASTSARPQRRTSSTRWSNCSCSS*PIRPSTTFWWTRDVRSSLRSSPAPGPPVPG
NTKTC*PSSASPRWAS*TSTARTIGSMETL*PGSSRPKTSKSSRSRRNHEIADITGTRRRHE

Figure 5.8: Representative protein sequence alignment between semaphorin3Fb WT and semaphorin3Fb mutant. Semaphorin3Fb mutant revealed a large number of stop codons (shown as red highlighted star) compared to WT.

5.2.3 Semaphorin3F mutation induced by TALENs showed the same phenotype as semaphorin3F whole fish knockdown.

To investigate the inflammatory responses of neutrophils of semaphorin3F mutation induced by TALENs, the F1 generation mutants with heterozygous mutation of each gene were in-crossed. This resulted in predicted genotypes for the offspring of 50% heterozygous, 25% homozygous mutation (knockout), and 25% WT genotype. Tail transection was performed at 2 dpf. Green fluorescent neutrophil cells were assessed by counting at injured sites at 6 and 24 hours after injury. Embryos of *mpx:*GFP were used as a negative control.

To retrospectively identify the genotype of each embryo after neutrophil counting, genomic DNA of each embryo was extracted and tested using the previously described mutation analysis (methods chapter 2 section 2.2.3.9). According to the digest array, WT revealed 2 bands caused by complete digestion, whereas homozygous mutation showed only 1 band caused by absolute modification of the cleavage site. Heterozygous mutation revealed 3 bands because of partial digestion (Figure 5.9).

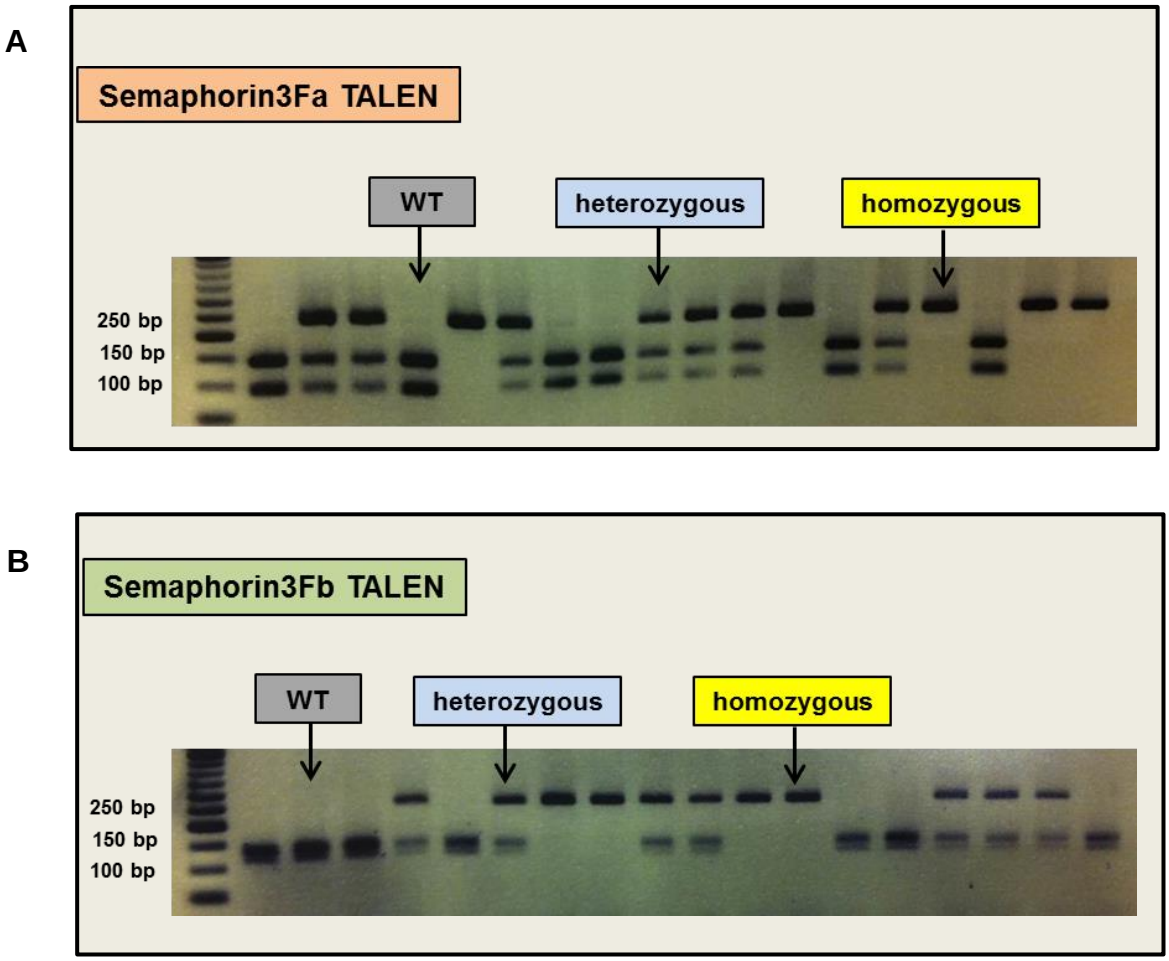

Figure 5.9: Digest array of a single embryo. (A) Gel showing MwoI digestion of PCR products amplified from genomic DNA of a single embryo of semaphorin3Fa mutated gene by TALENs. (B) Gel showing BslI digestion of PCR products amplified from genomic DNA of a single embryo of semaphorin3Fb mutated gene by TALENs. The uncleaved and cleaved PCR products are indicated.

During the recruitment phase, both semaphorin3Fa and semaphorin3Fb mutated embryos showed no significant difference in neutrophil numbers at the site of injury (semaphorin3Fa mean=26.9±0.38, semaphorin3Fb mean=26.2±0.34) compared to *mpx*:GFP control (mean=26.7±0.40) (n= 50 performed as 4 independent experiments) (Figure 5.10A). Likewise, semaphorin3F mutated embryos with genotype identification revealed no significant changes in recruited neutrophil numbers (semaphorin3Fa WT mean=27.0±0.67, semaphorin3Fa het mean=27.0±0.54, semaphorin3Fa hom mean=26.1±0.88, semaphorin3Fb WT mean=26.3±0.90, semaphorin3Fb het mean=26.3±0.48, semaphorin3Fb hom mean=26.2±0.62) compared to control (mean=26.7±0.40) (n= 50 performed as 4 independent experiments) (Figure 5.10B).

In contrast, at resolution phase, semaphorin3Fa and semaphorin3Fb mutated embryos showed significantly fewer neutrophil numbers at the injury site (semaphorin3Fa mean=9.6±0.31, semaphorin3Fb mean=9.6±0.37) compared to control (mean=11.1±0.34) (*P<0.001*, n= 50 performed as 4 independent experiments) (Figure 5.11A).

Subsequently, I compared the results with genotype identification. Semaphorin3Fa or semaphorin3Fb with WT genotype showed no significant difference in neutrophil numbers (semaphorin3Fa WT mean=10.7±0.52, semaphorin3Fb WT mean=11.1±0.71) compared to control (mean=11.1±0.34). Semaphorin3Fa or semaphorin3Fb with heterozygous mutation showed fewer neutrophil numbers at the site of injury (semaphorin3Fa het mean=9.8±0.47, semaphorin3Fb het mean=9.7±0.45). Semaphorin3Fa or semaphorin3Fb with homozygous mutation caused significantly decreased neutrophil numbers at the site of injury at 24 hpi (semaphorin3Fa hom mean=8.0±0.41, semaphorin3Fb hom mean=7.8±0.54) compared to control (mean=11.1±0.34) (*P<0.0001*, n= 50 performed as 4 independent experiments) (Figure 5.11B). These findings give evidence that semaphorin3F mutant accelerates neutrophil resolution.

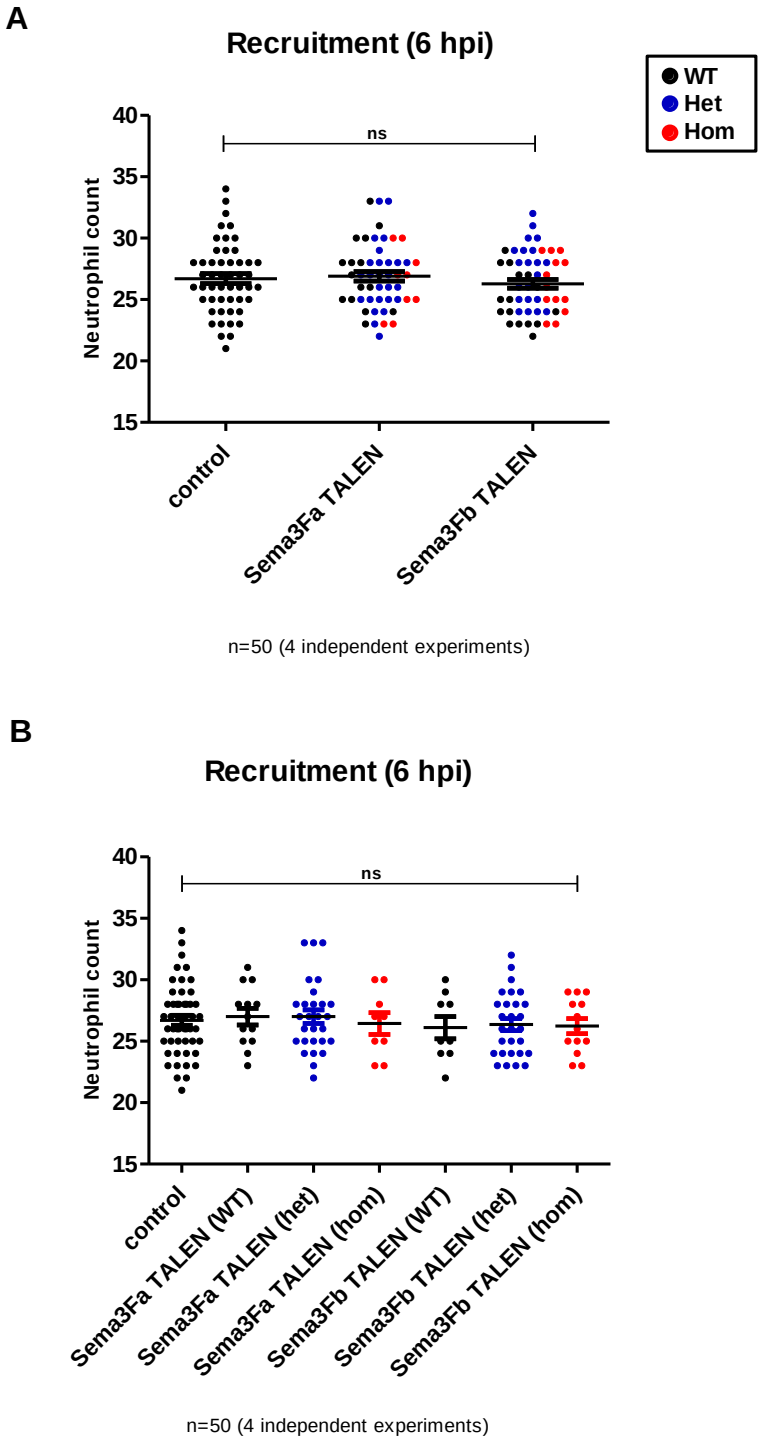

Figure 5.10: Semaphorin3F mutation induced by TALENs had no effect on neutrophil recruitment. Semaphorin3Fa or semaphorin3Fb mutated F1 fish were incrossed. Mpx:GFP was used as control. Tailfin transection was performed at 2dpf, and neutrophils counted at 6 hpi. (A) Semaphorin3F WT, heterozygous mutation and homozygous mutation were shown as black, blue and red dots, respectively. (B) Identification of genotype with separate column. Data shown are mean ± SEM. n= 50 performed as 4 independent experiments.

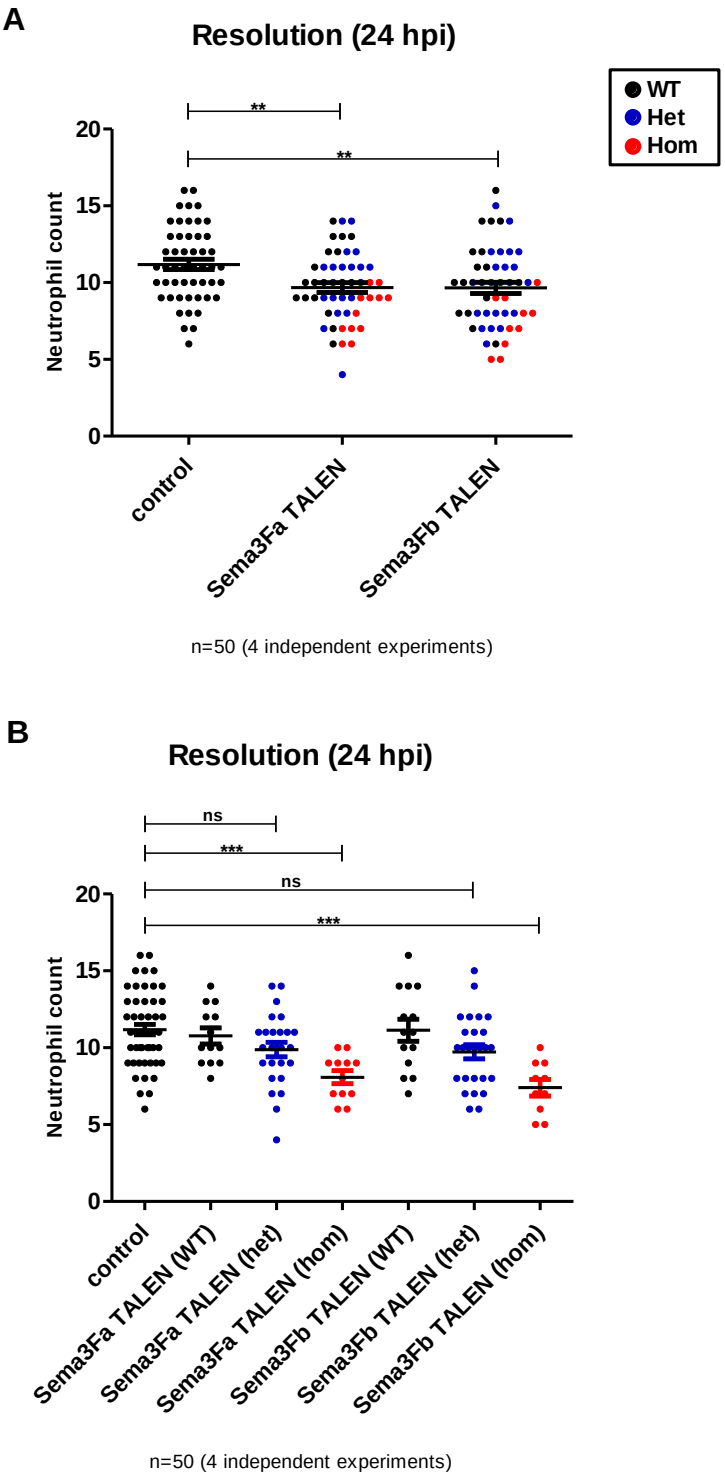

Figure 5.11: Semaphorin3F mutation induced by TALENs accelerated neutrophil resolution. Semaphorin3Fa or semaphorin3Fb mutated F1 fish were incrossed. Mpx:GFP was used as control. Tailfin transection was performed at 2dpf, and neutrophils counted at 24 hpi. (A) Semaphorin3F WT, heterozygous mutation and homozygous mutation were shown as black, blue and red dots, respectively. (B) Identification of genotype with separate column. Data shown are mean ± SEM. n= 50 performed as 4 independent experiments, **P<0.01, ***P<0.001*.

To determine whether TALENs caused any effects on whole body neutrophil numbers, total neutrophils in each mutated embryos were counted. Both semaphorin3Fa and semaphorin3Fb mutated embryos showed no significant changes in the whole body neutrophil population compared to the controls (Figure 5.12).

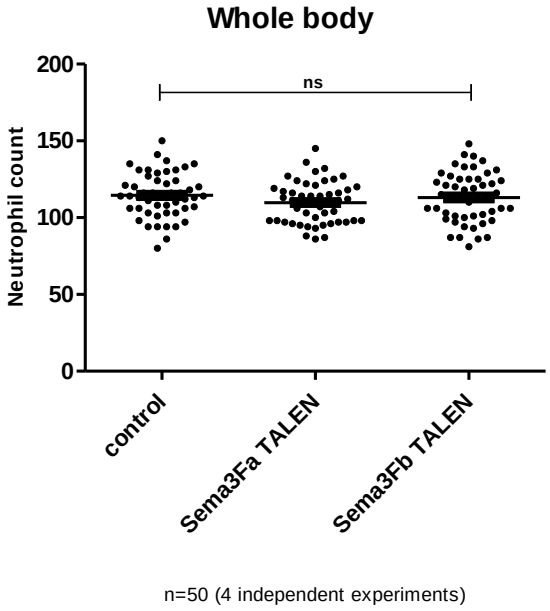

Figure 5.12: TALENs had no effect on the whole body neutrophil numbers. Whole body total neutrophil numbers were counted at 3dpf. n= 50 performed as 4 independent experiments.

In summary, semaphorin3F mutation induced by TALENs did not affect neutrophil recruitment to the site of injury, but accelerated neutrophil resolution. Thus, semaphorin3F mutant lines replicated our observed morpholino phenotypes. Together, these data indicate that semaphorin3F plays an important role in orchestrating the persistence of neutrophils at the inflammatory site through the regulation of reverse migration from the wound site.

5.3 Discussion

The zebrafish presents a powerful genetic model organism offering a diverse range of approaches to study human diseases. Several methods have been developed that enable the perturbation of a number of gene functions within the organism as a whole. In this chapter, I have created semaphorin3Fa and semaphorin3Fb mutant zebrafish lines using TALENs technology to investigate the role of semaphorin3F in the migratory behaviour of neutrophils during inflammation. Following the successful mutation of the semaphorin3F genes in zebrafish, the consequence on neutrophil recruitment and neutrophil resolution were determined, confirming the neutrophil phenotypes compared to the previous results of semaphorin3F knockdown induced by antisense morpholino injection.

5.3.1 TALENs as a new tool for genome editing in zebrafish

TALENs are one of the genome editing methods for altering specific gene sequences using artificially engineered nucleases. Site-specific double-strand DNA breaks are induced at a locus of interest by these synthetic nucleases that increase the ability to knockout or alter the expression of that gene. Targeted gene function can be attenuated in zebrafish embryos by morpholino injections (Nasevicius and Ekker, 2000), but morpholinos frequently have off-target effects on zebrafish development, and may only interfere with gene expression transiently (Eisen and Smith, 2008). TALENs have been applied in a variety of organisms including yeast, flies, rat and plants (Li et al., 2011) (Liu et al., 2012) (Tesson et al., 2011) (Li et al., 2012). In addition to zinc finger nucleases (ZFNs), TALENs have been shown to provide an alternative genome editing method for introducing DNA mutation into zebrafish (Sander et al., 2011). However, TALENs offer a number of advantages over ZFNs. They are able to target larger gene sequences with higher specificities, and are easily constructed. Design tools such as accessible reagents and software, are freely available. TALENs can target a wide range of sequences by virtue of their more flexible RVD-based

recognition (Mussolino et al., 2011). TAL effector proteins are also readily stacked to recognise long sequences. In zebrafish, TALENs show a high success rate of active nuclease capacity, and high mutation rates leading to targeted gene inactivation (Moore et al., 2012). Moreover, TALENs have fewer off-target effects and lower toxicity than ZFNs (Mussolino et al., 2011). However, TALENs have the disadvantage that assembly of TAL effectors is complicated because of their large size and abundant repeat regions. Their weakness is thus the difficulty of delivery of their large and repeat-prone sequences.

Although semaphorin3F knockdown demonstrates the significant phenotypes of neutrophilic inflammation, these findings need to be explicitly investigated. Gene knockdown using morpholinos requires optimisation of the injection dosage given the potential risk of off-target effects (Eisen and Smith, 2008). Thus, the effectiveness of the morpholino-based knockdown needs to be carefully considered. Therefore, I considered using TALENs as a tool to generate semaphorin3F mutation in zebrafish.

Here, I have demonstrated that TALENs are effective at introducing double-strand breaks resulting in mutations at the target sites. Up to 50% of embryos injected with RNA encoding semaphorin3Fa or semaphorin3Fb TALEN obtained multiple independently targeted mutations. Moreover, injection of semaphorin3F TALEN construct resulted in less than 30% mortality. The selected founders for both semaphorin3Fa and semaphorin3Fb were frameshift mutations, with 1bp deletions observed at the somatic cell level, known as indel, in that targeted gene. The mutated founders subsequently transmitted their mutation to 80% of their progeny indicating that TALENs have been successfully used to generate targeted mutations of semaphorin3Fa and semaphorin3Fb genes and, therefore, led to effective induction of heritable loss-of-function mutations in zebrafish.

5.3.2 Phenotype of neutrophil migration in the semaphorin3F mutant lines

As shown in chapter 4, semaphorin3F knockdown causes no significant changes in recruited neutrophil numbers at the injury site compared to controls, but at the resolution phase, there are fewer neutrophil numbers at the site of inflammation. As a consequence, semaphorin3F knockdown accelerates resolution of inflammation. In order to confirm these findings, the numbers of neutrophils at recruitment and resolution phase at the site of injury in mutated zebrafish embryos generated by TALENs were assessed. Homozygous null fish revealed the same phenotype of semaphorin3F whole fish knockdown by morpholino. They facilitated inflammation resolution with a semaphorin3F-dependent reduction in neutrophil numbers at the site of injury. Although fish heterozygous for semaphorin3F displayed lower numbers of neutrophils at the site of inflammation, this did not reach statistical significance with the number of fish studied. This may be reflective of a partial phenotype in the heterozygous offspring. Further studies of other migratory behaviour of neutrophils including speed and meandering index of neutrophil apoptosis at the site of injury, and of movement of neutrophils away from the wound region will be carried out to elucidate this finding in the future.

Taken together, these findings suggest that semaphorin3F mutant reduces the number of retained neutrophils at the wound site leading to acceleration of inflammation resolution. It also modulates the resolution rather than recruitment phase of inflammation. This phenomenon is similar to semaphorin3F knockdown induced by morpholinos.

5.3.3 Conclusions

In conclusion, I have demonstrated that TALENs-induced mutations are sufficient to generate semaphorin3F gene mutation in zebrafish. Moreover, the TALENs-introduced mutant alleles are stably inherited by their progeny. Neutrophils in these semaphorin3F mutant lines display similar phenotypes to semaphorin3F knockdown confirming that semaphorin3F plays an important role in neutrophil migration during inflammation, especially in the resolution phase. Semaphorin3F is also a potential target for inflammatory disorders associated with persistence of neutrophils at the site of inflammation.

Chapter 6: Investigating potential mechanisms of semaphorin3F modulation of neutrophilic inflammation

6.1 Introduction

The previous results in chapters 3, 4 and 5 demonstrated that semaphorin3F expression could be modulated in response to hypoxia and pro-inflammatory mediators in human neutrophil culture. Semaphorin3F was markedly expressed in inflammatory tissues in murine acute lung injury models. *In vivo*, semaphorin3F whole fish overexpression delayed neutrophil recruitment and inflammation resolution, in contrast, semaphorin3F knockdown resulted in significantly faster neutrophil clearance from the injury site. Notably, semaphorin3F mutant transgenic lines induced by TALENs accelerated inflammation resolution, confirming the role of semaphorin3F in neutrophil migration during inflammation. These findings together led me to question the mechanisms by which neutrophil movement is regulated by semaphorin3F during inflammation.

As previously mentioned, class 3 semaphorin binding to neuropilins requires a member of the plexin family in order to form a complex enabling the activation of downstream signal transduction cascades. In this complex, neuropilins function as the ligand-binding subunit, whereas plexins act as the signal-transducing subunit (Pueschel, 2002). Recently, neuropilin-2, as well as the plexin-A family have been identified as co-receptors of semaphorin3F (Negishi et al., 2005). I therefore hypothesised that co-expression of neuropilin-2 or plexin-As with semaphorin3F might modulate neutrophil responses to hypoxia or inflammation. To investigate this, I initially examined the protein expression of neuropilin-2, plexin A1, plexin A2 and plexin A3 in isolated human neutrophils in response to hypoxia and in the presence of pro-inflammatory cytokines (TNF-α and IL-1β). In addition, expression of neuropilin-1 and plexin D1 was investigated to confirm the specificity of

neuropilin-2 and plexin-As. Moreover, mRNA expression of neuropilin-1 and neuropilin-2 in murine bronchoalveolar lavage (BAL) neutrophils was quantified.

Given the phenotype of delayed neutrophil recruitment and delayed neutrophil resolution in the context of semaphorin3F whole fish overexpression, I questioned a role for semaphorin3F in neutrophil chemotactic responses. Chemotaxis is the process by which an external-signal gradient detected by cell-surface receptors is translated into the directed movement of the cell toward or away from the sources (Ridley et al., 2003). Neutrophils migrate to inflammatory sites through this chemotaxis process. The directional movement of neutrophils requires the regulation of intracellular signalling pathways allowing neutrophils to detect a gradient of attractant, then polarize and migrate toward the highest concentration of the chemoattractant (Nuzzi et al., 2007). The source of chemoattractants includes bacterial products such as formylated peptides, e.g. *N*-formyl-methionyl-leucyl-phenylalanine (fMLP), products of phospholipid metabolism such as leukotriene B4, components of the complement cascade (C5a) and chemokines such as IL-8, and they are detected by cell-surface receptors (Zachariae, 1993). In this chapter, I therefore investigated the chemotactic ability of isolated human neutrophils to a classical chemoattractants fMLP in the presence of semaphorin3F *in vitro*.

Next, to gain specific insight into the mechanism of semaphorin3F regulating neutrophil migration to the injury site during inflammation, I sought to investigate the role of Phosphoinositide 3-Kinase (PI-3K) in neutrophil recruitment. It is well known that PI-3K is functionally important in neutrophil chemotaxis. Chemoattractants like fMLP or IL-8 can activate neutrophil receptors coupled to heterotrimeric G proteins (Puri et al., 2004). PI-3Ks in turn are a family of enzymes which have been identified to be downstream of the G-protein-coupled receptors in neutrophils that trigger signalling pathways to regulate neutrophil chemotaxis towards the inflamed tissue (Cicchetti et al., 2002). The major lipid products of the PI-3K are phosphatidylinositol-3-phosphate [PI(3)P], phosphatidylinositol-3,4-biphosphate [$PI(3,4)P_2$] and phosphatidylinositol-3,4,5-triphosphate

[PI(3,4,5)P_3]. [PI(3,4)P_2] and [PI(3,4,5)P_3] are involved in a wide variety of cellular processes, including cell survival, cell transformation, cell polarisation and re-arrangements of the actin cytoskeleton (Toker et al., 1997, Rameh et al., 1999). Furthermore, production of [PI(3,4,5)P_3] was demonstrated in neutrophils stimulated with fMLP (Traynor-Kaplan et al., 1989).

Once a chemoattractant binds to its cell surface receptor, it triggers a series of cytoplasmic events that result in the activation of the cytoskeletal machinery. As a result, neutrophils acquire a polarised morphology characterised by expansion of the leading-edge into a lamellipod involving localised actin assembly (Benard et al., 1999). Recent observation has shown that neutrophil polarisation is blocked by the PI-3K inhibitor wortmannin (Okada et al., 1994). Moreover, neutrophils from PI-3Kγ knockout mice are unable to produce PI(3,4,5)P_3 upon stimulation resulting in a severe defect in chemotaxis and cell polarisation, and suggesting that PI-3K activity is important in cell polarity (Hirsch et al., 2000). In zebrafish, it has been shown that inhibition of PI-3Kγ disrupts neutrophil polarisation and directionality, and that zebrafish neutrophils migrate towards the wound site in a PI-3K-signalling-dependent manner (Yoo et al., 2010).

To investigate the involvement of PI-3K signalling in polarity, the zebrafish transgenic line *Tg(lyz:PHAkt-EGFP)* was used, which expresses the Pleckstrin Homology (PH) domains of Akt/PKB (protein kinase B) fused to EGFP under the *lyz* promoter. This line expresses an *in vivo* sensor of PI(3,4,5)P_3 to probe PI-3K subcellular localisation which is normally accumulated at the leading edge of neutrophils during chemotaxis (Wang et al., 2014). In addition, translocation of PHAkt-EGFP to the plasma membrane can be visualised in real time, observing the activity of PI-3K to produce PI(3,4,5)P_3. The loss of PHAkt-EGFP localisation indicates an inhibition of PI-3K signalling. This model provides the regulation of dynamics of neutrophil chemotaxis *in vivo*. In this chapter, *Tg(lyz:PHAkt-EGFP)* embryos were injected with semaphorin3F RNA, inducing whole fish semaphorin3F overexpression. Embryos were then injured at 3 dpf by tail transection, neutrophils were imaged, and the polarity index of each neutrophil was calculated.

Aims and hypotheses

The aim of this chapter is to investigate the mechanisms by which semaphorin3F regulates neutrophil movement during inflammation. The expression of semaphorin3F co-receptors was examined in response to inflammatory mediators and by regional hypoxia. The chemotaxis of human neutrophils to the chemoattractant fMLP in the presence of semaphorin3F *in vitro* was also determined. Finally, PI-3K activity was investigated in the whole fish semaphorin3F overexpression model by dynamic study.

6.2 Results

6.2.1 Neuropilin-2 and Plexin A3 expression were modulated by hypoxia and pro-inflammatory mediators.

To investigate how hypoxia or pro-inflammatory mediators (TNF-α and IL-1β) regulate the expression of predicted receptors of semaphorin3F including neuropilin-1, neuropilin-2, plexin A1, plexin A2, plexin A3 and plexin D1, freshly isolated peripheral blood neutrophils from healthy volunteers were cultured in normoxic and hypoxic conditions for 4 hours. In addition, neutrophils were incubated in parallel in the presence or absence of TNF-α and IL-1β for 4 hours either in normoxia or hypoxia. Cells were lysed using hypotonic sonication lysis buffer, the lysates were then separated by SDA-PAGE with 8% resolving gels, and p38-MAPK was used as a loading control.

Neuropilin-1 has an approximate molecular weight of 103 kDa, neuropilin-2 105 kDa, plexin A1 211 kDa, plexin A2 212 kDa, plexin A3 207 kDa, and plexin D1 212 kDa. Human neutrophils constitutively expressed all six of these co-receptor proteins. The expression of neuropilin-1 was unchanged in all conditions (Figure 6.1 & 6.2A), in contrast, neuropilin-2 expression was significantly downregulated in response to hypoxia compared to normoxia. Expression of neuropilin-2 was upregulated compared to unstimulated neutrophils when aged neutrophils were incubated with TNF-α or IL-1β (Figure 6.1 & 6.2B) (densitometry performed relative to p38, $*P<0.05$, n=3 performed as 3 independent experiments).

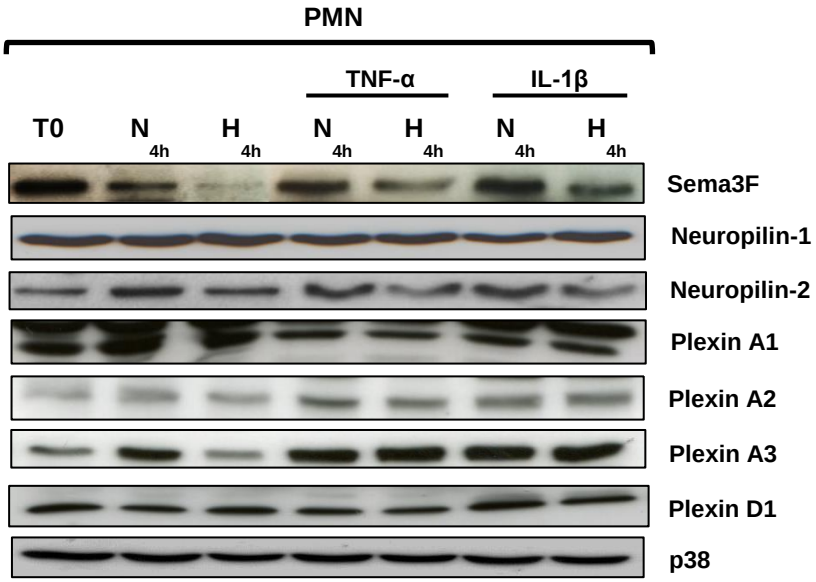

Figure 6.1: Hypoxia and pro-inflammatory mediators (TNF-α or IL-1β) can modulate the expression of neuropilin 2 and plexin A3. Western blot analysis of semaphorin3F, neuropilin-1, neuropilin-2, Plexin A1, plexin A2, plexin A3 and plexin D1 protein in human neutrophils. Human peripheral blood neutrophils (PMNs) were lysed at time 0 or following 4 hours +/- TNF-α or IL-1β culture in normoxia (N) or hypoxia (H), with p38-MAPK used as a loading control.

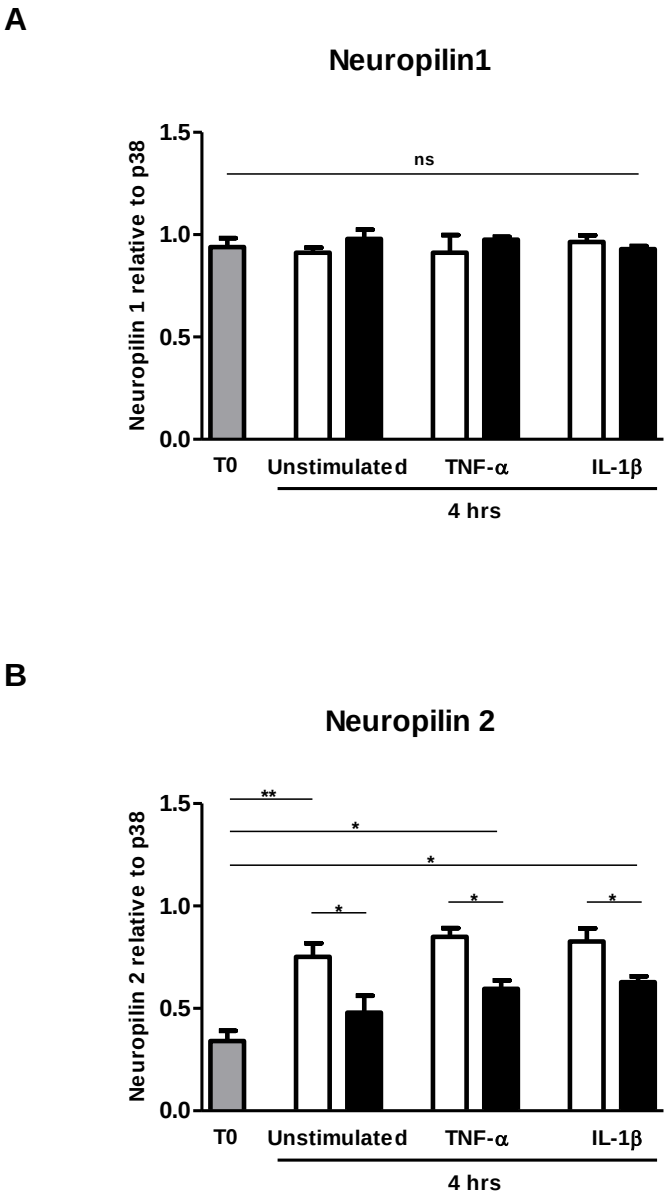

Figure 6.2: Hypoxia and pro-inflammatory mediators (TNF-α or IL-1β) can modulate the expression of neuropilin 2. (A) Densitometry performed relative to p38 of neuropilin 1 or (B) of neuropilin 2 at time 0 or following 4 hours in normoxia and hypoxia in the presence or absence of TNF-α or IL-1β (n=3), P values were calculated using one-way ANOVA **P<0.05, **P<0.01*.

Plexin A1 expression demonstrated no significant change between normoxia and hypoxia both in the presence or absence of pro-inflammatory mediators (Figure 6.1 & 6.3A). Likewise, hypoxic conditions did not markedly affect the expression of plexin A2 in human neutrophils (Figure 6.1 & 6.3B). By contrast, plexin A3 expression was significantly downregulated in response to hypoxia compared to normoxia, but this hypoxic suppression of plexin A3 was partially rescued by co-incubation of neutrophils with TNF-α and IL-1β (Figure 6.1 & 6.3C). Plexin D1 was significantly unchanged by hypoxic conditions or TNF-α and IL-1β (Figure 6.1 & 6.3D).

In summary, neuropilin-2 and plexin A3 expression were altered in hypoxia and in the presence of TNF-α or IL-1β. These studies revealed that hypoxia and pro-inflammatory mediators could modulate the expression of these two receptors.

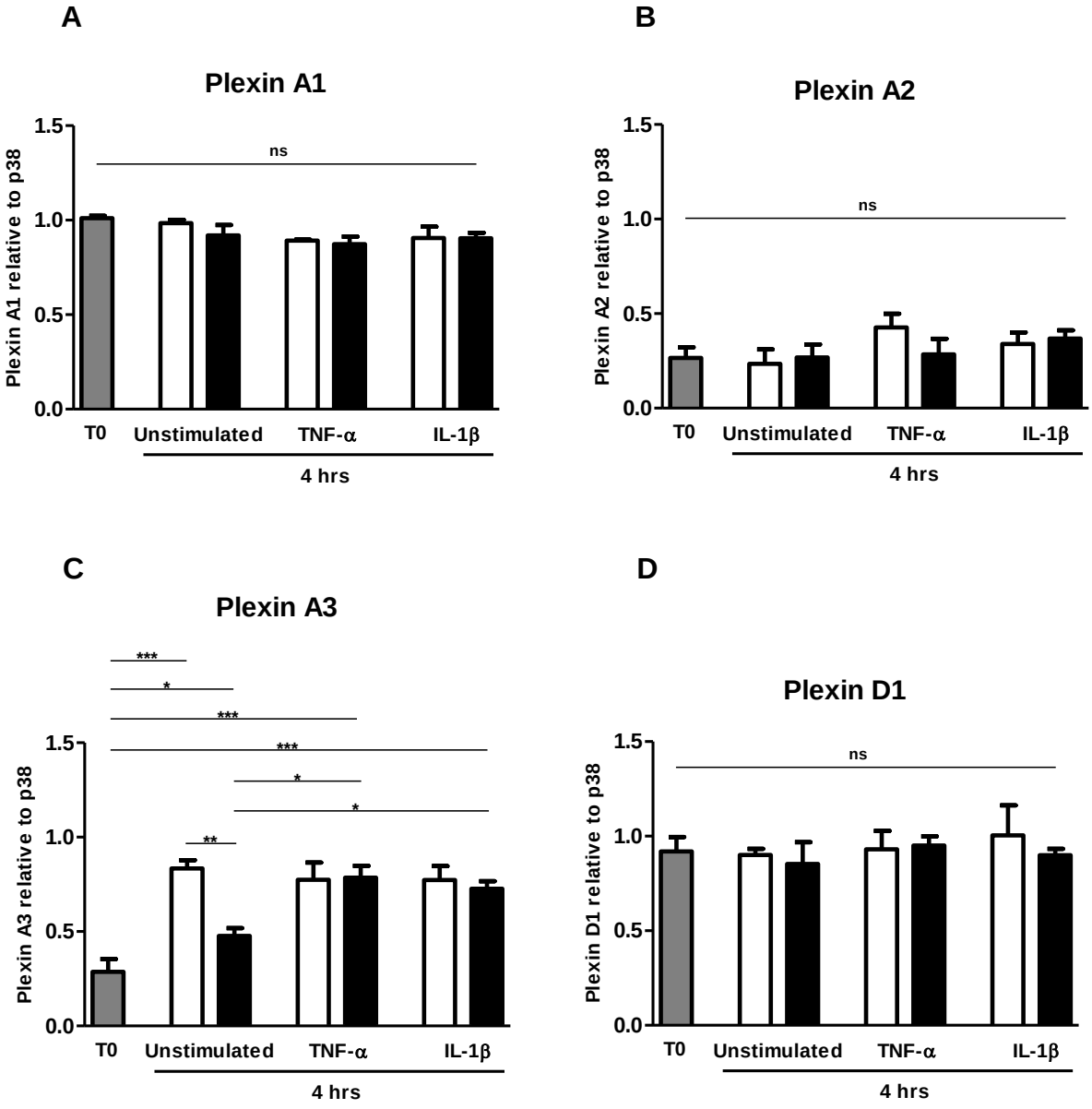

Figure 6.3: Hypoxia and pro-inflammatory mediators (TNF-α or IL-1β) could modulate the expression of plexin A3. (A) Densitometry performed relative to p38 of plexin A1 or (B) of plexin A2 or (C) plexin A3 or (D) plexin D1 at time 0 or following 4 hours in normoxia and hypoxia in the presence or absence of TNF-α or IL-1β (n=3), P values were calculated using one-way ANOVA **P<0.05, **P<0.01, ***P<0.0001*.

6.2.2 Neuropilin-1 and Neuropilin-2 expression in acute models of neutrophilic inflammation

To further investigate the expression of neuropilin-1 and -2 in neutrophilic inflammation in *vivo,* an acute model of lung injury in mice was performed. LPS was directly instilled intratracheally inducing acute lung injury. Six hours after LPS, mice were recovered in environmental normoxia or hypoxia. Mice were sacrificed at 24 hours, lung sections were stained with neuropilin-1 or neuropilin-2 isotypecontrol and neuropilin-1 or neuropilin-2 antibody, respectively (data reproduced with permission from Dr.Sarah Walmsley).

Both neuropilin-1 and neuropilin-2 were co-localised to neutrophils (shown as deep brown cells). Neuropilin-1 expression was not obviously different between normoxia and hypoxia. Moreover, neuropilin-1 isotype was quite dirty with non-specific background (Figure 6.4), whereas neuropilin-2 appeared to be more highly induced in hypoxic acute models of neutrophilic inflammation. High number of neutrophils was co-detected with neuropilin-2 (Figure 6.5) (data with permission from Dr.Sarah Walmsley).

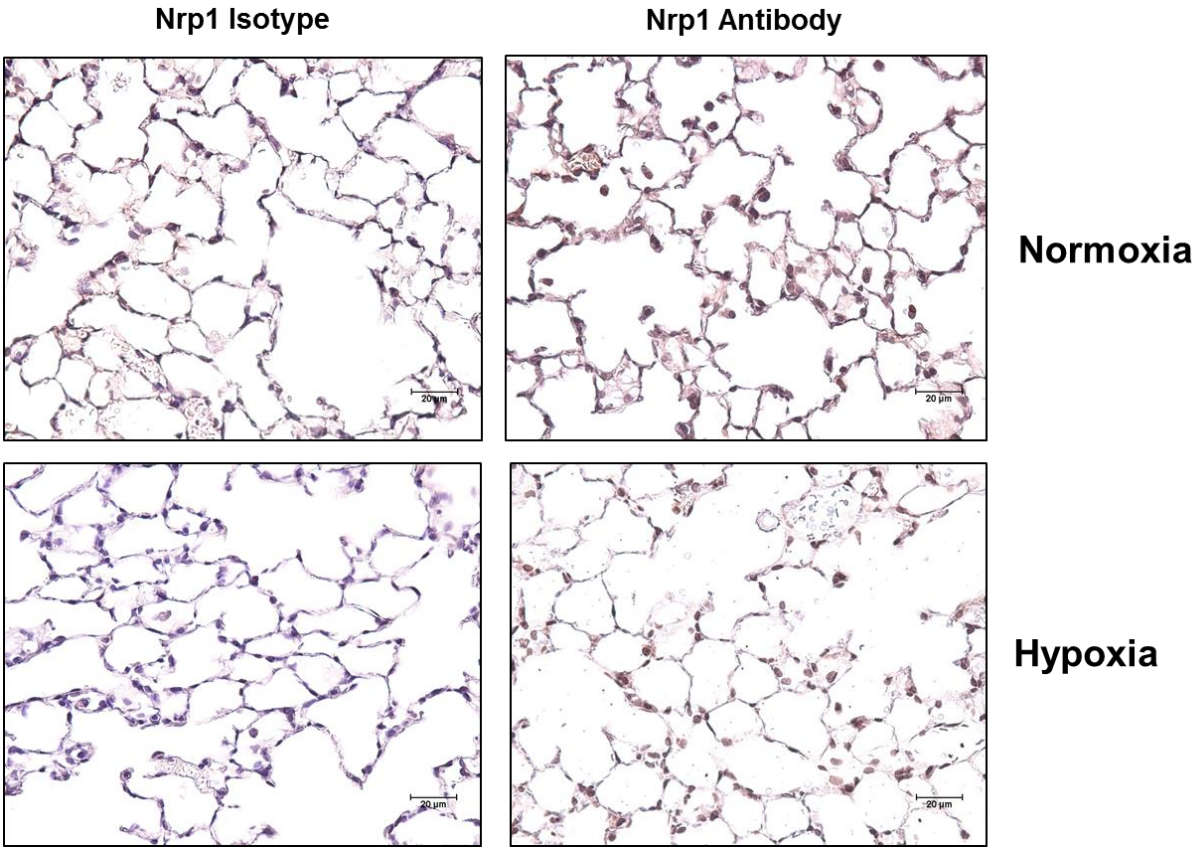

Figure 6.4: Neuropilin-1 expression was unchanged in acute models of neutrophilic inflammation. An acute lung injury was induced by intratracheal LPS installtion. Six hours after LPS, mice were recovered in environmental normoxia or hypoxia. Mice were sacrificed, lung sections were stained with neuropilin-1 isotype and neuropilin-1 antibody (deep purple staining) (data with permission from Dr.Sarah Walmsley).

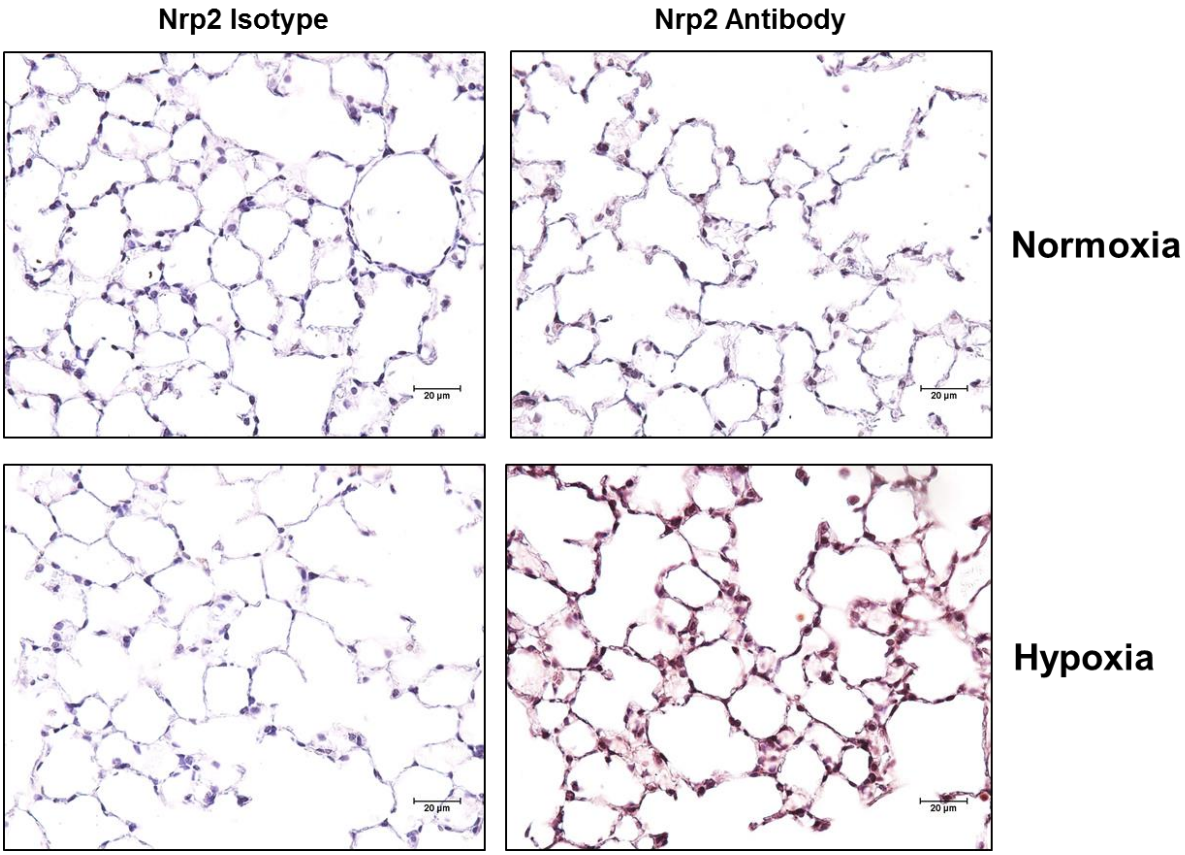

Figure 6.5: Neuropilin-2 expression appeared to be more highly induced in hypoxic acute models of neutrophilic inflammation. An acute lung injury was induced by intratracheal LPS installtion. Six hours after LPS, mice were recovered in environmental normoxia or hypoxia. Mice were sacrificed, lung sections were stained neuropilin-2 isotype and neuropilin-2 antibody (deep purple staining) (data with permission from Dr.Sarah Walmsley).

6.2.3 Neuropilin-2 mRNA expression was upregulated in murine bronchoalveolar lavage (BAL) neutrophils.

To further investigate the expression of neuropilin-1 and neuropilin-2 in response to inflammation *in vivo*, neuropilin-1 and neuropilin-2 mRNA in murine bronchoalveolar lavage (BAL) neutrophils were quantified. Acute lung injury in mice was induced by intratracheal LPS installtion. Then, 6, 24 and 48 hours after LPS, mice were recovered in environmental hypoxia. Mice were sacrificed, BAL cells were collected, and cDNA was then extracted. The cDNA samples of each condition were applied to TaqMan® gene expression assays. Beta-actin (ACTB) was selected as the endogenous control as it is highly expressed and expression is not altered by hypoxia (data with permission from Dr.Sarah Walmsley).

Consistent with the previous finding of lung section staining, the mRNA expression of neuropilin-1 was unchanged in BAL neutrophils at 6, 24 and 48 hours after LPS compared to peripheral blood neutrophils (T0). This finding was also consistent with the previous result of neuropilin-1 protein expression in human neutrophils (data normalized to beta-actin expression, n=4) (Figure 6.6A).

In contrast, the expression of neuropilin-2 mRNA was significantly upregulated in BAL neutrophils at 6, 24 and 48 hours after LPS compared to peripheral blood neutrophils (T0) (data normalized to beta-actin expression, *$P<0.05$, ***$P<0.001$, n=4) (Figure 6.6B). These results demonstrated that neuropilin-2 was markedly induced in neutrophilic inflammation at an mRNA level (data with permission from Dr.Sarah Walmsley).

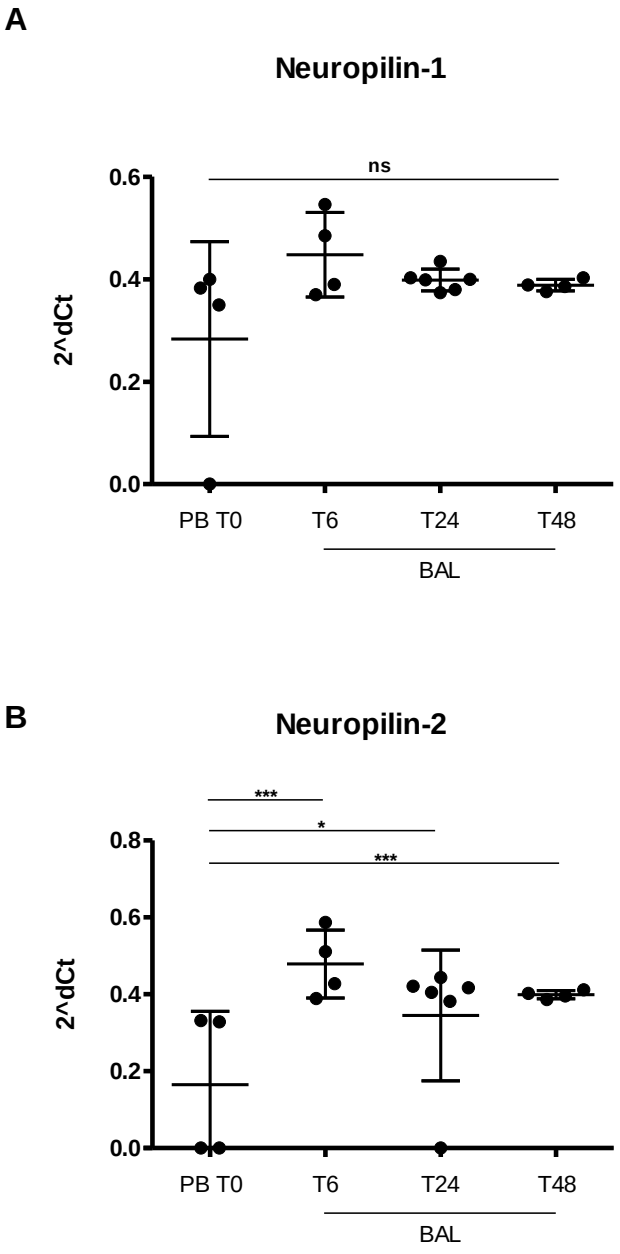

Figure 6.6: Neuropilin-2 mRNA expression was upregulated in murine bronchoalveolar lavage (BAL) neutrophils. Fold change in expression of (A) neuropilin-1 or (B) neuropilin-2 following acute lung injury with LPS. Mice were recovered for 6, 24 and 48 hours in hypoxia. BAL neutrophils were then collect, and cDNA was extracted. TaqMan analysis of cDNA was performed with data normalized to beta-actin (*ACTB)* expression. Data show mean and SEM of fold change compared to peripheral blood neutrophils (T0), n=4, analysed by ANOVA, **P<0.05, ***P<0.0001* (data with permission from Dr.Sarah Walmsley).

6.2.4 Semaphorin3F inhibited neutrophil chemotaxis to the chemoattractant fMLP.

To dissect the mechanism by which semaphorin3F regulates neutrophil movement, we planned a parallel experiment in human peripheral blood neutrophils. We first sought to characterise neutrophil chemotactic responses in the presence of exogenous semaphorin3F. To address this question, freshly isolated peripheral blood neutrophils from healthy volunteers were treated with recombinant semaphorin3F, and the chemotactic behaviour of neutrophils to fMLP was determined by chemotaxis assay using modified Boyden chambers (Boyden, 1962). Neutrophils were placed in the presence of semaphorin3F (10 nM or 100 nM) (Atwal et al., 2003) into the upper chamber, while fMLP (10 nM or 100 nM) was put into the lower chamber. Neutrophils were allowed to migrate through the pores of membrane from the upper into the lower chamber. After incubation for 1 hour at 37^{o} C, the number of neutrophils that had migrated to the lower chamber was counted using a haemocytometer. In addition, to test whether semaphorin3F is itself a chemoattractant, neutrophils were placed into the upper chamber without semaphorin3F, and the chemotactic effect of semaphorin3F in the lower chamber was evaluated. Migratory behaviours of neutrophils to media and fMLP were used as controls. Moreover, fMLP or semaphorin3F chemokinesis randomly directed or non-directional neutrophil migration, was used as negative control (data with permission from Dr.Sarah Walmsley).

Incubation of human neutrophils with semaphorin3F demonstrated significantly fewer neutrophils migrated toward the chemoattractant fMLP in the lower chamber compared to neutrophils without semaphorin3F (*$P<0.05$, **$P<0.001$, ***$P<0.0001$, n=3). The number of neutrophils migrated to semaphorin3F was unchanged compared to media, fMLP chemokinesis and semaphorin3F chemokinesis negative control, but was significantly fewer than fMLP positive controls (***$P<0.0001$, n=3) (Figure 6.7). These results indicated that semaphorin3F inhibited neutrophil chemotaxis to fMLP. Semaphorin3F itself was unable to induce neutrophil chemotaxis (data with permission from Dr.Sarah Walmsley).

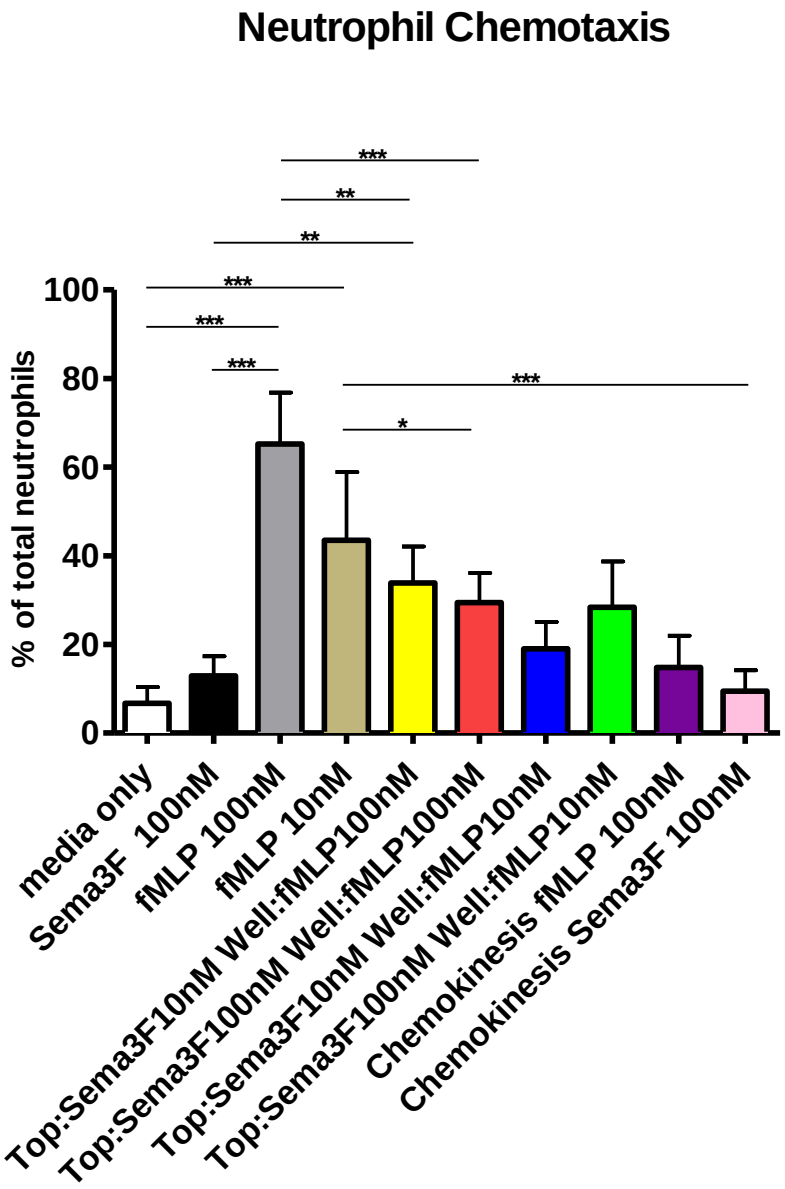

Figure 6.7: Semaphorin3F inhibited neutrophil chemotaxis to a chemoattractant fMLP. A graph to show the percentage of neutrophils undergoing chemotaxis demonstrating modulation of chemoattraction to fMLP by semaphorin3F. Isolated peripheral blood neutrophils from healthy volunteers were treated with recombinant semaphorin3F, and the chemotactic behaviour of neutrophils to fMLP was determined by chemotaxis assay using Boyden chambers (Boyden, 1962). Neutrophils were placed in the presence or absence of semaphorin3F (10 nM or 100 nM) in the upper chamber, while fMLP (10 nM or 100 nM) was put into the lower chamber. Neutrophils were allowed to migrate through the pores of membrane from the upper into the lower chamber. After incubation for 1 hour at 37^{o} C, the number of neutrophils that had migrated to the lower chamber was counted using a haemocytometer. Semaphorin3F inhibited neutrophil chemotaxis to fMLP. Semaphorin3F itself was not a chemoattractant. Data show mean and SEM, n=3, analysed by ANOVA, **P<0.05, **P<0.001, ***P<0.0001* (data with permission from Dr.Sarah Walmsley).

6.2.5 Semaphorin3F overexpression had no effect on PI-3K activity and neutrophil polarisation.

On the basis of previous findings showing semaphorin3F inhibited neutrophil chemotaxis, I subsequently extended my study into PI-3K signalling and neutrophil polarisation. In order to investigate the effect of semaphorin3F on neutrophil migration towards the wound site and on dynamic PI-3K-signalling, the zebrafish transgenic line *Tg(lyz:PHAkt-EGFP)* (obtained through collaboration with Dr.Xingang Wang and Professor Philip Ingham (IMCB, Singapore)) was used. Semaphorin3Fa or semaphorin3Fb RNA was injected into 1-cell stage embryos of *lyz*/PHAkt lineage to induce semaphorin3F whole fish overexpression. Tail transection was performed at 3 dpf, and embryos were then mounted in agarose. Neutrophils in the region between the site of injury and the posterior blood island were individually imaged on an Ultra*VIEWVoX* spinning disk confocal imaging system with an inverted Olympus IX81 microscope at 60x magnification. Non-injected *lyz*/PHAkt embryos were used as controls.

To quantify the polarity index from the images, the difference in EGFP intensity at the leading edge of the cell compared to the trailing edge and compared to the fluorescence within the cell was analysed using ImageJ. The word ‘polarity’ in this analysis means localised accumulation of PHAkt-EGFP with PI(3,4,5)P_3 at the leading edge. In this, using the straight-line tool, a transecting line was drawn through each cell from the trailing edge towards the leading edge. A plot profile was generated to measure the fluorescence intensity per pixel along the length of the line. Using Microsoft Excel, the mean intensity values for each parameter (more detail in section 2.2.3.10) were entered into the equation:

$$\text{Polarity index} = (\log_{10} a / b) \times [(a + b) / c]$$

where a = trailing edge of cell; b = leading edge of cell; c = whole cell

Neutrophils with semaphorin3Fa or semaphorin3Fb overexpression displayed PHAkt-EGFP localisation at the cell membrane, and had a defined leading edge. This localisation was equivalent to the PHAkt-EGFP signal observed in non-injected controls. Plot profile of the fluorescence intensity from the trailing edge towards the leading edge of semaphorin3Fa or semaphorin3Fb overexpression as well as the control demonstrated a similar pattern (Figure 6.8). Using the polarity index equation, neutrophils of semaphorin3F overexpression showed no significant difference in polarity index (semaphorin3Fa mean = 0.0412 $\pm$ 0.013, semaphorin3Fb mean = 0.0416 $\pm$ 0.0097) compared to control (mean = 0.0428 $\pm$ 0.0118) (n=9, 1 independent experiment) (Figure 6.9).

Interestingly, although the polarity index of all conditions was not altered, neutrophil shape was obviously different. Neutrophils of control fish displayed stretched body with pseudopodia, whereas most neutrophils of semaphorin3Fa or semaphorin3Fb overexpressing fish were round or oval (Figure 6.10).

Subsequently, I quantified neutrophil roundness using the 'analyse' function of imageJ (Yoo et al., 2012). In this, a freehand line was drawn around each cell, and the roundness of each neutrophil was quantified by 'measure' of the analyse function.

$$Roundness = 4 \times [Area] / \pi \times [Major\ axis]^2$$

The value is between 0 and 1, which 0 is a line segment, and 1 is actually a circle.

Semaphorin3Fa or semaphorin3Fb overexpression was associated with rounder neutrophils than the non-injected controls (semaphorin3Fa mean = 0.743 $\pm$ 0.043, semaphorin3Fb mean = 0.762 $\pm$ 0.061, control mean = 0.446 $\pm$ 0.039) (****P<0.0001*, n=9, 1 independent experiment) (Figure 6.10). These results suggested that semaphorin3F overexpression had no effect on PI-3K activity and neutrophil polarisation, but might affect neutrophil shape during inflammation.

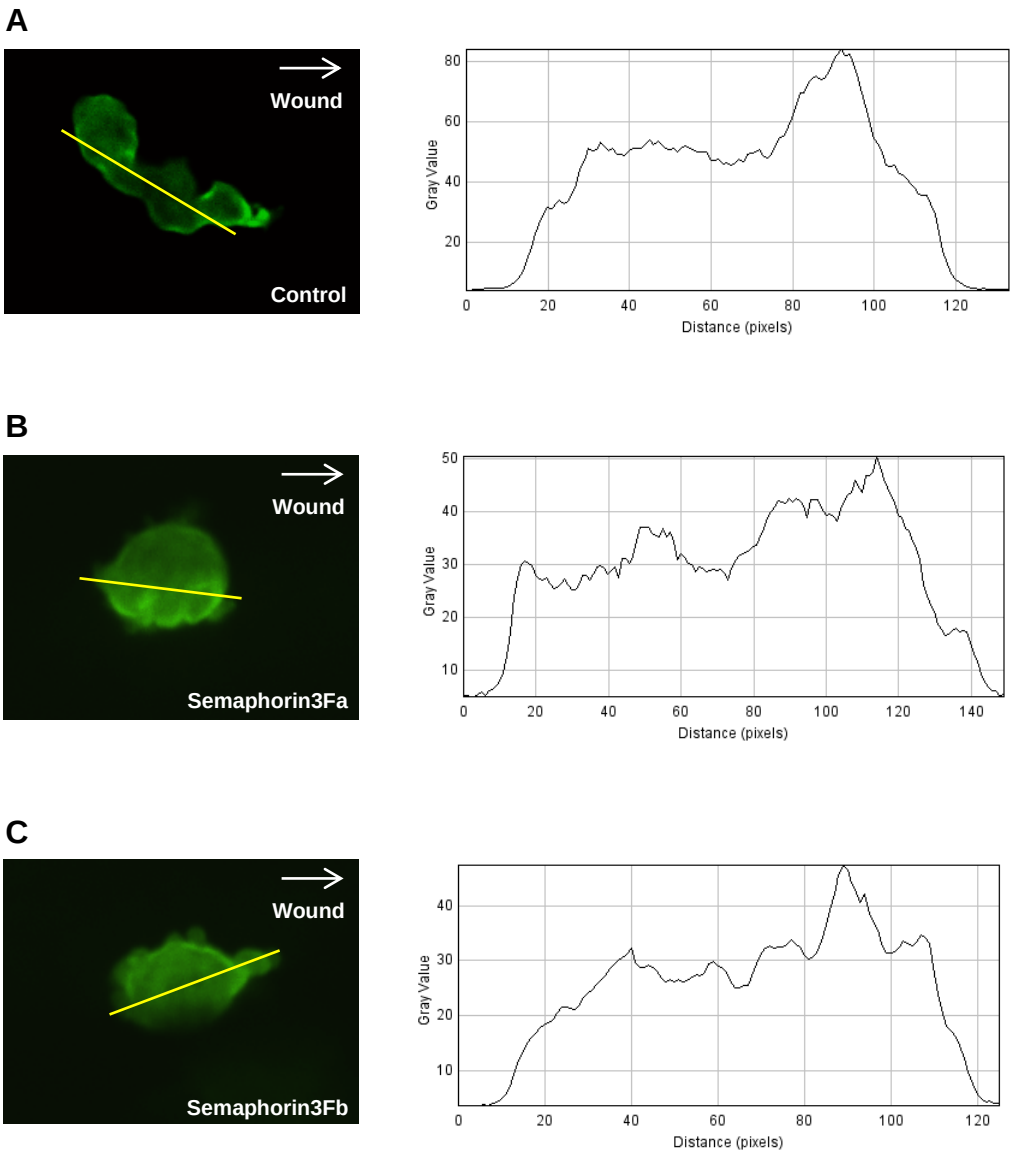

Figure 6.8: Semaphorin3F whole fish overexpression showed no significant difference in neutrophil polarity index in Tg(lyz:PHAkt-EGFP) embryos. Semaphorin3Fa or semaphorin3Fb RNA (50ng/µl) was injected into 1-cell stage Tg(lyz:PHAkt-EGFP) embryos. In addition, lyz:PHAkt-EGFP embryos without injection were used as control. Tailfin transection was performed at 3 dpf, and embryos were imaged as described previously. A representative recruited neutrophil of (A) control or (B) semaphorin3Fa overexpression or (C) semaphorin3Fb overexpression with straight-line tool as illustrated in yellow line is matched to a representative intensity plot.

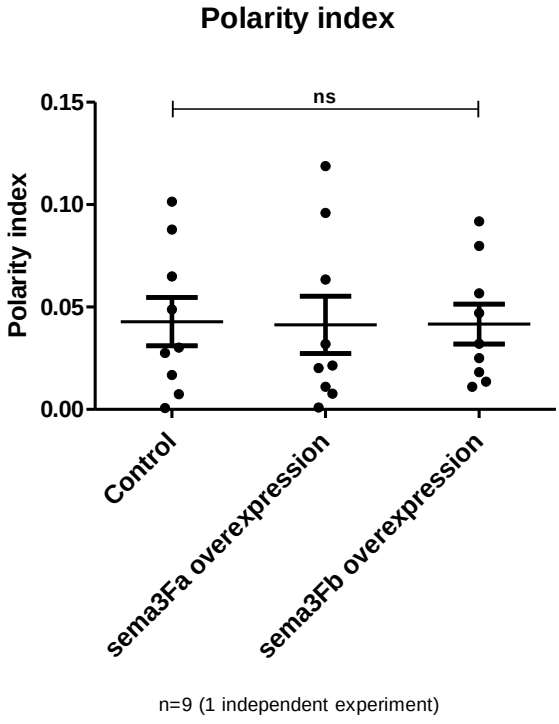

Figure 6.9: Semaphorin3F whole fish overexpression showed no significant difference in neutrophil polarity index in Tg(lyz:PHAkt-EGFP) embryos. Semaphorin3Fa or semaphorin3Fb RNA (50ng/µl) was injected into 1-cell stage Tg(lyz:PHAkt-EGFP) embryos. In addition, lyz:PHAkt-EGFP embryos without injection were used as control. Tailfin transection was performed at 3 dpf, and embryos were imaged as described previously. Polarity index of each neutrophil was calculated. Data shown are mean ± SEM. n= 9 performed as 1 independent experiment.

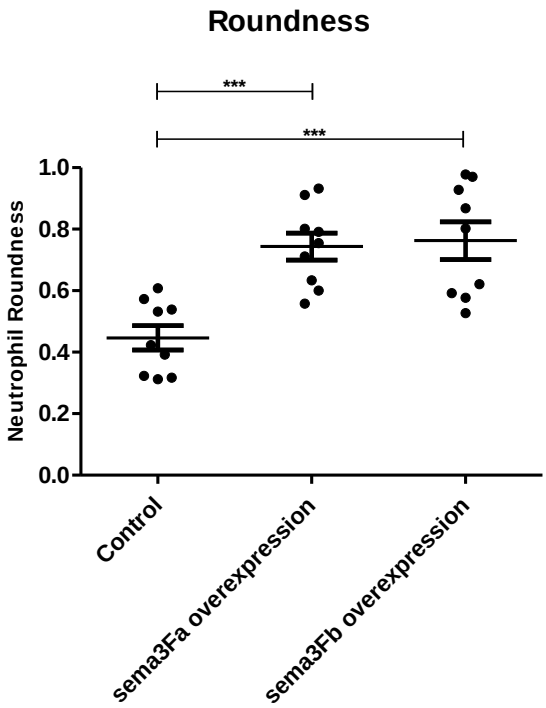

n=9 (1 independent experiment)

Figure 6.10: Semaphorin3F whole fish overexpression induced a more round morphology of recruited neutrophils in Tg(lyz:PHAkt-EGFP) embryos. Semaphorin3Fa or semaphorin3Fb RNA (50ng/µl) was injected into 1-cell stage Tg(lyz:PHAkt-EGFP) embryos. In addition, lyz:PHAkt-EGFP embryos without injection were used as control. Tailfin transection was performed at 3 dpf, and embryos were imaged as described previously. Neutrophil roundness of each neutrophil was calculated. Data shown are mean ± SEM. n= 9 performed as 1 independent experiment, ****P<0.0001*.

6.3 Discussion

Whilst a role for semaphorin3F in tumour progression has begun to emerge, the function of semaphorin3F in the immune system remains largely unknown. Here I explored for the first time the role of semaphorin3F in neutrophilic inflammation. In this chapter, I have investigated the mechanism of semaphorin3F regulation of neutrophil migration. Characterisation of semaphorin3F receptors, neutrophil chemotactic responses, and PI-3K-triggered polarisation are then determined.

6.3.1 Receptors of semaphorin3F in regulating neutrophil migration during inflammation

Neuropilin-1 and neuropilin-2 are receptors for axon guidance factors belonging to the class 3 semaphorins. Most of these semaphorins bind to one or to both of the neuropilin family exhibiting different binding-specificities (Kolodkin et al., 1997). Neuropilin-1 was initially identified as a semaphorin3A receptor (He and Tessier-Lavigne, 1997), whereas neuropilin-2 was originally characterised as a receptor for semaphorin3C and semaphorin3F (Kolodkin et al., 1997). In addition, neuropilin-2 is a receptor of $VEGF_{165}$, and binds semaphorin3F and VEGF with similar affinities in a competitive manner (Geretti et al., 2007).

Interestingly, experiments with hypoxia have revealed conflicting results regarding neuropilin-2 expression in different cell types. Hypoxia leads to decreased expression of neuropilin-2 in glioblastoma and melanoma cells at both transcriptional and translational level (Coma et al., 2011), whereas neuropilin-2 expression is maintained in human umbilical vein endothelial cells (HUVECs) (Bae et al., 2008) and in human pulmonary microvascular endothelial cells (Blythe et al., 2012) under hypoxic conditions, and is in contrast downregulated in murine hepatoma cells in response to hypoxia (Raskopf et al., 2012). However, in inflammatory tissues such as rheumatoid synovium, neuropilin-2 is markedly increased (Fassold et al., 2009), as it is in chronic bladder inflammation (Saban et al., 2010). In this study, I observe

that neuropilin-2 protein is downregulated in response to hypoxia in peripheral blood neutrophils, but this can be rescued by co-stimulation with TNF-α or IL-1β. Moreover, neuropilin-2 mRNA and protein are significantly upregulated in murine BAL and tissue recruited neutrophils respectively, suggesting that neuropilin-2 is regulated by additional factors released in the inflammatory microenvironment. In contrast, neuropilin-1 expression is unchanged both at mRNA and protein level.

Neuropilins have short intracellular domains and are thus through to act as independent signalling receptors. Several studies demonstrate that the class 3 semaphorin signals are transduced by plexins, with neuropilins functioning as high-affinity binding receptors (Takahashi et al., 1999). Current studies in neurons suggest that neuropilin-2/plexin A3 complexes mediate responses to semaphorin3F (Cheng et al., 2001) (Yaron et al., 2005). Other research groups have shown that plexin A3 and semaphorin3F have a similar expression pattern. For instance, a significant decreased expression of plexin A3 and semaphorin3F was observed in human ovarian cancer cells (Capparuccia and Tamagnone, 2009), in human breast neoplasia (Staton et al., 2011) and in endometrial carcinomas (Nguyen et al., 2011). Here, I found that only plexin A3 expression is decreased in response to hypoxia, but upregulated in response to inflammatory cytokines, displaying the same pattern as the expression of semaphorin3F, and of neuropilin-2 as well. By contrast, other class A plexins, plexin A1and plexin A2, and another control plexin, plexin D1, are not altered in all conditions. This led me to postulate that neuropilin-2 and plexin A3 may represent the critical receptors for semaphorin3F in inflammatory neutrophils.

Given that semaphorin3F affects neutrophil migration during inflammation, I hypothesise that semaphorin3F triggers signalling through neuropilin-2/plexin A3 complexes regulating neutrophil motility. To support this, other groups have shown the ability of this combination to regulate cell migration. Specific binding of semaphorin3F and its ligand, neuropilin-2, can inhibit VEGF-A and VEGF-C-induced endothelial cell migration (Favier et al., 2006). Tumour studies also suggest that semaphorin3F directly inhibits cancer cell migration

by reducing the level of integrin αvβ3, a key mediator of cell motility, through a neuropilin-2 dependent pathway (Wu et al., 2011).

Furthermore, semaphorin3F mediates sympathetic neuron migration during development in mice (Waimey et al., 2008), and oligodendrocyte precursor cell migration (Xiang et al., 2012) through plexin A3. Although no direct evidence has been shown that semaphorin3F acts via binding of neuropilin-2 and plexin A3 in modulating cell migration in the immune system, their similar expression pattern and their increased expression depending on inflammatory stimuli convince us that thisis very probable.

6.3.2 Semaphorin3F regulated chemotactic signalling pathway

In vivo, neutrophils navigate effectively through tissue microenvironments towards a chemoattractant source (Ridley et al., 2003). Here, we provided an *in vitro* experiment using Boyden chambers to investigate the chemotactic behaviour of neutrophils to fMLP in the presence of exogenous semaphorin3F. We found that semaphorin3F inhibits neutrophil chemotaxis to fMLP. Moreover, semaphorin3F itself is not chemoattractive. Conversely, other class 3 semaphorins have been reported to act as chemoattractants, for instance, semaphorin3A is a chemoattractant for cortical apical dendrites during neuron development (Polleux et al., 2000). The inhibition of neutrophil chemotaxis by semaphorin3F led me to further investigate the cellular mechanisms behind this response.

During chemotaxis, directional migration of neutrophils requires cell polarisation, resulting in formation of a leading edge characterised by actin-rich lamella and a tail-like uropod (Ciccahetti et al., 2002). Studies on the mechanism of chemotaxis have shown that PI-3K activity regulates the establishment of cell polarity (Stephens et al., 2002). PI3Kγ have been identified to be downstream of the βγ complex of G-protein-coupled receptors (GPCRs), which is released after stimulation by chemoattractants (Gerard and Gerard, 1994). Gβγ proteins activate their downstream

effectors, including PI3Kγ, guanosine triphosphatases of the Rho family (Rho GTPases), protein kinase C, cytosolic phospholipase A2 (cPLA2), and cytosolic tyrosine kinases. Inactivation of Gβγ proteins or inhibition of those downstream effectors causes defects of neutrophil motility in response to chemoattractants (Weiner et al., 2000). Studies of PI3Kγ signalling have reported that inhibition of PI3Kγ activities results in impairment of leading edge formation and suppression of neutrophil chemotaxis (Hirsch et al., 2000). Furthermore, localised accumulation of PI(3,4,5,)P_3, a major lipid product of PI3K, is a key event directing the activation of signalling components required for cell polarity and chemotaxis (Orlando and Guo, 2009). In this study, *lyz*/PHAkt zebrafish embryos were used to determine the localisation of PHAkt-EGFP observed in neutrophils during recruitment to the wound site. Akt binds directly to PI(3,4,5,)P_3 at the membrane through its PH domain. Trafficking of PHAkt-EGFP to the neutrophil membrane is thus dependent on the amount of PI(3,4,5,)P_3 which also refers to PI-3K activity.

Although semaphorin3F inhibits neutrophil chemotaxis *in vitro*, it shows no significant effect on PI-3K activity. The localised accumulation of PHAkt-EGFP at the membrane between fish with semaphorin3F overexpression and control fish is similar. They all also have a defined leading edge, and reveal the same polarity suggesting that semaphorin3F does not affect signalling either directly on or upstream of PI-3K involve in neutrophil polarisation. I hypothesise that semaphorin3F might be implicated in activities of other Gβγ downstream effectors such as Rho GTPases, protein kinase C, or cytosolic tyrosine kinases that could be further elucidated in the future. Moreover, besides PI-3K, the establishment of PI(3,4,5)P_3 gradients in neutrophils is regulated by the phosphatase with tensin homology (PTEN) and the Src homology2-containing inositol phosphatase (SHIP). PTEN dephosphorylates PI(3,4,5)P_3 into PI(4,5)P_2, thereby switching off PI3-K/Akt signalling (Cantley and Neel, 1999). SHIP hydrolyses the 5’ phosphatase of the inositol ring from PI(3,4,5)P_3 to PI(3,4)P_2 (. Both enzymes are important regulators of phosphoinositide pools and also thought to be important in establishing polarity in signalling (Leslie et al., 2008).

Interestingly, the observed neutrophil shape of semaphorin3F overexpression is obviously different from the control. Neutrophils of the control display stretched bodies with pseudopodia, whereas most neutrophils of semaphorin3F overexpressing fish are round or oval. One possible explanation is the activity of small GTPases of the Rho subfamily which have been reported to act as active regulators of cell shape change and also motility (Hall and Nobes, 2000). Besides being downstream effector of Gβγ proteins, Rho GTPases are also downstream targets of PI-3K that are activated by PI(3,4,5,)P_3 accumulation (Benard et al., 1999). The spatially distinct activation of different members of the small GTPases of the Rho subfamily reveals specific functional responses within the cytoskeleton. For instance, RhoA plays a role in the regulation of cell shape and polarity through actin polymerisation and actomyosin contractility (Wheeler and Ridley, 2004). Activated Rac triggers extension of lamellipodia containing arborized actin polymers, and stimulation of actin polymerisation, whereas Cdc42 activation induces fine finger-like protrusions formed by actin filaments called filopodia, and also activates Rac (Nobes and Hall, 1995). Notably, studies using differentiated HL60 (dHL-60) cells, a neutrophil-like cell line, have shown that fMLP induces polarisation and cell migration by triggering ‘frontness’ and ‘backness’ of the cells. The frontness is characterised by a protruding pseudopod composed of actively polymerising F-actin mediated by a trimeric G protein, which has positive feedback loops to PI(3,4,5,)P_3 and Rac (Weiner et al., 2002). In contrast, the backness is characterised by a rounded shape induced by contracting actomyosin complexes, which are stimulated by RhoA, Rho-dependent kinase and myosin II (Xu et al., 2003). In polarised cells, Rac-dependent frontness constrains backness to the trailing edge, whereas RhoA-dependent backness confines frontness to pseudopods. Furthermore, frontness and backness have an ability to inhibit one another (Wong et al., 2006). Consistently, studies of epithelia shape demonstrate that a balance of RhoA- and Rac-activities is critical for control of cell shape. RhoA mutant cells display longer and less apically constricted cells than control, whereas Rac1 deficient cells are shorter and more apically restricted (Chauhan et al., 2011). This led me to hypothesis that semaphorin3F might excessively stimulate the

RhoA-activity or inhibit the Rac-activity. Thus, neutrophils of semaphorin3F overexpression form rounded shape during chemotaxis, and as a consequence, the migratory ability of neutrophils is inhibited compared to controls.

6.3.3 Conclusions

In conclusion, I have identified the probable receptors of semaphorin3F in regulating neutrophilic inflammation, namely neuropilin-2 and plexin A3. Furthermore, the mechanism of semaphorin3F modulation of neutrophil chemotaxis was investigated. I demonstrated that semaphorin3F inhibits neutrophil chemotaxis to chemoattractants. However, semaphorin3F does not affect the chemotaxis-downstream PI-3K activity controlling cell polarisation. Semaphorin3F appears to be implicated in neutrophil shape change during directed migration, which may be affected by members of Rho GTPases families.

Chapter 7: Final discussion and future work

In response to injury or infection, neutrophils migrate to the site of infection or to eliminate potentially injurious stimuli. A critical active process following the elimination of invading pathogens is resolution of inflammation. This requires removal of neutrophils from inflamed sites, since they themselves can release their own injurious contents. Inflammation resolution therefore contributes to the prevention of propagation of host tissue damage caused by release of oxidants and proteinases from persistent neutrophilic activity that leads to pathology of many chronic inflammatory diseases. In recent years, much research has focussed on the regulation of neutrophilic inflammation, especially mechanisms involved in resolution of inflammation. Semaphorins, originally identified as axon guidance factors functioning in the nervous system, have recently emerged as regulators of the immune system. These semaphorins play critical roles in various phases of immune responses such as B-or T-cell activation, T-cell differentiation, T-cell-macrophage interaction, and in the functional activity of macrophages (Takamatsu et al., 2010) (Casazza et al., 2013). At inflamed sites, neutrophils are functionally regulated by hypoxia-inducible transcription factors (HIFs) and their hydroxylation by the prolyl hydroxylase (PHDs) (Thompson et al., 2013). Interestingly, our group has found that semaphorin3F is significantly induced in PHD3-deficient neutrophils following hypoxic stimulation (Walmsley et al., 2011). This led me to question whether semaphorin3F is involved in regulating neutrophil functions in inflammation. To address this, investigation of semaphorin3F expression in human neutrophils and *in vivo* experiments were carried out. Most of experiments in this study were performed in the zebrafish because it is an ideal alternative model for the study of vertebrate innate immune responses *in vivo*, especially neutrophil behaviour during inflammation (Renshaw et al., 2006). This model effectively enables the visualisation and tracking of neutrophils in real-time to investigate the role of semaphorin3F in parallel with experiments in human cells and in mouse models. Moreover, genome editing techniques for altering specific gene sequences such as morpholino-based knockdown and Transcription Activator-Like Effector Nucleases (TALENs)-induced

mutation, are reliable and easily applied to the zebrafish models. However, for microinjections, it's difficult to quantify how much the injected message is diluted or degraded by cell division, and how reproducible this effect is between different microinjections. At least, phenotypic changes e.g. in neutrophil counts at recruitment and resolution phase or shape of injected embryos (such as curly tail of morpholino-injected embryos).

7.1 Is semaphorin3F involved in neutrophil function in inflammation?

As previously mentioned, the hypoxic PHD3-deficient neutrophils have increased levels of semaphorin3F transcript (Walmsley et al., 2011). This evidence persuaded me of a correlation between neutrophil function and semaphorin3F expression during inflammation. Although semaphorin3F has only been reported to be involved in nervous system and tumour progression, other class 3 semaphorins, such as semaphorin3A affect cells of the myeloid lineage, especially macrophages. Semaphorin3A/neuropilin-1 signalling enhances tumour-associated macrophage recruitment to hypoxic tumour areas. However, semaphorin3A can interact with macrophages in the absence of neuropilin-1. This action of semaphorin3A can antogonise VEGF-induced attraction (Casazza et al., 2013). Thus, it is interesting to further investigate the expression of semaphorin3F in neutrophils in various conditions. As suggested by the PHD3 study, semaphorin3F expression is altered by inflammatory culture conditions, both at transcriptional and translational levels in human neutrophils. In response to hypoxia, semaphorin3F exhibits the opposite expression to VEGF, a known HIF target gene and regulator of neutrophil function (Taichman et al., 1997) (Gong and Koh, 2010). Semaphorin3F mRNA expression in iflammed neutrophils is significantly upregulated compared to peripheral blood neutrophils. The hypoxia-downregulation of semaphorin3F in peripheral blood neutrophils is also in contrast to the significant induction of semaphroin3F in inflammation and suggests that semaphorin3F is strongly regulated by the activity of additional factors released in the inflammatory microenvironment. All findings

support that semaphorin3F expression in inflamed neutrophils is obviously different to that in peripheral blood neutrophils. Although it's difficult to interpret the results of zebrafish linking to those of human according to unknown cellular sources of semaphorin3F in zebrafish, semaphorin3F is thought to play a crucial role in regulating neutrophil function during inflammation. The effect of exogenous semaphorin3F on neutrophil chemotaxis, and the consistent convincing upregulation of semaphorin3F in inflamed tissues in mouse lung section and in zebrafish support my hypothesis. Furthermore, I found that semaphorin3F receptor components, neuropilin-2 and plexin A3, have a similar expression profile, raising the possibility that semaphorin3F may act in an autocrine fashion on neutrophils during inflammation.

7.2 Novel role of semaphorin3F in neutrophil migration during inflammation

Semaphorin3F has been recently found to be involved in regulating cell migration of a variety of cell types, including neural cells, endothelial cells, and tumour cells (Gammill et al., 2007) (Coma et al., 2011) (Xiang et al., 2012). Here, I demonstrate for the first time the role of semaphorin3F in regulating neutrophil migration in inflammation. As shown by overexpression and by knockdown both by morpholino suppression and TALENs-generated mutation, semaphorin3F affects not only neutrophil migration to the site of injury, but also the reverse migration from the inflamed site. This suggested that semaphorin3F affects neutrophil chemotaxis, the key process governing neutrophil migration during inflammation. Chemotactic cells are characterised by three abilities, namely direction sensing, polarisation, and motility (Swaney et al., 2010). I found that semaphorin3F has effects only on speed, not direction of neutrophils suggesting that neutrophil directional sensing is not affected by semaphorin3F, but that cell motility is impaired. Consistent with this, I found that the polarisation of neutrophils, as indicated by the localisation of PI-3K to the leading edge during migration, is not affected by semaphorin3F. By contrast, neutrophil shape is obviously

different when semaphorin3F is overexpressed. Neutrophils of the control fish displayed stretched bodies with pseudopodia, whereas when semaphorin3F was overexpressed, most neutrophils were round or oval. Cell motility occurs through random extension of pseudopodia driven through the cytoskeleton (Chung et al., 2000). Therefore, the finding that semaphorin3F-affected neutrophil shape and motility raises the possibility that semaphorin3F may be associated with cytoskeleton directly or via related signalling pathways.

This is consistent with a plethora of studies of the effects of class 3 semaphorins on neuron growth cones, most particularly of semaphorin3A, that demonstrate their ability to disassemble the actin cytoskeleton (Fan et al., 1993) (Mann et al., 2007). More recently, semaphorin3F has been shown to have similar effects on the actin cytoskeleton of endothelial and tumour cells (Nasarre et al., 2003) (Bielenberg and Klangsbrun, 2007).

Studies of tumour cell migration have demonstrated that semaphorin3F inhibits cell migration by inactivating RhoA, followed by inactivation of Rho kinase. As a result, F-actin cytoskeleton depolymerisation is stimulated. Moreover, semaphorin3F inactivates small GTPase Rac1, so that lamellipodia formation at the cell leading edge is disrupted. The migration and contractility of this cell are then inhibited (Shimizu et al., 2008). Therefore, it is possible that semaphorin3F affects RhoA-activity or Rac-activity in neutrophils. As a consequence, semaphorin3F can regulate migratory behaviour of neutrophils during inflammation.

7.3 Is semaphorin3F expression associated with resolution of inflammation?

The clearance of neutrophils from inflamed sites is necessary for successful resolution of inflammation. Besides neutrophil apoptosis at the site of inflammation, neutrophil reverse migration away from the wound is an alternative important mechanism of neutrophil clearance. The work presented here has demonstrated that semaphorin3F does not affect rates of

neutrophil apoptosis at the site of injury, whereas it has considerable influence on neutrophil reverse migration. Although semaphorin3F overexpression affected both recruitment and resolution, the loss of function experiments specifically affected the clearance of neutrophils from the injury site, accelerating reverse migration. Coupled with the fact that semaphorin3F overexpression resulted in persistence of neutrophils at the site of inflammation, and that semaphorin3F expression in human neutrophils appears to be modulated antagonistically by hypoxia and inflammatory cytokines, this is consistent with the idea that modulation of semaphorin3F signalling during inflammation may govern the persistence of neutrophils at the injury site. One possibility is that as neutrophils arrive at the injury site, their movement is slowed by upregulation of semaphorin3F, causing them to 'pause' where the inflammation is greatest. However, increased hypoxia may have the opposite effect, downregulating semaphorin3F expression and initiating resolution. Unfortunately, according to limited availability of the reverse migration assay, speed and meandering index of neutrophils during the resolution phase could not be quantified. Volocity® sorfware of this assay can only calculate the numbers of neutrophils reverse migrating from the site of injury into a defined distal region. For further study of the effects of semaphorin3F on migratory behaviour of neutrophils in that phase, additional experiments have to be investigated.

Moreover, the use of zebrafish to study the effect of semaphorin3F in regulating neutrophil migration is possibly limited. Most of neutrophils have been reported to migrate away from sites of inflammation through the tissues rather than true "reverse migration" and return to the blood vessels (Robertson et al., 2014). This is distinct from mammalian systems, in which neutrophils have a return migration to the vasculature (Woodfin et al., 2011). Therefore, despite our finding that semaphorin3F is involved in both zebrafish and mammal, it is possible that some details of the molecular mechanisms or signalling pathways regulating this process in zebrafish may be different from those in mammalian systems. Thus, the effect of semaphorin3F on neutrophil reverse migration has to be further investigated in mammalian models of inflammation.

7.4 Is semaphorin3F a possible therapeutic target in chronic inflammatory diseases?

Unresolved neutrophilic inflammation often leads to a wide variety of inflammatory diseases. Persistently activated neutrophils release excessively cytotoxic molecules such as proteinases, and reactive oxygen species (ROS). Uncontrolled or impaired neutrophil activation can also leads to persisting tissue damage from these cytotoxic molecules. An ideal drug to treat inflammatory diseases should be able to reduce inflammatory responses or activate resolution of inflammation. Currently, most of the anti-inflammatory therapies target key inflammatory responses controlling infiltration of neutrophils into the site of inflammation, such as use of chemokine receptor CXCR2 inhibitors reducing neutrophil recruitment during acute and chronic inflammatory responses (Goncavalves and Appelberg, 2002) (Donnelly and Barnes, 2011), or use of laser therapy inhibiting inflammatory mediator (TNF-α, IL-1β and IL-6) expression during inflammation (Alves et al., 2013). However, these do not effectively reduce permanent inflammation, because different microenvironments composed of tissue-specific cell types can themselves activate inflammatory responses. For instance, some cell types such as fibroblasts play an important role in the switch from acute resolving to chronic persistent inflammation. Fibroblasts can provide survival and retention signals for neutrophils, leading to their persistent accumulation within inflamed sites (Buckley et al., 2001). More recently, attention has turned to inflammatory disease treatments that target the resolution phase and anti-inflammatory mechanisms that lead to the return of homeostasis. Particular emphasis has been placed on drugs that might accelerate resolution by enhancing neutrophil apoptosis (Burgon et al., 2014). Treatment promoting neutrophil clearance from the site of injury by neutrophil reverse migration may also become an alternative solution for chronic inflammatory diseases (Robertson et al., 2014).

Semaphorin3F has been shown to affect neutrophil migration during inflammation. Loss of semaphorin3F can accelerate inflammation resolution by enhancing neutrophil reverse migration from the inflamed site.

Semaphorin3F therefore would be a potential therapeutic target for inflammatory diseases caused by persistent neutrophilia. However, semaphorin3F has also been reported to be a tumour suppressor (Bielenberg et al., 2004) (Kusy et al., 2005) (Nasarra et al., 2005) (Futamura et al., 2007) (Guttmann-Raviv et al., 2007). Use of semaphorin3F antagonists as drugs for inflammatory conditions therefore must be carefully considered in light of its potential effect on tumour progression.

7.5 Future work

Further work determining *in vivo* whether neuropilin-2 and plexin A3 are important receptor components of semaphorin3F, expression of plexin A3 in lung sections of acute neutrophilic inflammation, as well as in murine bronchoalveolar lavage neutrophils should be performed. Moreover, TALENs-generated neuropilin-2 or plexin A3 mutation in zebrafish may enable dissection of the mechanism of semaphorin3F regulating neutrophil migration. In this study, one could demonstrate only the action of exogenous semaphorin3F in modulating neutrophil persistence at the site of inflammation as contrasted to whole fish in which overexpression or knockdown/knockout of semaphroin3F was generated. To specifically define the function of neutrophil-derived semaphorin3F, neutrophil-specific semaphorin3F overexpression or knockdown zebrafish lines are an alternative future approach. Nonetheless, the molecular mechanisms or signalling pathways regulating neutrophil reverse migration in zebrafish may be different from those in mammalian systems. Thus, the effect of semaphorin3F on neutrophil reverse migration has to be further investigated in mammalian models of inflammation.

As thought that semaphorin3F plays a role in neutrophil function at inflamed tissues, semaphorin3F expression in chronic inflammatory tissues such as samples of COPD patients would be important for the further work. It will also be important to discover those mechanisms involved in neutrophil chemotaxis which are affected by semaphorin3F, perhaps factors involved in

RhoA- and Rac-activity or the cytoskeleton such as RhoA kinase (ROCK), cofilin, STAT3, actin, myosin, or microtubule, to determine whether semaphorin3F is associated with or affects their functions. Class 3 semaphorins have been suggested to modulate cell adhesion, notably through effects on integrins and their trafficking (Zhou et al., 2008), but also on other adhesion systems, for example cadherins (Nasarre et al., 2005), all of which are likely to have a role in neutrophil migration. Discovering which of these mechanisms is critical to the effects we see, should provide further insight into the mechanisms regulating neutrophil migration. This research is currently underway.

7.6 Thesis summary

To summarise, in this thesis I have discovered a novel role of semaphorin3F in regulating neutrophil migration during inflammation. The expression of semaphorin3F, and also its receptors neuropilin-2 and plexin A3, in neutrophils has been characterised. *In vivo* investigation of the role of semaphorin3F in neutrophil behaviour in inflammation was performed in transgenic zebrafish embryos accompanied with use of genomic editing techniques, including TALENs. I found that semaphorin3F affects the migratory behaviour of neutrophils and leads to changes in the recruitment and resolution phases of inflammation. Semaphorin3F overexpression reduces neutrophil motility causing retention of neutrophils at the inflamed site, whereas loss of semaphorin3F promotes inflammation resolution by accelerating neutrophil movement away from the site of injury. I further determined the mechanism of semaphorin3F involvement in neutrophil migration. I demonstrated that semaphorin3F inhibits chemotactic response of neutrophils to chemoattractants, but it does not affect PI-3K activity which generates polarisation during chemotaxis. Notably, distinct changes in neutrophil shape between semaphorin3F overexpression and the controls were observed. This may be affected by involvement of semaphorin3F in cytoskeletal signalling pathways that must be further elucidated in the future. Coupled with the fact that semaphorin3F knockdown/knockout shows no considerable effect on neutrophil recruitment, and that semaphorin3F expression in human neutrophils appears to be modulated antagonistically by hypoxia and inflammatory cytokines released at the inflammatory site, these suggest that semaphorin3F may not be induced until neutrophils reach the site of inflammation. As neutrophils arrive at the injury site, their movement is slowed by upregulation of semaphorin3F caused by cytokines, causing them to stop where the inflammation is greatest. Once the pathogens are destroyed, increased hypoxia may have the opposite effect, downregulating semaphorin3F expression and initiating resolution, resulting in neutrophil reverse migration (Figure 7.1). This work will hopefully extend the study of neutrophilic inflammation, and provide a new concept of drug discovery for inflammatory diseases.

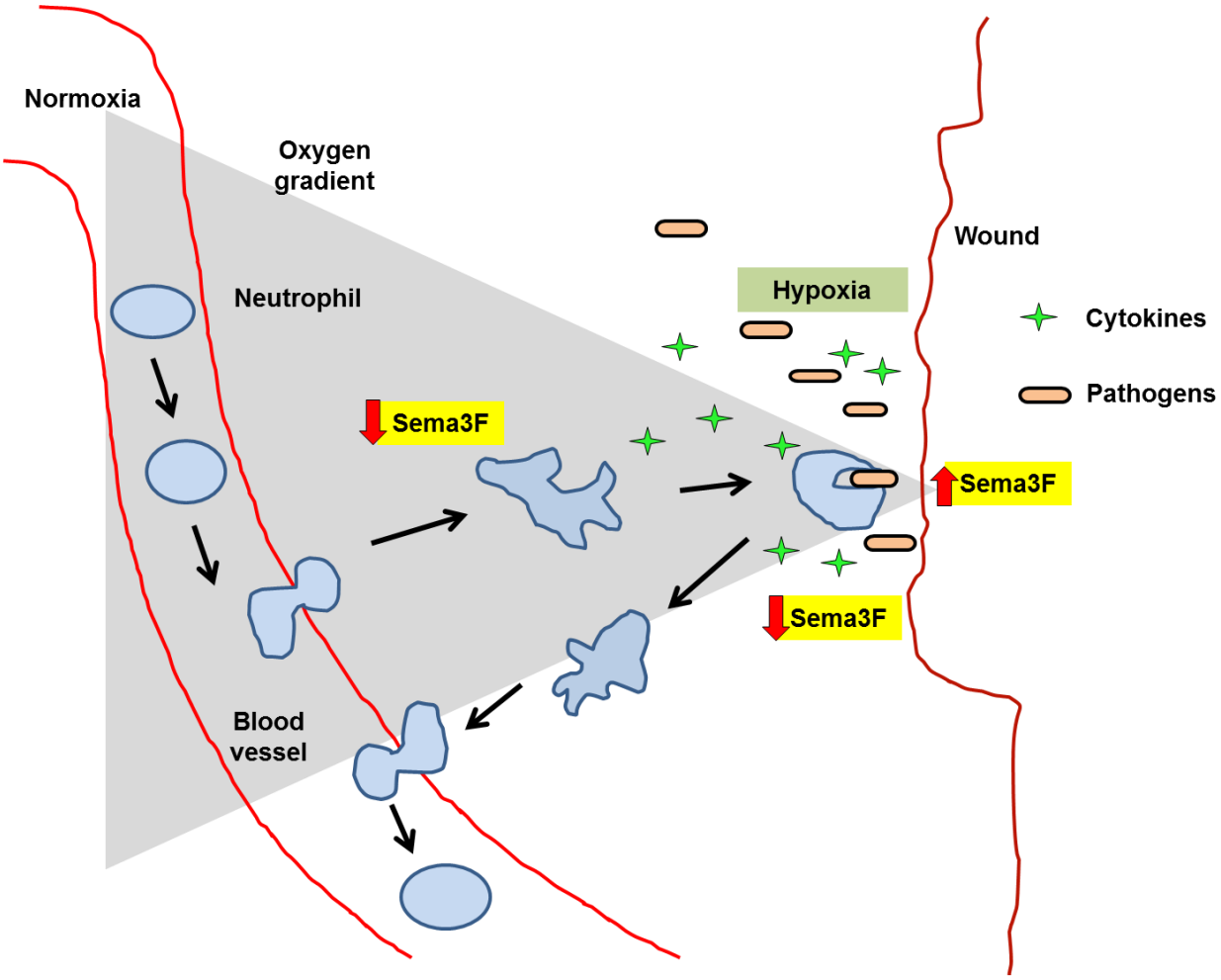

Figure 7.1: Semaphorin3F regulates neutrophil migration during inflammation. Once an injury occurs, neutrophils are recruited from the circulation to the site of inflammation by alarm signal from hypoxia and pro-inflammatory cytokines though chemotaxis. At the beginning of recruitment phase, semaphorin3F is thought to be downregulated. As neutrophils arrive at the site of injury, released cytokines upregulate semaphorin3F expression, causing neutrophil movement to slow or stop where the inflammation is greatest. Once the pathogens are destroyed, increased hypoxia downregulates semaphorin3F expression and initiate resolution, resulting in neutrophil reverse migration.

References

Akira S, Takeda K. (2004) **Toll-like receptor signalling.** *Nat.Rev.Immunol.* **4:** 499-511.

Alves ACA, Vieira RP, Leal-Junior ECP, dos Santos SA, Ligeiro AP, Albertini R, Silva Junior JA, de Carvallo PT. (2013) **Effect of low level laser therapy on the expression of inflammatory mediators and on neutrophils and macrophages in acute joint inflammation.** *Arthr.Res.Therap.* **15:** R116.

Atwal JK, Singh KK, Tessier-Lavigne M, Miller FD, Kaplan DR. (2003) **Semaphorin3F antagonizes neurotrophin-induced phosphatidylinositol 3-kinase and mitogen-activated protein kinase kinase signalling: A mechanism for growth cone collapse.** *J.Neurosci.* **23(20):** 7602-7609.

Bae D, Lu S, Taglienti CA, Mercurio AM. (2008) **Metabolic stress induces the lysosomal degradation of neuropilin-1 but not neuropilin-2.** *J.Biol.Chem.* **283:** 28074-28080.

Banu N, Teichman J, Dunlap-Brown M, Villegas G, Tufro A. (2006) **Semaphorin3C regulates endothelial cell function by increasing integrin activity.** *FASEB.* **20(12):** 2150-2152.

Bedell VM, Westcot SE, Ekker SC. (2011) **Lessons from morpholino-based screening in zebrafish.** *Brief.in.func.genom.* **doi:** 10.1093/bfgp/elr021.

Bedell VM, Wang Y, Campbell JM, Poshusta TL, Starker CG, Krung II RG, Tan W, Penheiter SG, Ma AC, Leung AYH, Fahrenkrung SC, Carlson DF, Voytas DF, Clark KJ, Essner JJ, Ekker SC. (2012) ***In vivo* genome editing using a high-efficiency TALEN system.** *Nat.* **491(7422):** 114-118.

Benard V, Bokoch GM, Diebold BA. (1999) **Potential drug targets: small GTPases that regulate leucocyte function**. *Trends.Phamacol.Sci.* **20:** 365-370.

Bennett CM, Kanki JP, Rhodes J, Liu TX, Paw BH, Kieran MW, Langenau DM, Delahaye-Brown A, Zon LI, Fleming MD, Look AT. (2001) **Myelopoiesis in the zebrafish, *Danio rerio*.** *Blood.* **98:** 643-651.

Berndt JD, Halloran MC. (2006) **Semaphorin3D promotes cell proliferation and neuron crest cell development downstream of TCF in the zebrafosh hindbrain.** *Devel.* **133(20):** 3983-3992.

Bielenberg DR, Hida Y, Shimizu A, Kaipainen A, Kreuter M, Kim CC, Klagsbrun M. (2004) **Semaphorin3F, a chemorepulsant for endothelial cells, induces a poorly vascularized, encapsulated, nonmetastatic tumour phenotype.** *J. Clin. Inv.* **114(9):** 1260-1271.

Bill BR, Balciunas D, McCarra JA, Young ED, Xiong T, Spahn AM, Garcia-Lecea M, Korzh V, Ekker SC, Schimmenti LA. (2008) **Development and Notch signalling requirements of the zebrafish choride plexus.** *Plos.One.* **3(9):** e3114.

Blond D, Campbell SJ, Butchart AG, Perry VH, Anthony DC. (2002) **Differential induction of interleukin-1 beta and tumour necrosis factor-alpha may account for specific patterns of leukocyte recruitment in the brain.** *Brain.Res.* **958(1):** 89-99.

Blythe TA, Jarrett CE, Barratt SL, Welsh GI, Millar AB. (2012) **Regulation of VEGF receptors and co-factors by hypoxia and hyperoxia in A549 and human pulmonary microvascular endothelial cells.** *ATS.J.* **DOI:** 10.1164/ajrccm.

Boch J, Scholze H, Schornack S, Landgraf A, Hahn S. (2009) **Breaking the code of DNA binding specificity of TAL-type III effectors.** *Sci.* **326:** 1509-1512.

Boch J, Bonas U. (2010) **Xanthomonas AvrBs3 family-type III effectors: discovery and function.** *Annu.Rev.Phytopathol.* **48:** 419-436.

Bork P, Doerks T, Springer TA, Snel B. (1999) **Domains in plexins: links to integrins and transcription factors.** *Trend.Biochem.Sci.* **24:** 261-263.

Borregaard N, Cowland JB. (1997) **Granules of human neutrophilic polymorphonuclear leukocyte.** *Blood.* **89(10):** 3503-3521.

Boyden S. (1962) **The chemotactic effect of mixtures of antibody and antigen on polymorphonuclear leucocytes.** *J.Exp.Med.* **115(3):** 453-466.

Brambilla E, Constantin B, Drabkin H, Roche J. (2000) **Semaphorin SEMA3F localization in malignant human lung and cell lines: a suggested role in cell adhesion and cell migration.** *Am.J.Pathol.* **156:** 939-950.

Bratton DL, Henson PM. (2011) **Neutrophil clearance: when the party is over, clean-up begins.** *Trends in Immun.* **32(8):** 350-357.

Breier G, Albrecht U, Sterrer S, Risau W. (1992) **Expression of vascular endothelial growth factor during embryonic angiogenesis and endothelial cell differentiation.** *Devel.* 114: 521-532.

Brown LF, Yeo KT, Berse B, Yeo TK, Senger DR, Dvorak HF, Van de Water L. (1992) **Expression of vascular permeability factor (vascular endothelial growth factor) by epidermal keratinocytes during wound healing.** *J.Exp.Med.* **176:** 1375-1379.

Brown LF, Olbrich SM, Berse B, Jackman RW, Matsueda G, Tognazzi K, Manseau EJ, Dvorak HF, Van de Water L. (1995) **Overexpression of vascular permeability factor (VPF/VEGF) and its endothelial cell receptors in delayed hypersensitivity skin reactions.** *J.Immunol.* **154:** 2801-2807.

Brown SB, Savill J. (1999) **Phagocytosis triggers macrophage release of Fas ligand and induces apoptosis of bystander leukocytes.** *J.Immunol.* **162(1):** 480-485.

Buckley CD, Pilling D, Lord JM, Scheel-Toellner D, Salmon M. (2001) **Fibroblasts regulate the switch from acute resolving to chronic persistent inflammation.** *Trends.Immunol.* **22(4):** 199-204.

Buckley CD, Ross EA, McGettrick HM, Osborne CE, Haworth O, Schmutz C, Stone PC, Salmon M, Matharu NM, Vohra RK, Nash GB, Rainger GE. (2006) **Identification of a phenotypically and functionally distinct population of long-lived neutrophils in a model of reverse endothelial migration.** *J.Leukoc.Biol.* **79(2):** 303-311.

Burgon J, Robertson AL, Sadiku P, Wang X, Hooper-Greenhill E, Prince LR, Walker P, Hoggett EE, Ward JR, Farrow SN, Zuercher WJ, Jeffrey P, Savage CO, Ingham PW, Hurlstone AF, Whyte MK, Renshaw SA. (2014) **Serum and glucocorticoid-regulated kinase 1 regulates neutrophil clearance during inflammation resolution.** *J.Immunl.* **192(4):** 1796-1805.

Burridge K, Wennerberg K. (2004) **Review Rho and Rac take center stage.** *Cell.* **116(2):** 167-179.

Callander DC, lamont RE, Childs SJ, McFarlane S. (2007) **Expression of multiple class three semaphorins in the retina and along the path of zebrafish retinal axons.** *Devel.Dynam.* **236(10):** 2918-2924.

Cantley LC, Neel BG. (1999) **New insights into tumor suppression: PTEN suppresses tumor formation by restraining the phosphoinositode 3-kinase/Akt pathway.** *Proc.Natl.Acad.Sci.USA.* **96(8):** 4240-4245.

Capparuccia L, Tamagnone L. (2009) **Semaphorin signalling in cancer cells and in cells of the tumour microenvironment-two sides of a coin.** *J.Cell.Sci.* **122:** 1723-1736.

Cartwright GE, Athens JW, Wintrobe MM. (1964) **The kinetics of granulopoesis in normal man.** *Blood.* **24:** 780-803.

Casazza A, Laoui D, Wenes M, Rizzolio S, Bassani N, Mambretti M, Desschoemaeker S, Van Ginderachter JA, Tamagnone L, Mazzone M. (2013) **Impeding macrophage entry into hypoxic tumour areas by sema3A/Nrp1 signalling blockade inhibits angiogenesis and restores antitumour immunity.** *Cancer. Cell.* **24(6):** 695-709.

Cascao R, Rosario HS, Fonseca JE. (2009) **Neutrophils: warriors and commanders in immune mediate inflammatory diseases.** *Acta.Reumatologica.Portuguesa.* **34(2):** 313-326.

Castellani V, Chedotal A, Schachner M, Faivre-Sarrailh C, Rougon G. (2000) **Analysis of the L1-deficient mouse phenotype reveals cross-talk between sema3A and L1 signaling pathways in axonal guidance.** *Neuron.* **27(2):** 237-249.

Castro-Rivera E, Ran S, Thorpe P, Minna JD. (2004) **Semaphorin3B (SEMA3B) induces apoptosis in lung and breast cancer, whereas VEGF165 antagonises this effect.** *PNAS.* **101(31):** 11432-11437.

Catalano A, Caprari P, Rodilossi S, Betta P, Castellucci M, Casazza A, Tamagnone L, Procopio A. (2004) **Cross-talk between vascular endothelial growth factor and semaphorin-3A pathway in the regulation of normal and malignant mesothelial cell proliferation.** *FASEB J.* **18(2):** 358-360.

Catalano A, Caprari P, Moretti S, Faronato M, Tamagnone L, Procopio A. (2006) **Semaphorin-3A is expressed by tumour cells and alters T-cell signal transduction and function.** *Blood.* **107:** 3321-3329.

Cermark T, Doyle EL, Christian M, Wang L, Zhang Y, Schmidt C, Baller JA, Somia NV, Bogdanove AJ, Voytas DF. (2011) **Efficient design and assembly of custom TALEN and other TAL effector-based constructs for DNA targeting.** *Nucleic Acids Res.* **39(12):** e82.

Chakravarti A, Rusu D, Flamand N, Borgeat P, Poubelle PE. (2009) **Reprogramming of s subpopulation of human blood neutrophils by prolonged exposure to cytokines.** *Lab.Invest.* **89(10):** 1084-1099.

Chauhan BK, Lou M, Zheng Y, Lang RA. (2011) **Balanced Rac1 and RhoA activities regulate cell shape and drive invagination morphogenesis in epithelia.** *PNAS.* **Doi:** 10.1073/pnas.1108993108.

Chen H, Chedotal A, He Z, Goodman CS, Tessier-Lavigne M. (1997) **Neuropilin-2, a novel member of the neuropilin family , is a high affinity**

receptor for thesemaphorins Sema E and Sema IV but not Sema III. *Neuron.* **19:** 547-559.

Cheng HJ, Bagri A, Yaron A, Stein E, Pleasure SJ, Tessier-Lavigne M. (2001) **Plexin-A3 mediates semaphorin signalling and regulates the development of hippocampal axonal projections.** *Neuron.* **32:** 249-263.

Chung CY, Lee S, Firtel RA. (2000) **Role of Rac in controlling the actin cytoskeleton and chemotaxis in motile cells.** *Proc.Natl.Acad.Sci.USA.* **97(10):** 5225-5230.

Choi YI, Duke-Cohan JS, Ahmed WB, Handley MA, Mann F, Epstein JA, Clayton LK, Reinherz EL. (2008) **Plexin D1 glycoprotein controls migration of positively selected thymocytes into the medulla.** *Immunity.* **29(6):** 888-898.

Christian M, Cermark T, Doyle EL, Schmidt C, Zhang F, Hummel A, Bogdanove AJ, Voytas DF. (2010) **Targeting DNA double-strand breaks with TAL effector nucleases.** *Gen.* **186(2):** 757-761.

Cicchetti G, Allen PG, Glogauer M. (2002) **Chemotactic signalling pathways in neutrophils: from receptor to actin assembly.** *Crit.Rev.Oral.Biol.Med.* **13(3):** 220-228.

Clark RA. (1999) **Activation of the neutrophil respriratory burst oxidase.** *J.Infect.Dis.* **179:** 309-317.

Coma S, Shimizu A, Klangsbrun M. (2011) **Hypoxia induces tumour and endothelial cell migration in a semaphorin3F- and VEGF-dependent manner via transcriptional repression of their common receptor neuropilin-2.** *Cell.Adh.Migr.* **5(3):** 266-275.

Corey RD, Abrams JM. (2001) **Morpholino antisense oligonucleotides: tools for investigating vertebrate development.** *Genom. Bio.* **2(5):** 1015.1-1015.3.

Cramer T, Yaminishi Y, Clausen BE, Forster I, Pawlinski R, Mackman N, Haase VH, Jaenisch R, Corr M, Nizet V, Firestein GS, Gerber H-P, Ferrara

N, Johnson RS. (2003) **HIF-1α is essential for myeloid cell-mediated inflammation.** *Cell.* **112:** 645-657.

Damen JE, Lui L, Rosten P, Humphries RK, Jefferson AB, Majerus PW, Krytal G. (1996) **The 145-kDa protein induced to associate with Shc by multiple cytokines is an inositol tetraphosphate and phosphatidylinositol 3,4,5-triphosphate 5- phosphatase.** *Proc.Natl.Acad.Sci.USA.* **93(4):** 1689-1693.

Degenhardt K, Singh MK, Aghajanian H, Massera D, Wang Q, Li J, Li L, Choi C, Yzaguirre AD, Francey LJ, Gallant E, Krantz ID, Gruber PJ, Epstein J. (2013) **Semaphorin3D signalling defects are associated with anomalous pulmonary venous connections.** *Nat.Med.* **19:** 760-765.

Dekker RJ, Boon RA, Rondaij MG, Kragt A, Volger OL, Elderkamp YW, Meijiers JC, Voorberg J, Pannekoek H, Horrevoets AJ. **KLF2 provokes a gene expression pattern that establishes functional quiescent differentiation of the endothelium.** *Blood.* **107:** 4354-4363.

Delaire S, Billard C, Tordjman R, Chedotal A, Elhabazi A, Bensussan A. (2001) **Biological activity of soluble CD100.II. Soluble CD100, similarly to H-SemaIII, inhibits immune cell migration.** *J.Immunol.* **166:** 4348-4354.

De Nardin E, Radel SJ, Genco RJ. (1991) **Isolation and partial characterization of the formyl peptide receptor components on human neutrophils.** *Biochem.Biophys.Res.Commun.* **174:** 84-89.

Dickson BJ. (2002) **Molecular mechanisms of axon guidance.** *Sci.* **298:** 1959-1964.

Donnelly LE, Barnes PJ. (2011) **Chemokine receptorCXCR2antagonism to prevent airway inflammation.** *Drugs.Future.* **36:** 465-472.

Edwards SW. (1994) **Biochemistry and Physiology of the Neutrophil.** *Cambridge University Press.*

Eisen JS, Smith JC. (2008) **Controlling morpholino experiments: don't stop making antisense.** *Devel.* **135:** 1735-1743.

EL Kebir D, Filep JG. (2010) **Role of neutrophil apoptosis in the resolution of inflammation.** *TheSci.World.J.* **10:** 1731-1748.

Elizur A, Cannon CL, Ferkol TW. (2008). **Airway inflammation in cystic fibrosis.** *Chest.* **133:** 489-495.

Elks PM, van Eeden FJ, Dixon G, Wang X, Reyes-Aldasoro CC, Ingham PW, Whyte MK, Walmsley SR, Renshaw SA. (2011) **Activation of Hif-1alpha delays inflammation resolution by reducing neutrophil apoptosis and reverse migration in a zebrafish inflammation model.** *Blood* **doi:**10.1182/blood-2010-12-324186.

Fassold A, Falk W, Anders S, Hirsch T, Mirsky VM, Straub RH. (2009) **Soluble neuropilin-2, a nerve repellent receptor, is increased in Rheumatoid Arthritis synovium and aggravates sympathetic fiber repulsion and arthritis.** *Arth.Rheu.* **60(10):** 2892-2901.

Fava RA, Olsen NJ, Spencer-Gteen G, Yeo KT, Yeo TK, Berse B, Jackman RW, Dvorak HF, Brown LF. (1994) **Vascular permeability factor/endothelial growth factor (VPF/VEGF): accumulation and expression in human synovial fluids and rheumatoid synovial tissue.** *J.Exp.Med.* **180:** 341-346.

Favier B, Alam A, Barron P, Bonnin J, Laboudie P, Fons P, Mandron M, Herault JP, Neufeld G, Savi P, Herbert JM, Bono F. (2006) **Neuropilin-2 interacts with VEGF-2 and VEGF-3 and promotes human endothelial cell survival and migration.** *Blood.* **108:** 1243-1250.

Feiner L, Webber AL, Brown CB, Lu MM, Jia L, Feinstein P, Moombaerts P, Epstein JA, Raper JA. (2001) **Targeted disruption of semaphorin3C leads to persistent truncus arteriosus and aortic arch interruption.** *Devel.* **128(16):** 3061-3070.

Frede S, Berchner-Pfannschmidt U, Fandrey J. (2007) **Regulation of hypoxia-inducible factors during inflammation.** *Methods.Enzymol.* **435:** 405-419.

Fujioka S, Masuda K, Toguchi M, Ohoka Y, Sakai T, Furuyama T, Inagaki S. (2003) **Neurotrophic effect of semaphorin4D in PC12 cells.** *Biochem.Biophys.Res.Commun.* **301(2):** 304-310.

Fujiwara N, Kobayashi K. (2005) **Macrophages in inflammation**. *Curr. Drug Targets Inflamm. Allerg.* **4(3):** 281-286.

Fukasawa M, Matsushita A, Korc M. (2007) **Neuropilin-1 interacts with integrin beta 1 and modulates pancreatic cancer cell growth, survival and invasion.** *Cancer.Biol.Ther.* **6:** 1173-1180.

Futamura M, Kamino H, Miyamoto Y, Kitamura N, Nakamura Y, Ohnishi S, Masuda Y, Arakawa H. (2007) **Possible Role of Semaphorin 3F, a Candidate Tumour Suppressor Gene at 3p21.3, in p53-Regulated Tumour Angiogenesis Suppression.** *Cancer Res.* **67 (4)**: 1451-1460.

Gammill LS, Gonzalez C, Bronner-Fraser M. (2007) **Neuropilin-2/semaphorin3F signaling is essential for cranial neural crest migration and trigeminal ganglion condensation.** *Dev.Neurobiol.* **67(1):** 47-56.

Gaudry M, Bregerie O, Andrieu V, El Benna J, Pocidalo MA, Hakim J. (1997) **Intracellular pool of vascular endothelial growth factor in human neutrophils.** *Blood.* **90:** 4153-4161.

Gaur P, Bielenberg DR, Samuel S, Bose D, Zhou Y, Gray MJ, Dallas NA, Fan F, Xia l, Lu J, Ellis LM. (2009) **Role of class 3 semaphorins and their receptors in tumour growth and angiogenesis.** *Clin.Cancer.Res.* **15:** 6763-6770.

Gerard C, Gerard NP. (1994) **The pro-inflammatory seven-transmembrane segment receptors of the leukocyte.** *Curr.Opin.Immunol.* **6(1):** 140-145.

Geretti E, Shimizu A, Kurschat P, Klangsbrun M. (2007) **Site-directed mutagenesis in the B-neuropilin-2 domain selectively enhances its affinity to $VEGF_{165}$, but not to semaphorin3F.** *J.Biol.Chem.* **282:** 25698-25707.

Glinka Y, Prud'homme GJ. (2008) **Neuropilin-1 is a receptor for transforming growth factor beta-1, activates its latent form, and promotes regulatory T-cell activity.** *J.Leukoc.Biol.* **84:** 302-310.

Gluzman-Poltorak Z, Cohen T, Herzog Y, Neufeld G. (2000) **Neuropilin-2 is a receptor for the vascular endothelial growth factor (VEGF) forms VEGF-145 and VEGF-165.** *J. Biol. Chem.* 275(24): 18040-18045.

Gomez F, Ruiz P, Schreiber AD. (1994) **Impaired function of macrophage Fc gamma and bacterial infection in alcoholic cirrhosis.** *N.Engl.J.Med.* **331:** 1122-1128.

Goncalves AS, Appelberg R. (2002) **The involvement of the chemokine receptor CXCR2 in neutrophil recruitment in LPS-induced inflammation and in Mycobacterium avium infection.** *Scan.J.Immunol.* **55:** 585-591.

Gong Y, Koh DR. (2010) **Neutrophils promote inflammatory angiogenesis via release of preformed VEGF in an in vivo corneal model.** *Cell.Tissue.Res.* **339:** 437-448.

Goodman CS, Kolodkin AL, Luo Y, Pueschel AW, Raper JA. (1999) **Unified nomenclature for the semaphorins/collapsins.** *Cell.* **97(5):** 551-552.

Guo HF, Li X, Parker MW, Waltenberger J, Becker PM, Vander Kooi CW. (2013) **Mechanistic basis for the potent anti-angiogenic activity of semaphorin3F.** *Biochem.* **52(43):** 7551-7558.

Guttmann-Raviv N,Shraga-HeledN, Varshavsky A, Guimaraes Sternberg C, Kessler O, Neufeld G. (2007) **Semaphorin-3A and semaphorin-3F work together to repel endothelial cells and to inhibit their survival by induction of apoptosis.** *J. Biol. Chem.* **282:**26294–305.

Hall A, Nobes CD. (2000) **Rho GTPases: molecular switches that control the organization and dynamics of the actin cytoskeleton.** *Philos.Trans.R.Soc.Lond.B.Biol.Sci.* **355(1399):** 965-970.

Hallett MB, Lloyds D. (1995) **Neutrophil priming: the cellular signals that say 'amber' but not 'green'.** *Immunol.Today.* **16:** 264-268.

Haslett C. (1999) **Granulocyte apoptosis and its role in the resolution and control of lung inflammation.** *Am. J. Respir. Crit. Care Med.* **160:** S5-11.

He Z, Tessier-Lavigne M. (1997) **Neuropilin is a receptor for the axonal chemorepellent semaphorin III.** *Cell*. **90:** 739-751.

Hirsch E, Katanaev VL, Garlanda C, Azzolino O, Pirola L, Silengo L. (2000) **Central role for G protein-coupled phosphoinositide 3-kinase gamma in inflammation.** *Science.* **287(5455):** 1049-1053.

Huang P, Xiao A, Zhou M, Zhu Z, Lin S, Zhang B. (2011) **Heritable gene targeting in zebrafish using customized TALENs.** *Nat.Biotechnol.* **29:** 699-700.

Iijima K, Yoshikawa N, Connolly DT, Nakamura H. (1993) **Human mesangial cells and peripheral blood mononuclear cells produce vascular endothelial growth factor.** *Kidney.Int.* **44:** 959-966.

John AS. (1944) **Neutrophils, host defense, and inflammation: a double-edged sword.** *J. Leuko. Biol.* **56:** 672-685.

Joseph D, Ho SM, Syed V. (2010) **Hormonal regulation and distinct functions of semaphorin3B and semaphorin3F in ovarian cancer.** *Mol.Cancer.Ther.* **9(2):** 499-509.

Joung JK, Sander JD. (2013) **TALENs: a widely applicable technology for targeted genome editing.** *Nat.Rev.Mol.Cell Biol.* **14(1):** 49-55.

Kaelin WG Jr, Ratcliffe PJ. (2008) **Oxygen sensing by metazoans: the central role of the HIF hydroxylase pathway.** *Mol.Cell.* **30(4):** 393-402.

Kagoshima M, Ito T. (2001) **Diverse gene expression and function of semaphorins in developing lung: positive and negative regulatory roles of semaphorins in lung branching morphogenesis.** *Gen.Cell.* **6(6):** 559-571.

Kardash E. (2012) **Current methods in zebrafish research.** *Mater.Metho.* **doi:** 10.13070/mm.en.2.109.

Kassahn KS, Dang VT, Wilkins SJ, Perkins AC, Ragan MA. (2009**) Evolution of gene function and regulatory control after whole-genome duplication: comparative analyses in vertebrates.** *Genome.Res.* **19:** 1404-1418.

Kessler O, Shraga-Heled N, Lange T, Gutmann-Raviv N, Sabo E, Baruch L, Machluf M, Neufeld G. (2004) **Semaphorin-3F is an inhibitor of tumour angiogenesis.** *Cancer Res.* **64:**1008–1015.

Kim J, Oh WJ, Gaiano N, Yoshida Y, Gu C. (2011) **Semaphorin3E-plexin-D1 signalling regulates VEGF function in developmental angiogenesis via a feedback mechanism.** *Genes&Dev.* **25:** 1399-1411.

Kobayashi SD, Voyich JM, Braughton KR, DeLeo FR. (2003) **Down-regulation of proinflammatory capacity during apoptosis in human polymorphonuclear leukocytes.** *J.Immunol.* **170:** 3357-3368.

Kobayashi SD, Voyich JM, Burlak C, DeLeo FR. (2005) **Neutrophils in the innate immune response.** *Arch.Immunol.Ther.Exp.* **53:** 505-517.

Koehne P, Willam C, Strauss E, Schindler R, Eckardt KU, Buehrer C. (2000) **Lack of hypoxic stimulation of VEGF secretion from neutrophils and platelets.** *Americ.J.Physiol.Heart and Circ.Physiol.* **279:** 817-824.

Kolodkin AL, Matthes D, O'Connor T, Patel NH, Admon A,Bentley D, Goodman CS. (1992) **Fasciclin IV: sequence, expression, and function during growth cone guidance in the grasshopper embryo.** *Neuron.* **9:** 831-845.

Kolodkin AL, Levengood DV, Rowe EG, Tai YT, Giger RJ, Ginty DD. (1997) **Neuropilin is a semaphorinIII receptor.** *Cell.* **90:** 739-762.

Koppel AM, Feiner L, Kobayashi H, Raper JA. (1997) **A 70 amino acid region within the semaphorin domain activates specific cellular response of semaphorin family members.** *Neuron.* **19:** 531-537.

Kruger RP, Aurandt J, Guan KL. (2005) **Semaphorins command cells to move.** *Nat.Rev.Mol.Cell.Biol.* **6:** 789-800.

Kumanogoh A, Watanabe C, Lee I, Wang X, Shi W, Araki H. (2000) **Identification of CD72 as a lymphocyte receptor for the class IV semaphorin CD100: a novel mechanism for regulating B cell signalling.** *Immunity.* **13:** 621-631.

Kumanogoh A, Marukawa S, Suzuki K, Takegahara N, Watanabe C, Chong E, Ishida I, Fujimura H, Sakoda S, Yoshida K, Kikutani H. **Semaphorin4A Sema4A enhances T-cell activation and interacts with Tim-2.** *Nat.* **419:** 629-633.

Kusy S, Nasarre P, Chan D, Potiron V, Meyronet D, Gemmill RM, Conatantin B, Drabkin HA, Roche J. (2005) **Selective suppression of in vivo tumourigenicity by semaphorin SEMA3F in lung cancer cells.** *Neoplasia.* **7:** 457-465.

Kusy S, Potiron V, Zeng C, Franklin W, Brambilla E, Minna J, Drabkin HA, Roche J. (2005) **Promoter characterisation of semaphorin SEMA3F, a tumour suppressor gene.** *Biochem.Biophys.Acta.* **1730(1):** 66-76.

Kutschera S, Weber H, Weick A, De Smet F, Genove G, Takemoto M, Prahst C, Riedel M, Mikelis C, Baulande S, Champseix C, Kummerer P, Conseiller E, Multon MC, Heroult M, Bicknell R, Carmeliet P, Betsholtz C, Augustin HG. (2011) **Differential endothelial transcriptomics identifies semaphorin3G as a vascular class 3 semaphorin.** *Arterioscler.Thromb.Vasc.Biol.* **31(1):** 151-159.

Lee A, Whyte MK, Haslett C. (1993) **Inhibition of apoptosis and prolongation of neutrophil functional longevity by inflammatory mediators.** *J.Leukoc.Biol.* **54:** 283-288.

Leslie NR, Batty IH, Maccario H, Davidson L, Downes CP. (2008) **Understanding PTEN regulation: PIP_2, polarity and protein stability.** *Oncogene.* **27:** 5464-5476.

Ley K. (2002) **Integration of inflammatory signals by rolling neutrophils.** *Immunol.Rev.* **186:** 8-18.

Levy NS, Chung S, Furneaux H, Levy AP. (1998) **Hypoxic stabilization of vascular endothelial growth factor mRNA by the RNA-binding protein HuR.** *J.Biol.Chem.* **273:** 6417-6423.

Li M, O'Sullivan KM, Jones LK, Lo C, Semple T, Kumanogoh A, Kikutani H, Holdsworth SR, Kitching R. (2009) **Endogenous C100 promotes glomerular injury and macrophage recruitment in experimental crescentic glomerulonephritis.** *Immun.* **128:** 114-122.

Li T, Huang S, Zhao X, Wright DA, Carpenter S, Spalding MH, Weeks DP, Yang B. (2011) **Modularly assembled designer TAL effector nucleases for targeted gene knockout and gene replacement in eukaryotes.** *Nucleic Acids. Res.* **39(14):** 6315-6325.

Li T, Lui B, Spalding MH, Weeks DP, Yang B. (2012) **High-efficiency TALEN-based gene editing disease-resistant rice.** *Nat.Biotechnol.* **30(5):** 390-392.

Lieschke GJ, Oates AC, Crowhurst MO, ward AC, Layton JE. (2001) **Morphologic and functional characterization of granulocytes and macrophages in embryonic and adult zebrafish.** *Blood.* **98(10):** 3087-3096.

Liu J, Li C, Yu Z, Huang P, Wu H, Wei C, Zhu N, Shen Y, Chen Y, Zhang B, Deng WM, Jiao R. (2012) **Efficient and specific modification of the**

Drosophila genome by means of aneasy TALEN strategy. *J.Genet.Genom.* **39(5):** 209-215.

Loynes CA, Martin JS, Robertson A, Trushell DMI, Ingham PW, Whyte MKB, Renshaw SA. (2010) **Pivotal advance: Pharmacological manipulation of inflammation resolution during spontaneously resolving tissue neutrophilia in the zebrafish.** *J. of Leuko. Biol.* **87(2):** 203-212.

Luchino J, Hocine M, Amoureux MC, Gibert B, Bernet A, Royet A, Treilleux I, Lecine P, Borg JP, Mehlen P, Chauvet S, Mann F. (2013) **Semaphorin3E suppresses tumour cell death triggered by the plexin D1 dependence receptor in metastatic breast cances.** *Cell.* **24(5):** 673-685.

Luo Y, Raible D, Raper JA. (1993) **Collapsin: a protein in brain that induces the collapse and paralysis of neuronal growth cones.** *Cell.* **75:** 217-227.

Maione F, Capano S, Regano D, Zentillin L, Giacca M, Casanovas O, Bussolino F, Serini G, Giraudo E. (2012) **Semaphorin3A overcomes cancer hypoxia and metastatic dissemination induced by antiangiogenetic treatment in mice.** *J.Clin.Invest.* **122(5):** 1832-1848.

Mathias JR, Perrin BJ, Liu TX, Kanki J, Look AT, Huttenlocher A. (2006) **Resolution of inflammation by retrograde chemotaxis of neutrophils in transgenic zebrafish.** *J. of Leuko. Biol.* **80(6):** 1281-1288.

Matin JS, Renshaw SA. (2009) **Using *in vivo* zebrafish models to understand the biochemical basis of neutrophilic respiratory disease.** *Bio.Chem.Soc.Trans.* **37:** 830-837.

Matthes DJ, Sink H, Kolodkin AL, Goodman CS. (1995) **Semaphorin II can function as a selective inhibitor of specific synaptic arborisations.** *Cell.* **8(4):** 631-639.

McGovern NN, Cowburn AS, Porter L, Walmsley SR, Summers C, Thompson AAR, Anwar S, Willcocks LC, Whyte MKB, Condliffe AM, Chivers ER. (2011) **Hypoxia selectively inhibits respiratory burst activity and**

killing of *Staphylococcus aureus* in human neutrophils. *J.Immunol.* **186(1):** 453-463.

McPhail LC, Clayton CC, Snyderman R. (1984) **The NADPH oxidase of human polymorphonuclear leukocytes: Evidence for regulation by multiple signals.** *J.Biol.Chem.* **259:** 5768-5775.

Meda C, Molla F, De Pizzol M, Regano D, Maione F, Capano S, Locati M, Mantovani A, Latini R, Bussolino F, Giraudo E. (2012) **Semaphorin4A exerts a proangiogenic effect by enhancing vascular endothelial growth factor-A expression in macrophages.** *J. of Immunol.* **Doi:**10.4049.

Meszaros AJ, Reichner JS, Albina JE. (2000) **Macrophage-induced neutrophil apoptosis.** *J.Immunol.* **165(1):** 435-441.

Moore FE, Reyon D, Sander JD, Martinez SA, Blackburn JS, Khayter C, Ramirez AL, Joung JK, Langenau DM. (2012) **Improved somatic mutagenesis in zebrafish using TALENs.** *Plos.One.* **DOI:** 10.1371/journal.pone.0037877.

Moreno-Flores MT, Martin-Aparicio E, Martin-Bermejo MJ, Aqudo M, MaMahon S, Avila J, Diaz-Nido J, Wandosell F. (2003) **Semaphorin3C preserves survival and induces neuritogenesis of cerebellar granule neurons in culture.** *J.Neurochem.* **87(4):** 879-890.

Moriya J, Minamino T, Tateno K, Okada S, Uemura A, Shimizu I, Yokoyama M, Nojima A, Okada M, Koga H, Komuro I. (2010) **Inhibition of semaphorin as a novel strategy for therapeutic angiogenesis.** *Circ.Res.* **106:** 391-398.

Morote-Garcia J, Napiwotzky D, Koehler D, Rosenberger P. (2012) **Endothelial semaphorin7A promotes neutrophil migration during hypoxia.** *PNAS.* **109(35):** 14146-14151.

Mussolino C, Morbitzer R, Luetge F, Dannemann N, Lahaye T, Cathomen T. (2011) **A novel TALE nuclease scaffold enables high genome editing activity in combination with low toxicity.** *Nucleic Acids.Res.* **39(21):** 9283-9293.

Nakamura F, Goshima Y. (2002) **Structural and functional relation of neuropilins.** *Adv.Exp.Med.Biol.* **515:** 55-69.

Nasarre P, Constantin B, Rouhaud L, Harnois T, Raymond G, Drabkin N, Bourmeyster N, Roche J. (2003) **Semaphorin SEMA3F and VEGF have opposing effects on cell attachment and spreading.** *Neoplas.* **5:** 83-92.

Nasarra P, Kusy S, Constantin B, Castellani V, Drabkin HA, Bagnard D, Roche J. (2005) **Semaphorin 3F has a repulsing activity on breast cancer cells and inhibits E-cadherin-mediated cell adhesion.** *Neoplas.* **7:** 180-189.

Nasevicius A, Ekker SC. (2000) **Effective targeted gene knockdown in zebrafish.** *Nat. Genet.* **26(2):** 216-220.

Nathan C. (2006) **Neutrophil and immunity; challenges and opportunities.** *Nat.Rev.Immunol.* **6(3):** 173-182.

Neufeld G, Kessler O. (2008) **The semaphorins: versatile regulators of tumour progression and tumour angiogenesis.** *Nat.Rev.Cancer.* **8:** 632-645.

Negishi M, Oinuma I, Katoh H. (2005) **Plexin: axon guidance and signal transduction.** *Cell.Mol.Life Sci.* **62:** 1363-1371.

Nguyen H, Ivanova VS, Kavandi L, Rodriguez GC, Maxwell GL, Syed V. (2011) **Progesterone and 1,25-dihydroxyvitamin D inhibit endometrial cancer cell growth by upregulating semaphorin3B and semaphorin3F.** *Mol.Cancer.Res.* **9:**1479-1492.

Nobes CD, Hall A. (1995) **Rho, rac and cdc42 GTPases regulate the assembly of multimolecular focal complexes associated with actin stress fibers, lamellipodia, and filopodia.** *Cell.* **81:** 53-62.

Nusslein-Volhard C and Dahm R. (2002) **Zebrafish: a practical approach.** Oxford, Oxford University Press.

Nuzzi PA, Lokuta MA, Huttenlocher A. (2007) **Analysis of neutrophil chemotaxis.** *Methods.Mol.Biol.* **370:** 23-36.

Okada T, Sakuma L, Fukui Y, Hazeki O, Ui M. (1994) **Blockage of chemotactic peptide-induced stimulation of neutrophils by Wortmannin as a result of selective inhibition of phospotidylinositol-3-kinase.** *J.Biol.Chem.* **269(5):** 3563-3567.

Orlando K, Guo W. (2009) **Membrane organisation and dynamics in cell polarity.** *Cold.Spring.Harb.Perspect.Biol.* **1:** a001321.

Pasterkamp RJ, Peschon JJ, Spriggs MK, Kolodkin AL. (2003) **Semaphorin7A promotes axon outgrowth through integrins and MAPKs.** *Nat.* **424(6947):** 398-405.

Peyssonnaux C, Datta V, Cramer T, Doedens A, Theodorakis EA, Gallo RL, Hurtado-Ziola N, Nitzet V Johnson RS. (2005) **HIF-1alpha expression regulates the bactericidal capacity of phagocytes.** *J.Clin.Invest.* **115(7):** 1806-1815.

Peyssonnaux C, Zinkernagel AS, Schuepbach RA, Rankin E, Vaulont S, Haase VH, Nitzet V Johnson RS. (2007) Regulation of iron homeostasis by the hypoxia-inducible transcription factors (HIFs). *J.Clin.Invest.* **117(7):** 1926-1932.

Polleux F, Morrow T, Ghosh A. (2000) **Semaphorin3A is a chemoattractant for cortical apical dendrites.** *Nat.* **404(6778):** 567-573.

Potiron VA, Nasarre P, Roche J, Healy C, Boumsell L. (2007) **Semaphorin signalling in the immune system.** *Adv.Exp.Med.Biol.* **600:** 132-144.

Potiron VA, Sharma G, Nasarre P, Clarhaut JA, Augustin HA, Gemmill RM, Roche J, Drabkin HA. (2007) **Semaphorin SEMA3F affects multiple signalling pathways in lung cancer cells.** *Cancer.Res.* **67:** 8708-8715.

Pueschel AW. (2002) **The function of neuropilin/plexin complexes.** *Adv.Exp.Med.Biol.* **515:** 71-80.

Puri KD, Doggett TA, Douangpanya J, Hou Y, Tino WT, Wilson T, Graf T, Clayton E, Turner M, Hayflick JS, Diacovo TG. (2004) **Mechanisms and**

implications of phosphatidylinositol-3-kinase δ in promoting neutrophil trafficking into inflamed tissue. *Blood.* **103:** 3448-3456.

Quint JK, Wedzicha JA. (2007). **The neutrophil in chronic obstructive pulmonary disease.** *J.Allergy.Clin.Immunol.* **119:** 1065-1071.

Rahme LE, Cantley LC. (1999) **The role of phosphatidylinositol-3-kinase lipid products in cell function.** *J.Biol,Chem.* **274:** 8347-8350.

Raskopf E, Vogt A, Decker G, Hirt S, Daskalow K, Cramer T, Standop J, Gonzales-Carmona MA, Sauerbruch T, Schmitz V. (2012) **Combination of hypoxia and RNA-interference targeting VEGF induces apoptosis in hepatoma cells via autocrine mechanisms.** *Curr.Phama.Biotechnol.* **13(11):** 2290-2298.

Renshaw SA, Parmar JS, Singleton V, Rowe SJ, Dockrell DH, Dower SK, Bingle CD, Chilvers ER, Whyte MK. (2003) **Acceleration of human neutrophil apoptosis by TRAIL.** *J.Immunol.* **170:** 1027-1033.

Renshaw SA, Loynes CA, Trushell DM, Elworthy S, Ingham PW, Whyte MK. (2006) **A transgenic zebrafish model of neutrophilic inflammation.** *Blood*. **108(13):** 3976-3978.

Ridley AJ, Schwartz MA, Burridge K, Firtel RA, Ginsberg MH, Borisy G, Parsons JT, Horwitz AR. (2003) **Cell migration: integrating signals from front to back.** *Sci.* **302:** 1704-1709.

Robertson AL, Holmes GR, Bojarczuk AN, Burgon J, Loynes CA, Chimen M, Sawtell AK, Hamza B, Willson J, Walmsley SR, Anderson SR, Coles MC, Farrow SN, Solari R, Jones S, Prince LR, Irimia D, Ed Rainger G, Kadirkamanathan V, Whyte MKB, Renshaw SA. (2014) **A zebrafish compounds screen reveals modulation of neutrophil reverse migration as an anti-inflammatory mechanism.** *Sci.Transl.Med.* **DOI:** 10.1126/scitranslmed.3007672.

Rolny C, Capparuccia L, Casazza A, Mazzone M, Vallario A, Cignetti A, Medico E, Carmeliet P, Comoglio PM, Tamagnone L. (2008) **The tumour**

suppressor semaphorin3B triggers a prometastatic program mediated by interleukin 8 and the tumour microenvironment. *J. Exp. Med.* **205(5):** 1155-1171.

Saati AA. (2013) **Regulatory role of semaphorin3E on human neutrophil migration.** *Thesis submitted to the U of Manitoba.*

Sabag AD, Bode J, Fink D, Kigel B, Kugler W, Neufeld G. (2012) **Semaphorin3D and semaphorin3E inhibit the development of tumours from gliioblastoma cells implanted in the cortex of the brain.** *Plos.One.* **DOI:** 10.1371/journal.pone.0042912.

Saban MR, Sferra TJ, Davis CA, Simpson C, Allen A, Maier J, Fowler B, Knowlton N, Birder L, Wu XR, Saban R. (2010) **Neuropilin-VEGF signalling pathway acts as a key modulator of vascular, lymphatic, and inflammatory cell responses of the bladder to intravesical BCG treatment.** *Am.J.Physiol.Renal.Physiol.* **299(6):** 1245-1256.

Sakurai A, Gavard J, Annas-Linhares Y, Basile JR, Amornphimoltham P, Palmby TR, Yagi H, Zhang F, Randazzo PA, Li X, Weigert R, Gutkind S. (2010) **Semaphorin3F initiates antiangiogenic signalling through plexin D1 by regulating Arf6 and R-Ras.** *Mol.Cell.Biol.* **30(12):** 3086-3098.

Sahay A, Molliver ME, Ginty DD, Kolodkin AL. (2003) **Semaphorin3F is critical for development of limbic system circuitry and is required in neurons for selective CAN axon guidance events.** *J.Neurosci.* **23(17):** 6671-6680.

Sahay A, Kim CH, Sepkuty JP, Cho E, Huganir RL, Ginty DD, Kolodkin AL. (2005) **Secreted semaphorins modulate synaptic transmission in the adult hippocampus.** *J.Neurosci.* **25(14):** 3613-3620.

Sander JD, Cade L, Khayter C, Reyon D, Peterson RT, Keith Joung J, Yeh JJ. (2011) **Targeted gene disruption in somatic zebrafish cells using engineered TALENs.** *Nat.Biotechnol.* **29:** 697-698.

Savill JS, Wyllie AH, Hanson JE, Wal[ort MJ, Hanson PM, Haslett JC. (1989) **Macrophage phagocytosis of aging neutrophils in inflammation. Programmed cell death in the neutrophils leads to its recognition by macrophages**. *J.Clin.Invest.* **83:** 865-875.

Schofield CJ, Ratcliffe PJ. (2004) **Oxygen sensing by HIF hydroxylases.** *Nat.Rev.Molecul.Cell.Biol.* **5:** 343-354.

Schornack S, Meyer A, Roemer P, Jordan T, Lahaye T. (2006) **Gene-for gene-mediated recognition of nuclear-targeted AvrBs3-like bacterial effector proteins.** *J.Plant.Physiol.* **163:** 256-272.

Schmidt RF. (1989) **Human physiology 2nd edition** (ed Schmidt RF and Thews G); (Springer-Verlag, Berlin, Germany).

Schwarz Q, Vieira JM, Howard B, Eickholt BJ, Ruhrberg C. (2008) **Neuropilin-1 and 2 control cranial gangliogenesis and axon guidance through neural crest cells.** *Devel.* **135:** 1605-1613.

Serhan CN, Brain SD, Buckley CD, Gilroy DW, Haslett C, O'Neill LAJ, Perretti M, Rossi AG, Wallace JL. (2007) **Resolution of inflammation: state of the art, definitions and terms.** *FASEB.* **21(2):** 325-332.

Serini G, Maione F, Bussolino F. (2009) **Semaphorins and tumour angiogenesis.** *Angio.* **12:** 187-193.

Servant G, Weiner OD, Herzmark P, Balla T, Sedat JW, Bourne HR. (2000) **Polarisation of chemoattractant receptor signalling during neutrophil chemotaxis.** *Sci.* **287:** 1037-1040.

Shimizu A, Mammoto A, Italiano JE Jr, Pravda E, Dudley AC, Ingber DE, Klagsbrun M. (2008) **ABL2/ARG tyrosine kinase mediates SEMA3F-induced RhoA inactivation and cytoskeleton collapse in human glioma cells.** *J.Biol.Chem.* **283(40):** 27230-27238.

Shweiki D, Itin A, Soffer D, Keshet E. (1992) **Vascular endothelial growth factor induced by hypoxia may mediate hypoxia-initiated angiogenesis.** *Nat.* **359:** 843-845.

Soker S, Takashima S, Miao HQ, Neufeld G, Klagsbrun M. (1998) **Neuropilin-1 is expressed by endothelial and tumour cells as an isoform-specific receptor for vascular endothelial growth factor.** *Cell* **92:**735–745.

Spassky N, De Castro F, Le Bras B, Heydon K, Queraud-LeSaux F, Bloch-Gallego E, Chedotal A, Zalc B, Thomas JL. (2002) **Directional Guidance of oligodendroglial migration by class 3 semaphorins and netrin-1.** *Neurosci.* **22(14):** 5992-6004.

Starnes TW, Huttenlocher A. (2012) **Neutrophil reverse migration becomes transparent with zebrafish.** *Adv. In Hematol.* **DOI:** 10.1155/2012/398640.

Sun Q, Zhou H, Binmadi NO, Basile JR. (2009) **Hypoxia-inducibla factor-1-mediated regulation of semaphorin4D affects tumour growth and vascularity.** *J.Biol.Chem.* **284:** 32066-32074.

Staton CA, Shaw LA, Valluru M, Hoh L, Cross SS, Reed MW, brown NJ. (2011) **Expression of class 3 semaphorins and their receptors in human breast neoplasia.** *Histopathol.* **59(2):** 274-282.

Stephens L, Ellson C, Hawkins P. (2002) **Roles of PI3Ks in leukocyte chemotaxis and phagocytosis.** *Curr,Opin.Cell.Biol.* **14:**203.

Swaney KF, Huang CH, Devreotes PN. (2010) **Eukaryotic chemotaxis: a network of signalling pathways controls motility, directional sensing, and polarity.** *Annu.Rev.Biophys.* **39:** 265-289.

Taichman NS, Young S, Cruchley AT, Taylor P, Paleolog E. (1997) **Human neutrophils secrete vascular endothelial growth factor.** *J.Leukoc.Biol.* **62:** 397-400.

Takagi S, Hirata T, Agata K. (1991) **The A5 antigen, a candidate for the neuronal recognition molecule, has homologoes to complement components and coagulation factors.** *Neuron.* **7(2):** 295-307.

Takahashi T, Fournier A, Nakamura F, Wang LH, Murakami Y, Kalb RG. (1999) **Plexin-neuropilin-1 complexs from functional semaphorin3A receptors.** *Cell.* **99:** 59-69.

Takahashi T, Strittmatter SM. (2001) **Plexin A1 autoinhibition by the plexin sema domain.** *Neuron.* **29:** 429-439.

Takamatsu H, Okuno T, Kumanogoh A. (2010) **Regulation of immune cell responses by semaphorins and their receptors.** *Cell.Mole.Immunol.* **7:** 83-88.

Tanaka H, Maeda R, Shoji W, Wada H, Masai I, Shiraki T, Kobayashi M, Nakayama R, Okamoto H. (2007) **Novel mutations affecting axon guidance in zebrafish and a role for plexin signalling in the guidance of trigeminal and facial nerve axons** *Devel.***134:** 3259-3269.

Taylor CT, Colgan SP. (2007). **Hypoxia and gastrointestinal disease.** *J.Mol.Med.* **85:** 1295-1300.

Tesson L, Usal C, Menoret S, Leung E, Niles BJ, Remy S, Santiago Y, Vincent AL, Meng X, Zhang L, Gregory PD, Anegon I, Cost GJ. (2011) **Knockout rats generated by embryo microinjection of TALENs.** *Nat.Biotechnol.* **29(8):** 695-696.

Thompson AA, Binham J, Plant T, Whyte MK, Walmsley SR. (2013) **Hypoxia, the HIF pathway and neutrophilic inflammatory responses.** *Biol.Chem.* **394(4):** 471-477.

Thompson AA, Elks PM, Marriott H, Eamsamarng S, Higgins KR, Lewis A, Williams L, Parmar S, Shaw G, McGrath EE, Formenti F, Van Eeden FJ, Kinnula VL, Pugh CW, Sabroe I, Dockrell DH, Chivers ER, Robbins PA, Percy MJ, Simon MC, Johnson RS, Renshaw SA, Whyte MKB, Walmsley SR. (2013) **Hypoxia-inducible factor 2α regulates key neutrophil functions in humans, mice, and zebrafish.** *Blood.* **123(3):** 366-376.

Toker A, Cantley LC. (1997) **Signalling through the lipid products of phosphatidylinositol-3-OH kinase.** *Nature.* **387(6634):** 673-676.

Toyofuku T, Zhang H, Kumanogoh A, Takegahara N, Suto F, Kamei J, Aoki K, Yabuki M, Hori M, Fujisawa H. (2004) **Dual roles of sema6D in cardiac morphogenesis through region-specific association of its receptor, plexin A1, with off-track and vascular endothelial growth factor type 2.** *Genes.Dev.* **18:** 435-447.

Toyofuku T, Yoshida J, Sugimoto T, Zhang H, Kumanogoh A, Hori M, Kikutani H. (2005) **FARP2 triggers signals for sema3A-mediated axonal repulsion.** *Nat.Neurosci.* **8(12):** 1712-1719.

Tran TS, Kolodkin AL, Bharadwej (2007) **Semaphorin regulation of cellular morphology.** *Annu.Rev.Cell Dev.Biol.* **23:** 263-292.

Traynor-Kaplan AE, Thompson BL, Harris AL, Taylor P, Omann GM, Sklar LA. (1989) **Transient increase in phosphatidylinositol-3,4-biphosphate and phosphatidylinositol-3,4,5-triphosphate during activation of human neutrophils.** *J.Biol.Chem.* **264(26):** 15668-15673.

Trede NS, Langenau DM, Traver D, Look AT, Zon LI. (2004) **The use of zebrafish to understand immunity.** *Immun.* **20:** 367-379.

Urnov FD, Rebar EJ, Holmes MC, Zhang HS, Gregory PD. (2010) **Genome editing using zinc-finger nucleases.** *Nat.Rev.Genet.* **11:** 636-646.

Vieira SM, Lemos HP, Grespan R, Napimoga MH, Dal-Secco D, Freitas A, Cunha TM, Verri WA, Souza-Junior DA, Jamur MC, Fernandes KS, Oliver C, Silva JS, Teixeira MM, Cunha FQ. (2009) **A crucial role for TNF-alpha in mediating neutrophil influx induced by endogenously generated or exogenous chemokines, KC/CXCL1 and LIX/CXCL5.** *Br.J.Phamacol.* **158(3):** 779-789.

Waimey KE, Huang PH, Chen M, Cheng HJ. (2008) **Plexin A3 and plexin A4 restrict the migration of sympathetic neurons but not their neural crest precursors.** *Dev.Biol.* **315(2):** 448-458.

Walmsley SR, Print C, Farahi N, Peyssonnaux C, Johnson RS, Cramer T, Sobolewski A, Condliffe A, Cowburn AS, Johnson N, Chilvers ER. (2005) **The role of HIF-1α and NF-κB in hypoxia-induced survival in human and murine neutrophils.** *J.Exp.Med.* **201:** 105-115.

Walmsley SR, Chilvers ER, Thompson AA, Vaughan K, Marriott HM, Parker LC, Shaw G, Parmar S, Schneider M, Ian Sabroe I, Dockrell DH, Milo M, Taylor CT, Johnson RS, Pugh CW, Ratcliffe PJ, Maxwell PH, Carmeliet P, Whyte MK. (2011) **Prolyl hydroxylase 3 (PHD3) is essential for hypoxic regulation of neutrophilic inflammation in humans and mice.** *J.Clin.Invest.* **121(3):** 1053-1063.

Walzer T, Galibert L, De Smedt T. (2005) **Poxvirus semaphoringA39R inhibits phagocytosis by dendritic cells and neutrophils.** *Eur.J.Immunol.* **35:** 391-398.

Wang X, Robertson AL, Li J, Chai RJ, Haishan W, Sadiku P, Ogryzko NV, Everett M, Yoganathan K, Luo HR, Renshaw SA, Ingham PW. (2014) **Inhibitors of neutrophil recruitment identified using transgenic zebrafish to screen a natural product library.** *Dis.Model.Mech.* **7(1):** 163-169.

Webb NJ, Myers CR, Watson CJ, Bottomley MJ, Brenchley PE. (1998) **Activated human neutrophils express vascular endothelial growth factor (VEGF).** *Cytokine.* **10(4):** 254-257.

Weiner OD, Servant G, Parent CA, Devreotes PN, Bourne HR. (2000**) Cell polarity in response to chemoattractants. In cell polarity: frontiers in molecular biology.** *Oxford University Press.*

Weiner OD, Neilsen PO, Prestwich GD, Kirschner MW, Cantley LC, Bourne HR. (2002) **A PtdInsP(3_- and Rho GTPase-mediated positive feedback loop regulates neutrophil polarity.** *Nat.Cell.Biol.* **4:** 509-513.

Wheeler AP, Ridley AJ. (2004) **Why three Rho proteins? RhoA, RhoB, RhoC, and cell motility.** *Exp.Cell.Res.* **301(1):** 43-49.

Williams A, Piaton G, Aigrot MS, Belhadi A, Theaudin M, Petermann F, Thomas JL, Zalc B, Lubetzki C. (2007) **Semaphorin3A and 3F: key players in myelin repair in multiple sclerosis?** *Brain.* **130:** 2554-2565.

Williams LT, Snyderman R, Pike MC, Lefkowitz RJ. (1977) **Specific receptorsites for chemotactic peptides on human polymorphonuclear leucocytes.** *Proc.Natl.Acad.Sci.USA.* **74:** 1204-1208.

Wong K, Pertz O, Hahn K, Bourne H. (2006) **Neutrophil polarisation: spatiotemporal dynamics of RhoA activity support a self-organizing mechanism.** *Proc.Natl.Acad.Sci.USA.* **103:** 3639-3644.

Woodfin A, Voisin MB, Imhof BA, Dejana E, Engelhardt B, Nourshargh S. (2009) **Endothelial cell activation leads to neutrophil transmigration as supported by the sequential roles of ICAM-2, JAM-a and PECAM-1**. *Blood.* **113:** 6246-6257.

Woodfin A, Voisin MB, Beyrau M, Colom B, Caille D, Diapouli FM, Nash GB, Chavakis T, Albelda SM, Rainger GE, Meda P, Imhof BA, Nourshargh S. (2011) **The junctional adhesion molecule JAM-C regulates polarized transendothelial migration of neutrophils *in vivo*.** *Nat.Immunol.* **12(8):** 761-769.

Wright HL, Moots RJ, Bucknall RC, Edwards SW. (2010) **Neutrophil function in inflammation and inflammatory diseases.** *Rheumatol.* **49:** 1618-1631.

Wu F, Zhou Q, Yang J. (2011) **Endogenous axon guiding chemorepulsant semaphorin3F inhibits the growth and metastasis of colorectal carcinoma.** *Clin.Cancer.Res.* **17:** 2702-2711.

Xiang R, Hensel C, Garcia D, Carlson H, Kok K, Daly M, Kerbacher K, Van Den Berg A, Veldhuis P, Buys C, Naylor S. (1996) **Isolation of the human semaphorin III/F gene (SEMA3F) at chromosome 3p21, a region deleted in lung cancer.** *Genom.* **32:** 39-48.

Xiang R, Davalos AR, Hensel C, Zhou XJ, Tse C, Naylor SL. (2002) **Semaphorin 3F gene from human 3p21.3 suppresses tumour formation in nude mice.** *Cancer Res.* **62:** 2637-2643.

Xiang X, Zhang X, Huang QL. (2012) **Plexin A3 is involved in semaphorin3F-mediated oligodendrocyte precursor cell migration.** *Neurosci.Letters.* **530(2):** 127-132.

Xu J, Wang F, Van Keymeulen A, Herzmark P, Straight A, Kelly K, Takuwa Y, Sugimoto N, Michison T, Bourne HR. (2003) **Divergent signals and cytoskeletal assemblies regulate self-organizing polarity in neutrophils.** *Cell.* **114:** 201-214.

Xu Y, Yaun L, Mak J, Pardanaud L, Caunt M, Kasman I, Larrivee B, Del Toro R, Suchting S, Medvinsky A, Silva J, Yang J, Thomas JL, Koch AW, Alitato K, Eichmann A, Bagri A. (2010) **Neuropilin-2 mediates VEGF-C-induced lymphatic sprouting together with VEGFR3.** *J.Cell.Biol.* **188(1):** 115-130.

Yaron A, Huang PH, Cheng HJ, Tessie-Lavigne M. (2005) **Differential requirement for plexinA3 and –A4 in mediating responses of sensory and sympathetic neurons to distinct class 3 semaphorins.** *Neuron.* **45:** 513-523.

Yazdani U, Terman JR. (2006) **The semaphorins.** *Genom.Biolo.* **7:** 211-221.

Yoo SK, Deng Q, Cavnar PJ, Wu YI, Hahn KM. (2010) **Differential regulation of protrusion and polarity by PI(3)K during neutrophil motility in live zebrafish.** *Devel.Cell.* **18(2):** 226-236.

Yoo SK, Huttenlocher A. (2011) **Spatiotemporal photolabeling of neutrophil trafficking during inflammation in live zebrafish.** *Pro.Nat.Acad.Sci.USA.***101:** 15706-15711.

Yoo SK, Lam P, Eichelberg MR, Zasadil L, Bement WM, Huttenlocher A. (2012) **The role of microtubules in neutrophil polarity and migration in live zebrafish.** *J.Cell.Sci.* **125:** 5702-5710.

Yu HH, Araj HH, Ralls SA, Kolodkin AL. (1998) **The transmembrane semaphorin Sema I is required in drosophila for embryonic motor and CNS axon guidance.** *Neuron.* **20:** 207-220.

Yu HH, Moens CB. (2005) **Semaphorin signaling guides cranial neural crest cell migration in zebrafish.** *Devel.Biol.* **280:** 373-385.

Zachariae CO. (1993) **Chemotactic cytokines and inflammation. Biological properties of the lymphocyte and monocyte chemotactic factors ELCF, MCAF and IL-8.** *Acta.Derm.Venereol.Suppl.* **181:** 1-37.

Zhou H, Yang YH, Binmadi NO, Proia P, Basile JR. (2012) **The hypoxia-inducible factor-responsive proteins semaphorin4D and vascular endothelial growth factor promote tumour growth and angiogenesis in oral squamous cell carcinoma.** *Exp.Cell.Res.* **318(14):** 1685-1698.

Zhou Y, Gunput RA, Pasterkamp RJ. (2008) **Semaphorin signaling: progress made and promises ahead.** *Trends Biochem. Sci.* **33**, 161-170.

Zu Y, Tong X, Wang Z, Liu D, Pan R, Li Z, Hu Y, Luo Z, Huang P, Wu Q, Zhu Z, Zhang B, Lin S. (2013) **TALEN-mediated precise genome modification by homologous recombination in zebrafish.** *Nat.Meth.* **DOI:**10.1038/NMETH.2374.

Appendix 1

Primary antibodies

Name	Producer species	Species reactivity	Isotype	Dilution	Source
Anti-semaphorin3F	Rabbit	Human, Mouse, Rat	Polyclonal	1:200	#ab39956 Abcam
Anti-neuropilin1	Rabbit	Human, Mouse, Rat	IgG	1:500	#ab81321 Abcam
Anti-neuropilin2	Rabbit	Human, Mouse, Rat	Polyclonal	1:200	#ab135456 Abcam
Anti-plexin A1	Rabbit	Human, Mouse, Rat	Polyclonal	1:500	#ab23391 Abcam
Anti-plexin A2	Mouse	Human, Mouse, Rat	IgG2b	1:500	#ab88130 Abcam
Anti-plexin A3	Rabbit	Human, Mouse	Polyclonal	1:500	#ab41564 Abcam
Anti-plexin D1	Rabbit	Human, Mouse, Rat	Polyclonal	1:500	#ab96313 Abcam
Anti-p38 MAPK	Rabbit	Human, Mouse, Rat, Monkey, Guinea pig	Polyclonal	1:1000	#9212 Cell Signaling Technology

Secondary antibodies

Name	Producer species	Species reactivity	Isotype	Dilution	Source
Anti-Rabbit Immunoglobulins/HRP	Goat	Rabbit	Polyclonal	1:2000	#P0448 Dako
Anti-Mouse Immunoglobulins/HRP	Rabbit	Mouse	Polyclonal	1:2000	#P0260 Dako

Cytokines

Name	Concentration	Source
Recombinant Human TNF-alpha	10 ng/ml	#210-TA-100 R&D Systems
Recombinant Human IL-1 beta	10 ng/ml	#201-LB-025 R&D Systems

Plasmid constructs

Name	Information	Source
Full length Zebrafish semaphorin3Fa in pCR4 vector	Insert size: 2.6 kb Antisense cut with PmeI Transcription with T7	From Prof.Cecilia B. Moens (University of Washington)
Full length Zebrafish semaphorin3Fb in pCR4 vector	Insert size: 2.2 kb Antisense cut with NotI Transcription with T3	From Prof.Cecilia B. Moens (University of Washington)

Morpholino oligonucleotides

Name	Sequence	Type	Source
Zebrafish semaphorin3Fa	5'-TATCCATAAAACCCACAAGAGATTT-3’	Translation blocker	Yu and Moens, 2005
Zebrafish semaphorin3Fb	5’-CATAGACTGTCCAAGAGCATGGTGC-3’	Translation blocker	Tanaka et al., 2007
Zebrafish semaphorin3Fb	5'-TATGAAGCGATACTCACGTTTGTGT-‘3	Splice blocker	Dr.Stephen Renshaw
Control	5’-CCTCTTACCTCAGTTACAATTTATA-3’	-	Gene Tools

Primer for morpholino test

Name	Sequence
Sema3fb-splice blocker (F)	5’-CATGTATGTGGGCAGCAAAG-3’
Sema3fb-splice blocker (R)	5’-CATAGGCTTGCGTCCTCTGT-3’
Ef1α (F)	5’-CTTCTCAGGCTGACTGTGC-3’
Ef1α (R)	5’-CCGCTAGCATTACCCTCC-3’

Primer for TALEN

Name	Sequence
TAL_R2	5’-GGCGACGAGGTGGTCGTTGG-3’
SeqTALEN_5-1	5’-CATCGCGCAATGCACTGAC-3’
Sema3Fa MwoI (F)	5’-ATGGATGGGCTCATTTTGTC-3’
Sema3Fa MwoI (R)	5’-GTAGTATGCCACGGTTCAAA-3’
Sema3Fb BsII (F)	5’-TCTCCCTGCATTGTCTTGC-3’
Sema3Fb BsII (R)	5’-TTTGAGCTCACCAGGCAGAT-3’

Appendix 2

Resolving gels

To make 1 gels for 1.5 mm gel plates:	3	ml	40% Acrylamide
	3.8	ml	1.5 M Tris pH 8.8
	8	ml	dH_2O
	75	µl	20% SDS
	150	µl	20% APS
	6	µl	TEMED

Stacking gels

To make 1 gels for 1.5 mm gel plates:	620	µl	40% Acrylamide
	1260	µl	1.5 M Tris pH 6.8
	3	ml	dH_2O
	25	µl	20% SDS
	50	µl	20% APS
	5	µl	TEMED

20% Ammonium persulfate (APS)

To make 1 ml of 20% APS stock:	0.2	g	APS
	1	ml	dH_2O

This can be stored in aliquots at -20°C for up to 1 month, but do not freeze-thaw.

Hypotonic sonication lysis buffer

To make 100 ml:	10	ml	1 M Tris pH 7.8
	55.84	mg	1 M EDTA
	74.56	mg	KCl
	7.71	mg	DTT
	18.39	mg	Sodium orthovanadate
	48.15	mg	Tetramisole
	dH_2O up to 100 ml		

Immediately before use the following were added:

Complete mini EDTA-free protease inhibitor cocktail tablets (1 tablet in 1 ml water)	1:20
Phenylmethanesulfonyl fluoride (PMSF)	1:100

2x SDS lysis buffer

To make 10 ml:	308.5	mg	DTT
	2	ml	20% SDS
	2	ml	Glycerol
	2	ml	1 M Tris-HCl pH 6.8
	100	µl	Bromophenol blue
	200	µl	Protease inhibitor cocktail
	dH_2O up to 10 ml		

Running buffer

To make 1 L of 10x stock:	190	g	Glycine
	30.3	g	Tris base
	50	ml	20% SDS
	dH_2O up to 1 L		

Transfer buffer

To make 1 L of 10x stock:	145	g	Glycine
	29	g	Tris base
	dH_2O up to 1 L		
To make 1 L of 1x stock:	100	ml	10x Transfer buffer
	200	ml	Methanol
	700	ml	dH_2O

This should be made immediately before use.

Tris-buffered saline (TBS)

To make 1 L of 10x stock:	97.3	g	NaCl
	100	ml	1 M Tris-HCl pH 8.0
	dH_2O up to 1 L		

Tris-buffered saline + 0.1% tween 20 (TBS-Tween)

To make 1 L of 10x stock:	97.3	g	NaCl
	100	ml	1 M Tris-HCl pH 8.0
	5	ml	Tween-20
	dH_2O up to 1 L		

Blocking buffer

To make 100 ml:	5	g	Skim milk powder
	100	ml	1x TBS

E3 medium

To make 1 L of 60x stock:	5	mM	NaCl
	0.17	mM	KCl
	0.33	mM	$CaCl_2$
	0.33	mM	$MgSO_4$
	dH_2O up to 1 L		
To make 1 L of 1x stock:	16.6	ml	60x E3 stock
	1% methylene blue		
	dH_2O up to 1 L		

In all cases, the 60x E3 stock was autoclaved before dilution and use in *in vivo* inflammation assays, to avoid contamination.

Hybridisation wash buffer (HybWash)

To make 50 ml:	25	ml	50% formamide
	12.5	ml	20x SSC
	460	µl	Citric acid
	50	µl	Tween 20

Pre-hybridisation buffer (PreHyb)

As HypWash, with	50	µg/ml	Heparin
	500	µg/ml	tRNA

Probe-hybridisation buffer (ProbeHyb)

As PreHyb, with	1:200 dilution of probe in formamide

20x Saline sodium citrate buffer (SSC)

To make 200 ml:	35.06 g NaCl
	17.64 g Sodium citrate
	dH_2O up to 200 ml
	pH 7.0 using citric acid

Blocking solution

PBT, with	2% Sheep serum
	2 mg/ml BSA

Staining wash

To make 50 ml:	5 ml 100 mM Tris-HCl pH 9.5
	2.5 ml 50 mM $MgCl_2$
	5 ml 100 mM NaCl
	dH_2O up to 50 ml

Staining solution

As staining wash, with	100 mg/ml NBT
	50 mg/ml BCIP

Appendix 3

Transgenic line	Abbreviation	Application	Reference
Tg(mpx:GFP)i114	*mpx*:GFP	Recruitment, Resolution, Total neutrophil number assays TUNEL assays In situ hybridisation	Renshaw et al., 2006
Tg(mpx:Gal4;UAS:Kaede)i222	*mpx*/Kaede	Reverse migration assays	Elks et al., 2011
Tg(fms:GAL4;UNM)	*fms*:UNM	Recruitment, Resolution assays	Gray et al., 2011
Tg(lyz:PHAkt-EGFP)	*lyz*/PHAkt	PI-3K assays	Wang et al., 2014